An Interferon Regulatory Factor Element Controls the Major Immune Modulator of Murine Cytomegalovirus

Dissertation
submitted for the degree
“Doktor der Naturwissenschaften“

At the Faculty of Biology
of the Johannes Gutenberg-University Mainz

Vanessa Wilhelmi
born 19.10.1981 in Wiesbaden

Mainz, 24.01.2012

Dekan:

1. Berichterstatter:

2. Berichterstatter:

Tag der mündlichen Prüfung: 24.02.2012

Res aspera verum gaudium est
(by my father; modified from Seneca)

Summary

Immune modulation by herpesviruses, such as cytomegalovirus, is critical for the establishment of acute and persistent infection confronting a vigorous antiviral immune response of the host. Therefore, the action of immune-modulatory proteins has long been the subject of research, with the final goal to identify new strategies for antiviral therapy.

In the case of murine cytomegalovirus (mCMV), the viral m152 protein has been identified to play a major role in targeting components of both the innate and the adaptive immune system in terms of infected host-cell recognition in the effector phase of the antiviral immune response. On the one hand, it inhibits cell surface expression of RAE-1 and thereby prevents ligation of the activating natural killer (NK)-cell receptor NKG2D. On the other hand, it decreases cell surface expression of peptide-loaded MHC class I molecules thereby preventing antigen presentation to CD8 T cells. Ultimately, the outcome of CMV infection is determined by the interplay between viral and cellular factors.

In this context, the work presented here has revealed a novel and intriguing connection between viral m152 and cellular interferon (IFN), a key cytokine of the immune system: the *m152* promoter region contains an interferon regulatory factor element (IRFE) perfectly matching the consensus sequence of cellular IRFEs.

The biological relevance of this regulatory element was first suggested by sequence comparisons revealing its evolutionary conservation among various established laboratory strains of mCMV and more recent low-passage wild-derived virus isolates. Moreover, search of the mCMV genome revealed only three IRFE sites in the complete sequence. Importantly, the functionality of the IRFE in the *m152* promoter was confirmed with the use of a mutant virus, representing a functional deletion of the IRFE, and its corresponding revertant virus. In particular, *m152* gene expression was found to be inhibited in an IRFE-dependent manner in infected cells. Essentially, this inhibition proved to have a severe impact on the immune-modulatory function of m152, first demonstrated by a restored direct antigen presentation on infected cells for CD8 T-cell activation. Even more importantly, this effect of IRFE-mediated IFN signaling was validated *in vivo* by showing that the protective antiviral capacity of adoptively-transferred, antigen-specific CD8 T cells is also significantly restored by the IRFE-dependent inhibition of *m152*. Somewhat curious and surprising, the decrease in m152 protein simultaneously prevented an enhanced activation of NK cells in acute-infected mice, apparently independent of the RAE-1/NKG2D ligand/receptor interaction but rather due to reduced ‘missing-self’ recognition.

Taken together, this work presents a so far unknown mechanism of IFN signaling to control mCMV immune modulation in acute infection.

Table of Contents

Abbreviations

AAF	IFN alpha activated factor
ADCC	antibody-dependent cellular toxicity
AIDS	aquired immune deficiency syndrome
AIM-2	absence in melanoma 2
APC	antigen presenting cell
APAAP	alkaline phosphatase α-alkaline phosphatase
Aq.dist	distilled water
ASGM1	Asialo GM1
AT	adoptive transfer
ATCC	American Type Culture Collection
ATF	activating transcription factor
BAC	bacterial artificial chromosome
b.i.	before infection
Blimp-1	B lymphocyte-induced maturation protein
bp	base pairs
BSA	bovine serum albumin
CBP	cAMP response element binding protein (CREB) binding protein
CD	cluster of differentiation
CDC	complement-dependent cytotoxicity
cDC	conventional Dendritic Cell
cDNA	complementary DNA
CEI	centrifugal enhancement of infection
CL	confidence limit
CMV	Cytomegalovirus
CPE	cytopathic effect
CTL(L)	cytolytic T lymphocyte line
ca.	circa
d	day
DAI	DNA-dependent activator of IFN-regulatory factor
DC	Dendritic Cell
DMEM	Dulbecco`s Modified Eagle Medium

DNA	deoxyribonucleic acid
dNTP	deoxyribonucleotide triphosphate
E	Early
EBV	Epstein-Barr Virus
e.g.	exempli gratia
ELISPOT	Enzyme-Linked Immunospot
ER	Endoplasmic Reticulum
ERGIC	ER *cis*-Golgi intermediate compartment
FACS	Fluorescence Activated Cell Sorter
FCS	fetal calv serum
fig	figure
GAF	Interferon–gamma activated factor
GAS	Interferon-gamma activated sequence
gp	glycoprotein
h	hours
hCMV	human Cytomegalovirus
HHV	Human Herpesvirus
HSV	Herpes-Simplex Virus
Hz	Hertz
IE	Immediate Early
i.e.	id est
IFN	Interferon
IFNAR	Interferon alpha receptor
IFNGR	Interferon gamma receptor
IHC	Immunohistochemistry
IL	Interleukin
i.p.	intra peritoneal
i.pl.	intra plantar
IRF	Interferon regulatory factor
IRF(-)E	Interferon regulatory factor element
ISGF3	Interferon-stimulated gene factor 3
ISRE	Interferon stimulated response element

JAK	Janus-kinase
KSHV	Kaposi`s sarcoma-associated herpesvirus
L	Late
LT	lymphotoxin
MACS	Magnetic Cell Separation
mCMV	murine Cytomegalovirus
MEF	mouse embryonic fibroblasts
MHC	Major Histocompatibility Complex
MIE	Major Immediate Early
MIEP	Major Immediate Early Promoter
MIEPE	Major Immediate Early Promoter Enhancer
min	minute
m	month
MOI	multiplicity of infection
MPN	most probable number
MyD88	Myeloid differentiation primary response gene 88
NFκB	nuclear factor kappa-light-chain-enhancer of activated B-cells
NK cell	Natural Killer cell
NLR	NOD-like receptors
NOD	nucleotide-binding oligomerization domain
NTC	no transfer control
OAS	2´,5´oligoadenylate cyclase
OD	optical density
ORF	open reading frame
p.a.	pro analysis
PAMP	pathogen-associated molecular pattern
pDC	plasmacytoid dendritic cell
PFU	plaque-forming unit
p.i.	post infection

PKR	protein kinase RNA-activated
PRDI-BF1	positive regulatory domain I-binding factor 1
PRR	pattern-recognition receptors
PTHRP	parathyroid hormone-related peptide
qPCR	quantitative real-time polymerase chain reaction
qRT-PCR	quantitative real-time reverse transcriptase polymerase chain reaction
RIG-I	retinoic-acid-inducible gene I
RLR	RIG-like receptors
RLU	relative luminescence unit
ROX	5-carboxy-x-Rhodamine
sec	second
SPF	specified pathogen free
STAT	signal transducer and activator of transcription
Tab.	table
TCR	T-cell receptor
TDY	Male sex (Testes)-determining gene
TLR	Toll-like receptor
TNFα	tumor necrosis factor alpha
TRIF	TIR-domain-containing adapter inducing interferon-beta
Tyk	tyrosine kinase
UV	ultraviolet
vol.	volume
v/v	volume per volume
VZV	Varicella-Zoster Virus
WT	wildtype
w/v	weight per volume
wk	week

1 Introduction

1.1 Cytomegalovirus

1.1.1 Classification

Cytomegaloviruses (CMV) are members of the family *Herpesviridae*. Family members share a common virion structure (Plummer, 1967), are characterized by a core containing linear double-stranded DNA, an icosahedral capsid composed of capsomers, the tegument consisting of viral phosphoproteins and certain RNA species, and a lipid bilayer (envelope) containing viral glycoproteins, which mediate attachment to and penetration into the host cell (Boyle & Compton 1998; Compton et al., 1992 & 1993). Moreover, they share 4 crucial biological properties: high coding capacity, nuclear DNA synthesis and capsid assembly, lytic infection, and the establishment of latent infection. The family *Herpesviridae* is subdivided into 3 subfamilies, namely *Alpha-, Beta-, and Gammaherpesvirinae*. So far, 8 human herpesviruses have been identified in all subfamilies (Tab. 1.1). Cytomegalovirus belongs to the subfamily of *Betaherpesvirinae* (reviewed in Pellett & Roizman, 2006).

Designation	Abbreviation	Synonym	Sub-family	Reference
Human HV 1	HHV-1	Herpes simplex virus 1 (HSV1)	α	Gruter, 1924
Human HV 2	HHV-2	Herpes simplex virus 2 (HSV2)	α	Schneweis, 1962
Human HV 3	HHV-3	Varicella-zoster virus (VZV)	α	Dumas et al., 1980
Human HV 4	HHV-4	Epstein-Barr virus (EBV)	γ	Epstein et al., 1965
Human HV 5	HHV-5	Cytomegalovirus (CMV)	β	Smith, 1956
Human HV 6	HHV-6 A/B	HHV-6 variant A/B	β	Lindquester & Pellett, 1991
Human HV 7	HHV-7		β	Frenkel et al., 1990
Human HV 8	HHV-8	Kaposi's sarcoma-associated HV (KSHV)	γ	Chang et al., 1994

Tab. 1.1 Human herpesviruses (HHV). Modified from Pellett & Roizman, 2006.

Alphaherpesvirinae

They have a broad host range, a short replication cycle, display rapid spread in cell culture, efficiently destroy infected cells, and establish latency mainly in sensory ganglia.

Betaherpesvirinae

They are species-specific, have a long replication cycle, induce the enlargement of cells (cytomegaly), and establish latency in secretory glands, lymphoreticular cells, kidneys, and other tissues.

Gammaherpesvirinae

They have a limited host range, replicate in lymphoblastoid cells or in some cases in epithelioid and fibroblastic cells. Viruses of this subfamily are mainly specific for T or B lymphocytes, and establish latency in lymphoid tissues.

(summarized from Pellett & Roizman, 2006)

1.1.2 Genetics and Propagation

The DNA genome of wild-type (WT) human CMV (hCMV) comprises ~230kbp in length (Dolan et al., 2004), which also accounts for murine CMV (mCMV) (Rawlinson et al., 1996). The genomes encode ~165-200 or ~170 open reading frames (ORF), in the case of hCMV (Dolan et al., 2004; Novotny et al., 2001) or mCMV (Rawlinson et al., 1996), respectively, most of which have so far unknown functions. Among the betaherpesvirus genomes, only 70 protein-coding regions of hCMV have been reported to be conserved, including 40 core functions common to all mammalian herpesviruses (Davison et al., 2006).

In the natural host, hCMV is able to replicate in various cell types, but most studies have been performed in fibroblasts, endothelial cells, and monocytes/macrophages with the use of laboratory strains that have been adapted to this situation. Independent of cell type or virus strain, gene expression is carried out in a coordinately regulated manner during productive infection (summarized from Mocarski et al., 2006). Consecutively, immediate-early (*ie*), early (*e*), and late (*l*) genes are transcribed in the corresponding phase (Emery & Griffiths, 1990; Honess & Roizman, 1974). In hCMV, the genes *ie1* and *ie2*, in mCMV *ie1*, *ie2*, and *ie3*, comprise the major IE (MIE) locus, which is transcriptionally regulated by the MIE promoter (MIEP) and MIEP enhancer (MIEPE) (Stenberg et al., 1984; overview in Meier & Stinski, 2006). The IE phase starts directly after nuclear entry of the viral DNA. The E phase is induced by the *ie* gene products (Bühler et al., 1990; Keil et al., 1984) 1.5h (mCMV) or 4-24h (hCMV) after infection and results in the expression of *e* genes. The corresponding gene products are necessary for viral replication, which is carried out according to the principle of rolling circle, producing concatenates that are later cleaved (Marks & Spector, 1988). Meanwhile, the L phase starts, generating mainly structural proteins, which are required for the assembly of the virus particles (summarized from Mocarski et al., 2006).

The infectious cycle in cell culture, including infection, gene expression, replication, morphogenesis, and release, takes ~24h in the case of mCMV and ~72h in the case of hCMV.

1.1.3 Epidemiology

CMV is ubiquitiously distributed among human populations. The prevalence of infection varies depending on age, occupation, place of residence, sex, and socioeconomic status. For instance, in central Europe studies have reported a prevalence of ~50% in adults (summarized from Mocarski et al., 2007).

CMV is transmitted by direct contact with body fluids containing infectious virus, such as cervical secretions, saliva, semen, tears, and urine. Horizontal transmission is reported to occur mainly by intense contact with young children particularly at home and in day care centers, or by sexual activity. Moreover, CMV can be transmitted vertically from mother to fetus or newborn either transplacental, intrapartum, or by breast feeding. Vertical transmission is a characteristic feature of CMV (summarized from Mocarski et al., 2007). Intrauterine transmission can occur both after primary or recurrent infection of the mother (Boppana et al., 2001; reviewed in Kenneson & Cannon, 2007).

1.1.4 Clinical Features

In the immune-competent host the acquired CMV infection proceeds inapparently. However, sometimes the initial CMV infection manifests clinically as mononucleosis, with fever, fatigue, malaise, myalgia, or lymphocytosis among other possible features.

Congenital CMV infection clinically manifests in the CNS (microcephaly, seizures, generalized hypotonia, lethargy), organs (hepatitis with jaundice, hepatosplenomegaly), and blood system (petechiae, thrombocytopenia), and often leads to life-long neurological sequelae (deafness, blindness, mental retardation).

In the immunocompromised host, primary infection, re-infection, or reactivation from latency all result in a clinically evident infection. In this context, transfusion or transplantation can be the cause of infection. Most severe infections have been reported for patients with acquired immune deficiency syndrome (AIDS) and low counts of CD4 T cells, or recipients of allogeneic stem-cell transplants or organ transplants, but also for patients receiving chemotherapy, and in the case of congenital immune deficiency. Among the direct manifestations are pneumonitis, esophagitis, gastritis, enterocolitis, hepatitis, and retinitis, whereas often indirect effects occur, such as opportunistic infection, and impaired graft function in the case of transplantation.

(chapter summarized from Mocarski et al., 2007)

1.1.5 The Murine Model of CMV Infection

The host-species specificity of CMVs with regard to viral replication requires the establishment of suitable animal models to study common principles of CMV infections paradigmatically. The murine model, mCMV, provides comparability due to structural, biological, and genetic similarities to hCMV (Rawlinson et al., 1996), and has been applied particularly in studies on immune surveillance (Reddehase, 2002). Pathogenesis and clinical manifestations during infection with mCMV in the immune-competent or immune-deficient host have been reported to be similar to hCMV infection (Krmpotić et al., 2003). Moreover, immune control of CMV infection has been reported to be carried out under similar kinetics, with CD8 T cells adopting a major role (Reddehase, 2002). In this respect, the mouse model has been used for experimental antiviral cytoimmunotherapy of mCMV infections (Holtappels et al., 2008a; Reddehase et al., 1985). Accordingly, clinical trials of CD8 T-cell-based immunotherapy in humans have been successfully used to reduce post-transplantation CMV disease (Cobbold et al., 1995; Riddell et al., 1992). Furthermore, the murine model has been used extensively for the study of the immune-modulatory function of certain viral proteins. Both mCMV and hCMV encode proteins that interact with components of the innate and adaptive immune response, having related functions in this respect without sharing sequence homology (Reddehase, 2002). Taken together, this experimental model offers the possibility to genetically modify viruses and hosts, which is important to investigate the function of viral genes *in vitro* and *in vivo*, on the basis of immunological characteristics of the host.

1.2 Immune Response to CMV Infection

The immunological control of CMV infection is achieved by components of the innate and adaptive immune system (Paludan et al., 2011; Reddehase, 2002). Type I interferons (IFN) and natural killer (NK) cells adopt major roles in the early containment of CMV infection, as being part of the innate immune response (Arase et al., 2002; Biron et al., 1989; Bukowski et al., 1984; Hwang et al., 1995; Salazar-Mather et al., 2002). However, NK cells were shown to be unable to control mCMV infection in the long run (Welsh et al., 2001). This task is taken on by CD8 T cells, which are among the major components of the adaptive immune response, together with antibody-producing B cells, which have been shown to play a subordinate role in the control of primary CMV infection, but restrict virus dissemination after recurrent infection (Jonjić et al., 1994; Reddehase et al., 1994).

1.2.1 The Innate Immune Response to CMV Infection

Recognition of pathogen invasion, including viruses, into the cells relies on germ-line encoded pattern-recognition receptors (PRR), which specifically detect conserved

structures of pathogens (pathogen associated molecular patterns = PAMP), and induce downstream signal transduction for the antiviral response (Akira et al., 2001; Janeway & Medzhitov; 2002; reviewed in Kawai & Akira, 2010).

Toll-like receptors (TLR) are transmembrane proteins residing in various cellular compartments such as the plasma membrane or intracellular vesicles (endoplasmic reticulum (ER), endosomes, lysosomes, and endolysosomes) (Akira et al., 2006; reviewed in Kawai & Akira, 2010). In general, plasma-membrane resident TLR bind hydrophobic PAMP ligands, such as lipids, lipoproteins, and proteins, whereas endosome-resident TLR recognize nucleic acids, all of which are derived from bacteria, fungi, parasites, or viruses (reviewed in Paludan et al., 2011; see Fig. 1.1).

The selective recruitment of adaptor molecules by each TLR determines the distinct pattern of gene induction, and hence the immunological reaction. Thus far, 10 and 12 functional TLR have been identified in humans and mice, respectively (reviewed in Kawai & Akira, 2010).

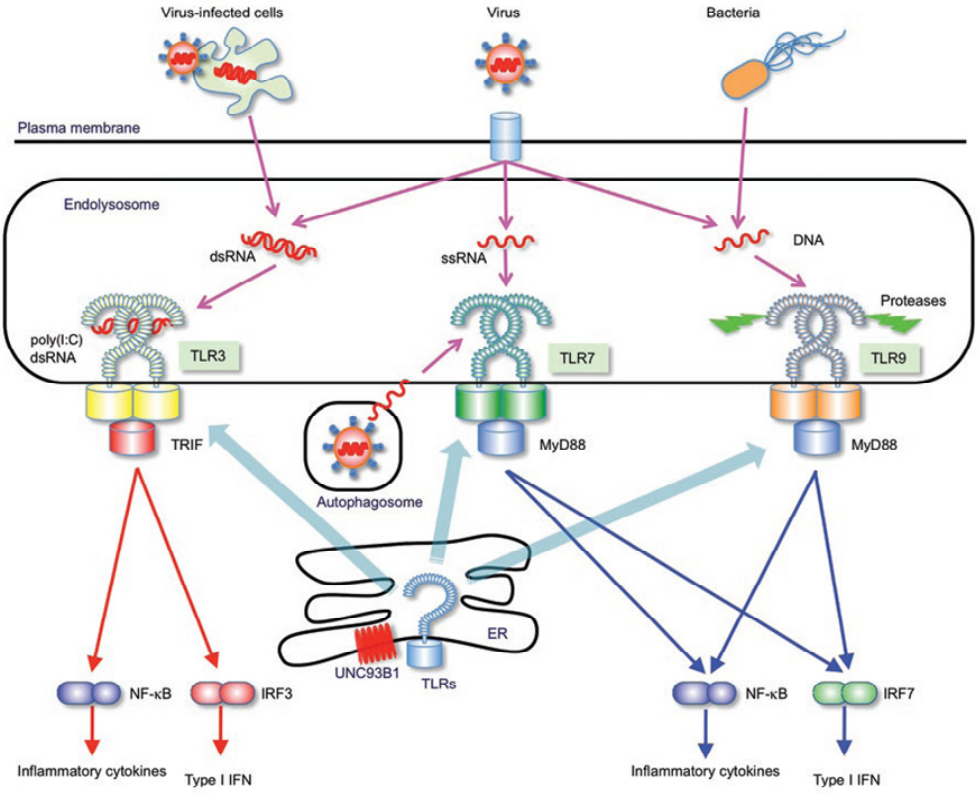

Fig. 1.1 PAMP recognition by intracellular TLR. Reproduced from Kawai & Akira (2010) with permission from the Nature Publishing Group under license number 2831410897136. ER: endoplasmic reticulum. MyD88: Myeloid differentiation primary response gene 88. TRIF: TIR-domain-containing adapter inducing interferon-β.

In addition, cytosolic PRR have been discovered, such as the retinoic-acid-inducible gene I (RIG I)-like receptors (RLR), which detect RNA viruses, and the nucleotide-binding oligomerization domain (NOD)-like receptors (NLR), responding to a variety of PAMP,

non-PAMP, and cellular stress. Furthermore, so-far unidentified PRR have been reported to recognize double-stranded (ds) DNA that triggers type I IFN production (reviewed in Kawai & Akira, 2010; reviewed in Stetson & Medzhitov, 2006), which depends on the activation of IFN regulatory factors (IRF) in the case of IFNα, and on IRF and nuclear factor kappa-light-chain-enhancer of activated B-cells (NF-κB) in the case of IFNβ (reviewed in Honda et al., 2006).

In the specific case of hCMV and mCMV, viral DNA, proteins, and RNA of both are recognized by various PRR (Tab. 1.2).

PRR	Location	Virus	Proposed PAMP	Reference
TLR1	Cell surface	hCMV	gB and/or gH	Boehme et al., 2006
TLR2	Cell surface	hCMV mCMV	gB and/or gH	Boehme et al., 2006 Szomolanyi-Tsuda et al., 2006
TLR3	Intracellular vesicles	mCMV	dsRNA	Tabeta et al., 2004
TLR7	Intracellular vesicles	mCMV	ssRNA	Zucchini et al., 2008
TLR9	Intracellular vesicles	hCMV mCMV	Genomic DNA	Varani et al., 2007 Tabeta et al., 2004 Krug et al., 2004
DAI	Cytosol	hCMV	Genomic DNA	DeFilippis et al., 2010
AIM2	Cytosol	mCMV	Genomic DNA	Rathinam et al., 2010

Tab. 1.2 PRR and PAMP in the innate recognition of CMV. Modified from Paludan et al., 2011. AIM-2: absence in melanoma 2. DAI: DNA-dependent activator of IFN-regulatory factor.

In this context, the attachment of viral glycoproteins of hCMV to the cell surface is sensed by TLR2 probably in complex with TLR1 (Boehme et al., 2006), which leads to downstream activation of NF-κB and proinflammatory cytokines (reviewed in Paludan et al., 2011; Wang et al., 2005). In the case of mCMV infection, studies from TLR2 knock-out mice have reported elevated viral loads in the spleen and liver, which are associated with a reduced activation of NK cells (Szomolanyi-Tsuda et al., 2006). In this respect, it could be shown later that viral ligands, including ligands of mCMV, are selectively recognized by TLR2 on inflammatory monocytes, and induce type I IFN production (Barbalat et al., 2009).

In the case of TLR3, dsRNA structures of mCMV can function as agonists (Tabeta et al., 2004). Studies from TLR3-deficient mice infected with mCMV have demonstrated increased viral loads in the spleen, and reduced serum-cytokine levels, but no difference in survival as compared to WT mice. Moreover, TLR3 signaling was shown to augment

cross-presentation by DC thereby stimulating an increased cross-priming response of CTL (Schulz et al., 2005).

TLR7, expressed in plasmacytoid (p)DC, senses ssRNA after mCMV infection, and mounts an IFNα response. Mice deficient in TLR7 were shown to be more susceptible to mCMV infection as compared to WT mice (Zucchini et al., 2008).

TLR9 recognizes genomic DNA of both hCMV and mCMV in endosomes (Krug et al., 2004; Tabeta et al., 2004; Varani et al., 2007). TLR9 expression in humans is restricted to B cells and pDC, whereas in mice it is expressed in a wide range of cells (Mogensen, 2009; Takeuchi & Akira, 2010). Recognition by TLR9 leads to downstream activation of IRF7, thereby inducing type I IFN expression in pDC. TLR9-deficient mice were shown to be more susceptible to mCMV infection, which might in part be due to an impaired IFNγ production by NK cells (Delale et al., 2005).

With regard to the cytosolic PRR, it has been shown that transfection of hCMV DNA into fibroblasts induces IFNβ production independent of TLR signaling (Ishii et al., 2006), and that this effect is mediated by DNA-dependent activator of IFN-regulatory factor (DAI) (DeFilippis et al., 2010).

IRF have been described as being the major regulators of pathogen recognition and initiation of the innate immune response by TLR and cytosolic PRR (Honda & Taniguchi, 2006). The IRF constitute a family of 9 members in humans and mice, which are ubiquitously expressed, except for the hematopoietic cell restricted IRF-4 and IRF-8 (Mamane et al., 1999; Sato et al., 2001; Taniguchi et al., 2001). In addition, viral members of this family have also been described for HHV-8 (Li et al., 1998; Moore et al., 1996; Zimring et al., 1998). The first two cellular IRF had been identified in studies investigating type I IFN gene regulation, and were termed IRF-1 and IRF-2. These factors were demonstrated to be `*trans*-acting factors´ with IRF-1 activating type I IFN gene expression and IRF-2 repressing the effect through direct competition for binding to the common motif (Fujita et al., 1988 & 1989; Harada et al., 1989; Tanaka et al., 1993). Subsequently, homologous factors had been identified, all containing a well-conserved N-terminal DNA-binding domain (DBD) with five tryptophan-rich repeats, which forms a helix-turn-helix domain that recognizes defined consensus DNA sequences present in enhancers and promoters of type I IFN genes and IFN-stimulated genes (ISG) (Honda & Taniguchi, 2006; preceding review by Nguyen et al., 1997; Sato et al., 2001; Taniguchi et al., 2001). The C-terminal region of IRF however, is less well conserved and has been described to direct interactions with other TF and coactivators (reviewed in Savitsky et al., 2010). In the beginning, sequences responsive to IFN had been identified in various ISG (overview in

Taniguchi et al., 1993), and were termed IFN stimulated response element (ISRE), with the consensus sequence:

ISRE 5`A/G NGAAANNGAAACT 3´ (Darnell et al., 1994) (N denotes any nucleotide).

The recognition sequence of IRF-1 and IRF-2, which resides in the promoters of genes encoding IFNα and IFNβ, and in various ISG (e.g. those encoding H-2D^d and β_2-microglobulin) was termed IRF element (IRF-E, here referred to as IRFE), defined by the following consensus sequence:

IRFE 5` G(A)AAA G/C T/C GAAA G/C T/C 3´ (Taniguchi et al., 1993).

The expression of the IRF has been shown to be inducible by virus and IFN, whose expression in turn is regulated by IRF (Fujita et al., 1989; Harada et al., 1989; Myamoto et al., 1988). With respect to CMV, so far IRF-3 has been shown to be induced by hCMV (Preston et al., 2001) and mCMV (Navarro et al., 1998) infection. The function of the IRF, as being transcription factors (TF), depends on the target gene, cell type, nature of stimulus, modification, stability, and interaction with other TF (Taniguchi et al., 2001; Tijan & Maniatis, 1994). In this respect, their functional diversity ranges from regulation of the immune response and immune-cell development, to regulation of cell growth and apoptosis (reviewed in Savitsky et al., 2010). An overview of the functions in the innate immune response of selected IRF is given in table 1.3.

IRF	Role in Immune Responses
IRF-1	Stimulates expression of IFN & ISG Enhances TLR signaling by binding to MyD88
IRF-2	Attenuates type I IFN response by antagonizing IRF-1 & IRF-9 In some cases cooperates with IRF-1 to activate transcription
IRF-3	Induces type I IFN and chemokines upon virus infection Stimulates TLR and cytosolic PRR signaling
IRF-5	Induces type I IFN upon virus infection Binds to MyD88 and positively regulates TLR-dependent induction of proinflammatory cytokines
IRF-7	Induces type I IFN upon virus infection Binds to MyD88 and induces type I IFN upon TLR signaling
IRF-9	Binds to STAT1 and STAT2 to form ISGF3 and stimulates type I ISG via ISRE

Table 1.3 Role of IRF in immune response and immune-cell development. Modified from Savitsky et al., 2010. ISGF3: IFN-stimulated gene factor 3.

As mentioned above, IRF play a crucial role in the induction of type I IFN genes via the IRFE, with IRF-1, IRF-3, IRF-5, and IRF-7 being positive regulators (reviewed in Mamane et al., 1994, Taniguchi et al., 2001). However, only IRF-3 and IRF-7 have been shown in studies from knock-out mice to be essential for the induction of IFNα and IFNβ in virus-infected cells (reviewed in Honda & Taniguchi, 2006; reviewed in Sato et al., 2001; see

Fig. 1.2). IRF-3 is constitutively expressed and resides in the cytoplasm in an inactive form until virus infection triggers (via TLR3 signaling) its phosphorylation and nuclear translocation, where it binds to the IRFE in the *IFNβ* promoter to induce mRNA expression. (Kawai & Akira, 2010; see Fig 1.1). IRF-7 is expressed at low levels in most cell types, but is induced by IFNα and IFNβ through binding of IRF-9 to its promoter. Newly produced IRF-7 can then induce type I IFN gene expression, which provides a positive feedback regulation of type I IFN production (Marié et al., 1998; Sato et al., 1998a; Sato et al., 1998b, reviewed in Sato et al., 2001; Yoneyama et al., 1998). In pDC, IRF-7 is constitutively expressed but upon ligation of TLR7 or TLR9 to their corresponding ligands, the adaptor molecule MyD88 along with other factors is recruited and activates IRF-7. Thereby, a multiprotein complex is formed, which induces phosphorylation of IRF-7 and its subsequent translocation to the nucleus to induce type I IFN gene expression (Kawai & Akira, 2010; see Fig. 1.1).

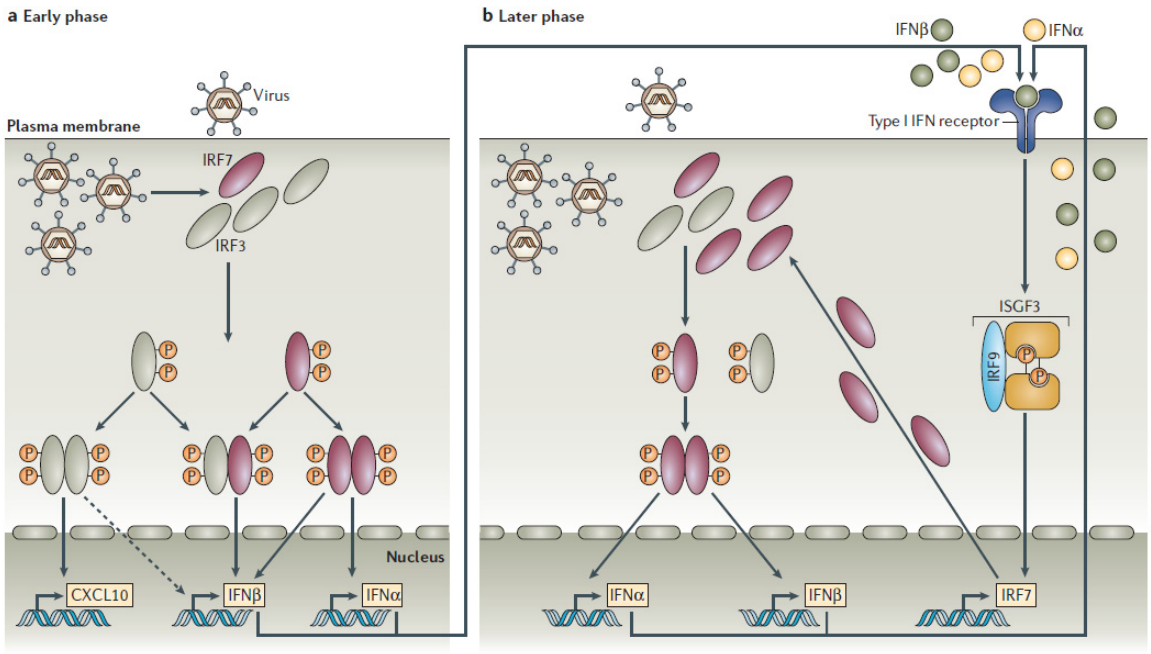

Fig. 1.2 IRF in positive-feedback regulation of type I interferon genes. Reproduced from Honda & Taniguchi, 2006, with permission from the Nature Publishing Group under license number 2831411086428. **a** | In the early phase of virus infection, IRF-3 and -7 are phosphorylated and dimerized, which leads to their translocation to the nucleus and induction of gene expression. CXCL10: CXC-chemokine ligand 10. **b** | Secreted IFN bind and activate the type I IFN receptor (IFNAR) in an autocrine or paracrine manner. This results in downstream activation of ISGF3, which translocates to the nucleus and induces transcription of the *IRF-7* gene. Activation of newly synthesized IRF-7, following recognition of viral nucleic acids by PRR, leads to the expression of large amounts of IFNβ and many of the IFNα proteins (positive-feedback loop).

In the context of gene regulation by IRF, another murine TF termed B lymphocyte-induced maturation protein (**Blimp**)**-1** has been shown to selectively compete with IRF-1 and IRF-2

for binding sites containing the GAAAG sequence, and that the consensus sequence of the transcriptional repressor Blimp-1 (5´ A/C AG T/C GAAAG T/C G/T 3´) is very similar to both the IRFE (matching bases are underlined) and ISRE (Kuo & Calame, 2004). Initially, this TF had been discovered and reported to 'drive the maturation of B lymphocytes into immunoglobulin-secreting plasma cells' (reviewed in Calame, 2010; Turner et al., 1994), and had been reported to be a homolog of the human transcriptional repressor positive regulatory domain (PRD)I-binding factor (BF)1 (Huang, 1994; Keller & Maniatis, 1991). Later, Blimp-1 was demonstrated to also play a 'dominant opposing' role by repressing the MHC class I antigen-presentation pathway (Doody et al., 2007).

IFN were originally identified as a 'substance that protects cells from viral infection' (Isaacs & Lindenmann, 1957). A variety of stimuli induces the secretion of these antiviral proteins from cells (Pestka et al., 1987). Today, they are well-known not only for their antiviral properties (Levy & García-Sastre, 2001; reviewed in Samuel, 2001), but also for their regulatory role in cell growth (Grandér et al., 1997), and their immune-modulatory effects (Biron, 2001). Moreover, their functions, such as induction of MHC class I gene expression (Bukowski et al., 1985; Israel et al., 1986; Korber et al., 1988; Sugita et al., 1987) and activation of NK-cell cytotoxicity (Biron et al., 1996 & 1999), provide a link between innate and adaptive immune responses (Biron, 2001). Two main types of IFN have been described in humans and mice. Type I IFN consists, among others, of IFNβ (single gene), which is expressed by almost all nucleated cells and particularly by fibroblasts, as well as of different species of IFNα (multigene family), which are mainly expressed in leukocytes but can also be induced by IFNβ in fibroblasts (Erlandsson et al., 1998; reviewed in Taniguchi & Takaoka, 2001; Zimmermann & Hengel, 2006). The structurally unrelated type II IFN consists only of IFNγ, which is produced in response to virus-infected cells by certain immune cells, including NK cells, CD4 T cells (T_H1) and CD8 T cells (reviewed in Taniguchi & Takaoka, 2001; Zimmermann & Hengel, 2006). Studies from IFNα/β and IFNγ receptor knock-out mice (IFNAR-/- and IFNGR-/-, respectively), where transmission of the IFN signal is abrogated, have disclosed the necessity and non-redundance of these cytokines for the antiviral immune response (Hwang et al., 1995; Müller et al., 1994), and in particular for mCMV infection (Gil et al., 2001; Presti et al., 1998). IFNα and IFNβ are constitutively produced in cells at very low levels (Gresser, 1990). This has been shown to enhance the cellular responsiveness to these cytokines and stimulate an amplified type I IFN production as well as responses to other cytokines (Sato et al., 2000; Taniguchi & Takaoka, 2001). Moreover, this weak constitutive IFNα/β signaling was demonstrated to be crucial for the cross-talk between type I and type II IFN

signaling (Gough et al., 2010; Takaoka et al., 2000). Binding of IFN to its receptor induces a signal-transduction pathway to the nucleus (Fig. 1.3).

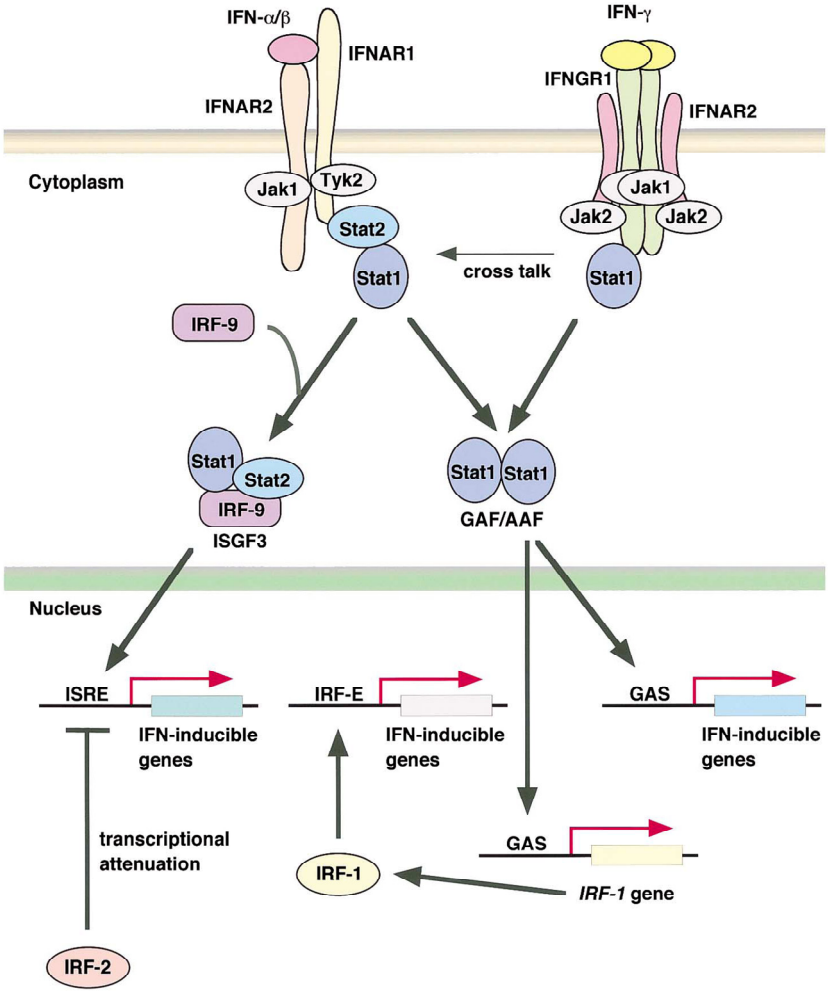

Fig. 1.3 Signal transduction and transcriptional regulation in IFNα/β and IFNγ. Reproduced from Sato et al, 2001, with permission from Elsevier under license number 2831411310344. Jak: Janus-kinase. Tyk2: tyrosine kinase 2. AAF: IFNα activated factor. GAF: IFNγ activated factor. Stat: signal transducer and activator of transcription. GAS: IFNγ activated sequence.

In detail, binding of type I and type II IFN to the corresponding receptor IFNAR1 or IFNAR2 and IFNGR1 or IFNGR2, respectively, results in complex formation at the cell surface. Thereby, receptor-associated Janus kinases (Jak) are activated, which in turn phosphorylate signal transducers and activators of transcription (STAT) 1 and STAT 2. These are converted to their transcriptionally active form either by homodimerization (STAT1) to form the IFNα activated factor (AAF) / IFNγ activated factor (GAF), or by heterodimerization (STAT1 & STAT2) and binding of IRF-9 to form ISGF3. These TF translocate to the nucleus and bind to their target genes via the IFNγ activated site (GAS) or the ISRE, respectively (Darnell et al., 1994; Sato et al., 2001; reviewed in Stark et al., 1998). Induction of the ISG, which mainly encode antiviral proteins, is crucial for the antiviral effect of IFN. One of the best-studied genes is that of dsRNA-activated

serine/threonine protein kinase (PKR) (Meurs et al., 1990), which, in its activated form, can inhibit the process of transcription and translation, and thereby prevent virus replication and generation of virus progeny. Hence, it is not surprising that PKR is a common target of immune modulation by viruses (reviewed in Katze et al., 2002). Other ISG, for instance, encode the 2´,5´oligoadenylate cyclase (OAS) and RNaseL, which are responsible for mRNA degradation.

Regarding the viral host, type I IFN gene induction by virus infection is temporally regulated, which results in a biphasic response. In the early phase, at ~6-8h p.i. (i.p.), systemic type I IFN is mainly produced by splenic stromal cells (accounts for 80-90% of total IFN levels), and depends on B cells expressing lymphotoxin (LT)$\alpha\beta$, a ligand for the LTβ receptor (Schneider et al., 2008). Moreover, as mentioned above (Fig. 1.2), constitutively expressed IRF-3 can induce early IFNβ expression when activated by virus entry into the cells via TLR. At a later stage, at ~36h p.i., splenic and systemic type I IFN have been reported to be produced mainly by splenic pDC in a TLR9/MyD88-dependent manner (Krug et al., 2004; reviewed in Loewendorf & Benedict, 2010). As mentioned above, the activation of early-endosome resident TLR7 or TLR9 by viral nucleic acids leads to induction of type I IFN production via IRF-7 in pDC (see Fig. 1.1) (reviewed in Gilliet et al., 2008). Furthermore, early-produced IFN via LTβ-receptor signaling or IRF-3 leads to downstream induction of IRF-7 via ISGF3 in the later phase, which constitutes the positive feedback regulation of type I IFN induction (Fig. 1.2). Another mechanism for type I IFN production in the later phase has been reported to be due to CD11b+ DC in a TLR9/MyD88-independent manner (Delale et al., 2005).

With regard to pDC, depletion of this population in mCMV-infected mice has been shown to reduce early type I IFN production and augment viral burden, thereby facilitating the expansion of Ly49H-positive NK cells (Swiecki et al., 2010).

NK cells are another important component of the innate immune system (Biron et al., 1999; Trinchieri et al., 1998). Studies from patients deficient in these lymphocytes have displayed their significance for the immunological control of viral infections (Biron et al., 1989). NK cells express both activating receptors and MHC class I-specific inhibitory receptors (Ortaldo & Young, 2005; Yokoyama et al., 1998). Integration of the signals from both receptor types determines the function of NK cells (Orr et al., 2010; Ortaldo & Young, 2005). Engagement of activating receptors can lead to activation of NK cells, characterized by the release of perforin and granzymes, which mediate target cell lysis, and production of cytokines such as IFNγ (Lanier et al., 2000). This activation can be blocked by co-ligation of inhibitory receptors with MHC class I molecules, which hinders NK cells from attacking ‘self’ (Lanier 2008). NK cells expressing inhibitory receptors are

termed ‘licensed’ and are generally more responsive as compared to the ‘unlicensed’ maturation forms which are rather hyporesponsive (reviewed in Yokoyama & Kim, 2006). Yet, in the case of mcmv infection *in vivo* it has been shown that for the most part ‘unlicensed’ NK cells mediate NK-cell control (Orr et al., 2010). However, if cell surface expression of MHC class I molecules is decreased in response to immune modulation by viruses, such as CMV (see 1.3), this ‘missing-self recognition’ (Kärre et al., 1986) is in favor of the activating signals (Fig. 1.4).

In addition to that, NK cells were shown to be activated by type I IFN and other cytokines (Biron et al., 1996 & 1999).

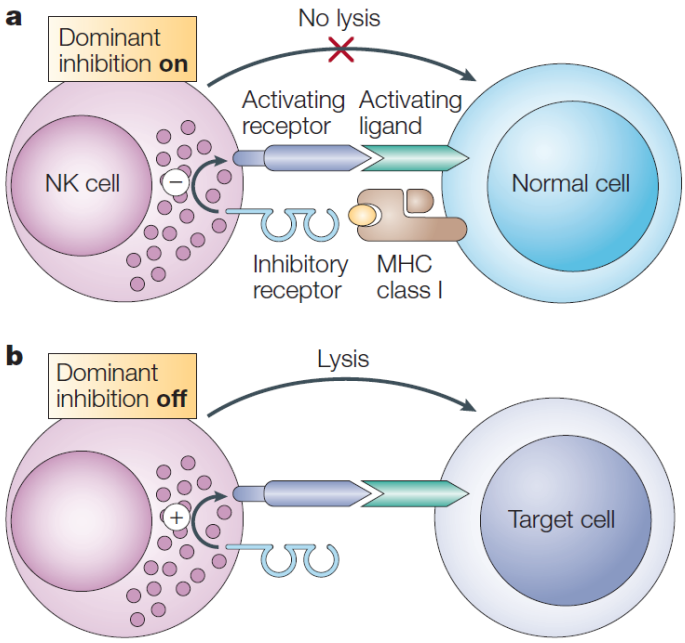

Fig. 1.4 NK cell recognition of target cells. Reproduced from Fauci et al., 2005, with permission from the Nature Publishing Group under license number 2831411441106. NK-cell recognition of target cells is influenced by the level of expression of MHC class I molecules at the cell surface. **a** | In the presence of MHC class I molecules on another cell, inhibitory NK-cell receptors are triggered, leading to the delivery of inhibitory signals, and, consequently, to lack of target-cell lysis. **b** | In the case of virus-infected cells or tumor cells, the cell surface expression of MHC class I molecules is downmodulated, so inhibitory NK-cell receptors are not triggered. Instead, positive signals through activating receptors dominate, which induces lysis of target cells.

Early studies have shown that mCMV infection augments the cytotoxic activity of NK cells (Bancroft et al., 1981). Later studies reported a general connection between viral infection and an increase in NK cell-mediated cytotoxicity, due to their enhanced proliferation and activation (Biron et al., 1983), which was reported to be promoted by type I IFN during mCMV infection (Orange & Biron, 1996). Moreover, a significant NK-cell response to mCMV infection was demonstrated to take place 3-6d p.i. (Quinnan et al., 1982). Experiments investigating the effects of NK-cell depletion demonstrated an enhanced

susceptibility to infection, an increase in virus replication, and higher mortality rates, thereby underlining the significance of the early innate immune control of mCMV infection mediated by these lymphocytes (Bukowski et al., 1983 & 1984). NK cells in the uninfected host have been reported to reside in the splenic red pulp, lymph nodes, and thymus, but not in the liver. In contrast, 2d p.i. (i.p.) with mCMV splenic NK cells are located mainly in lymphoid follicles and the marginal zone, which is the place of type I IFN production (6h-36h p.i.) by splenic stromal cells and pDC (Loewendorf & Benedict, 2010). By 3d p.i., the number of liver NK cells has increased significantly (Dokun et al., 2001).

In early studies, differences in the susceptibility of various mouse strains to mCMV infection had been observed, and were found to correlate with the NK-cell response (Bancroft et al., 1981). Subsequently, this strain-dependent resistance was investigated by genetic analyses, which have attributed this effect to the expression of the activating NK-cell receptor Ly49H (Brown, 2001; Lee, 2001; Scalzo et al., 1990). In mouse strain BALB/c, for instance, Ly49H is not expressed, whereas in strain C57BL/6 it is. In this context, a viral ligand (m157) was identified to bind the activating NK-cell receptor Ly49H. In conclusion, engagement of this ligand confers resistance to mCMV infection of C57BL/6 mice (Arase et al., 2002), and deletion of m157 results in gain of virulence (Bubić et al., 2004). In this respect, previous studies in mCMV-infected C57BL/6 have demonstrated that the activation of NK cells at early time points p.i. is nonspecific, in that IFNγ production at 36h p.i. by splenic NK cells does not correlate with the expression of Ly49H, and proliferation 2d p.i. is not selective for Ly49H+ cells. However, they also demonstrated that by 6d p.i. the number of Ly49H+ NK cells has increased in spleen and liver, which is suggested to be due to the virus-specific NK-cell receptor (Dokun et al., 2001b). In this respect, it is important to consider that the m157-Ly49H ligation, as being an activatory interaction, is particularly important for the effector phase of NK cells.

Another function of NK cells has been revealed to provide a link to adaptive immunity. In this context, the early control of CMV infection by NK cells was reported to be important to reduce the activation of pDC and preserve the compartment of conventional (c)DC, thereby limiting the production of type I IFN to levels being `not immunosuppressive´ and accelerate CD8-T-cell responses against mCMV infection *in vivo* (Robbins et al., 2007).

1.2.2 The Adaptive Immune Response to CMV Infection

CD8 T cells are a major component of the adaptive immune system. Like other T-cell populations, CD8 T cells are characterized by the expression of a T-cell receptor (TCR) on their cell surface. In addition, they express the CD8 coreceptor. Activation of a T cell is achieved by interaction of the TCR with a specific peptide-MHC class I complex and simultaneous interaction of co-stimulatory molecules with ligands on the target cell

(reviewed in Rudolph et al., 2006). This results in the exertion of effector functions, such as production of cytokines (e.g. IFNγ, TNFα), and target cell lysis (Doherty et al., 1993; reviewed in Harty et al., 2000), and in clonal expansion of the T cell. A population of memory-CD8 T cells is maintained in the host, which upon infection migrate to nonlymphoid tissues where they exert their effector functions (Masopust et al., 2001).
The essential role of CD8 T cells with regard to long-term protection from CMV infection has been demonstrated repeatedly. In early studies, the virus specific H-2-restricted CTL response in the mCMV-infected host was shown to be operational at 6-20d p.i. (Quinnan et al; 1978). An early proof of principle was given by an experiment demonstrating that a preemptive T-cell transfer into immunocompromised and mCMV-infected mice results in a protective effect (Reddehase et al., 1985). The antiviral protective capacity of polyclonal CD8 T cells was later confirmed for mCMV-peptide specific cytolytic T lymphocyte lines (CTLL) (Holtappels et al., 2006; Holtappels et al., 2008a), as well as for *ex vivo* isolated peptide-specific CD8 T cells (Böhm et al., 2008a; Pahl-Seibert et al., 2005).
So far, 9 antigenic mCMV-peptides have been identified in haplotype H-2^d, which are recognized by specific CD8 T cells and lead to a protective effect *in vivo* (reviewed in Holtappels et al., 2008a). In haplotype H-2^b, 24 antigenic mCMV-peptides have been described (Munks et al., 2006).

1.3 Immune Modulation by CMV

For herpesviruses to establish acute and persistent viral infection, confronting a vigorous antiviral immune response of the host, evolution of a wide range of counter strategies has been vital, and is a common feature of this virus family (Cloutier & Flamand, 2010; Jaworska et al., 2007; Melroe et al., 2004; Moore et al., 1996; Sen et al., 2010; Taylor & Bresnahan, 2006; Wu et al., 2009). The mechanisms range from avoidance of recognition by PRR and inhibition of IFN signaling to prevent the antiviral state of the cell, to targeting the actions of immune cells (reviewed in Hansen & Bouvier, 2009; Paludan et al., 2010; Reddehase et al., 2002; Tortorella et al., 2000; Yewdell & Hill, 2002).
Thus far, the class of viral proteins exerting these functions have been mostly referred to as immune evasion proteins or `immunoevasins´ (Wagner et al., 2002), or viral regulators of antigen presentation (vRAP). However, the term `evasion´ somehow implies that viruses escape immune surveillance because they cannot be cleared from the host. Yet, infection is kept in check by the competent immune system. Thus, the outcome of infection is determined by the interplay of viral and host factors, and viruses rather modulate than evade immune responses. For that reason, the term immune modulators is used throughout this work for viral proteins carrying out this function, and the process is referred to as immune modulation.

In the case of CMV, both hCMV and mCMV encode various immune-modulatory proteins with related functions, yet without displaying sequence homology of the corresponding genes (Reddehase et al., 2002). The three best-studied immune modulators of mCMV all interfere with the MHC class I peptide-presentation pathway, but the whole range of functions is still not fully understood:

m04 (gp34) is known to form a stable complex with MHC class I molecules and to move to the cell surface (Kavanagh et al., 2001; Kleijnen et al., 1997). This effect appears to prevent NK-cell activation via 'missing-self recognition' (Babić et al., 2010; Kielczewska et al., 2009; reviewed in Lemmermann et al., 2011). In this respect, it could be shown that a decrease in inhibitory signals leads to NK-cell activation via stimulatory receptors (Babić et al., 2010) and that 'unlicensed' NK cells mediated control from mCMV infection *in vivo* (Orr et al., 2010).

m06 (gp48) stably binds MHC class I molecules in the ER and reroutes the complexes to lysosomes for degradation (Reusch et al., 1999).

m152 (gp40) has been described as a major immune modulator of mCMV (Fig. 1.5). It binds transiently to peptide-loaded MHC class I complexes and retains them in the ER-Golgi intermediate compartment (ERGIC) *cis*-Golgi network, thereby preventing peptide presentation at the cell surface (Del Val et al., 1992; Thäle et al., 1995; Ziegler et al., 1997; Ziegler et al., 2000). In this respect, the hCMV protein gp23, encoded by open reading frame (ORF) US3, has been implicated with a similar function. In addition, m152 was shown to exert another function on the innate immune response to infection, namely the downmodulation of RAE-1 (Krmpotić et al., 2002; Lodoen et al., 2003), which is a ligand for the activating NK-cell receptor NKG2D. Thereby, it reduces the number of activating signals and shifts the balance to inhibitory interactions (Lanier 2008; Ortaldo and Young, 2005; Yokoyama et al., 1998). Presumably, this function directly compensates for the negative effect of MHC class I downregulation, which leads to an activation of NK cells via the 'missing-self' axis (Kärre et al., 1986). The importance of m152 for viral replication *in vivo* is demonstrated by the CD8 T-cell- and NK-cell-mediated attenuated phenotype of the ∆m152 deletion mutant (Krmpotić et al., 1999; Slavuljica et al., 2010).

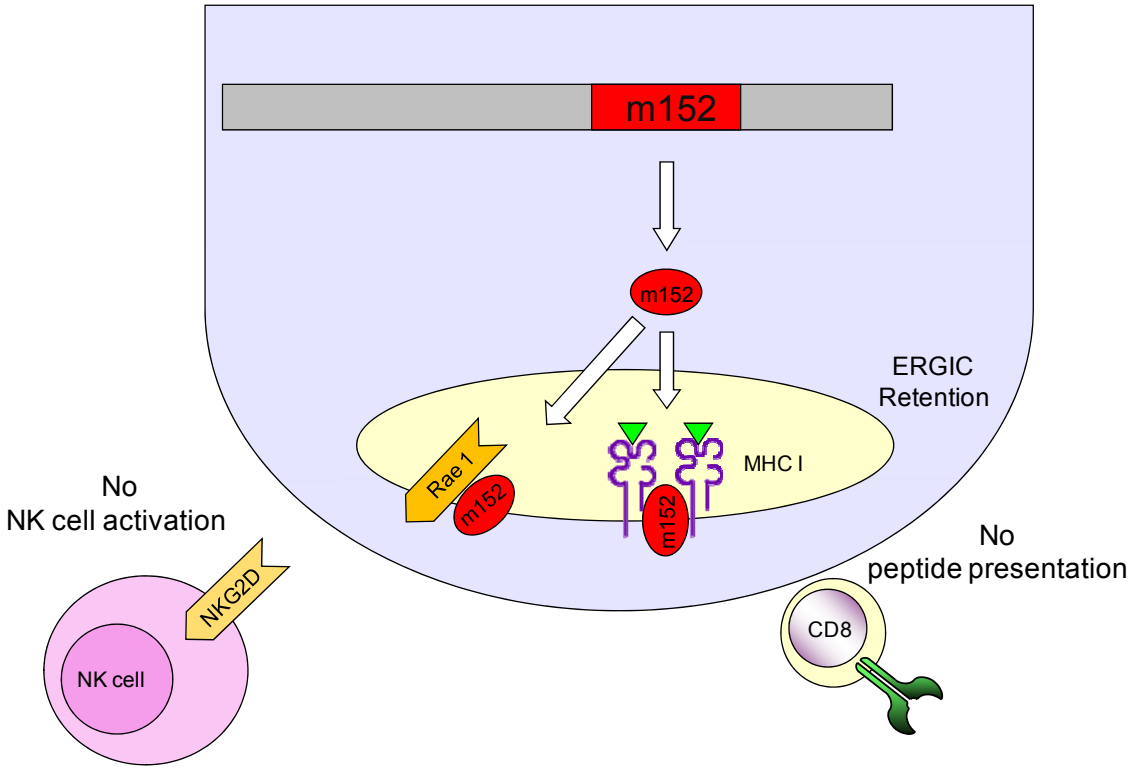

Fig. 1.5 Schematic overview of immune modulation by m152. Gene expression of viral m152 leads to the retention of peptide-loaded MHC class I molecules in the ERGIC, and to downmodulation of RAE-1, thereby preventing both peptide presentation to CD8 T cells and activation of NK cells.

1.4 Main Objective

Immune-modulatory proteins, as being critical for CMV to establish acute and persistent infection, have long been the object of research with the final goal to identify new strategies for antiviral therapy.

In this respect, we have identified here an intriguing connection between the major cytokine of the host´s innate and adaptive immune response, IFN, and the major immune modulator of mCMV, m152: the *m152* promoter region contains an interferon regulatory factor element (IRFE).

The aim of this study was to investigate the importance and the function of this virus-adopted cellular regulatory element on *m152* gene expression, its immune modulatory function, and control of infection in the host.

At first, the conservation of this element and thus its evolutionary relevance for the virus should be figured out by sequence alignments of various established laboratory strains of mCMV and more recent low-passage wild-derived virus isolates, and by analyzing the complete genome of mCMV for the presence of this motif. Then, as a main point of interest the functionality of this element with regard to its influence on *m152* promoter activity and gene expression, should be investigated using various methods. In order to

show the direct effect by selective destruction of the motif a mutant virus and its corresponding revertant were included in the experiments.

As another major focus of the study, the impact of the regulatory element on the immune-modulatory function of m152 should be investigated. In this respect, both the downmodulation of MHC class I molecules and the downmodulation of RAE-1 (see 1.3), and thereby the effect on CD8 T-cell effector function and NK-cell activity, respectively, should be investigated with the final aim to corroborate the results with *in vivo* studies.

2 Materials and Methods

2.1 Materials

2.1.1 General Equipment

Centrifuges	5417 (Eppendorf, Hamburg)
	5417C (Eppendorf, Hamburg)
	5417R (Eppendorf, Hamburg)
	5424 (Eppendorf, Hamburg)
	Labofuge 200 (Heraeus, Hanau)
	Labofuge 400 (Heraeus, Hanau)
	Megafuge 2.0 (Heraeus, Hanau)
	Multifuge 3 S-R (Heraeus, Hanau)
	Multifuge 3 L (Heraeus, Hanau)
	Sorvall Combi Plus (Sorvall, Langenselbold)
	Sorvall RC 5C (Sorvall, Langenselbold)
Flow cytometer	Cytomics FC 500 (Beckman Coulter, Krefeld)
Fluorescence microscope	Axiophot (Carl Zeiss GmbH, Jena)
Gamma-Counter Cobra II	(Packard Canberra, Frankfurt/Main)
Gel documentation	Digit Store (INTAS, Göttingen)
Hybridization oven	OV1 (Biometra, Labotech, Wiesbaden)
Incubator (cells)	B12, B5060 (Heraeus, Hanau)
Incubator (bacteria)	B6, T18 (Heraeus, Hanau)
Irradiator (small animals)	Type OB 58-BA (Buchler, Braunschweig)
Irradiator (cells)	Gammacell 2000 (MØlsgard Medical, Danmark)
Liquid Nitrogen Tank	(Messer, Griesheim)
Luminometer	Lumat LB 9507 (Berthold, Bad Wildungen)
MACS MultiStand	(Miltenyi Biotech, Bergisch Gladbach)
Magnetic stirrer (with heating)	IKA Combimag RET/RCT (Janke & Kunkel, Staufen)
Microscope (cells)	Nikon SE (Nikon, Düsseldorf)
	Olympus CKX31 (Olympus, Hamburg)
	DM IL (Leica, Wetzlar)
Microscope (ELISPOT)	Olympus SZX 12 (Olympus, Hamburg)
Microtome	RM 2255 (Leica, Wetzlar)
Microwave oven	(Privileg, Fürth)
Mixer Mill	MM300 (QIAGEN, Hilden)
Paraffin heater	HistoTAPplus (Leica, Bensheim)

Pipets	(Biohit, Finnland)
	(Eppendorf, Hamburg)
	(Gilson, Villies Le Bel, France)
	Rainin (Mettler Toledo, Oakland, CA, USA)
	(Socorex, Schweiz)
	Pipetboy (INTEGRA Biosciences, Fernwald)
Multichannel pipet	(Socorex, Schweiz), (Abimed, Langenfeld)
Multi dispenser pipet	(Eppendorf, Hamburg) (Gilson, Villies Le Bel, France)
Plate reader	Labsystems Multiskan MS (Thermo Scientific, Langenselbold)
Power supply	EPS 301, EPS 600 (Pharmacia, Erlangen)
	E802 (Consort, Belgium)
Real-Time instrument	ABI 7500 Real-Time PCR System
	(Applied Biosystems, Foster City, CA, USA)
Safety cabinet	HERA safe HS 12/2 and HS 15/2 (Heraeus, Hanau)
Scales	BP 61 (Sartorius, Göttingen)
	UW 2200H (Shimadzu Deutschland GmbH, Duisburg)
Shaker (bacteria)	Certomat MaxQ 4000 (Labotec, Wiesbaden)
	Cellstar (Nunc, Wiesbaden)
Shaker (blots)	ST 5 CAT (neoLab, Heidelberg)
	IKA HS 250 basic (Janke & Kunkel, Staufen)
Shaker (organs)	IKA KS 260 basic (Janke & Kunkel, Staufen)
Spectrophotometer	NanoDrop ND-1000 (PEQLAB, Erlangen)
Table-top sealer	Polystar 244 (Rische + Herfurth GmbH, Hamburg)
Template tamers	Captair bio (Erlab, Köln)
Thermocycler	GenAmp PCR System 9700 (Perkin Elmer, Foster City, USA)
Thermomixer	(Eppendorf, Hamburg)
Tissue Ruptor	(QIAGEN, Hilden, No. 9001272)
Ultraviolet lamp	UVC 30 (Thermo Scientific, Langenselbold)
	UVC-CRL 400 (Umwelt und Technik GmbH, Horb)
UV transilluminator (312nm)	FluoLink (Bachofer, Reutlingen)
	UV Star 30 (Biometra, Göttingen)
Vortexing device	Vortex-Genie 2 (Scientific Industries, USA)
	IKA MS 1 Minishaker (Janke & Kunkel, Staufen)
	IKA VF 2 (Janke & Kunkel, Staufen)
Water bath	(GFL, Burgwedel)

2.1.2 Laboratory Products

Cell culture dishes	60mm (Tube, Becton Dickinson, Heidelberg, No. 353004) 100mm (Tube, Becton Dickinson, Heidelberg, No. 353003) 150mm (Tube, Becton Dickinson, Heidelberg, No. 353025)
Cell culture flasks	25cm^2 (Tube, Becton Dickinson, Heidelberg, No. 353024) 75cm^2 (Tube, Becton Dickinson, Heidelberg, No. 353135)
Cell culture plates (adherent)	6-well plate (Tube, Becton Dickinson, Heidelberg, No. 353046) 24-well plate (Tube, Becton Dickinson, Heidelberg, No. 353047) 48-well plate (Tube, Becton Dickinson, Heidelberg, No. 353078) 96-well plate (Tube, Becton Dickinson, Heidelberg, No. 353072)
Cell culture plates (suspension)	24-well plate (Greiner Bio-One, Nürtingen, No. 662102) 96-well plate (Greiner Bio-One, Nürtingen, No. 650180) 96-well plate (Greiner Bio-One, Nürtingen, No. 650101)
Cell scraper	25cm (Sarstedt, Nümbrecht, No. 83.1830)
Cell strainers	40µm (Tube, Becton Dickinson, Heidelberg, No. 352340) 100µm (Tube, Becton Dickinson, Heidelberg, No. 352360)
Centrifuge tubes	4ml round (Greiner Bio-One, Nürtingen, No. 115261) 15ml conical (Tube, Becton Dickinson, Heidelberg, No. 352096) 50ml conical (Tube, Becton Dickinson, Heidelberg, No. 352070)
Chromatography paper	3MM Chr (Whatman International Ltd., England, No. 3030690)

Counter tubes	6.0x38mm GLKL 0.6ml (Greiner Bio-One, Nürtingen, No. 101101)
Cryo tubes	1.8ml CryoTube Vials (Nalgene Nunc International, Danmark, No. 375418)
ELISPOT plates	96-well plate MultiScreen$_{HTS}$ (Millipore GmbH, Schwalbach, No. MSIPN4550)
Embedding cassettes	Tissue Tek III (Sakura Finetek BV, Zoeterwoude, Netherlands)
FACS tubes	Test tube, 12x75mm (Beckman Coulter, Monheim, No. 2523749)
Luminometer tubes	12x75mm RIA tube (Tube, Becton Dickinson, Heidelberg, No. 2008)
MACS equipment	LS columns (Miltenyi Biotech, Bergisch Gladbach, No. 130-042-401)
Needles	0.40x12mm (Braun, Melsungen, No. 46654062499682) 0.45x12mm (Henke Sass Wolf GmbH, Tuttlingen, No. 65045X2500) 0.90x40mm (Henke Sass Wolf GmbH, Tuttlingen, No. 65090)
Neubauer counting chamber	(LO Laboroptik GmbH, Friedrichsdorf, No. 11022022)
Nylon membrane	(Roche, Mannheim, No. 11417240001)
Poly-allomer centrifuge tube	36ml (Sorvall, Newtown, USA, No. 03141)
Pipet filter tips	Rainin 10µl (Mettler Toledo, Oakland, CA, USA, No. GP-L10F) Rainin 20µl (Mettler Toledo, Oakland, CA, USA, No. GP-L200F) Rainin 1000µl (Mettler Toledo, Oakland, CA, USA, No. GP-L1000F) 20µl (Sarstedt, Nümbrecht, No. 70.760.213) 200µl (Sarstedt, Nümbrecht, No. 70.760.211) 1000µl (Sarstedt, Nümbrecht, No. 70.762.211)
Polypropylene tubes (sterile)	5ml 12.0x75mm (Greiner Bio-One, Nürtingen, No. 115261)
PVDF transfer membrane	Immobilon-FL (Millipore GmbH, Schwalbach, No. IPFL00010)
QIAshredder	250x (QIAGEN, Hilden, No. 79656)

Reaction tubes	1.5ml (Sarstedt, Nümbrecht, No. 72.690)
	2ml Safe Seal (Sarstedt, Nümbrecht, No. 72.695)
Reaction tubes (sterile)	0.5ml Safe Lock (Eppendorf, Hamburg, No. 35325)
	0.5ml (Biozym, Hessisch Oldendorf, No. 710051)
	1.5ml (Biozym, Hessisch Oldendorf, No. 710052)
	2ml (Biozym, Hessisch Oldendorf, No. 710053)
Reaction tubes (PCR)	PCR Strips 1x8 tubes 0.2ml (Greiner Bio-One, Nürtingen, No. 673210)
	Strip Cap for 8 tubes, flat (Greiner Bio-One, Nürtingen, No. 373250)
Scalpels	(Braun, Aesculap AG & Co. KG, Tuttlingen, No. 5518075)
Serological pipets (sterile)	5ml (Greiner Bio-One, Nürtingen, No. 606180)
	10ml (Greiner Bio-One, Nürtingen, No. 607180)
	25ml (Greiner Bio-One, Nürtingen, No. 760180)
Stainless steel beads, 3mm	Wälzlager-Vertrieb Wiesbaden GmbH, Mainz-Kastel
Sterile filter	250ml Stericup Express plus 0.22µm (Millipore GmbH, Schwalbach, No. SCGPU02RE)
	500ml Stericup Express plus 0.22µm (Millipore GmbH, Schwalbach, No. SCGPU05RE)
Syringes	1ml (Braun, Melsungen, No. 916 6017)
	2ml (Braun, Melsungen, No. 460 6027)
	5ml (Becton Dickinson, Heidelberg, No. 309050)
	10ml (Becton Dickinson, Heidelberg, No. 309110)
	20ml (Terumo Europe, Belgium)
	DistriTip Maxi 12.5ml (Gilson, Villies Le Bel, France)
Thermo-cooler racks	(Biozym, Hessisch Oldendorf, No. 733350)

2.1.3 Chemicals

All chemicals and reagents listed below were purchased in p.a. quality unless otherwise noted. For the preparation of buffers and solutions, mainly VE-water (H_2O_{demin}, Millipore, Molsheim, France) or Aqua B. Braun (Braun, Melsungen, No. 0088992) was used. For some preparations, however, aq. dist (*Aqua ad iniectabilia*, Delta Select GmbH, via pharmacy of the University Medical Center) was utilized.

Acetic acid 100% (v/v)	Roth, Karlsruhe, No. 3738.2
Acetone	AppliChem, Darmstadt, No. A1582
Acetonitrile	LGC Promochem, Wesel, No. SO-9128-B025

Agarose (SeaKem LE)	BioWhittaker Molecular Applications, Rockland, ME, USA, No. 840004 (Biozym, Hessisch Oldendorf)
Ammonium nickel (II) sulfate hexahydrate ($NiSO_4x6H_2O$)	Sigma-Aldrich Chemie GmbH, Steinheim, No. 09885
Ammonium persulfate (APS)	Roth, Karlsruhe, No. 9592.2
Ampicillin (Amp)	Roth, Karlsruhe, No. K029.1
Arabinose	Roth, Karlsruhe, No. 5118.2
Bacto agar	Becton Dickinson, Heidelberg, No. 214010
Bacto tryptone	OXOID LTD, Hampshire, England, No. CM0129
Bovine serum albumin (BSA):	
MACS buffer	PAA Laboratories, Pasching, Austria, No. K41-001-500
Histology	Sigma-Aldrich Chemie GmbH, Steinheim, No. A-7906
Brilliant blue R250	Roth, Karlsruhe, No. 9598.1
Bromophenol blue	150µM, Sigma-Aldrich Chemie GmbH, Steinheim, No. B-5525
Chloramphenicol (CAM)	Roth, Karlsruhe, No. 3886.2
^{51}Cr-sodium-chromate ($Na_2{}^{51}CrO_4$)	Perkin Elmer, Zaventem, Belgium, No. NEZ030; 2mCi/0.4ml,
Deoxyribonucleoside triphosphates (dNTPs)	MBI Fermentas, St-Leon-Rot, No. 120192
3,3'-Diaminobenzidine-tetrahydrochloride (DAB)	Sigma-Aldrich Chemie GmbH, Steinheim, No. D 5637
Diethyl pyrocarbonate (DEPC)	Roth, Karlsruhe, No. K028.1
Dimethyl sulfoxide (DMSO)	Merck KGaA, Darmstadt, No. 1.02951.1000
Dithiothreitol (DTT)	Roth, Karlsruhe, No. 6908.2
Entellan	Merck KGaA, Darmstadt, No. 1.07960
Erythrocyte lysis buffer	Sigma-Aldrich Chemie GmbH, Steinheim, No. R7757
Ethanol 100% (v/v)	AppliChem, Darmstadt, No. A1613
Ethidium bromide	Roth, Karlsruhe, No. 2218.1
Ethylenediamine tetraacetic acid disodium salt dihydrate (EDTA)	Roth, Karlsruhe, No. 3619.1
Fluoromount	Sigma-Aldrich Chemie GmbH, Steinheim, No. F-4680
Formaldehyde 37%	Merck KGaA, Darmstadt, No. K31602203302

Glycerol	Roth, Karlsruhe, No. 4043.1
Glycine	Roth, Karlsruhe, No. 3908.2
Hematoxylin	Waldeck GmbH & Co. KG, Division Chroma, Münster, No. 2E 010
HEPES	Roth, Karlsruhe, No. 91054
Hoechst 33342	Invitrogen, USA, No. 43570
Hydrochloride (HCl) 25%	AppliChem, Darmstadt, No. A1434
Hydrogen peroxide 30% (v/v) (H_2O_2)	Roth, Karlsruhe, Rotipuran, No. 8070.1
Isopropanol	Hedinger, Stuttgart, via pharmacy of the University Medical Center, Mainz
Kanamycin (Kan)	Roth, Karlsruhe, No. T832.2
Magnesium chloride ($MgCl_2$)	Roth, Karlsruhe, No. 2189.1
2-Mercaptoethanol (βME)	Roth, Karlsruhe, No. 42271
Methanol	Roth, Karlsruhe, No. 8388.5
Milk powder	Roth, Karlsruhe, No. T145.3
Paraclear®	Quartett GmbH, Berlin, Earth Safe Industries, Inc., No. BP 400301105
Paraffin	Vogel Histo-Comp, Gießen, No. V0-5-1002
Paraformaldehyde (PFA)	Merck KGaA, Darmstadt, No. 4005
Paramount®	BioCyc, Luckenwalde, No. BP-167H
Peroxidase (HRPO)-conjugated streptavidin	Jackson ImmunoResearch Europe Ltd., UK, No. 016-030-084
PolyFect	Qiagen, Hilden, No. 301107
Poly(dA-dT)-Poly(dA-dT) oligonucleotides	Roche, Mannheim, No. 11763000
Potassium chloride (KCl)	Roth, Karlsruhe, No. 6781.1
Potassium dihydrogen phosphate (KH_2PO_4)	Merck KGaA, Darmstadt, No. 4873
Protease inhibitor	Roche, Mannheim, No. 1697498
Restore™ Western Blot Stripping Buffer	Pierce, USA, No. 21059
Rotiphorese® Gel 30 (37.5:1)	Roth, Karlsruhe, No. 3029.1
Sucrose ($C_{12}H_{22}O_{11}$)	Roth, Karlsruhe, No. 4621.1
Sodium acetate trihydrate ($C_2H_3NaO_2x3H_2O$)	Roth, Karlsruhe, No. 6779.2
Sodium carbonate (Na_2CO_3)	Roth, Karlsruhe, No. 8563.1

Sodium chloride (NaCl)	Roth, Karlsruhe, No. 4360.2
Sodium citrate dihydrate ($C_6H_5Na_3O_7x3H_2O$)	Roth, Karlsruhe, No. 3580.1
Sodium dihydrogen phosphate ($NaH_2PO_4xH_2O$)	Roth, Karlsruhe, No. 2370.1
Sodium hydrogen phosphate ($Na_2HPO_4x2H_2O$)	Roth, Karlsruhe, No. P030.2
Sodium dodecyl sulfate (SDS)	Roth, Karlsruhe, No. 4360.1
Sodium hxdroxyde (NaOH)	Roth, Karlsruhe, No. P031.1
Sodium hydrogen carbonate ($NaHCO_3$)	Roth, Karlsruhe, No. 6885.1
Sodium phosphate (Na_3PO_4)	Roth, Karlsruhe, No. 8613.1
Temed	Roth, Karlsruhe, No. 2367.3
Trichloroacetic Acid (CCl_3COOH)	Roth, Karlsruhe, No. 4360.2
Tris(hydroxymethyl)-aminomethane	Roth, Karlsruhe, No. 4360.2
Triton X-100	Roth, Karlsruhe, No. 3051.3
Trypsin	DIFCO Laboratories, Detroit, MI, USA, No. 0152-1
Tween 20	Sigma-Aldrich Chemie GmbH, Steinheim, No. P9416
X-Rhodamin (ROX)	Genova Diagnostics Europe, No. 80-3315-10
Xylene cyanole	Sigma-Aldrich Chemie GmbH, Steinheim, No. X4126
Xylene	Merck, Darmstadt KGaA, No. 1.08685.2500
Yeast extract Servabacter	Serva, Heidelberg, No. 24540

2.1.4 Media and Supplements for Cell Culture

Sterile media were purchased from Gibco-BRL (Invitrogen GmbH, Karlsruhe), stored at 4°C, and supplements listed below were added if necessary. Unless otherwise noted, listed media already contain L-glutamine in the form of L-Glutamax.

DMEM (Dulbecco's Modified Eagle Medium): No. 61965-062

NCS	10% (v/v)
Penicillin	100U/ml
Streptomycin	0.1mg/ml

MEM (Minimum Essential Medium): No. 41090-028

FCS	0.5-10% (v/v)
Penicillin	100U/ml

Streptomycin	0.1mg/ml

MEM 10x (Minimum Essential Medium 10x): No. 21430-20

MEM Alpha (Minimum Essential Medium Alpha): No. 32561-029

FCS	7.5% (v/v)
HEPES	10mM
+/- rh Interleukin-2	200U/ml
β-Mercaptoethanol	$5x10^{-5}$M
Penicillin	100U/ml
Streptomycin	0.1mg/ml

DPBS 1x (Dulbecco's Phosphate-Buffered Saline): No. 14190

NaCl	136mM
KCl	26mM
$Na_2HPO_4x2H_2O$	8mM
KH_2PO_4	1.5mM

RPMI (Roswell Park Memorial Institute): No. 81870-010

Penicillin	100U/ml
Streptomycin	0.1mg/ml
β-Mercaptoethanol	$5x10^{-5}$M
Hepes	10mM
FCS	5% (v/v)

Amphotericin B: This antimycoticum was purchased from Sigma-Aldrich Chemie GmbH (Steinheim, No. A-2411). It was added to culture media for long-term storage of *ex vivo* isolated organs at -80°C to prevent fungal contaminations. The reagent was reconstituted at 1.4mg/ml, apportioned in tubes of 500µl and stored at -20°C. The final concentration used in culture media was 1.4µg/ml.

Fetal Calf Serum/Newborn Calf Serum (FCS/NCS) (v/v): The sterile and mycoplasma-free sera were purchased from PAA Laboratories (Cölbe, No. A15-151/B15-001). They were stored at -20°C. Prior to use, they were thawed at 4°C and subsequently incubated for 30min at 56°C to inactivate factors of the complement system. The heat-inactivated FCS/NCS can be stored at 4°C. Culture media were supplemented with the above mentioned concentrations of these sera.

Geneticin (G418 Sulphate): Geneticin was purchased from Invitrogen (Darmstadt, No. 11811-031). It is an aminoglycoside related to Gentamicin and toxic to prokaryotic and eukaryotic cells. In order to select for geneticin resistant cells it was added to the culture media of P815/B7 cells at a final concentration of 0.176mg/ml.

L-Glutamine: The stock solution (200mM at a final concentration of 29.2mg/ml in 0.85% (w/v) NaCl) was purchased from Gibco-BRL (No. 25030-24). It was apportioned to 5ml tubes and stored at -20°C. For culture media or methyl-cellulose media a final concentration of 20nM was used.

Hepes: The buffer was purchased from Gibco-BRL (No. 15630-056) as 1M stock solution. Its buffering capacity ranges from pH 6.8 to 8.2. It was particularly used in cell culture media of fast growing cells to prevent acidification. The final concentration used therein was 10mM.

Recombinant human interleukin 2 (rh IL-2): This cytokine is a growth and differentiation promoting factor for certain immune cells. It was used at a final concentration of 200U/ml for long time cultivation of CD8 T-cell lines. It was kindly provided by the Sandoz Forschungsinstitut, Vienna (lot. 89050/84802, specific activity 7.3×10^6U/mg).

Recombinant mouse interferon α/β/γ: The cytokines were purchased from PBL interferon source (USA, No. 12100-1/12400-1/12500-1). They were apportioned in separate tubes and stored at -80°C. In cell culture, different amounts and incubation periods were used, as indicated.

β-Mercaptoethanol (β-ME): The reagent was purchased from Sigma-Aldrich Chemie GmbH (No. M7522). It reduces protein disulfide bonds. It was added to some of the cell culture media at a final concentration of 5×10^{-5}M. For this purpose, a stock solution of 100µl β-ME/100ml aq.dist. was prepared and stored at -20°C.

Methyl-cellulose medium: Methyl cellulose was purchased from VWR International GmbH (Darmstadt, No. 25499.182). For media prepared to overlay cell cultures, 8.8g of methyl cellulose were suspended in 360ml aq.dist. and were autoclaved in a 500ml flask together with a magnetic stirring bar. After having cooled off, the methyl cellulose was dissolved by stirring at 4°C and stored at this temperature. Before use in cell culture, the following materials were added:

MEM 10x	40ml

Penicillin	100U/ml
Streptomycin	0.1mg/ml
L-Glutamine	2mM
FCS (v/v)	4%
adjust to pH 7.5 ($NaHCO_3$, stock 55g/l)	

Penicillin/Streptomycin: A Penicillin-Streptomycin antibiotic stock solution (10,000U Penicillin + 10mg/ml Streptomycin in 0.9% (w/v) NaCl) was purchased from Gibco-BRL (No. 15140-122). It was used to supplement cell culture media to prevent contamination with gram positive and gram negative bacteria. The stock solution was stored in 5ml aliquots at -20°C and was added to the culture media at a final concentration of 100U/ml Penicillin and 0.1mg/ml Streptomycin.

Trypan blue: This vital dye (0.5% (w/v) in physiological saline) was purchased from Biochrom AG (Berlin, No. L 6323). It was used at a concentration of 0.1% to count the number of living cells in organ suspensions and cell cultures. Dead cells are permissive for the dye and become stained immediately which can be seen under the light microscope.

Trypsin/EDTA: The solution was purchased from Gibco-BRL (No. 15400-054). It was used for the detachment of adherent cells in a 1:10 dilution with PBS at a final concentration of 0.5g/l trypsin, 0.2g/l EDTA, pH 7.4-7.6.

Türk's solution: The solution was purchased from Merck (Darmstadt, No. 109277). It was used for counting leukocytes in organ suspensions. All nucleus containing cells are stained by the dye whereas erythrocytes are hemolyzed. However, a differentiation between dead and living cells is not possible.

2.1.5 Kits

ABC-POD-Kit	VECTASTAIN Elite ABC-Kit standard, Vector Laboratories Inc., Burlingame, CA, USA, No. PK-6100
APAAP-Complex	Sigma-Aldrich Chemie GmbH, Taufkirchen, No. A 7827
BCA™ Protein Assay Kit	Pierce, USA, No. 23225
DNeasy Blood and Tissue Kit	QIAGEN, Hilden, No. 69506
ECL Plus Western Blotting Detection System	GE Healthcare, UK, No. RPN 2132

Fuchsin+Substrate-Chromogen Kit	DakoCytomation, Hamburg, No. K0625
High Pure Viral Nucleic Acid Kit	Roche, Mannheim, No. 11858874001
HotStar HiFidelity Polymerase	QIAGEN, Hilden, No. 202602
Neufuchsin Kit	DakoCytomation, Hamburg, No. K0624
NucleoBond® PC 500	MACHEREY-NAGEL, Düren, No. 740.574.25
One Step RT-PCR Kit	QIAGEN, Hilden, No. 210212
QuantiTect SYBR Green PCR Kit	QIAGEN, Hilden, No. 204143
RNeasy Mini Kit	QIAGEN, Hilden, No. 74104
Plasmid Maxi Kit	QIAGEN, Hilden, No. 12163

2.1.6 Ladders for DNA, Protein, and RNA

Low Molecular Weight DNA Ladder	New England BioLabs, Frankfurt, No. N3233S
1kb DNA Ladder	Invitrogen, Darmstadt, No. 15615-016
PageRuler™ Prestained Protein Ladder	Fermentas, St-Leon-Rot, No. SM0671
ssRNA Ladder	New England BioLabs, Frankfurt, No. N0362S
RNA Molecular Weight Marker I, DIG-labeled	Roche, Mannheim, No. 11526529910

2.1.7 Enzymes

All enzymatic reactions were carried out under conditions recommended by the particular manufacturer, and with the buffers provided.

DNaseI (RNase free)	QIAGEN, Hilden; No. 79254
HotStar HiFidelity Polymerase Kit	QIAGEN, Hilden; No. 202602
Proteinase K	QIAGEN, Hilden; No. 19133
Taq DNA Polymerase	QIAGEN, Hilden; No. 201205
*Bam*HI	New England BioLabs; No. R0136S
*Dpn*I	New England BioLabs; No. R0176S
*Eco*RI	New England BioLabs; No. R0101L
*Hind*III	New England BioLabs; No. R0104S
I-*Sce*I	New England BioLabs; No. R0694S

2.1.8 Antibodies

Antibody	Clone	Host	Dilution	Source
Western Blot:				
α β-actin	N-210	rabbit	1:500	Santa Cruz

				Biotechnology, USA sc-130656
α-IE1	Croma 101	mouse	1:1,000	Prof. S. Jonjić University of Rijeka
α-m152	3D10	rat	1:250	Helmholtz Zentrum, Munich, Dr. E. Kremmer
α-mouse HRP	polyclonal	rabbit	1:1,0000	DakoCytomation, Denmark, No. P0260
α-rat HRP	polyclonal	rabbit	1:1,0000	DakoCytomation, Denmark, No. P0162
α-rabbit HRP	polyclonal	swine	1:1,0000	DakoCytomation, Denmark, No. P0217
Histology:				
α-IE1	Croma101	mouse	1:250	Prof. S. Jonjić University of Rijeka
α-m152	3D10	rat	1:200	Helmholtz Zentrum, Munich, Dr. E. Kremmer
α-CD3ε	CL CD3-12	mouse, human	1:300	Acris, USA, No. SM1754P
α-mouse (Fab)-biotin	polyclonal	goat	1:200	Sigma, Deisenhofen, No. B0529
α-rat (Fab)-biotin	polyclonal	goat / mouse	1:100	BD Biosciences, No. 554014 / 553880
α-mouse alkaline phosphatase	polyclonal	goat	1:100	AbD Serotec, No. OBT 1172
Normal serum rabbit	polyclonal	rabbit	1:10	Invitrogen Life Technologies, Karlsruhe, No. 16120099
Normal serum goat	polyclonal	goat	1:10	Invitrogen Life Technologies, Karlsruhe, No. 16210064
Normal serum horse	polyclonal	horse	1:10	Invitrogen Life Technologies, Karlsruhe, No. 16050130
APAAP-mouse-complex	polyclonal	rabbit	1:10	Sigma, Deisenhofen, No. A9811
ELISPOT assay:				
α-mouse IFNγ	RMMG-1	rat	5µg/ml	Biosource Europe, Solingen, No. AMC4834
α-mouse IFNγ biotin-labeled	XMG1.2	rat	0.5mg/ml	BD Pharmingen™, Heidelberg, No. 18112D
Flow cytofluorometry:				
α-CD16/CD32 (Fcγ III/II receptor)	2.4G2	rat	1µg/10^6cells	BD Pharmingen™, Heidelberg, No. 553140
α-mouse CD3ε (TC) FITC	145-2C11	hamster	0.5µg/10^6cells	Beckman Coulter, Krefeld, No. 737985A
α-mouse CD335 (NKp46) PE	29A1.4	rat	2.5µg/10^6cells	eBioscience, USA, No. 12-3351-80
α-mouse NKG2D APC	CX5	rat	0.5µg/10^6cells	eBioscience, USA, No. 17-5882-82
α-CD49b/Pan-NK cells FITC	DX5	rat	0.5µg/10^6cells	BD Pharmingen™, Heidelberg, No. 553857
α-mouse CD8α FITC	53-6.7	rat	0.5µg/10^6cells	BD Pharmingen™, Heidelberg, No. 553031

α-mouse TCRβ chain PE	H57-597	hamster	0.5µg/10^6cells	BD Pharmingen™, Heidelberg, No. 553172
PE hamster IgG1,κ	A19-3		0.2µg/10^6cells	BD Pharmingen™, Heidelberg, No. 553972
PE rat IgG1	R3_34		0.2µg/10^6cells	BD Pharmingen™, Heidelberg, No. 554685
FITC rat IgG1	eBRG1		0.2µg/10^6cells	eBioscience, USA, No. 11-4301-85
In vivo depletion:				
α-mouse asialo GM1	polyclonal	rabbit	20µl/mouse	WAKO Chemicals GmbH, Osaka, Japan, No. 986-10001
α-mouse CD8	YTS169.4	mouse	1mg/mouse	Prof. S. Jonjić Univ. of Rijeka
α-mouse NKG2D	C7	hamster	300µg/mouse	Prof. S. Jonjić Univ. of Rijeka
Magnetic Cell Sorting:				
α-mouse CD8a (Ly-2) MicroBeads	-	rat	10µl/10^7cells	Miltenyi Biotech, Bergisch Gladbach, No. 130-049-401

Tab. 2.1 Antibodies.

2.1.9 Laboratory Animals

Mice were bred and housed under specified pathogen free (SPF) conditions in the Central Laboratory Animal Facility (CLAF) of the University Medical Center Mainz. For the experiments, female mice of the inbred strains BALB/c (haplotype H-2^d) and C57BL/6 (haplotype H-2^b) were used. Moreover, the transgenic mouse strain OT1, which expresses SIINFEKL-peptide-specific T cells (Hogquist et al., 1994) was used.
In addition to that, IFNAR-/- knock-out mice (C57BL/6 backpassed) which lack expression of the type I interferon receptor were used (http://www.research.ucla.edu/tech/ucla09-214.htm). These mice were kindly provided by Dr. Z. Waibler, Paul Ehrlich Institut, Langen. All animal experiments were approved according to German federal law under approval number G09-1-004.

2.1.10 Primary Cells and Cell Lines

NIH 3T3 BAM25 (mouse embryonic fibroblasts): This NIH 3T3 cell line is stably transfected with mCMV IE proteins 1 and 3 (Angulo et al., 2000), and was kindly provided by Prof. M. Messerle, Institute for Immunology & Institute for Virology, Hannover Medical School. It was used in this work for the Dual-Luciferase reporter gene assay in order to examine the influence of the IRFE on *m152* expression. Here, the cell line is briefly referred to as BAM25.
Culture medium: DMEM + 10% (v/v) NCS

EL4 (mouse T lymphocyte, C57BL/6, ATCC No. TIB-39™): This cell line (haplotype H-2^b) was used as antigen presenting cell (APC) in an ELISPOT assay investigating mCMV-peptide recognition by memory mCMV-WT.Smith splenic lymphocytes (C57BL/6).
Culture medium: DMEM + 10% (v/v) FCS

MEF (murine embryonic fibroblasts): These primary, adherent cells are permissive to mCMV infection. They were used for *in vitro* reconstitution of mCMV as well as for several cell culture studies. The cells were prepared from 14-17d old embryos of mouse strains BALB/c, C57BL/6, IFNAR-/-. After 3-4d of *in vitro* cultivation, they were conserved in cryo tubes (FCS + 10% DMSO v/v) at -196°C in liquid nitrogen.
Culture medium: MEM + 10% (v/v) FCS

NIH 3T3 (mouse embryonic fibroblasts, ATCC No. CRL-1658): This cell line is known to be transfected easily and was used in this work for the Dual-Luciferase reporter gene assay in order to examine the influence of the IRFE on *m152* expression.
Culture medium: DMEM + 10% (v/v) NCS

P815: This immortalized mouse lymphoblast-like mastocytoma cell line was used as antigen presenting cell (APC) in ELISPOT assay and cytolysis assay. This line was originally isolated from the DBA/2 mouse and obtains the haplotype H-2^d. The cells were cultivated in suspension.
Culture medium: RPMI + 5% (v/v) FCS

P815/B7: This P815 cell line was stably transfected with cDNA for the human CD80/B7-1 molecule (Azuma et al., 1992). It was used for restimulation of H-2^d-restricted T cells. The cell line was kindly provided by Prof. Lanier, Department of Human Immunology, DNAX Research Institute, Palo Alto, USA.
Culture medium: RPMI + 5% (v/v) FCS + 0.167mg/ml G418

2.1.11 Viruses

mCMV-WT.BAC (MW97.01): This chimeric recombinant virus was generated from the genome of laboratory strain Smith as well as in part (*HindIII-E* fragment) from strain K181. After cloning of the whole mCMV genome into a BAC (bacterial artificial chromosome), and subsequent transfection into MEF, the reconstituted virus MW97.01 could be isolated from the supernatant (Messerle & Crnković, 1997; Wagner et al., 1999). *In vivo* experiments with MW97.01 did not display any differences in the biological characteristics in comparison with mCMV-WT.Smith (Wagner et al., 1999). It was kindly provided by Prof. U. H. Koszinowski, Max von Pettenkofer-Institute for Hygene and Microbiology, Munich.

mCMV-WT.Smith (strain Smith, ATCC VR-1399): Mice were infected with this laboratory strain of mCMV and used as CD8 T-cell donors in ELISPOT assays and adoptive transfers.

mCMV-Δm152 & mCMV-Δm152rev: The deletion mutant of the major immune-modulator m152 and its revertant were generated by M. Wagner (Wagner et al., 2002) and kindly provided by Prof. U. H. Koszinowski, Max von Pettenkofer-Institute for Hygene and Microbiology, Munich.

mCMV-Δm157Luc-m164SIINFEKL: This virus was generated in our laboratory. The deletion of m157 facilitates virus replication in the C57BL/6 strain. The K^b-presented antigenic peptide SIINFEKL is expressed in place of the immunodominant viral peptide of the protein m164. This virus was used in an adoptive transfer experiment to infect IFNAR-/- and C57BL/6 (Lemmermann et al., 2010).

mCMV-Δm152m06-m164SIINFEKL: This virus was generated in our laboratory. The K^b-presented antigenic peptide SIINFEKL is expressed in place of the immunodominant viral peptide of the protein m164. Two immune modulators of mCMV, m152 and m06, are deleted. This virus was used in an adoptive transfer experiment to infect IFNAR-/- and C57BL/6 (Lemmermann et al., 2010).

mCMV-mutIRFE & mCMV-mutIRFErev: Our group identified that the *m152* promoter region contains an interferon regulatory factor element (IRFE). The sequence (5'-GAAAGCGAAAGT-3') fully overlaps with the IRFE consensus sequence (5'-G(A)AAA G/C T/C GAAA G/C T/C-3') (Taniguchi et al., 2002). In order to examine the significance of this regulatory element, the mutant virus mCMV-mutIRFE and its revertant were generated (S. Emde & V. Wilhelmi) using the 2-step Tischer recombination. The characteristic adenosins in the consensus IRFE were exchanged by cytosins (5'-GCCCGCGCCCGT-3') to functionally delete the motif. In this work, the influence of this regulatory element of the type I IFN signaling pathway on *m152* gene expression, and the effect on pathogenicity of the mutant virus compared to mCMV-WT virus (mCMV-mutIRFErev), was examined.
Note: Recombinant viruses are in the following briefly referred to as e.g. mCMV-WT.BAC → WT.BAC.

2.1.12 mCMV Peptides

The MHC class I-restricted antigenic mCMV peptides used herein were synthesized by JERINI Biotools GmbH, Berlin. The HPLC-purified peptides were purchased as lyophilisates (~1mg) with 80% purity. They were used for restimulation of mCMV-specific

T cells as wells as for loading of APC in ELISPOT assay and cytolysis assays. The lyophilisates were dissolved in 1% DMSO (or Acetonitril for cysteine-containing peptides) and 99% PBS to yield final concentrations of 10^{-3} or 10^{-4}M. The stocks were stored at -70°C.

ORF	Peptide sequence	MHC I restriction	Reference
Haplotype H-2D^d:			
M105	^{207}TYWPVVSDI^{215}	K^d	Holtappels et al., 2008
m145	^{451}CYYASRTKL^{459}	K^d	Holtappels et al., 2008
m164	^{167}AGPPRYSRI^{175}	D^d	Holtappels et al., 2002a,b
Haplotype H-2D^b:			
M38	^{316}SSPPMFRV^{323}	K^b	Munks et al., 2006a,b
M45	^{985}HGIRNASFI^{993}	D^b	Munks et al., 2006a,b
M57	^{816}SCLEFWQRV^{824}	K^b	Munks et al., 2006b
m139	^{419}TVYGFCLL^{426}	K^b	Munks et al., 2006a,b
m141	^{16}VIDAFSRL^{23}	K^b	Munks et al., 2006a,b
m164	^{150}AGPPRYSRI^{158}	D^b	Munks et al., 2006b
IE3	^{416}RALEYKNL^{423}	K^b	Munks et al., 2006a
OT-1 mice:			
Ovalbumin	257SIINFEKL264	K^b	Rötzschke et al., 1991

Tab. 2.2 Antigenic mCMV peptides. * CTLL= cytolytic T-lymphocyte line.

2.2 Methods

2.2.1 Methods in Cell Culture

In order to avoid contamination of cell cultures with airborne germs (fungal spores, bacteria), work was performed at sterile safety cabinets using sterile glass and plastic ware. The cells were cultivated in CO_2-incubators (37°C, 5% (v/v) CO_2) in 95% (v/v) relative humidity. Under these conditions, the physiological pH of the CO_3^{2-}/HCO_3^--buffered media can be maintained.

2.2.1.1 Preparation of Murine Embryonic Fibroblasts (MEF)

Trypsin/EDTA pH 6.4:	Trypsin		1.25g
	EDTAx2H_2O	3.4mM	1.25g
	Adjust to 1l (aq.dist.), pH 6.4 (1M NaOH), filter sterile		

Primary fibroblasts were isolated (sterile) from 14-17d old embryos. In brief, the embryonic tissue except for inner organs, eyes, and brain was cut with scalpels to a homogenous mass. The tissue was transferred to a sterile flask containing glass beads. It was lysed 3x for 30min with 15ml trypsin/EDTA pH 6.4 + 15ml PBS by stirring at 37°C. Afterwards, the cell suspension was filtered through a metal sieve and centrifuged for 10min at 300xg. The pellet was resuspended in medium and the cell number was determined. The cells (passage 0; 2-3x10^7cells/150mm dish) were cultivated for two days. Afterwards, they were frozen in liquid nitrogen for long-term storage (passage 1; 4 aliquots/150mm dish → 1 aliquot/ 3-4 100mm dishes). Only cells up to passage 3 were used. For a detailed description of the protocol, see Podlech et al., 2002.

2.2.1.2 Cryo-Conservation and Recultivation of Cells

Freezing medium: FCS 90% (v/v)
DMSO 10% (v/v)

Cryo-conservation is the storage of cells at -196°C in liquid nitrogen. For this purpose, cells (1-5x10^6cells/ml) were suspended in 4°C freezing medium, and were then apportioned to cryo tubes (1ml aliquots). The tubes were frozen slowly at -70°C and after 1-2d they were transferred to liquid nitrogen for long-term storage.
In order to recultivate the cells, the aliquots were thawed immediately in the water bath at 37°C. They were suspended in fresh culture medium and washed 2x before further cultivation.

2.2.1.3 Determination of the Cell Number and Viability

The vital dye trypan blue is an acidic anion-dye which binds easily to proteins, and facilitates the discrimination of living cells from dead cells. Dead cells take up trypan blue instantly which leads to a blue stain of the cytoplasm. In contrast, the cell membrane of living cells is impermeable to the dye for 5-10min. However, Türk's solution stains all nucleus-containing cells and is suitable only for the discrimination between lymphocytes and erythrocytes (see 2.1.4).
For the determination of the cell number, a small amount of the cell suspension was mixed in a suitable dilution with the dye, and was pipeted into a Neubauer counting chamber (depth: 0.1mm). Cells per large square (subdivided into 25 small squares) were counted, and the calculation of the cell number per ml was made with the following formula:

$$\text{Cell number/ml} = N/n \times d \times 10^4$$

N = Number of cells counted in all large squares
n = number of large squares counted

d	=	dilution factor
10^4	=	chamber factor

2.2.1.4 Centrifugal Enhancement of Infectivity

Routinely, infection of cell cultures was performed by centrifugal enhancement of infectivity (CEI; Hudson et al., 1976; Kurz et al., 1997). Thereby, the infectivity enhancement factor is ~20. In order to infect cells, the appropriate amount of virus in culture medium was added to the cells (in case of a multiplicity of infection (MOI) of 4 = 0.2 plaque-forming units (PFU) per cell), and cell culture dishes or plates were centrifuged at 760xg for 30min. Thereafter, the cells were further incubated at 37°C.

2.2.2 Virus Reconstitution from BAC Plasmids

Transfection reagent:	PolyFect (QIAGEN)
Culture medium:	MEM + 10% (v/v) FCS

MEF were cultured in 6-well plates to a confluence of ~80%. Graded volumes of BAC DNA (5, 7.5, 10, 15µl) were diluted with MEM in a total volume of 100µl. 15µl PolyFect were added to each sample and the transfection mix was incubated for 10min at ~20°C. Meanwhile, the cells were washed 1x with PBS, and 1.5ml fresh culture medium was pipetted per well. After that, 600µl of the transfection mix was added per well and incubated for 6.5h at 37°C. Thereafter, the transfection supernatant was removed, and the cells were incubated in 3ml fresh culture medium at 37°C for 5-7d. When most cells showed a cytopathic effect (CPE), the supernatants were collected and centrifuged for 5min at 800xg. In order to eliminate the BAC vector sequence, six rounds of passaging in MEF were performed. For the first propagation passage, confluent MEF in 6-well plates were infected with 1ml of the viral supernatant for 30min at 37°C. For all further propagations, 1µl virus supernatant + 999µl culture medium were used for infection. After infection, the cells were incubated in 2ml culture medium at 37°C until 80% showed CPE. All cell-free viral supernatants were stored at -70°C. Mutant virus mutIRFE was generated by a colleague (S. Emde) up to the 3rd propagation on cell cultures (viral supernatant p3). In this work, the supernatant of the 3rd propagation was further propagated as described above. Successful elimination of the BAC vector sequence of both, mutant and revertant virus mutIRFE, was verified by plaque purification and subsequent quantitative real-time PCR (qPCR). For this, confluent MEF were infected with 1µl and 1µl of 1:10 diluted supernatant from p6, as described above. The cultures were covered with 2ml methyl-cellulose medium to prevent formation of secondary plaques. 4d after infection, single plaques were picked with a sterile pipet tip (200µl), and were used to infect MEF for clonal expansion of the virus population. From these cultures, viral DNA was isolated and used

in qPCR (see 2.2.15.8-10). For description of a general protocol for virus reconstitution and propagation, see Lemmermann et al., 2010.

2.2.3 Virus Propagation and Purification

Virus standard buffer (VSB):	Tris	50mM	6.1g
	EDTAx2H_2O	5mM	1.86g
	KCl	12mM	0.895g
	Adjust to 1l (aq.dist.), pH 7.8 with HCl, autoclave		
15% (w/v) sucrose/VSB:	Sucrose	15g	
	Adjust to 100ml with VSB		
Culture medium:	MEM + 10% (v/v) FCS		

The viruses used in this work were propagated on infected BALB/c MEF cultures and purified as described below (for a more detailed protocol, see Podlech et al., 2002).

Infection of MEF: In order to obtain large amounts of purified virus, approximately 50 cell culture dishes (150mm) containing almost confluent monolayers (~1x10^7cells/dish) were infected with 5x10^4-1x10^5 PFU per dish. The MOI was approximately 0.005-0.01 PFU per cell. In detail, the culture medium was removed and the virus was added in a volume of 5ml MEM-FCS. After 30min incubation at 20°C, 20ml medium were added, and the dishes were incubated for 4-5d at 37°C until CPE, rounding and detachment, was visible under the microscope.

Virus purification: Still adherent cells were collected with a cell scraper, and together with the supernatants they were transferred to a 500ml centrifuge tube. All further steps were performed at 4°C or on ice. After 20min centrifugation at 6,400xg, the supernatant was transferred to 250ml centrifuge tubes. The sedimented cells were collected in a low volume of culture medium (~10-20ml), and were homogenized with a Dounce homogenizer. Then, the homogenate was transferred to a 50ml centrifugation tube and centrifuged for 20min at 3,600xg. The supernatant containing the virus particles was pooled with the supernatant from the first centrifugation. By 3h centrifugation at 26,000xg, the virus particles were sedimented so that afterwards the supernatants were discarded carefully and the sediment covered with little medium was stored overnight at 4°C. The next day, the sediment was resuspended in the residual medium, homogenized, and carefully loaded on a 15% (w/v) sucrose/VSB density cushion in 20ml polyallomer ultracentrifugation tubes (ratio sucrose/buffer:virus = 10:1). This was followed by a further centrifugation step for 1h at 53,000xg. The supernatant was discarded, and the pellet (sedimented virus particles) was covered with 2-4ml sucrose/VSB and incubated for 4-12h on ice. Thereafter, the pellet was resuspended carefully with a Pasteur pipet, homogenized again with a Dounce homogenizer, and stored in aliquots of 20-100µl at

-70°C. The virus titer was determined using a standard virus plaque assay (see 2.2.4).
Note: Starting with 50 cell culture dishes, one can expect 3-4ml virus suspension with titers ranging from $5x10^8$-$2x10^9$ PFU/ml. Undiluted aliquots of the virus suspension can be thawed up to 3x without serious change in titer.

2.2.4 Virus Plaque Assay

Culture media: MEM + 10% (v/v) FCS
Methyl-cellulose medium

In general, this assay is used for PFU quantitation in purified virus stocks, supernatants of infected cell cultures, and homogenates of infected cells or organs. By definition, 1 PFU is the amount of virus required to form a single plaque in a monolayer of permissive cells. During plaque formation, infected cells in the center of the plaque are lysed, but they remain surrounded by uninfected cells. This can be visualized as 'gaps' in the monolayer. Methyl-cellulose medium limits virus spread to foci of cells at the sites of initial infection and prevents secondary plaques. For further information, see Podlech et al., 2002.

2.2.4.1 Quantitation of Virus Stocks

For the assay, MEF (BALB/c) of the second passage were cultivated in 48-well plates until complete confluence was achieved. The virus stock was serially diluted with $\log_{10}$ steps (6-8 dilutions) in culture medium. All procedures with virus-containing solutions were performed on ice and with pre-cooled culture medium. Most of the culture medium was removed from the monolayer, and 100µl of each dilution was added. Triplicate cultures were done for each dilution. The culture plates were incubated for 1h at 37°C for virus adsorption and penetration. Afterwards, they were covered with 500µl methyl-cellulose medium per well, and were incubated for 3-4d at 37°C. Finally, the virus plaques were counted under an inverted microscope, for the dilution that gives □10 and □100 plaques, and the titer of the stock solution was calculated as follows:

Virus titer (PFU/ml) = M x D x 10
M= mean value of the plaque no. counted for triplicate cultures
D= dilution factor

2.2.4.2 Quantitation of Virus in Organ Homogenates

Organs of infected mice (BALB/c or C57BL/6) were dissected (sterile) and transferred to 1ml culture medium, containing 1.4µg/ml amphotericin B. The organs were kept at -70°C until further processing. For the assay, the organs were thawed slowly in the water bath and kept on ice. Then, they were passed with the plunger of a 2ml syringe through a steel mesh, and were taken up in 2ml culture medium. After that, $\log_{10}$ dilutions of the

homogenate were prepared in 1ml culture medium, and 100µl were pipetted onto the cell monolayer. Duplicate cultures were done for each dilution. The culture plates were centrifuged at 760xg for 30min. Afterwards, they were covered with 500µl methyl-cellulose medium per well, and were incubated for 4d at 37°C. Finally, the virus plaques were counted under an inverted microscope and the titer of the organ homogenate was calculated (see 2.2.4).
Note that the titer per organ homogenate must be related to the 2ml suspension:

Virus titer (PFU/organ) = M x D x 10 x 2

2.2.5 Viral Replicative Fitness

Newly generated recombinant viruses must be characterized for their ability to replicate in cell culture as well as in the natural host in comparison to WT.BAC virus. Only then is it possible to selectively attribute any phenotype to the introduced mutation. mCMV is controlled very efficiently in the immunocompetent host. For this reason, viral replication is quantitated in the immunocompromised and genetically susceptible murine host (BALB/c). Therein, mCMV shows a very broad cell-type tropism (Podlech et al., 1998). In this work, the recombinant virus mutIRFE was tested for its viral replicative fitness *in vitro* and *in vivo*. For additional information, see Lemmermann *et al*., 2010.

2.2.5.1 Viral Replicative Fitness *In Vitro*

Low-serum starvation medium: MEM + 0.5% (v/v) FCS

To test the replicative potential of virus mutIRFE *in vitro*, multistep growth curves of the mutant virus were determined in cultures of quiescent MEF. These serum-starved MEF are more representative of the *in vivo* situation, because in tissues, cells are for the most part quiescent.DNA was isolated on the one hand from the cell pellets (DNeasy Blood and Tissue Kit, see 2.2.15.4) and on the other hand from 200µl supernatant (High Pure Viral Nucleic Acid Kit, see 2.2.15.5). Then, the number of viral genomes was quantitated by *M55*/*gB*-specific real-time PCR with normalization to the cellular gene *pthrp* (see 2.2.15.5). In addition, infectious virus in the supernatants was determined by virus plaque assay in MEF indicator cultures (2.2.4).

2.2.5.2 Viral Replicative Fitness *In Vivo*

To test the replicative potential of mutIRFE in host tissues, 3-5 BALB/c mice per time point were immunocompromised by γ irradiation, and were infected with 10^5 PFU intraplantar (i.pl., see below). At 2, 4, 6, 8, 10d p.i., organs were dissected and conserved. DNA was isolated from spleen and lungs (DNeasy Blood and Tissue Kit, see 2.2.15.3), and the number of viral genomes was quantitated by *M55*/*gB*-specific real-time PCR with

normalization to the cellular gene *pthrp* (2.2.15.5). Additionally, the number of infected cells in the liver was determined by IE1-specific immunohistochemistry (IHC, 2.2.17.2).

2.2.6 Intraplantar mCMV Infection

A virus solution was prepared at a concentration of $2x10^5$ PFU in 50µl PBS/mouse, which was injected subcutaneously into the right hind footpad (i.pl.) with a 1ml syringe and a needle of 0.4x12mm in diameter. In the immunosuppressed animal, a distinct hemorrhagic and locally swollen right posterior foot pad can be seen after 6-7d.

2.2.7 Immunosuppression

In order to exclude the immunological control of the host in experiments analyzing the replication potential of recombinant mCMV or the pathogenicity of certain viruses *in vivo*, mice were γ irradiated prior to infection. Irradiation was performed with a ^{137}Cs source (Type OB 58-BA, Buchler, Braunschweig) at a dose of 6.5 and 7Gy for BALB/c and C57BL/6 mice, respectively. The dose was calculated monthly according to the half-life of ^{137}Cs ($T_{1/2}$=30a). This treatment induces the extinction of hematopoietic stem and progenitor cells, characteristic of bone marrow aplasia (Mutter et al., 1998).

2.2.8 *Ex vivo* Isolation of CD8 T Cells from the Spleen

Material:	Red blood cell lysing buffer (Sigma-Aldrich Chemie GmbH)
Culture medium:	RPMI + 5% (v/v) FCS

Immunocompetent 8-10wk-old BALB/c or C57BL/6 mice were sensitized by i.pl. infection (see 2.2.6) with 10^5 PFU of either WT.BAC or WT.Smith. Lymphocytes were isolated from spleens of acute (1wk p.i.) or long-term (>3mon p.i., memory) infected donors, and were used in ELISPOT analyses, cytolytic assays, adoptive transfers, or for the generation of mCMV peptide-specific CTLL.

In brief, spleens from 3 mice were dissected sterilely and transferred to a 15ml tube containing RPMI medium. Then, they were passed with a 2ml syringe through a steel mesh and collected in a 60mm dish by rinsing the mesh with medium. The homogenate was transferred to a 50ml tube, and was washed 2x with medium (centrifugation 681xg, 5min). Afterwards, the suspension was filtered again through a 40µm cell strainer (on a 50ml tube) to remove remaining tissue debris. Then, the cell number was determined using Türk's solution. From this single-cell leukocyte suspension, CD8 T cells were isolated and enriched by immunomagnetic cell separation (see 2.2.9), so they could be used as effector cells in the above mentioned analyses. For the generation of peptide-specific cytolytic T-lymphocyte line (CTLL), erythrocytes in the organ homogenate were lysed by incubation in lysis buffer for 2min. Afterwards, centrifugation and filtering on a cell

strainer was performed as described above. The cell number was determined using trypan blue.

2.2.9 Immunomagnetic Cell Separation

Material:	CD8α (Ly-2) MicroBeads (Miltenyi Biotech)		
	LS columns for up to 10^8 cells (Miltenyi Biotech)		
Culture medium:	RPMI + 5% (v/v) FCS		
5x MACS buffer:	EDTA	10mM	1.86g
	BSA	2.5% (w/v)	12.5g
	Adjust to 500ml (PBS), filter sterile		
	Dilute 1:5 (PBS) before use.		

Positive immunomagnetic cell separation (MACS) was used to isolate and enrich for CD8 T cells from the single-cell leukocyte suspension which was obtained from spleens of infected mice (see 2.2.8).
For the isolation, the amount of cells required was incubated with the paramagnetic beads for 15min at 4°C under continuous soft shaking. For this, 10µl beads per $1x10^7$cells in 90µl MACS buffer were used. Then, the cells were washed with MACS buffer (10x volume; centrifugation 10min at 300g) to remove unbound beads. A 2-column separation was performed to achieve >95% purity. The cell pellet was resuspended in 500µl buffer and pipetted onto the first column, which was placed in the MACS separator. The pellet was washed 3x with buffer. The column was removed from the MACS separator, so the cells could be pressed through it into a tube. The eluate was given on a second column, placed in the magnetic stand, and was washed 2x. Then, the cells were eluted in 2ml buffer, washed with PBS to remove BSA (centrifugation 300xg, 5min) and counted. The remaining cells were taken up in a defined volume of medium, and could then be used as effector cells in an ELISPOT assay, a cytolytic assay, or an adoptive transfer.

2.2.10 Generation and Restimulation of CTLL

Solutions:	Synthetic peptide in PBS
Media:	RPMI + 5% (v/v) FCS
	MEM alpha + 7.5% (v/v) FCS +/- 200U/ml rh IL-2

Spleens from memory WT.BAC or WT.Smith-infected mice were processed (see 2.2.8) for the generation of a mCMV-peptide specific CTLL. The isolated cells were cultivated for 2-3wk in medium containing IL-2, and were stimulated with a defined synthetic mCMV-peptide in different molar concentrations.

The cells were obtained from the spleens, and counted as described under 2.2.8. A number of $1.5x10^7$cells/1.5ml MEM alpha, without IL-2, was seeded in 24-well plates (flat-bottomed). Synthetic peptide was added at a defined molarity, determining the specificity of the CTLL. After 4d of cultivation, 0.5ml/well of medium containing IL-2 were added (100U/ml). One week after the first encounter with peptide, the cells were restimulated with the synthetic peptide. Restimulation of the CTLL was done every week during the first 2 weeks, then, every second week. Thereby, the activity of IL-2 was 200U/well. Peptide-loaded antigen-presenting cells (APC) P815/B7 were used for restimulation. In order to prevent spread of the APC in the cultures, they were irradiated with 9,000rad and added to the cultures at a density of $8x10^5$cells/ml/well. CTLL were harvested and seeded at $5x10^5$cells/ml in 24-well plates together with the APC. In general, after 2-3 rounds of restimulation they had reached their epitope-monospecificity. They were tested for their functional avidity in assays of effector cell function (ELISPOT assay, cytolytic assay), before they were used in an adoptive transfer experiment.

2.2.11 Adoptive Transfer of CD8 T Cells

The adoptive transfer (AT) of *in vitro* generated peptide-specific CTLL, or *ex vivo* isolated memory CD8 T cells is a state-of-the-art approach to demonstrate their protective antiviral potential. Indicator recipients were immunoablated, mCMV-infected mice. Under these conditions, mice usually die due to multiple-organ CMV disease between 10-12d, unless protective T cells are transferred (Reddehase et al., 1985). AT of protective mCMV-specific CD8 T cells provides a model for preemptive cytoimmunotherapy of CMV disease (Podlech et al., 2002). Recipient mice were γ irradiated (see 2.2.7) prior to the transfer. Meanwhile, CTLL (see 2.2.10) or *ex vivo* isolated CD8 T cells from spleens of mice (see 2.2.8/9) were processed, and the numbers of cells transferred were titrated in a final volume of 0.5ml PBS/mouse. Then, the T cell suspension was injected intravenously in one of the 2 lateral tail veins. At least 5 mice per group were left without transfer, serving as no transfer control. Afterwards, the recipients were infected i.pl. (see 2.2.6) with 10^5 PFU/25µl/mouse of mCMV. Normally, organ infection is monitored at day 11 after cell transfer, when the no transfer group succumbs to multiple-organ CMV disease. However, the AT experiments performed herein had to be stopped earlier due to severe organ failure and dying of the recipients ahead of time. Virus replication in spleen and lungs was evaluated by quantitating infectivity (plaque assay, see 2.2.4) and the number of viral genomes (qPCR, see 2.2.15.10). In the liver, infected cells were detected by IE1-specific immunohistology (IHC, see 2.2.17). For the analyses, dissected spleens and lungs were stored in 1ml MEM + 10% (v/v) FCS + amphotericin B (1.4µg/ml) at -70°C, and livers were fixed in 37% (v/v) formalin before further processing.

2.2.12 *In Vivo* NK-Cell and CD8-T-Cell Depletion

In order to reveal the significance of NK cells and CD8 T cells for the immune control of acute mCMV infection, these lymphocyte subtypes were selectively depleted *in vivo*, according to current protocols (Krmpotić et al. 2002; Bantug et al., 2008; Babić et al., 2010; Slavuljica et al., 2010). The advantage of the system, to deplete cells only directly for the experiment with a specific antibody, is that up to then, lymphocyte subtypes of the host can interact with each other, which is essential for their development and activation. By depleting NK cells or CD8 T cells, we wanted to test whether this has an influence on acute infection of the host with mutIRFE as compared to WT.BAC. Depletions were always carried out 24h before infection to exclude any residual activities of the cell populations in question.

BALB/c mice were NK-cell depleted by i.v. injection of anti-asialo GM1 (ASGM1) antiserum (WAKO Chemicals GmbH, Japan) (20µl/500µl PBS), or NKG2D+ cells were blocked with α-mouse NKG2D antibody (300µg/mouse; Ho et al., 2002) (kindly provided by Prof. Jonjić, Croatia). For depletion of CD8 T cells, monoclonal anti-CD8α antibody (Prof. Jonjić, Croatia) was injected intravenously (1mg/500µl PBS). In the mice, the antibodies bind their target molecule, which is expressed on the cell surface, thereby leading to antibody-dependent cellular cytotoxicity (ADCC) or complement-dependent cytotoxicity (CDC). One day after depletion, mice were infected i.v. with $4x10^4$ or $2x10^5$PFU/500µl PBS of virus WT.BAC, mutIRFE, or Δm152. A control group which was not depleted but infected was always included in the experiments. 3d p.i., spleens and lungs were dissected (in 1ml MEM + 10% (v/v) FCS + amphotericin B (1.4µg/ml), -70°C) and used for plaque assay (see 2.2.4.2), and livers were used for IE-specific IHC (see 2.2.17.2). About $1/5^{th}$ of each spleen was excised and pooled for each group (5 mice), and processed for flow cytofluorometric control of depletion (see 2.2.13).

2.2.13 Control of Lymphocyte Depletion by Flow Cytofluorometry

FACS buffer: 1% FCS (v/v) in PBS

Sheath fluid: IsoFlow™ (Beckman Coulter)

In general, fluorescence activated cell sorting (FACS) was used to determine the amount of distinct cells in a heterogenous cell population by using fluorescence-labeled antibodies to bind and detect defined intra- or extracellular antigens. This method was applied herein to determine the amount of NK cells and CD8 T cells in organ homogenates from lymphocyte-depleted and infected spleens. In all analyses, 2-3 antigens were stained by using antibodies conjugated with different fluorochromes. For the antibodies, see 2.1.8.

In order to investigate the contribution of certain lymphocytes to acute mCMV infection *in vivo*, either NK cells, NKG2D-positive NK cells, or CD8 T cells were depleted or at least blocked by the use of the corresponding antibodies (see 2.1.8.). The efficiency of depletion was controlled by flow cytofluorometry. For this, 1/5th of a spleen was excised, pooled for 1 group of 5 animals, and processed to yield a single cell suspension (see 2.2.8). 1x10^6 cells were used for staining. The corresponding amount of cells was transferred to a tube, and 1µg Fc-block per 10^{6}cells was added for 5min at 4°C to reduce unspecific binding. For the specific staining of NK cells, 0.5µg CD3ε-FITC and 2.5µg CD335-PE were diluted in 50µl FACS buffer per sample. For the specific staining of NKG2D$^+$ NK cells, 0.5µg CD49b-FITC, 0.5µg TCRβ-PE, and 0.5µg NKG2D-APC were diluted in 50µl FACS buffer per sample. For the specific staining of CD8 T cells, 0.5µg CD3ε-FITC and 0.5µg TCRβ-PE were diluted in 50µl FACS buffer per sample (1x10^{6}cells). The antibodies were incubated for 15min at 4°C. Then, the cells were washed with 1ml FACS buffer and centrifuged for 5min at 250xg. Finally, cells were resuspended in 500µl FACS buffer, and were analyzed directly and stored at 4°C over night. The samples were analyzed by flow cytofluorometry the next day.

2.2.14 Methods in Protein Biochemistry

2.2.14.1 Preparation of Whole Cell Protein

Lysis buffer	50ml	Final concentration
	1ml (1M) Hepes pH 7.7	20mM
	2ml (5M) NaCl	0.2M
	75µl (1M) $MgCl_2$	1.5mM
	40µl (0.5M) EDTA	0.4mM
	5ml (10%) Triton X-100	1%
Filter sterile, store at 4°C		
Add freshly before lysis:	0.5mM DTT	
	1:25 protease inhibitor	

In order to analyze the expression of viral proteins *in vitro*, BALB/c, C57BL/6 or IFNAR-/- MEF were cultured in 100mm dishes. At a density of ~2x10^6 cells/dish, they were centrifugally infected at an MOI of 4. Then, they were incubated at 37°C, and at different time points p.i. cells were harvested. For this, cells were washed 1x by removing the culture medium from each dish, rinsing the cells with PBS, and aspirating it again afterwards. Then, the cells were scraped off from the bottom with residual PBS using a cell scraper, and were collected in a 1.5ml tube, one tube per dish. The cells were pelleted by centrifugation (960xg, 5min, 4°C). After that, the pellet was lysed with 100-200µl lysis

buffer (depending on the number of cells per dish), for an incubation period of 15min on ice. The lysis buffer contains protease inhibitor to prevent digest of the proteins, and DTT to reduce their amino acids. Then, the cell suspension was centrifuged again (21,000xg, 10min, 4°C) and the supernatant containing the proteins was transferred to a new 1.5ml tube and stored at -20°C. For western blot analyses, the concentration of protein in the solution was determined (see 2.2.14.2), and for each sample the same amount (mainly 50µg) was loaded onto the gel.

2.2.14.2 Quantification of Protein

Material: BCA™ Protein Assay Kit (Pierce, USA)

The amount of protein in cell lysates prepared from cell culture experiments (see 2.2.14.1) was determined using the BCA (bicinchoninic acid) assay (Smith et al., 1985). This is a cupper-based protein assay which takes advantage of the Biuret reaction. Tripeptides and larger polypeptides form a chelate complex with cupric ions (Cu^{2+}) in an alkaline environment. Thereby, Cu^{2+} is reduced to cuprous ions (Cu^{+}), and the complex becomes colored (faint-blue) and absorbs light at 540nm. By addition of BCA to the assay, this biuret reaction is followed by a second chelation of BCA with Cu^{+} after removal of the weakly chelated peptides. This new complex has an intense purple color. The color is stable and intensifies proportionally over a broad range of increasing protein concentrations. Since BCA and cupper are in excess, the protein assay does not reach an end point and has to be stopped at a defined time point. Advantages of the BCA are a higher detection limit, and a greater tolerance towards nonionic detergents and buffer salts. For further reading, see www.piercenet.com.

For performance of the assay, a standard row with BSA was titrated to be used as reference for the unknown samples. Frozen lysates were thawed on ice. The assay reagents were mixed according to the manufacturer's instructions. For each sample, duplicates of 200µl were pipetted per well of a 96-well plate and 10µl lysate were added. The reaction was incubated for 30min at 37°C. After that, the absorbance was measured photometrically (Thermo Scientific, Langenselbold). Then, the amount of protein in the samples was calculated using the BSA standard curve.

2.2.14.3 SDS Polyacrylamide Gel Electrophoresis

Laemmli buffer	10ml	Final concentration
	2.25ml (1M) Tris/HCl pH 6.8	0.225M
	5ml (100%) glycerol	50%
	2.5ml (20%) SDS	5%
	5mg bromophenol blue	0.05%

	2.5ml (1M) DTT	0.25M

In order to compare viral protein expression in cell cultures infected with different viruses (WT.BAC, mutIRFE, mutIRFErev), the amount of protein used in gel electrophoresis was set to a certain concentration for each sample (50µg). For this, the amount required for each sample was pipetted in a 1.5ml tube, and 5µl Laemmli buffer was added. The sample was incubated for 5min at 95°C, and could then be stored at -20°C until the western blot was performed. Laemmli buffer contains DTT, which reduces amino acids. This supports denaturation of the proteins by SDS, which is an ingredient of the buffer as well. Thereby, protein interactions and quaternary structures are prevented. Heating the sample to 95°C further destroys higher protein structures, and inactivates proteases. Now, the complexes of different proteins with SDS only differ in their size. In SDS-gel electrophoresis, these complexes move in the electric field towards the anode. The polyacrylamide matrix separates them according to their molecular weight.

Stacking gel:	1.5ml acrylamid 30%	4%
	2.8ml 4x stacking gel buffer	
	6.93ml aq.dist.	
	150µl APS	10%
	20µl TEMED	
Stacking gel buffer 4x:	20ml 10% SDS	0.4%
	30.29g (121.4g/mol) Tris/H_3PO_4 pH6.8	5M
	Adjust to 500ml (aq.dist.)	
Resolving gel:	7.2ml Acrylamid 30%	12.5%
	4.5ml 4x resolving gel buffer	
	6.3ml aq.dist.	
	144µl APS	10%
	14.4µl TEMED	
Resolving gel buffer 4x:	20ml 10% SDS	0.4%
	90.9g (121.4g/mol) Tris/HCl pH8.8	1.5M
	Adjust to 500ml (aq.dist.)	
5x running buffer:	100ml 10% SDS	0.5%
	144.13g (75.07g/mol) glycine	960mM
	30.29g Tris pH8.3	125mM
	Adjust to 2l (aq.dist.)	
Protein ladder:	PageRuler™ Prestained Protein Ladder (Fermentas)	

For the SDS gel, the resolving gel was pipetted between 2 glas plates (10x20cm) fixed in the electrophoresis apparatus. As soon as the resolving gel was solid, the stacking gel was pipetted above it and the comb (mainly 20 lanes) was put in. Often, the gel was prepared one day prior to the western blot performance. In this case, the solid gel was covered with humid tissues to prevent drying out, and it was kept at 4°C over night. The protein samples had to be thawed on ice before they could be loaded onto the gel together with a protein ladder as standard. The run was started with a voltage of 100V until the samples had moved to the resolving gel (app. 60min). Then, it was run at 150V until the loading buffer had run out of the gel, and the samples had separated enough, as was visible by the prestained protein ladder (app. 80min). The stacking gel was cut off, and only the resolving gel was used in the western blot procedure (see 2.3.14.4).

2.2.14.4 Western Blot

Transfer buffer:	5.8g Tris	
	2.9g glycine	
	200ml ethanol (100%)	
	Adjust to 1l (aq.dist.)	
10x PBS:	80g NaCl (58.44g/mol)	1.37M
	2g KCl (74.55g/mol)	26.8mM
	14g $Na_2HPO_4(2H_2O)$ (177.99g/mol)	78.1mM
	2g KH_2PO_4 (136.09g/mol)	14.7mM
	Adjust to 5l (aq.dist.), autoclave	
Blocking buffer:	5g milk powder	5%
	100ml wash buffer II	
Wash buffer I:	9g milk powder	1%
	900ml wash buffer II	
Wash buffer II:	200ml 10xPBS	
	1800ml aq.dist.	
	2ml TX-100	0.1%

While gel electrophoresis was running, 4 Whatman paper and the PVDF (polyvinylidenfluorid)-membrane were cut to the size of the gel (5.5x16.5cm). Note that the membrane must not be touched without safety gloves! The membrane was activated in methanol, then transferred to aq.dist., and was finally left in transfer buffer together with the Whatman paper for 10min. The lower part of the blot apparatus (cathode) was rinsed with transfer buffer. Two of the Whatman papers were laid inside. The membrane was put on top of these. The resolving gel was put onto the membrane. The sandwich structure was ended with the other two Whatman papers. Then, a 5ml glass pipette was rolled

along the sandwich to remove any air bubbles. Finally, the apparatus was closed (anode) and the gel was blotted onto the membrane according to the guide line:
2mA/1cm^2 gel → 2mA x (5.5cm x 16.5cm) = 180mA for 90min
After the 90min, a successful transfer was visible by the prestained ladder on the membrane. After this blotting procedure, the membrane was incubated in blocking buffer for 1h on a rocking platform. Distinct dilutions of the primary antibodies (see 2.1.8) were prepared in 7ml wash buffer I. If IE1 was to be detected on one membrane together with m152, the membrane was cut horizontally under the red band (72kDa) of the ladder. The upper part of the membrane was laminated with 7ml of the IE1 antibody solution. The lower part was laminated with 7ml of the m152 antibody solution. The membrane parts were incubated with the respective antibodies over night at 4°C on a rocking platform. The next day, they were washed 5x for 10min in wash buffer I. 1:10,000 dilutions (5µl in 50ml wash buffer I) of the corresponding Horseraddish-peroxidase (HRP)-labeled secondary antibodies (see 2.1.8) were prepared, and were incubated with the membrane for 1h on a rocking platform. Afterwards, unbound antibody was washed away 5x for 10min in wash buffer II. Finally, the western blot signal could be detected (see 2.2.14.5).

2.2.14.5 Detection

Material: ECL Plus Western Blotting Detection System (GE Healthcare)

The chemiluminescence detection reagent was stored at 4°C, and was taken from the fridge 10min before detection should start. Reagents A and B were mixed, according to the manufacturer's advice, 40:1 (2ml/membrane). The membrane was removed from the washing solution and put in a new dish. The detection solution was pipetted for 2min over the complete membrane. Then, the membrane was put between 2 overhead foils in a detection cassette. In the photo laboratory, the membrane was exposed to x-ray film for several time points. The film was then transferred through developing solution, water, fixation solution, and water again. Finally, the bands of the standard were marked on the film, before the membrane could be taken out of the cassette for staining of the protein bands (see 2.2.14.6).

2.2.14.6 Stripping

Material:	Restore™ Western Blot Stripping Buffer (Pierce)	
Blocking buffer:	5g milk powder	5%
	100ml wash buffer II	
Wash buffer I:	9g milk powder	1%
	900ml wash buffer II	
Wash buffer II:	200ml 10xPBS	

	1800ml aq.dist.	
	2ml TX-100	0.1%

In order to verify loading amounts, primary and secondary antibodies had to be removed from immunoblots before the membrane could be reprobed. For this, after detection of viral proteins m152/IE1 the membrane was washed 4x for 10min with wash buffer II. Then, the membrane was stripped by incubation in Restore™ Western Blot Stripping Buffer for 15min at 37°C. Afterwards, the antibodies were washed off 5x for 10min with wash buffer II. The membrane was blocked with blocking buffer for 1h on a rocking platform. A dilution of the primary antibody against β-actin (see 2.1.8) was prepared in 7ml wash buffer I, and the membrane was incubated over night at 4°C on a rocking platform. The next day, unbound antibody was washed off 5x for 10min with wash buffer I. Then, the membrane was incubated in a dilution of the corresponding Horseraddish-peroxidase (HRP)-labeled secondary antibody (see 2.1.8) in wash buffer I for 1h on a rocking platform. Finally, unbound secondary antibody was washed off 5x for 10min with wash buffer II, and the chemiluminescent signal was detected as described above (see 2.2.14.5).

2.2.14.7 Coomassie Stain

Coomassie:	20% ethanol	100ml
	10% acetic acid	50ml
	0.1% Coomassie Brillant Blue R250	500mg
	Adjust to 500ml (aq.dist.)	
Destaining:	7.5% acetic acid	150ml
	25% ethanol	500ml
	Adjust to 2l (aq.dist.)	

In order to verify the amounts of protein loaded onto the gel and blotted to the membrane, a staining solution containing Coomassie (Brillant Blue R250) was used, which resulted in an unspecific, blue staining of the protein bands. For this, the membrane was put for approximately 10min in the Coomassie staining solution on a rocking platform. Then, the solution was removed, and the membrane was washed shortly under tap water. After that, it was put for several hours in destaining solution before being dried.

2.2.15 Methods in Molecular Biology: DNA

In this work, studies were conducted investigating the replicative fitness of mutant virus mutIRFE compared to that of WT.BAC virus *in vitro* and *in vivo* (see 2.2.5). To illustrate that, the number of viral genomes per cell was determined. For this purpose, DNA was

isolated from mCMV-infected cells or organs (spleen and lungs), and was subjected to qPCR. The same method was used to verify the deletion of the BAC vector-derived sequence from mutant virus mutIRFE and revertant virus mutIRFErev after propagation of the viruses on MEF cultures, and isolation from supernatants.

2.2.15.1 Oligonucleotides

Oligonucleotides used for qPCR analyses and cloning procedures were purchased from biomers.net GmbH (Ulm), or Operon Biotechnologies (Köln). The specifications of mCMV-sequences results from Rawlinson et al., 1996 (GenBank Acc. No.: NC_004065). The primers were dissolved in sterile aq.dist., the TaqMan probes in sterile Tris buffer pH 8.0.

LCgB_For3	n 84,017-84,037; 5´ GAAGATCCGCATGTCCTTCAG 3´
LCgB_Rev3	n 84,151-84,131; 5´ AATCCGTCCAACATCTTGTCG 3´
	Amplicon length: 135bp; GenBank Acc. No. NC_004065
LCPTHrP_For2	5´ GGTATCTGCCCTCATCGTCTG 3´
LCPTHrP_Rev2	5´ CGTTTCTTCCTCCACCATCTG 3´
	Amplicon length: 142bp; GenBank Acc. No.: M60056
BAC_taq_For	5´ GTTCTGTCATGATGCCTGCAA 3´
BAC_taq_Rev	5´ AATCCGCTCCACTTCAACGT 3´
BAC_taq probe	5´ [6~FAM]CACCGCACGAAGATTTCTATTGTTCCT GA[TAMRA~6~FAM] 3´
pepKan-S_IRFErev-For	5´ ^{211,491}CTTTTTATACTATGTGTCCATGTTTACCTAACATC GAAAGCGAAAGTCCGGACTTTCC^{211,548}CAACAACCAATT AA CCAATTCTGATTAG 3´
pepKan-S_IRFErev_Rev	5´ ^{211,570}CCTCGGTCGGCTCAGGCCTTTGGGAAAGTCCGG ACTTTCGCTTTCGATGTTAGGTAAAC^{211,512}CAGGATGAC GACGACGATAAGTAGG G 3´
IRFE_for5	n 211,491-211,512; 5´ CTTTTTATACTATGTGTCCATG 3´ GenBank Acc. No. NC_004065
rev5	5´ CAGGATGACGACGATAAGTAGGG 3´
*Hind*III_m152Prom_rev	5´ TTAAGCTT^{211,378}TGTACAGGCTAGCGATCGGG^{211,397} 3´
*Kpn*I__m152Prom_for	5´ CCGGTACC^{212,000}AGAAGTCAGATCTTGAATAC^{211,981} 3´

2.2.15.2 Disruption and Homogenization of Lungs, Salivary Glands, and Spleens

Lysis Buffer: Buffer ATL (QIAGEN)

In order to purify DNA from lungs, salivary glands, and spleens of infected mice, these organs had to be efficiently disrupted and homogenized. Disruption of plasma membranes is necessary to release nucleic acids and proteins. Homogenization reduces the viscosity of the cell lysates by shearing of cellular proteins and carbohydrates. Here, the tissues were disrupted using a rotor-stator system (TissueRuptor, QIAGEN). The principle of this homogenizer is that samples are disrupted and homogenized simultaneously by a rotating blade, through combination of turbulence and mechanical shearing (see TissueRuptor handbook, QIAGEN).

Note: Sample material can be homogenized for up to 5min without adversely affecting the quality of DNA, but disruption generates heat. Therefore, it is advisable to keep the tissues on ice. Disruption in lysis buffer (ATL) causes foaming. Thus, the sample should either be left at 20°C for a few minutes, or be centrifuged briefly, before it is further processed.

Organ	Weight [mg]	Buffer ATL [µl]	Proteinase K [µl]	Lysate for DNeasy [µl]
Lungs	25	180	20	200
Salivary gland	100	180	20	200
Spleen	10	180	20	200

Tab. 2.3 Starting material for DNA purification.

In the replicative fitness study, an equally sized piece of each spleen and lung was cut and weighed. The rest of the organs was frozen for long-term storage at -70°C. Salivary glands were weighed as a whole (~100mg). For disruption, the organs were placed each in a 50ml tube and buffer ATL was added. The amounts of ATL used per mg of tissue were calculated for each weight (Tab. 2.3). The organs were disrupted with the TissueRuptor for at least 30s at full speed until no debris remained visible. Then, proteinase K was added to the homogenates (see above). The whole amount was transferred to a 2ml microcentrifuge tube, which was placed in a thermomixer, and was incubated at 56°C over night. The lysate was then used for the purification of DNA (see 2.2.15.3).

2.2.15.3 Purification of DNA from Lungs, Salivary Glands, and Spleens

Kit: DNeasy Blood and Tissue Kit (QIAGEN)

In order to purify DNA from lungs and spleens, the DNeasy Blood and Tissue Kit (QIAGEN) was used. This kit is suitable for rapid purification of total DNA from fresh or frozen tissues. DNeasy-purified DNA, which is free from contaminants and enzyme inhibitors, can be used in PCR analyses. During the purification procedure, the DNA in the lysate is bound reversibly to a silica-based membrane, and contaminants and enzyme inhibitors are removed in two washing steps. Then, the DNA can already be eluted (DNeasy Blood and Tissue Handbook, Qiagen).
From organ lysates of the replicative fitness study, only 200µl, corresponding to 25mg of lungs and 10mg of spleen, were used in the DNeasy procedure to prevent overload of the column. According to the manufacturer's protocol, buffer AL was mixed 2:1 with ethanol (100%). The lysates were then mixed 1:3 with this buffer, and transferred to a 1.5ml microcentrifuge tube. The DNA was purified according to the manufacturer's instructions, and was finally eluted in 100µl buffer AE. The DNA yield and its purity were determined afterwards (see, 2.2.15.6), and the DNA was stored at -20°C.

2.2.15.4 Purification of DNA from Cell Pellets

Kit: DNeasy Blood and Tissue Kit (QIAGEN)

DNA was purified from infected MEF cultures for the *in vitro* replicative fitness study (see 2.2.5.1) to determine the number of viral genomes per cell. For the purification, the cell pellets were thawed, and resuspended in 200µl PBS. Afterwards, 20µl proteinase K, and 4µl RNase A were added and incubated for 2min at ~20°C. Then, 200µl buffer AL was given to the lysate, and was incubated for 10min at 56°C in a thermomixer. After that, 200µl ethanol (100%) was added, and the whole amount was transferred to a DNeasy spin column. Further steps were performed according to the manufacturer's instructions, and DNA was eluted in 200µl buffer AE.

2.2.15.5 Purification of Viral DNA

Kit: High Pure Viral Nucleic Acid Kit (Roche, Mannheim)

Viral DNA was isolated from supernatants of infected cell cultures, and subjected to qPCR (see 2.2.15.8). This was required for the *in vitro* replicative fitness study (see 2.2.5.1), and to verify the deletion of BAC vector-derived sequences from mutant virus mutIRFE and revertant virus mutIRFErev after propagation of the virus (see 2.2.3).
Purification was performed with 200µl of each virus supernatant as starting material. As a positive control, 10µl of virus WT.BAC was mixed with 190µl H_2O, and included in the purification procedure. According to the manufacturer's protocol, 200µl binding buffer including poly A (per 2.5ml buffer 50µl poly A) was added to each sample, as well as 50µl

proteinase K. This mixture was incubated for 10min at 72°C in a thermomixer. Then, 100µl binding buffer was added, and the whole amount was loaded on a filter tube. The DNA was purified according to the manufacturer's instructions, and was finally eluted in 50µl elution buffer, and stored at -20°C. In the qPCR analysis, 2µl per sample were used.

2.2.15.6 Determination of Concentration and Purity of Nucleic Acids

In general, the concentrations of DNA or RNA in purified samples from cell cultures or mouse organs were determined by measuring the absorbance at 260nm (A_{260}) with a spectrophotometer (NanoDrop® ND-1000, PEQLAB). For an accurate measurement, 1.5µl of each sample were used. Note that absorbance measurements cannot discriminate between DNA and RNA. The relationship between absorbance and concentration is based on an extinction coefficient calculated for RNA/DNA in water.

Extinction A_{260} 1 = 40µg/ml ssRNA
= 50µg/ml dsDNA
= 33µg/ml ssDNA

Proteins can contaminate a sample. Therefore, the ratio of absorbance at 260nm and 280nm (maximum of extinction of proteins) is used to assess the purity of nucleic acids. Pure RNA has an A_{260}/A_{280} ratio of 1.9-2.1, whereas pure DNA has a ratio of 1.7-1.9. If the ratio is appreciably lower in either case, it may indicate the presence of protein, or phenol, or other contaminants that absorb strongly or near 280nm (http://www.nanodrop.com/nd-1000-overview.html).

2.2.15.7 Polymerase Chain Reaction (PCR)

Kit: HotStar HiFidelity DNA Polymerase (QIAGEN)

This important method was first described by Mullis & Faloona (1987), and was optimized by Saiki et al. (1988). Sequence-specific primers, which define the two ends of the product to be amplified, are among the main components. The program Primer Express 2.0 (Applied Biosystems) was used to design these sequence-specific primers. It is important to avoid inter-complementary sequences which would lead to the formation of secondary structures within the oligonucleotides. Another characteristic of primers for efficient and specific hybridization of DNA:DNA duplexes are 3'-ends with cytosine or guanine. Using the PCR method, it is possible to selectively amplify certain DNA fragments to a high extent. Another crucial component is a thermally-stable enzyme such as the *Thermus aquaticus* (*Taq)* polymerase. One PCR cycle is characterized by three steps. First, the template DNA double strand (ds) has to be separated, which is accomplished by heating the sample to 94-95°C (denaturing). In a second step, the temperature is cooled down to a degree at which the primers can bind their homologous sequences on the now single-

stranded (ss) DNA (between 50-68°C) (annealing). After that, the temperature is increased to 72°C so that *de novo* synthesis of DNA starting at the primer sides can be performed by the thermally stable polymerase (extension). This 3-step cycle is repeated several times to yield a huge amount of the DNA fragment in question (amplicon). The number of newly synthesized molecules is increased by factor 2 in each cycle under optimal conditions. Therefore, the number of amplicons after n cycles can be estimated to 2^n. Limiting factors of the amplification are the amounts of primers, nucleotides, and activity of the enzyme.

HiFidelity PCR pipetting-scheme:

Components	Volume/reaction	Final concentration
10xHiFidelity PCR buffer	5µl	1x
Primer-for (10pmol/µl)	2.5µl	0.5µM
Primer-rev (10pmol/µl)	2.5µl	0.5µM
HiFidelity DNA polymerase	1µl	2.5U
H_2O	variable	-
DNA template	variable	10ng
Final volume	50µl	

HiFidelity PCR profile (touchdown)

Initial activation step	15min	95°C	Activates HiFidelity DNA polymerase
Touchdown PCR:			
Denaturing	30s	94°C	
Annealing	2min	62°C	Temperature is decreased by 1C° per cycle
Extension	2min/1kbp	68°C	
Cycles	18	62-45°C	
Denaturing	30s	94°C	
Annealing	2min	45°C	
Extension	2min/1kbp	68°C	
Cycles	12	45°C	
End	∞	4°C	

HiFidelity PCR profile

Initial activation step	5min	95°C	Activates HiFidelity DNA polymerase
Denaturing	15s	94°C	
Annealing	1min	63°C	
Extension	1min	72°C	
Cycles	35	62-45°C	
Final extension	10min	72°C	
End	∞	4°C	

2.2.15.8 Quantitative Real Time PCR (qPCR)

In a conventional PCR, at the end point of the reaction, amplicons are detected by agarose gel electrophoresis and staining of the DNA with ethidium bromide. It is not possible to draw a conclusion about the starting amount of the DNA template from the intensity of the bands. Amplification reaches a plateau phase after a certain number of cycles, which is due to exhausted substrate and limited enzyme activity. In qPCR,

however, signals can be detected during the exponential phase, where they correlate with the initial amount of template DNA. In this phase, amplification can be described by the following formula: $N = N_0 \times (E_{const})^n$

E = PCR efficiency

N = Number of amplified molecules

N_0 = Initial amount of template

n = number of cycles

A reaction efficiency of 100% is reached by an exact doubling of the amplicons (E=2) in one cycle. In order to compare the amount of template in two PCR reactions, the PCR efficiency and the number of cycles should be the same. Detection can either be made with non sequence-specific, dsDNA-binding fluorochromes (e.g. SYBR Green I), or with sequence-specific, fluorescent probes (e.g. TaqMan probes). On account of the fact that the fluorescence signal is proportional to the copy number of the amplicon, the amount in an unknown sample can be determined using a defined standard to generate a standard curve (absolute quantification). All sequence-specific primers were designed with the program Primer Express 2.0 (Applied Biosystems, Foster City, CA, USA).

2.2.15.9 Plasmids for qPCR Standardization

In absolute quantification assays (see, 2.2.15.8), plasmids were used for standardization. In order to determine the number of viral genomes and the amount of cells in an 'unknown' sample, plasmid pDrive_gB_PTHrP_Tdy (Simon et al., 2005) was used. This plasmid standard encodes the sequences of the mCMV gene *M55/gB*, as well as of the cellular gene *pthrp* (mouse parathyroid hormone-related peptide-encoding gene) (Mangin et al., 1990), and *sry* (male-sex (testes)-determining gene) (Gubbay et al., 1990). *M55/gB*- and *pthrp*-specific primers and probes were used in this setting (see 2.2.15.1).

In order to verify the deletion of the BAC vector-derived sequence in newly propagated virus, plasmid pDrive_gB_PTHrP_BAC (Lemmermann et al., 2010) was used. In this setting, the ratio between the BAC vector-sequence and *M55/gB* was determined using the corresponding primer pairs and probe (see 2.2.15.1), and purified virus DNA from supernatants as template (2.2.15.5). A ratio of $\square 10^2$ BAC vector sequences/10^6 viral genomes was strived for.

Aliquots of a defined concentration (0.5×10^9plasmids/µl) of each plasmid were stored at -20°C. These plasmids were titrated in Tris buffer (pH 8.0) in $\log_{10}$ dilutions ranging from 0.5×10^7-0.5×10^1. Poly A was added to dilutions of 0.5×10^3 and less.

2.2.15.10 TaqMan qPCR

Kit: QuantiTect SYBR Green I PCR Kit (QIAGEN)

For the replicative fitness assay (see 2.2.5), productive replication of mCMV in cell culture as well as *in vivo* was quantified. Therefore, absolute quantifications of viral genomes per cell were performed using SYBR Green in qPCR. Moreover, this assay was used to verify that newly propagated virus was free of the BAC vector-derive sequence. SYBR Green is a dsDNA-specific dye. During DNA synthesis, SYBR Green binds to the PCR products. In the course of this process, fluorescence is emitted, and can be measured directly. It is crucial to perform a melting curve analysis at the end of the PCR, because SYBR Green binds unspecifically to every synthesized dsDNA. A master mix including buffer, primers, and water was prepared under a Template Tamer (Oncor Appligene, Heidelberg) in order to avoid contamination of the samples. It was mixed thoroughly, and equal volumes (18µl) were dispensed into PCR tubes, placed in a ThermoCooler rack (Biozym, Hessisch Oldendorf). Thereafter, the template DNA (2µl) was added to the PCR tubes, in a different room, and the mix was spun down. The PCR was run in a TaqMan instrument.

TaqMan 7500 PCR Pipetting scheme

Component	Volume/Reaction	Final concentration
2×QuantiTect SYBR Green I PCR Master Mix	10µl	1×
Primer-For (10µM)	1.5µl	0.75µM
Primer-Rev (10µM)	1.5µl	0.75µM
DNA	2-4µl (max 5µl)	100ng
RNase-free H_2O	variable	—
Total Volume	20µl	—

TaqMan 7500 PCR Profile

Initial Activation Step	15min	95°C	Activation of HotStar*Taq* DNA-Polymerase
3-Step Cycling			
Denaturation	15s	95°C	
Annealing	30s	62°C	
Extension	45s	72°C	Data acquisition
Number of Cycles	50		
Melting Curve			
Denaturation	15s	95°C	
Annealing	1min	60°C	
Set Ramp Time	auto		
Denaturation	15s	95°C	

2.2.15.11 Agarose Gel Electrophoresis of DNA

50x TAE buffer:	Tris base	242g
	Acetic acid glacial ($C_2H_4O_2$)	57.1ml
	0.5M EDTA-2H_2O	100ml
	Adjust to 1l (aq.dist.), pH 8.0 (glacial acetic acid), autoclave	
1x TAE working solution:	40mM Tris*acetate	

	1mM EDTA	
10x loading buffer:	25g bromophenol blue	0.25% (w/v)
	2ml 0.5M EDTA	10mM
	40g sucrose	40% (w/v)
	0.1g SDS	0.1%
	Adjust to 100ml (aq.dist.)	
DNA ladder:	1kb DNA ladder (Invitrogen)	
	Low Molecular Weight Marker (New England BioLabs)	

DNA fragments can be separated by gel electrophoresis on the basis of their net charge and molecular weight. Herein, electrophoresis was performed to control duplex quantitative real-time reverse transcriptase PCR (qRT-PCR) efficiency by separation of the 2 amplicons, for the clean-up of linear DNA fragments for electroporation, and for the verification of linear DNA fragments after restriction.

Generally, 1% agarose gels were prepared. However, to verify the amplicons produced in the duplex qRT-PCR, which were of relatively small size (68bp and 87bp, see 2.2.16.1), a 3% agarose gel was prepared for an accurate separation. Depending on the number of samples, large gels (20x10cm, 20x20cm), or small gels (10x6.5cm) were prepared. The required amount of agarose was weighed and transferred to a glass flask. Then, 1xTAE buffer was added, and the flask was swirled slightly for homogenous distribution. The mixture was boiled carefully in the microwave until all agarose was dissolved. After it had cooled down (~50°C), it was poured in the gel tray, and ethidium bromide (final concentration 1µg/ml) was added. The well comb was fixed. As soon as the gel was solid, it was put in the horizontal gel chamber and covered with 1xTAE as running buffer. The sample loading buffer was added to the samples (1:10) to facilitate their moving into the wells. Then they could be loaded onto the gel. The voltage was set depending on the size of the gel and amount of nucleic acid (0.5-5V/cm distance of the electrodes).

DNA was stained by ethidium bromide, which intercalates in the DNA double helix, and fluoresces under UV light. Documentation was made with a camera (CCD). In order to determine the size of the DNA fragments, DNA ladders of determined size were run together with the samples.

In addition to the indications for gel electrophoresis mentioned above, this method was also used to verify the integrity of an intact BAC-plasmid in bacterial colonies, after preparation (2.2.15.14.2) and restriction (2.2.15.15.1). In some aspects, a BAC-gel differs from the procedure described above:

10x TBE buffer:	Tris base	890mM

Boric acid	890mM
EDTA	20mM
adjust to 1l (aq.dist.), pH8, autoclave	

A BAC-gel (20x20cm) was prepared with 0.7% agarose (4g) in 1xTBE (500ml) according to the general procedure (see above). 20µl ethidium bromide was added to the gel when it had cooled off. Then it was poured into the tray, and a comb with large wells (100µl) was fixed. The whole samples from the restriction (80µl) were mixed with loading buffer, and were loaded onto the gel, and the gel was run at 70V over night (>12h) at 4°C (or at 80V for at least 6h).

2.2.15.12 Gel Extraction

Kit: QIAquick Gel Extraction Kit (QIAGEN)

Gel extraction can be used to purify a defined DNA sample from a gel band. The linearized PCR fragment which was generated for the reversion of the mutIRFE mutation was verified by gel electrophoresis. The DNA was then extracted and purified using the QIAquick Gel Extraction Kit. For this, the DNA fragment was excised from the gel under UV light with a sterile scalpel. The gel piece was weighed, cut in pieces of up to 400mg, and these were mixed with 3vol of buffer QG. The DNA was then extracted according to the QIAquick Spin Handbook, and was eluted in 50µl buffer EB. The amount of DNA was determined with the NanoDrop. A 1% agarose gel was prepared to verify the single band.

2.2.15.13 Cultivation of Bacteria

2.2.15.13.1 Single Colony Cultures

LB agar:	Bacto agar	15g
	Bacto tryptone	10g
	Bacto yeast extract	5g
	NaCl	10g
	Adjust to 1l (aq.dist.), pH 7.5 (NaOH), autoclave	
Ampicillin (Amp) stock solution:	100mg/ml in aq.dist.	
	filter sterile, store at -20°C	
	use 1:1,000 in autoclaved LB (100µg/ml)	
Chloramphenicol (Cam) stock solution:	34mg/ml in ethanol (100%)	
	filter sterile, store at -20°C	
	use 1:2,000 in autoclaved LB (17µg/ml)	

Kanamycin (Kan) stock solution:	10mg/ml in aq.dist. filter sterile, store at -20°C use 1:400 in autoclaved LB (25µg/ml)

Bacteria were cultivated on LB agar to grow single colonies, which could then be used to inoculate suspension cultures. For this, LB agar was boiled (microwave) and subsequently cooled down to ~40°C (water bath). Then, the required concentration of antibiotics was added, and the agar was poured into sterile 100mm dishes. When the agar was solid, the dishes were stored face-down at 4°C. Bacteria from glycerol stocks were streaked with a wire-loop in 3 separate compartments of the agar plate, thereby diluting bacteria by streaking from one compartment to the next. Colonies that should be grown for transformation were streaked with a Drigalski spatula. The agar plates were incubated at 32/37°C over night. The next day, single colonies were picked with a sterile pipet tip, which was then transferred to LB medium + antibiotics (see 2.2.15.13.2).

2.2.15.13.2 Bacteria in Suspensions

LB medium:	Bacto tryptone	10g
	Bacto yeast extract	5g
	NaCl	10g
	Adjust to 1l (aq.dist.), pH 7.5 (NaOH), autoclave	
Freezing medium:	Glycerol	50% (v/v)
	LB medium	50% (v/v)

Bacteria were grown in suspension for DNA purifications. For this, a starter culture was prepared either from a bacterial glycerol stock (pipet tip dipped in), or from a single colony (picked with a pipet tip, see 2.2.15.13.1), by transferring the pipet tip to 5ml/10ml LB medium containing the selective antibiotics. This starter culture was incubated for 6-8h/12-16h at 32°C/37°C, respectively, with vigorous shaking (250rpm). Then, it was diluted 1:1,000 in 250ml/500ml fresh LB medium incl. antibiotics, and was incubated for 12-16h at 37°C/32°C. A fresh glycerol stock was prepared with 1ml of the culture and 1ml freezing medium.

2.2.15.14 Plasmid-DNA Preparations

Plasmid DNA had to be prepared in relatively large amounts for transfection experiments (see 2.2.15.14.1). Furthermore, preparation of BAC-plasmid DNA was required for the generation of revertant virus mutIRFErev (see 2.2.15.14.2+3).

2.2.15.14.1 Plasmid Maxi Preparation

Kit: Plasmid Maxi Kit (QIAGEN)

Plasmid DNA for transfection experiments (see 2.2.17) was prepared using the QIAGEN Plasmid Maxi Kit. The principle of this protocol is an alkaline lysis of the bacterial cell by binding of the plasmid DNA to an anion-exchange column under certain conditions (salt, pH). Thereby, cellular components such as RNA, Proteins, and others are washed from the column. The purified plasmid DNA can then be eluted from the column in a solution with a high salt concentration. Finally, the DNA is desalted by isopropanol.
A suspension culture of the bacteria containing the plasmid in question was grown in 250ml/500ml fresh LB medium incl. antibiotics (see 2.2.16.12.2). The bacterial cells were harvested by centrifugation at 6000xg for 15min at 4°C (Sorvall RC5 Plus, rotor SLA 1500/SLA3000). Optionally, the cell pellets can be stored at -20°C at this point. Afterwards, the bacterial pellet was resuspended in 10ml buffer P1 containing RNase A, and mixed with 10ml buffer P2. The tube was then inverted carefully, and was incubated for 5min at RT. After that, 10ml chilled buffer P3 were added, and the tube was inverted to be mixed thoroughly. Then, it was incubated for 20min on ice. The DNA was separated from cell debris by centrifugation at 20,000xg for 30min at 4°C (rotor SLA 1500). Meanwhile, a QIAGEN-tip 500 column was equilibrated with 10ml buffer QBT. Then, the clear supernatant containing the DNA was applied to the QIAGEN-tip. It was washed 2x with 30ml buffer QC each. The DNA could then be eluted in 15ml buffer QF. It was precipitated with 0.7x volumes (10.5ml) isopropanol and centrifugation at 15,000xg for 30min at 4°C (rotor HB-6, Corex tubes). The supernatant was decanted carefully, and the DNA pellet was washed with 5ml 70% ethanol, and was centrifuged again for 10min at 15,000xg. Thereafter, the supernatant was discarded carefully, and the pellet was air-dried for 5-10min at ~20°C. Finally the DNA was dissolved in 250µl 10mM Tris-HCl, pH 8.5. The concentration and purity were determined with the NanoDrop (see 2.2.15.6). The purified plasmid DNA was stored at -20°C. For further reading, see QIAGEN Plasmid Purification Handbook.

2.2.15.14.2 BAC Mini Preparation

Buffer I:	EDTA	10mM
	Tris/HCl	50mM
	adjust to 1l (aq.dist.), pH 8.0 HCl, autoclave	
	RNase A	100µg/ml
Buffer II:	NaOH	200mM
	SDS	1% (v/v)
	adjust to 100ml (aq.dist.), pH 12.5-13, autoclave	

Buffer III:	KAc	3M
	(5M KAc 60ml + acetic acid 11.5ml)	
	adjust to 100ml (aq.dist.), autoclave	

BAC-plasmid DNA had to be purified at several steps during the generation of revertant virus mutIRFErev. It is important to stick to some rules when working with BAC DNA: no vortexing of the samples, use only cut pipet tips, no freezing of solutions (storage at 4°C).
A single colony was picked from a selective LB agar plate, and a culture of 10ml LB medium + Cam was inoculated and grown for 16-20h at 37°C. From this culture, a glycerol stock was prepared (500µl culture + 500µl freezing medium) and stored at -70C. The rest of the culture was transferred to a 15ml tube tube and centrifuged at 4°C for 10min at 3,950xg. The bacterial pellet was resuspended in 250µl buffer I, and was transferred to a 2ml microcentrifuge tube, before 350µl buffer II were added. The tube was inverted carefully and incubated for <5min at ~20°C. Then, 350µl buffer III were added, mixed likewise, and incubated for 10min on ice. Afterwards, the mixture was centrifuged for 10-15min at 21,000xg at 4°C. The supernatant was transferred to a 2ml microcentrifuge tube, and the DNA was precipitated with 0.8x volumes (700µl) isopropanol. It was centrifuged for 25min at 21,000xg at 4°C. The supernatant was discarded carefully, and the pellet was dried for 3min. Finally, it was resuspended in 100µl Tris buffer (10mM) (containing RNase 1:1,000) at ~20°C for 10min, and was then stored at 4°C. The purified BAC-plasmid DNA was linearized by restriction (see 2.2.16.13), and its integrity was finally visualized in a BAC-gel (see 2.2.15.15.1).

2.2.15.14.3 BAC Maxi Preparation

Kit:	Nucleo-Bond PC 500 (MACHEREY-NAGEL)	
TE buffer:	Tris/HCl	10mM
	EDTA	0.1mM
	pH 8.0	

For this, 500ml LB medium + Cam were inoculated with 1ml over night culture of the GS1783 clones containing the mutIRFE-rev BAC, and incubated for 18-20h at 32°C (250rpm). The DNA was purified with the Nucleo-Bond PC 500 kit, following the manufacturer's instructions for low copy BAC plasmids, and was dissolved in 200µl TE buffer. Afterwards, the DNA integrity was checked by restriction digest (see 2.2.15.15) and electrophoresis (2.2.15.11).

2.2.15.15 Restriction of Plasmid DNA

2.2.15.15.1 Restriction of Purified BAC-Plasmid DNA

Restriction enzymes:	*Eco*RI (20,000U/ml, New England BioLabs)
	I-*Sce*I (5,000U/ml, New England BioLabs)
Pipetting scheme *Eco*RI:	50µl BAC Mini preparation
	3µl *Eco*RI (30U)
	8µl *Eco*RI buffer
	19µl H_2O
	Incubate for at least 4h at 37°C
Pipetting scheme *Eco*RI + I-*Sce*I:	50µl BAC Mini preparation
	3µl *Eco*RI (60U)
	3µl I-*Sce*I (15U)
	8µl I-*Sce*I buffer 1x (100µg/ml BSA)
	16µl H_2O
	Incubate for at least 4h at 37°C

Purified BAC DNA was restricted with enzyme *Eco*RI to test its integrity, before separation by gel electrophoresis. To verify a successful 1st Red-recombination in the cloning process of mutIRFErev, BAC DNA of the clones was restricted with both enzymes *Eco*RI and I-*Sce*I in one sample.

2.2.15.15.2 Restriction Analysis

Plasmid:	pDrive_m152 (5,313bp)
Restriction enzyme:	*Bam*HI (20,000U/ml, New England BioLabs), buffer 3 + BSA
	*Hind*III (20,000U/ml, New England BioLabs), buffer 2
Pipetting scheme:	10µl DNA (30µg)
	2µl (20U) *Bam*HI or *Hind*III
	10µl 10x buffer 3 or 2
	78µl H_2O
	Incubate for 3h at 37°C

For the generation of a DIG-labeled RNA probe used in northern blot analyses (see 2.2.16.6), plasmid pDrive_m152 was restricted and subsequently *in vitro* transcribed.

2.2.15.15.3 PCR Template Digest

Restriction enzyme:	*Dpn*I (40,000U/ml, New England BioLabs), buffer 4

Pipetting scheme: 50µl PCR mix
2µl *Dpn*I (40U)
5µl 10x buffer
Incubate for 1.5h at 37°C

The purified PCR product from the 2nd PCR for Tischer recombination (see 2.2.15.16.2) was restricted with *Dpn*I to remove template DNA, before it was used for the transformation into GS1783 containing the mutated BAC plasmid mutIRFE.

2.2.15.16 Tischer Recombination

In this work, revertant virus mutIRFErev was generated using the two-step Red-mediated recombination (Tischer et al., 2006). The corresponding mutant virus mutIRFE had been generated by a colleague (S. Emde) with the same method.

2.2.15.16.1 First Red-Recombination

Glycerol: 10% (v/v), pre-cooled at 4°C

Starter cultures with single colonies of the GS1783 in 5ml LB + Cam were grown over night at 32°C. Of these cultures, 1:20 and 1:50 dilutions in 50ml LB + Cam were prepared and incubated at 32°C and 250rpm, until an OD_{600} of 0.5-0.7 was achieved. The cultures were incubated in a water bath shaker (250rpm) at exactly 42°C for 15min. Then, the cultures were transferred into pre-cooled 50ml tubes and cooled down in ice water for 20min with occasional stirring. After that, the bacteria were pelleted by centrifugation at 4,500xg for 5min at 4°C (Sorvall RC5 Plus, SLA 3000), and the pellet was washed (on ice) with 50ml 10% glycerol. This step was repeated 2x. After the last centrifugation, the pellet was dissolved in 500µl (1:100 volume of the culture) 10% glycerol, and aliquots of 50µl were dispensed in pre-cooled microcentrifuge tubes. The bacteria were kept on ice for the transformation.

2.2.15.16.2 Transformation

Different amounts of a freshly generated and purified PCR product (100-250ng) were added to 50µl of electrocompetent GS1783 (see 2.2.15.16), mixed carefully, and incubated for 5min on ice. The mixture was transferred to pre-cooled 0.1cm cuvettes, which were then put in the Gene Pulser for electroporation (1.8kV, 25µF, 200Ω). After that, 1ml LB medium (Ø antibiotics) was added per sample, and the bacteria were incubated for 1.5h at 32°C under agitation. Of these bacteria, 100µl were directly streaked on LB agar plates + Cam + Kan, the rest was pelleted and dissolved only in a small volume, which was then streaked on another plate. The plates were incubated at 32°C for

20-22h. The next day, single colonies were picked, and 10ml LB + Cam + Kan were inoculated with these and incubated over night at 32°C (250rpm). Glycerol stocks were prepared and stored at -70°C. The BAC DNA was purified (see 2.2.15.14) and subjected to restriction digest with *Eco*RI and I-*Sce*I with subsequent verification in a BAC gel (see 2.2.15.11).

2.2.15.16.3 Second Red-Recombination

Two positive GS1783 clones were streaked on LB agar plates + Cam and incubated for 20-22h. Thereof, two single colonies were picked and incubated each in 1ml LB +Cam at 32°C over night (250rpm). The next day, 2ml LB + Cam were inoculated with 100µl of the over-night culture and incubated at 32°C for 2h (250rpm). After that, 2ml pre-warmed LB + Cam + 1% arabinose (prepared freshly) were added, and the bacteria were incubated therein for exactly 30min at 32°C (250rpm). Then, the cultures were transferred to a pre-warmed water bath at 42°C and incubated for exactly 15min (250rpm). Afterwards, the cultures were incubated again at 32°C for 3h (230rpm). They were diluted 1:1,000 and 1:10,000, and 100µl of each were streaked on agar plates + Cam + 1%arabinose (fresh), the rest was pelleted and dissolved only in a small volume, and was then streaked on the plates (wire loop). The plates were incubated at 32°C until the next day. Fresh agar plates +Cam+1%arabinose were inoculated with single colonies and incubated over night. After that, single colonies were picked and transferred to replica plates, meaning one colony was used to inoculate first a plate + Cam and then a plate + Cam + Kan, and these plates were incubated at 32°C over night. Small colonies normally appear to carry the BAC mCMV-genome. Only the Kan-sensitive colonies were used to inoculate 10ml LB +Cam, and were incubated at 32°C over night. From these cultures, BAC DNA was prepared, restricted (*Eco*RI), and used as template in a PCR for sequencing of the mutated region (2.2.15.7).

2.2.15.17 m152 Promoter Activity

In order to investigate the influence of the IRFE on *m152* promoter activity, different luciferase reporter plasmid constructs were tested in Dual-Luciferase reporter-gene assays.

2.2.15.17.1 Transient Transfection of Plasmid DNA

Cells:	NIH 3T3
	BAM25
Culture media:	DMEM + 10% NCS
	DMEM (without serum, proteins, or antibiotics)

Reporter plasmids (pGL3):	pGL3 basic (negative control)
	m152 -IRFE
	m152IRFE
	m152-mutIRFE
	m152-perfISRE
Control plasmid:	pRL-TK (GenBank AFO25846; Promega, No. E 2241)
Kit:	PolyFect Transfection Reagent (QIAGEN)

Foreign genetic material (DNA, siRNA) can be introduced into eukaryotic or prokaryotic cells by transfection. Different methods for transfection can be applied. Here, transient transfection experiments were performed, which limit existence of the foreign DNA in the cells to a few days, before it is degraded. For the transfer, dendrimers (PolyFect®, QIAGEN) were used, which assemble with DNA into compact structures, thereby optimizing the entry of DNA into the cell. The positive charge of the complexes allows them to bind to negatively charged receptors on the cell surface. Probably, the cell incorporates the complexes by phagocytosis. The PolyFect buffer ensures stability and transport of the complexes into the nucleus, which is required to inhibit lysosomal nucleases (see PolyFect Transfection Reagent Handbook, 2000).

For the reconstitution of revertant virus mutIRFErev, BAC DNA was purified (2.2.14.3) from the newly generated clones, and was transfected into MEF cultures (2.2.2). Cells were seeded at a density of $2x10^5$ cells in 60mm dishes, and were then kept in the incubator for 18h. Thereafter, the cells were cotransfected with 20ng of *Renilla* luciferase-encoding control plasmid pRL-TK to standardize for transfection efficiency, and 2.5µg of one of the firefly luciferase-encoding reporter plasmids (see above). For transfection, the required amounts of the plasmid DNAs were diluted in DMEM (without serum, proteins, or antibiotics), in a total volume of 150µl per dish. Thereafter, 15µl of the transfection reagent (PolyFect) were added to each sample and mixed by pipetting. The samples were incubated for 10min at 20°C to allow complex formation. Meanwhile, the cells were washed once with 4ml PBS, and 3ml of fresh medium was added to each dish. After the 10min incubation period, 1ml fresh medium was added to the transfection mix, and the whole volume was added to the cells. The dishes were swirled slowly to ensure uniform distribution. After 5h incubation at 37°C, the transfection mix was removed, and the cells were washed 2x with medium. Then, they were incubated for 18h. The next day, the cells were treated with certain amounts of recombinant IFNα or IFNβ (500-2,000U), and IFNγ (20ng/ml) in the culture medium, and were incubated for 24h. In a different setting, cells were infected 1d after transfection with WT.BAC at an MOI of 4 and incubated for 24h. After the incubation period, the results were analyzed (see, 2.2.15.17.2).

2.2.15.17.2 Dual Luciferase Reporter Gene (DLR) Assay

Material: DLR-Assay System (Promega, No. E1910)

- 1xPassive Lysis Buffer (PLB): Dilution of 5xPLB with aq. dist, storage at 4°C ≤ 1mon, at -20°C ≤ 1year
- Luciferase-Assay-Reagent (LARII): Dissolve lyophilized LARII in 10ml Assay Buffer II, storage at -70°C ≤ 1year
- 1xStop&Glo Reagent (10 measurements): Dilution of 20µl 50xStop&Glo substrate with 1,000µl Stop&Glo Buffer. Note: Prepare freshly

24h after transfection, the cells were washed once with 4ml PBS per dish (all further steps were carried out on ice). Thereafter, they were lysed with 400µl 1xPLB per dish, and still adherent cells were scraped off with a cell scraper. The lysate was pipetted up and down to enhance lysis, and was then completely transferred into a 1.5ml microcentrifuge tube. The cell suspension was centrifuged for 3min at 20,000xg (4°C). Afterwards, the pellet was resuspended again to yield a larger amount of protein. For the measurement, 100µl LARII per sample were predispensed into a luminometer tube. 20µl of the cleared cell lysate was then added and mixed with a pipet. A single-sample luminometer was used to measure the luminescence, expressed as relative luminescence units (RLU). According to the read-inject-read format of the DLR assay, for each sample, signals from firefly and *Renilla* luciferase were detected sequentially. At first, the firefly-luciferase was measured (RLU^{FL}), and after addition of 100µl 1x Stop&Glo reagent the *Renilla*-luciferase was detected (RLU^{RL}).

Note: Blank samples containing the two reagents (LARII, 1x Stop&Glo) without any lysate were measured to subtract backpassed RLU from assay RLU, as recommended by the manufacturer. These normalized values were then used to calculate RLU of each sample, dividing RLU^{FL} by RLU^{RL}.

2.2.16 Methods in Molecular Biology: RNA

2.2.16.1 Oligonucleotides

β-actin_For1	n 809-830; 5´ GAC GGC CAG GTC ATC ACT ATT G 3´
β-actin _Rev1	n 873-896; 5´ CAC AGG ATT CCA TAC CCA AGA AGG 3´
β-actin _Probe	n 833-852; 5´ [Cy5] AAC GAG CGG TTC CGA TGC CC [BHQ-2~Cy5] 3´ Amplicon length: 88bp; GenBank Acc. No. NM_007393
m152_For1	n 210,672-210,692; 5´ CGT TCG CGA GAC TGA TGT TGT 3´

m152_Rev1	n 210,720-210,740; 5´ GCA ACG GCT ACG TGT CCT GTA 3´
m152_Probe	n 210,696-210,716; 5´ [6~FAM] CCA ACG GAA CCT GAG TGC GCA [TAMRA~6~FAM] 3´ Amplicon length: 69bp; GenBank Acc. No. NC_004065

Oligonucleotides used for qRT-PCR analyses were purchased from biomers.net GmbH, Operon Biotechnologies, or Applied Biosystems. The specifications of mCMV-sequences resulted from Rawlinson et al., 1996 (GenBank Acc. No.: NC_004065). The primers were dissolved in sterile aq.dist., the TaqMan probes in sterile Tris buffer, pH 8.0.

2.2.16.2 Pretreatment of Devices and Liquids

Ribonucleases (RNases) are very active and stable enzymes and normally do not require cofactors to function. Therefore, RNases are hard to handle, and even small amounts are sufficient to destroy RNA. RNase decontamination is vital for all methods dealing with RNA, such as RNA isolation, qRT-PCR, or northern blot analyses. This was accomplished by using only stringently cleaned or sterile devices, and pretreated solutions. For preparation of buffers and solutions, aq.dist. was supplemented with 0.2% diethyl pyrocarbonate (DEPC) and stirred over night. The next day, it was autoclaved, and could then be used (H_2O_{DEPC}). Devices for northern blot analyses (e. g. electrophoresis tank, tray, comb, dishes) were cleaned with 0.5% SDS in H_2O_{DEPC} for 1h at ~20°C, and were then dried with 70% ethanol. Alternatively, they were incubated with RNase Away™ (Roth) for 1min, and were then obligatorily rinsed with H_2O_{DEPC} (traces of the reagent degrade RNA). The RNase Away solution was also used to clean laboratory surfaces. Special RNA working spaces (template tamers, benches) were equipped with separate pipets and other materials.

2.2.16.3 Purification of RNA from Cell Cultures

Kit:	RNeasy Mini Kit (QIAGEN)
	RNase-free DNase Set (QIAGEN)
Materials:	Cell scraper (Sarstedt)
	QIAshredder (QIAGEN)

Total RNA was isolated from cell cultures using the RNeasy Mini Kit, and was then subjected to gene expression analyses. In this kit, a silica-gel-based membrane which selectively binds RNA is used. The lysis of cells with buffer RLT (see below), and the usage of ethanol create conditions that promote selective binding of RNA to the membrane. Traces of DNA, which might copurify, are removed by treatment with DNase.

Together with other contaminants, they are washed away in several washing steps, and by microspin technology so that finally total RNA can be eluted in RNase-free water. With the RNeasy Mini procedure, all RNA molecules longer than 200 nucleotides are isolated so that the procedure enriches for mRNA. The maximum binding capacity of the column is 100µg RNA. For a detailed description, see the RNeasy Mini Handbook (QIAGEN).

Harvested cells were washed 1x with PBS, and 350µl/well of buffer RLT containing β mercaptoethanol (βME) were pipetted onto the cells. Then, the cells were scraped off with a cell scraper, and the lysate from one well was loaded directly onto a QIAshredder homogenizer. Thereby, cells were quickly and effectively homogenized, without cross-contamination of the samples. The homogenates were stored at -70°C until the samples were further processed for RNA purification. The samples were thawed, mixed 1:1 with 70% ethanol, and loaded onto RNeasy Mini columns. RNA was purified according to the manufacturer's instructions, with an obligatory on-column DNase digest. RNA was eluted in 30µl RNase-free H_2O, and the amount and purity were determined with the NanoDrop (see 2.2.15.6). The samples were stored at -70°C.

2.2.16.4 Reverse Transcriptase Polymerase Chain Reaction (RT-PCR)

Kit: OneStep RT-PCR Kit (QIAGEN)

Total RNA purified from infected cell cultures or from infected mice was used in RT-PCR to amplify selected sequences, such as viral m152 and cellular β-actin. For this, the OneStep RT-PCR Kit was used. This kit contains enzymes for both, reverse transcription and PCR amplification. Omniscript and Sensiscript reverse transcriptases are highly specific and efficient in reverse transcription of any RNA quantity between 1pg and 2µg. The use of HotStar*Taq* ensures temporal separation of reverse transcription and PCR, allowing both processes to be performed sequentially in a single tube. During the hot-start procedure, the reverse transcriptases are inactivated and HotStar*Taq* is activated. The advantage of this system is that initially, RNA is selectively transcribed into cDNA with a sequence-specific primer, and that this cDNA is subsequently amplified.

2.2.16.5 Quantitative Real Time RT-PCR (qRT-PCR)

Transcription kinetics of viral genes were performed with qRT-PCR (for principles of real-time qPCR, see 2.2.15.8), using sequence-specific primers and fluorescence-labeled probes (see 2.2.16.1). In order to determine comparable C_T values, a common threshold has to be set at a point where the fluorescence signal is just separating from the backpassed signal, and amplification is exponential. Then, for each sample, the number of cycles necessary to reach this threshold is analyzed (i.e. C_T). However, it is important to

consider the amount of starting material when comparing these values. Although, the amount of total RNA was determined using the NanoDrop (see 2.2.15.6), and according to this, 500ng of each sample was used in qRT-PCR, deviations generally occur in measurements and by pipetting. Therefore, the C_T of *β-actin*, as being a housekeeping gene, was determined in each sample, and was used as a standard for the amount of starting material (relative quantification). For the calculation of the relative expression values, the C_T of *β-actin* was subtracted from the C_T of the viral gene in question (dC_T). These dC_T values could then be compared between different samples. However here, the change in expression of *m152* (target) at different times p.i. was determined in relation to the expression at time 0 p.i. (calibrator). For the calculation of this, the C_T values of the calibrator samples were subtracted from the dC_T values of each target sample in question (ddC_T). Relative expression was finally calculated according to the formula: 2^{-ddCT}.

To make the method even more accurate, a duplex qRT-PCR was performed, meaning that both, the cellular and the viral gene, were detected in one sample by using differently labeled probes e.g. β-actin-Cy5 and m152-FAM, respectively. Master mixes (MM) were prepared (see below) under a Template Tamer hood (Captair bio Erlab, Köln), and RNA was added under another. The fluorescent dye ROX was used as an internal reference for normalization of fluorescence signals. All qRT-PCRs were performed with the TaqMan 7500 (Applied Biosystems).

qRT-PCR pipetting scheme:

Component	Volume/Reaction	Final concentration
5x QIAGEN OneStep RT-PCR Buffer	4µl	1x
dNTP Mix (10mM each)	1.34µl	670µM
$MgCl_2$ (25mM)	1.2µl	1.5mM
Primer-For (10µM)	1.2µl	0,6µM
Primer-Rev (10µM)	1.2µl	0,6µM
Probe (10µM)	0.53µl	0,26µM
Primer-For (10µM)	1.2µl	0,6µM
Primer-Rev (10µM)	1.2µl	0,6µM
Probe (10µM)	0.53µl	0.26µM
ROX (10µM)	0.264µl	0.132µM
QIAGEN OneStep RT-PCR Enzyme Mix	1µl	—
RNA	5µl	500ng
RNase-free H_2O	1.336µl	—
Total Volume	20µl	—

TaqMan 7500 qRT-PCR Profile:

Step	Time	Temperature	Comment
Reverse Transcription	30min	50°C	
Initial PCR Activation Step	15min	95°C	Activation of HotStar*Taq*-DNA-Polymerase, denaturation of

			reverse transcriptases
2-Step Cycling:			
Denaturation	15s	95°C	
Annealing	60s	60°C	Depends on primer sequence
Number of Cycles	45		

2.2.16.6 Northern Blot

Viral RNA was isolated 60min p.i. from cell lysates using the RNeasy Mini Kit (QIAGEN) (see 2.2.16.3). The RNA was then separated by gel electrophoresis and transferred to a nitrocellulose membrane. A digoxigenin (DIG)-labeled m152-RNA probe was used to hybridize with the mRNA and subsequently visualize the signal.

2.2.16.6.1 Generation of a DIG-labeled m152 Probe

Kit:	MAXIScript in vitro transcription kit (Ambion)
	RNeasy MinElute Cleanup Kit (QIAGEN)
Nucleotides:	Digoxigenin-11-UTP 250nmol [25µl] (Roche)
Plasmid:	pDrive_m152

For the northern blot analysis of m152 mRNA, 2 DIG-labeled RNA probes (positive and negative control) were generated. The linearized plasmid DNA was used as a template for *in vitro* transcription with either SP6 or T7 RNA polymerase, respectively incorporating DIG-11-UTP into the RNA transcript. In addition to the DIG-labeled probes, unlabeled probes were generated as controls.

Pipetting scheme for *in vitro* transcription:

	labeled	unlabeled
Nuclease-free H_2O (ad 20µl)	ad 20 µl	ad 20 µl
DNA template (1µg)	4.2µl	4.2µl
ATP 10mM	1µl	1µl
CTP 10mM	1µl	1µl
GTP 10mM	1µl	1µl
UTP 10mM	1µl	0.6µl
DIG-UTP	-	0.4µl
Enzyme mix	2µl	2µl
10x transcription buffer 1h, 37°C	2µl	2µl
Turbo DNase 15min, 37°C	1µl	1µl

Afterwards, the RNA transcripts were adjusted to 100µl with RNase-free H_2O, and were cleaned up according to the RNeasy MinElute Cleanup Handbook. The samples were eluted in 40µl RNase-free H_2O, each. The eluates were pipetted on the same column and

eluted again for maximum yield of RNA. Finally, concentration and purity of the probes were determined with the NanoDrop (see 2.2.15.6). The probes were stored at -70°C.

2.2.16.6.2 Dot Blot

20xSSC_{DEPC}:	3M NaCl (58.44g/mol)	175.3g/l
	0.3M sodium citrate (294.1g/mol) ($C_6H5Na_3O_7x2H_2O$)	88.2g/l
	pH 7.0 with HCl	
	0.1% DEPC	1ml
	Adjust to 1l (aq.dist.), stir over night, autoclave	
Wash I:	2xSSC_{DEPC}	1l (dilute from 20x)
	SDS	1g (0.1%)
Wash II:	0.1xSSC_{DEPC}	1l (dilute from 20x)
	SDS	1g (0.1%)

DIG Wash and Block Buffer Set (Roche):

• Washing buffer:	1x washing buffer (dilute from 10x)	100ml
• Blocking solution:	1x maleic acid (dilute from 10x)	90ml
	10x blocking solution	10ml (1x)
• Detection buffer:	1x detection buffer (dilute from 10x)	50ml

Antibody: Anti-Digoxigenin-AP Fab fragments (Roche)

Substrate: CSPD (Roche)

All dilutions were made with H_2O_{DEPC}.

In order to check the efficiency of the labeling reaction, and determine the amount of DIG-labeled product, a dot blot was performed as described below.

A nylon membrane was shortly washed in H_2O_{DEPC}, and then incubated for 30min in 10xSSC. 10-fold dilutions (100-1ng/µl) of each probe were pipetted dropwise on the membrane. The membrane was laid on a Whatman 3MM paper, and the RNA probe was cross-linked to the membrane by UV irradiation (0.15J/cm^2). All succeeding stringency washes were carried out under slight agitation. The membrane was washed 2x for 5min with Wash I at ~20°C, 2x for 15min with pre-warmed Wash II at 68°C (in roller bottles in a hybridization oven), and 3min with 1x washing buffer at ~20°C. Then, the membrane was blocked for 30min in 1x blocking solution. The antibody was centrifuged for 5min at 10,600xg and was diluted 1:10,000 in 1x blocking solution (2µl/20ml/100cm^2 membrane), and the membrane was incubated therein for 30min. After that, the membrane was washed again 2x for 15min with washing buffer. Then, it was equilibrated for 3min in 40ml 1x detection buffer. The substrate was diluted 1:100 in 1x detection buffer (20µl/2ml), and the membrane was incubated therein with the RNA side facing up, in a sealed

development folder for 5min at ~20°C, and for 15min at 37°C. Finally, the chemiluminescence signal was detected on X-ray film.

2.2.16.6.3 RNA Gel Electrophoresis

10xFA buffer:	200mM MOPS (209.29g/mol)	41.6g/l
	50mM sodium acetate (136.08g/mol) ($C_2H_3NaO_2x3H_2O$)	6.8g/l
	10mM EDTA (380g/mol)	3.8g/l
	dissolve in 800ml H_2O_{DEPC}	
	pH 7.0 (NaOH)	
	adjust to 1l (H_2O_{DEPC}), autoclave	
Formaldehyde gel:	1% agarose	3g/300ml
	1xFA buffer	30ml10xFA buffer
	adjust to 300ml (H_2O_{DEPC})	
	boil in microwave	
	cool down to 60°C in water bath	
	formaldehyde 37% (v/v)	5.4ml
	0.5µg/ml ethidium bromide	15µl/300ml gel
1x running buffer (prepare freshly!):		
	200ml 10xFA buffer	
	40ml formaldehyde 37% (v/v)	
	1760ml H_2O_{DEPC}	
Loading buffer:	80µl 0.5M EDTA pH 8.0	
	720µl 37% formaldehyde (v/v)	
	2ml glycerol (sterile)	
	3,084µl formamide	
	4ml 10xFA buffer	
	100µl H_2O_{DEPC}	
	1 spatula-tip bromophenolblue	
	store at -20°C	
RNA marker:	RNA molecular weight marker I, digoxigenin-labeled (Roche)	
	ssRNA Ladder (New England Biolabs)	

All devices for gel electrophoresis (tray, comb, chamber) and surfaces had to be cleaned prior to use (see 2.2.16.2) to prevent contamination and degradation of the RNA.
The formaldehyde gel was poured in a 20x20cm tray. When it had become solid, it was pre-run at 80V for 30min in fresh electrophoresis buffer. Meanwhile, the RNA samples were prepared for loading. For this, 1µg of total RNA was diluted in 10µl RNase-free H_2O,

and the samples were mixed with 1vol of loading buffer (10µl). The RNA markers were also mixed with 1vol of loading buffer, 2.5µl (50ng) of the Roche marker were used, and 6µl (5µg) of the NEB marker were used. All samples and markers were then denatured for 10min at 65°C in a thermo mixer, chilled for 5min on ice, and spun down. Thereafter, all samples were loaded onto the prerun gel, and the gel was run at 80V for about 1h and then at 105V for 2-3h. After that, the RNA bands in the gel were documented under UV light, and the marker bands (NEB marker) were measured with a fluorescent ruler.

2.2.16.6.4 Northern Blot

After the RNA had been separated by gel electrophoresis, it was transferred to a nylon membrane for subsequent detection of the signals. Before that, the lower part of the gel was cut off (no RNA there, as verified under UV). Then, for the transfer, the membrane was washed with H_2O_{DEPC}, and then incubated in 20xSSC_{DEPC} for 30min on a shaker to remove formaldehyde. Then, the RNA was transferred to the nylon membrane by capillary transfer. For this purpose, 3 Whatman 3MM paper and the membrane were cut, each 20x10cm in size. The 3 papers were shortly rinsed with H_2O_{DEPC}, and were put together with the membrane for 30min in 10xSSC_{DEPC}. The blot was then assembled as follows:

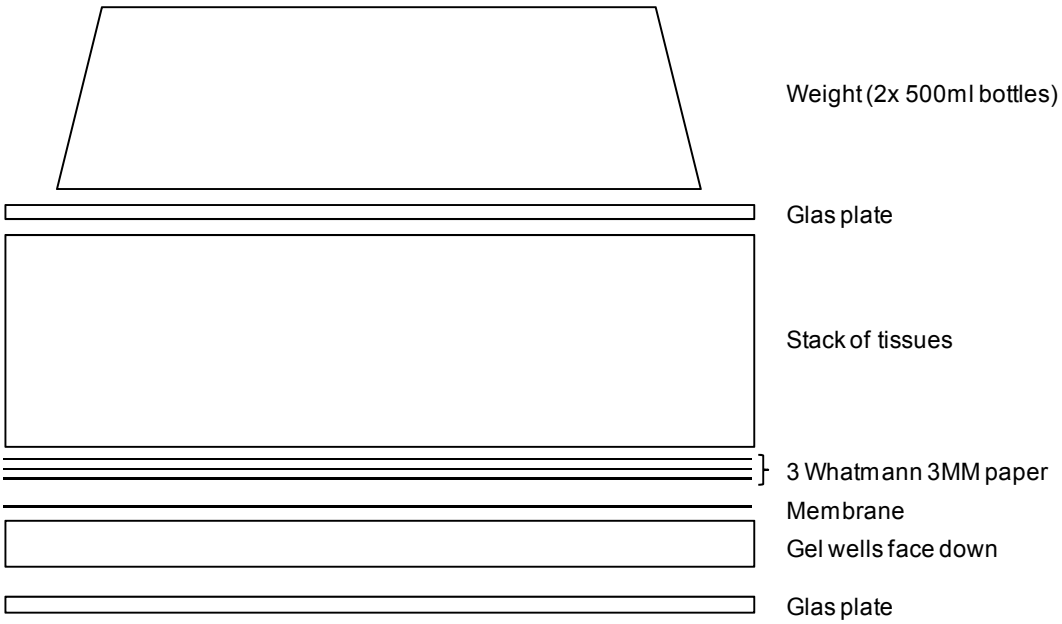

Fig. 2.3 Northern blot for capillary transfer.

After the gel, membrane, and 3 papers were put together, air bubbles were removed by rolling a pipet over the last paper. The capillary transfer was performed over night. The next day, the blue loading buffer was visible on the membrane. The localization of the wells was marked with a pencil on the membrane, and it was washed shortly in 6xSSC_{DEPC} (diluted from 20xSSC_{DEPC}). The membrane was laid on a Whatman 3MM

paper and the RNA probe was cross-linked to the membrane by UV irradiation (0.15J/cm^2).

2.2.16.6.5 Hybridization

Hybridization solution: DIG Easy Hyb (Roche)

As a next step, the probe had to hybridize with the RNA, linked to the membrane.
Firstly, the hybridization solution was pre-heated (20ml/100cm^2 membrane). In general, 68°C is recommended for RNA:RNA hybridization. The membrane was shortly incubated in 2xSSC_{DEPC} (diluted from 20x). Then, it was sealed with the pre-warmed hybridization solution, transferred into a roller bottle, and was incubated for 30min at 68°C (hybridization oven) under gentle rotation. Meanwhile, the DIG-labeled RNA probe was denatured (100ng/ml hybridization solution: 4ml/100cm^2 membrane) by boiling the required amount (2ml safe-cap tube) for 10min in a thermo mixer (99°C), it was rapidly cooled down on ice-water, and spun down shortly. First, 1ml of the pre-heated hybridization solution was added to the probe, and this was transferred to the rest of the solution (15ml tube), and the membrane was sealed in this solution, put in a roller bottle, and was incubated in the oven at 68°C over night.

2.2.16.6.6 Detection

For washing buffers, solutions, antibody, and substrate see 2.2.16.6.2.
The probe-target hybrids were detected with an alkaline-phosphatase-conjugated antibody (anti-DIG-AP) by a chemiluminescence reaction (CSPD). Light-emission was recorded by exposure to X-ray film. Stringency washes, blocking, antibody incubation, and detection was performed as described above (2.2.16.6.2), but with 10ml detection solution for 200cm^2 membrane. Multiple exposure times were applied to achieve an appropriate signal strength.

2.2.17 Immunohistochemistry (IHC)

In this work, IHC was applied to *in situ* quantify mutIRFE, ∆m152, and ∆m152rev or ∆m157Luc_m164SIINFEKL infected liver cells by staining of viral protein IE1, and to quantify and localize CD8 T cells after adoptive transfer by staining of CD3+ cells.

2.2.17.1 Organ Processing

Buffered formalin 4%:	KH_2PO_4	66mM	9.07g
	Na_2HPO_4	84mM	11.86g
	Formalin 37% (v/v)		140ml
	adjust to 1l (aq.dist.), pH 7.4 (NaOH)		

After organ dissection, livers were fixed in buffered formalin for about 18h at ~20°C. The next day, they were washed in tap water for 2h. After that, livers were dehydrated in graded alcohol for 45min each (isopropanol in aq.dist. (v/v) 20%, 40%, 60%, 80%, 90%) and then 2x 45min and 1x18h in 100% isopropanol. Thereafter, they were incubated 3x in xylene for 1h each, subsequently transferred to paraffin I (55C°) for 4h, and then to paraffin II (55C°) for 18h. Then, organs were embedded in paraffin. Prior to preparing 2µm micro sections, the paraffin-blocks were cooled down to -20°C. The slices were then stretched in a water bath (40°C) and mounted onto silanized microscope slides. Finally, the slides were dried at 37°C for 18h. Before immunohistochemical staining, slides were deparaffinized and rehydrated, by incubation 3x 5min in xylene, 2x 3min in 100% isopropanol, and 3min each in 90, 80, 70% (v/v) isopropanol.

2.2.17.2 Single-color IHC of the mCMV IE1 Protein

Trypsin:	NaCl	8g	137mM
	KCl	0.2g	2.7mM
	KH_2PO_4	0.2g	1.5mM
	Na_2HPO_4	1.15g	6.5mM
	EDTA	1.25g	3.4mM
	adjust to 1l (aq.dist.), pH 7.4, and autoclave		
	dissolve 1.25g trypsin after cooling, and store at 4°C		
Blocking solution:	H_2O_2 30% (v/v, aq.dist.)		0.6ml
	Methanol		59.4ml
Tris buffered saline (TBS):	Tris	12g	100mM
	NaCl	8.8g	150mM
	adjust to 1l (aq.dist.), pH 7.4		
Kit:	Vectastain ABC-peroxidase kit (Vector Laboratories)		
Substrate:	10mg 3,3' diaminobenzidine tetrahydrochloride hydrate (DAB) (Sigma)		
	75mg ammonium nickel (II) sulfate hexahydrate (Fluka) dissolve in 50ml Tris-HCl (50mM, pH 7.5), supplement with 17µl 30% (v/v) H_2O_2		

For antibodies, see Tab. 2.1.

The number of mCMV-infected liver cells after mutISRE or WT.BAC infection was determined and compared in the *in vivo* replicative fitness study (see 2.2.5.2), as well as after depletion of certain immune cells (see 2.2.13). *In situ* staining of the intranuclear viral immediate-early protein 1 (IE1) is the most sensitive alternative. This protein is expressed

and maintained from 2h p.i. on. It accumulates in the nucleus during the late phase of the replication cycle.

At first, tissue sections were treated with trypsin solution for 15min at 37°C to partially digest proteins, and were thereafter washed with aq.dist. for 3min. Endogenous peroxidases were blocked with blocking solution for 30min at 20°C, and the sections were subsequently washed with aq.dist. for 3min. Unspecific binding was inhibited by incubation of the sections in a 1:10 (v/v) dilution of normal serum rabbit in TBS, for 20min at ~20°C. All further steps were performed in a humid chamber to prevent drying of the sections. The first mCMV-specific antibody against IE1 diluted 1:250 in TBS (v/v) was a monoclonal antibody against IE1. Sections were incubated for 18h at 4°C. As an isotype control, sections were incubated accordingly with mouse IgG1. Thereafter, they were washed 2x with TBS for 3min. The secondary antibody goat α-mouse IgG diluted 1:200 in TBS (v/v) was added for 30min at ~20°C. The ABC solution was prepared 30min prior to use, and the slides were incubated therein for 30min at ~20°C, and then washed 3x with TBS for 10min. After that, slides were incubated in the peroxidase substrate (DAB) for 5-10min at 20°C, until the colored precipitate was visible. Excessive substrate was washed away 3x with aq.dist. for 1min, and the slides were counterstained with hematoxylin for 5s. Finally, the dried slides were sealed with a coverslip and PARAmount. The peroxidase-DAB-nickel stain resulted in a black color. Alternative staining procedures included peroxidase-DAB (brown).

2.2.17.3 Two-color IHC of IE1 and CD3

Unmasking solution:	Tri-sodium-citrate-dihydrate 10mM	2.941g/l aq.dist.
Blocking solution:	Dako Biotin Blocking System	
Antibodies and sera:	α-mouse CD3ε, mAB rat IgG1 (Acris)	
	goat α-rat Ig, biotinylated, polyclonal (BD Pharmingen)	
	goat α-mouse IgG , polyclonal (Sigma)	
	APAAP (alkaline phosphatase anti alkaline phosphatase) soluble complex, mouse MAb, clone AP1B9 (Sigma)	

For other buffers and solutions see also 2.2.17.1.

At first, the tissue sections were treated with trypsin solution for 15min at 37°C to partially digest protein. Thereafter, Heat Induced Epitope Retrieval was performed by boiling the slides (microwave) in unmasking solution for 5min. They were cooled down to ~20°C, and washed with tap water. Endogenous peroxidases were blocked, and the slides were further washed. Endogenous biotin was blocked with the Dako kit. After that, the slides were incubated in 1:20 diluted (TBS) antibody α-CD3ε for 18h at 4°C. Unbound antibody

was then washed away 2x with TBS for 3min. Then, tissues were incubated in 1:100 diluted (TBS) biotinylated α-rat Ab for 30min at ~20°C, and were washed 2x with TBS for 3min. This was followed by incubation with the ABC solution for 30min at ~20°C, and 3x washing with TBS for 10min. The slides were stained for 5-20min at ~20°C with DAB-nickel, and washed 3x with TBS for 10min. Afterwards, the slides were incubated in 1:10 diluted (TBS) normal rabbit serum for 20min at ~20°C, before being incubated for 18h at 4°C with monoclonal antibody to IE1. Unbound antibody was washed away 2x with TBS for 3min. This was followed by another incubation step in bridging antibody goat α-mouse, diluted 1:20 (TBS) for 30min at ~20°C, and 2 washing steps with TBS for 3min. The slides were further incubated with α-mouse APAAP complex, 1:50 (TBS), for 30min at 20°C, and washed 2x with TBS for 3min. The second stain was performed with Fuchsin for 10-30min at 20°C until a red precipitate was visible. Finally, the slides were washed with TBS for 3min, and were counterstained, and sealed as described above.

2.2.18 Methods of CD8 T Cell Effector Functions

2.2.18.1 Enzyme-Linked Immunospot (ELISPOT) Assay

ELISPOT plates:	MultiScreen$_{HTS}$-IP (Millipore), hydrophobic PVDF
Blocking medium:	MEMα + 10% (v/v) FCS
Washing solution:	PBS + 0.01% Tween 20 (50µl/500ml)
Secondary Ab dilution:	1µg Ab + 1ml PBS + 0.5% BSA (6ml/plate)
Enzyme dilution:	Streptavidine-alkaline phosphatase (MABTECH), 1:1,000 (PBS)
Substrate:	BCIP/NBT^{PLUS} (MABTECH), filter prior to use (0.45µm)

For antibodies, see 2.1.8.

Activated CD8 T cells produce and secrete IFNγ. Secretion of this cytokine can be detected by the ELISPOT assay, and the number of IFNγ-producing cells can be determined.

Antigen presenting cells (APC) were seeded together with the effector cells in 96-well ELISPOPT plates on a membrane which was covered with the first α-mouse IFNγ antibody. During cultivation, the effector cells are activated by the presented antigens. When they release IFNγ, the cytokine is bound by the antibody which is linked to the membrane. The bound cytokine is then visualized, by adding the second antibody (biotinylated α-mouse IFNγ), streptavidin-horseraddish peroxidase (HRPO), and a chromogen as substrate. This method allows for quantification of reactive effector cells, since 1 spot is caused by 1 cytokine-producing cell (Taguchi et al., 1990; Miyahira et al.,

1995). In this work, the assay was used to compare the activation of CD8 T cells isolated from either acute mCMV-infected or memory mCMV-infected mice, or of mCMV-peptide specific CD8 T cells, by stimulation with APC infected with either mutIRFE, mutIRFErev, ∆m152, ∆m152rev, or WT.BAC.

One day before the assay, the ELISPOT plate had to be coated with the primary antibody. At first, the membrane was activated with 20µl/well of 35% ethanol (prepared freshly) for exactly 1min at ~20°C, and was washed thereafter 3x with 200µl/well PBS. Then, 55µl of diluted α-mouse IFNγ antibody (5µg/ml PBS) were added and incubated for 18h at 4°C.

The next day, unbound antibody was washed off with 2x 200µl/well aq.dist. After that, unspecific bonds were blocked with 200µl/well blocking medium for at least 2h at 37°C. In the meantime, the APC and effector cells were prepared. In order to test *ex vivo* isolated effector cells from memory WT.Smith infected C57BL/6 mice (see 2.2.9), $1.8x10^5$ EL4 cells/90µl were exogenously loaded with a 10µl of a 10^{-6}M peptide stock solution, resulting in a final peptide loading concentration of 10^{-7}M. They were incubated for ~1h at 20°C. The cells were then washed 3x with medium, counted, and seeded at $1x10^5$cells/50µl medium/well. However, to test the avidities of the m164-CTLL, P815 cells were loaded with different concentrations of the synthetic m164 peptide (10^{-6}-10^{-13}M). Incubation, washing, and seeding were performed as described for EL4 cells. In order to compare the antigen presentation properties of MEF infected with different viruses, these APC were seeded in 100mm dishes, and were cultivated to almost complete confluence. If an IFNβ pretreatment was included in the experiment to enhance peptide presentation, MEF were incubated for 48h with 500U of the cytokine, prior to infection. Afterwards, they were centrifugally infected at an MOI of 4, and were incubated for 1h at 37°C. Then, the cells were washed, counted, and seeded at $1x10^5$cells/50µl medium/well.

Depending on the experiment, either e*x vivo* isolated effector cells from spleens of acute or memory infected mice, or m164-peptide specific CTLL (see 2.2.11) were added (different cell numbers, triplicate samples) to the APC in the ELISPOT plate. The cells were co-cultured for 18h at 37°C. The next day, the plate was washed 10x with 200µl/well washing solution. After that, the cells were incubated with 55µl of the secondary Ab dilution for 2h at 37°C. Unbound antibody was washed off 6x with 200µl/well washing solution, and 100µl/well of the enzyme dilution was added for 45min at ~20°C. This was followed by 6 washing steps, 3x 200µl/well washing solution and 3x 200µl/well PBS. Finally, 100µl/well substrate was added for ~20min at ~20°C until spots became visible, and the plate was washed under running tap water. As soon as the plates were dry, the number of spots could be counted under a microscope (Olympus SZX 12).

2.2.18.2 Cytolytic Assay (^{51}Cr-Release Assay)

Medium: RPMI + 5% (v/v) FCS

Cytolysis of APC is another effector function of activated CD8 T cells, and can be measured in the ^{51}Cr-Release Assay. Therein, APC are incubated with ^{51}Cr, and then co-cultured with the effector cells. Antigen-recognition via epitope-specific T-cell receptors (TCR) of CD8 T cells leads to cytolysis of the APC, and thus to the release of radioactivity, which can be quantified by a γ-counter.

P815 cells were used as APC, and were washed, counted, and 1x10^6 cells were incubated with 100µCi ^{51}Cr for 75min at 37°C. Then, the cells were washed 3x with medium and seeded at 1x10^{3}cells/50µl/well in a peptide plate which had been loaded before with triplicates of $\log_{10}$ titrations (10^{-7}-10^{-14} in 100µl) of the synthetic peptide. The cells were incubated with the peptide for 90min for exogenous loading of MHC class I molecules. Meanwhile, the CTLL were washed 3x with medium, and counted. 1.5x10^{4}cells/50µl/well (Effectors:APC = 15:1) were added to the APC. The cells were centrifuged for 5min at 110xg, and were incubated for 3.5h at 37°C. After that, the cells were sedimented by centrifugation at 550xg for 5min, and 100µl cell culture supernatant was transferred to counter tubes, and the released radioactivity was detected.

A high and a low lysis control were used to determine the number of specific and unspecific lysis, respectively. Therefore, 1x10^3 radioactively labeled APC/200µl medium/well were seeded in 2x9 wells. For the high control, the radioactivity in 9 wells of 100µl suspended cells was determined. For the low control, the radioactivity in 100µl culture supernatant was determined. Another control (no antigen) was included as well, by seeding P815 and effector cells without peptide added in 9 wells, and determining the radioactivity in 100µl cell culture supernatant. The calculation was made according to the following formula:

$$\text{Specific lysis [\%]} = \frac{cpm - lc}{hc - lc} \times 100$$

cpm = counts per min

lc = low control

hc = high control

3 Results

The ability of CMV to establish persistent infection in the face of the innate and adaptive immune response is due to modulation of infected host-cell recognition in the effector phase of the antiviral immune response. In this respect, the viral early protein m152 is a major immune modulator of mCMV, because it counteracts the action of two important components of the innate and adaptive immune system. On the one hand, it inhibits early NK-cell activation to viral infection by downregulating RAE-1, a ligand for the activating NK-cell receptor NKG2D (Krmpotić et al., 2002; Lodoen et al., 2003). On the other hand, it counteracts the CD8 T-cell response to infection by retaining peptide-loaded MHC class I complexes in the endoplasmic reticulum (ER)-Golgi intermediate compartment (ERGIC)-*cis* Golgi network, thereby decreasing cell surface expression (Del Val et al., 1992; Ziegler et al., 1997 & 2000). As part of the interplay of the immune system and the virus, both of these lymphocyte populations are regulated by interferons (IFN) with regard to their maturation, differentiation, and activity (Boehm et al., 1997; Biron et al., 1998 & 1999; Carnaud et al., 1999; Young & Hardy, 1995). Moreover, NK cells and CD8 T cells are the main producers of IFNγ themselves (Bach et al., 1997; Young, 1996). IFN are cytokines that were originally identified to interfere with viral replication and induce an antiviral state in cells (Isaacs & Lindermann, 1957). For this reason, it was interesting to find that the viral opponent m152 appeared to be regulated by these cytokines (preliminary data by S. Emde). In cells pretreated with IFNγ and subsequently infected with mCMV, the amount of m152 protein was selectively decreased as compared to non-IFN treated and infected cells. A search for transcription factor (TF) binding sites in the *m152* promoter region revealed a binding site for interferon regulatory factors (IRF-) 1 and 2. Upon that finding, luciferase reporter plasmids containing different constructs of the *m152* promoter were generated, as well as a virus carrying a mutation in the IRF binding site (S. Emde). In the present work, this binding site was identified as being an interferon regulatory factor element (IRFE, see 3.1). Of course, the question was raised about the influence of this element on the expression of the viral immune modulator m152, and on its effect on lymphocytes. To address this question herein, the influence of this IRFE on *m152* promoter activity was investigated at first, by performing reporter gene assays with the luciferase-encoding reporter plasmids in cells pretreated with IFN. Thereafter, the influence of this IRFE on m152 mRNA and protein levels was examined either by IFN pretreatment, by comparing mutant and WT virus, and by comparing IFNAR-/- receptor knock-out mice, which lack type I IFN signaling, with regular C57BL/6 mice. Lastly, the relevance of this IRFE was investigated first in cell culture experiments and eventually *in*

vivo. If m152 would be inhibited by IFN, this could possibly play a critical role for the protective effect of mCMV-specific CD8 T cells in the adoptive transfer model of cytoimmunotherapy in the immunocompromised host, as well as for the early control of mCMV infection by NK cells in the immunocompetent host. However, if that was really the case, the question of a benefit for the virus would arise.

3.1 The *m152* Promoter Contains an Interferon Regulatory Factor Element (IRFE)

As mentioned above, in preliminary experiments (S. Emde), a search for TF binding sites in the *m152* promoter had revealed a potential binding site for IRF-1 and IRF-2. In the present study, to currently confirm the findings with the use of a database (http://www.cbrc.jp/research/db/TFSEARCH.html), the promoter region of *m152* (Rawlinson et al., 1996) was searched again for TF binding sites. Fig. 3.1 displays the part of the promoter sequence which was analyzed (n211,552-211,359). Indeed, a sequence (n211,526-211,537) was found to be a potential binding site for mouse IRF-1 (score 86.4) and mouse IRF-2 (score 86.2), with location on the noncoding strand of *m152* (5'-GAAAGCGAAAGT-3'; upper strand). In the context of studies on IRF binding sites (Harada et al., 1989; Tanaka et al., 1993; Taniguchi et al., 2001), this site was identified herein to completely match the IRFE consensus sequence, being 5'-G(A)AAA G/C T/C GAAA G/C T/C-3' (matching bases are underlined), and in particular, match the IRF-2 recognition sequence: 5'-AANNGAAA-3'.

In order to check whether this is a more common motif in the mCMV genome, the whole sequence of the Smith strain (Rawlinson et al., 1996) was searched herein for the IRFE consensus sequence (Clone Manager Suite software). Interestingly, only 2 additional sites in the whole genome could be found, namely within the predicted open reading frames (ORF) *m29/m29.1* (Rawlinson et al., 1996) (n36,442-36,453, 5´-GAAAGCGAAAGT-3´), for which at present no function is known, and *M78* (Rawlinson et al., 1996) (n111,994-112,005, 5´-GAAACCGAAAGT-3´), which has been reported to code for a G-protein-coupled receptor (GPCR) homolog (Gompels et al., 1995; Rawlinson et al., 1996).

Moreover, hCMV proteins with analogous functions to mCMV *m152*, *m29*, and *M78* (AD169, Acc. no. X17403), which are *US3* (n194,130-194,690), *UL29* (n37,005-35,924), and *UL78* (n112,924-114,219), respectively, were searched for the presence of an IRFE. Remarkably, the element was only found in the ORF of *UL28* (n35,893-34,754, 5´-GAAAGTGAAAGT-3´, n35,130-38,616), which has previously been reported to encode a spliced mRNA together with ORF *UL29*, and this UL29/28 locus was suggested to play a role in activation of immediate-early gene expression (Mitchell et al., 2009).

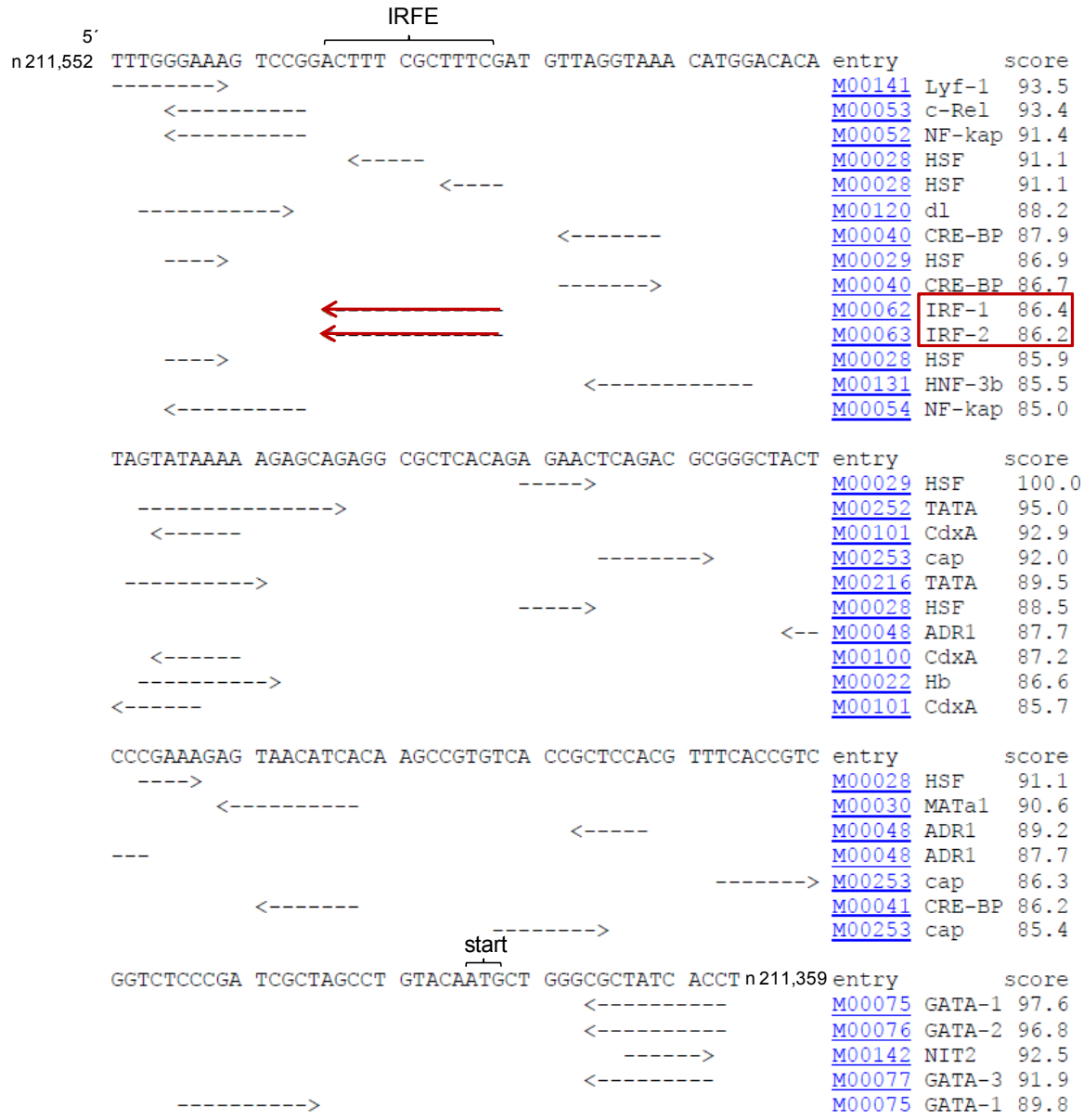

Fig. 3.1 Transcription factor binding-motif search of the *m152* promoter region (WT.Smith). Part of the *m152* promoter region (n 211,552-211,359) was searched for transcription factor binding sites (database http://www.cbrc.jp/research/db/TFSEARCH.html). Red arrows indicate a potential binding site for IRF-1 and IRF-2 (red box), connoted here as IRFE. Nucleotide positions (n) and the 5' start site of transcription (ATG) are indicated.

Fig. 3.2 presents a schematic overview of the *m152* locus in the mCMV-WT.Smith (WT.Smith) genome, with 3' and 5' untranslated regions (UTR) as determined by RACE analysis (S. Emde), and the *m152* promoter region with localization of the TATA box and the IRFE relative to the 5' start site of transcription. The *m152* IRFE sequence as well as IRFE and ISRE consensus sequences are given for direct comparison.

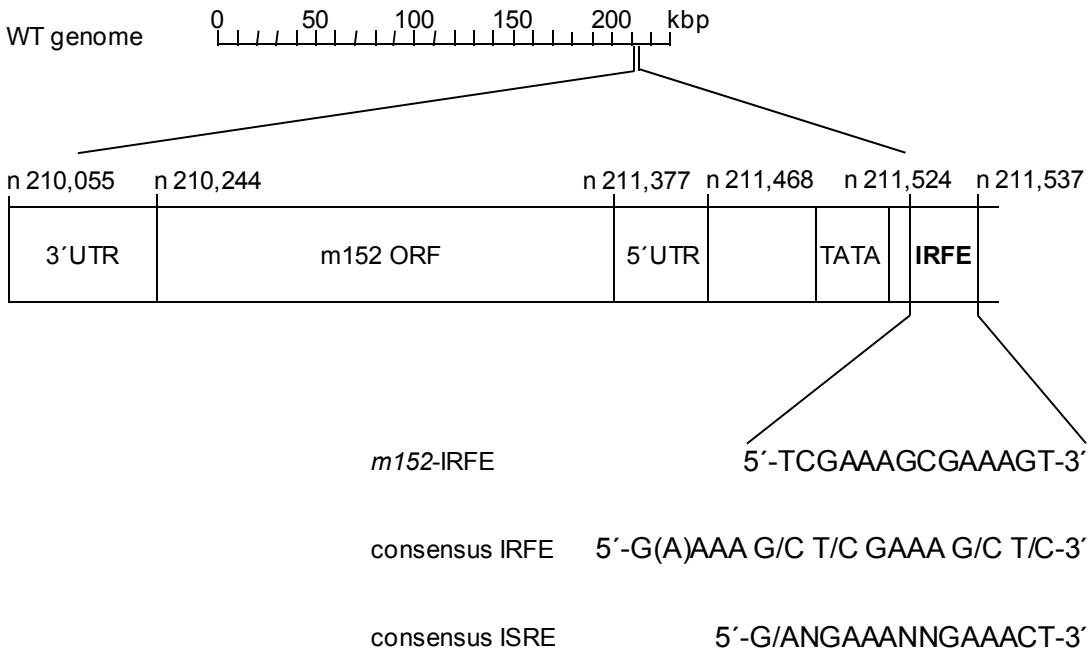

Fig. 3.2 Schematic map of the *m152* locus with promoter region highlighting the IRFE. WT.Smith genome is schematically presented with the *m152* locus highlighted. 3' and 5' UTR, *m152* ORF are indicated with their corresponding nucleotide (n) positions. The *m152* promoter region is presented with TATA box and IRFE site (in bold), which is highlighted with its nucleotide sequence. For a direct comparison, consensus IRFE and ISRE are also given. Figure not drawn to scale.

The IRFE consensus sequence has been described as being `almost indistinguishable´ from the consensus sequence of IFN stimulated response elements (ISRE) (Taniguchi et al., 2001). For that reason, the m152 IRFE sequence was also compared to the ISRE consensus sequence, being 5´-G/ANGAAANNGAAACT-3´ (Darnell et al., 1994), and was found to be identical except for 2 bases (matching bases are underlined). Interestingly, the search of the mCMV genome sequence for the presence of an IRFE revealed an ISRE in the *ie1/3* transcription unit, in intron 2 (n181,637-181,650; Rawlinson et al., 1996, 5´-AGGAAATGGAAACA-3´, matching bases are underlined).

To determine the evolutionary conservation of the IRFE in *m152*, the promoter region of *m152* in WT.Smith (Rawlinson et al., 1996) was compared to the sequences from 3 different virus strains isolated from wild mice, namely C1A, G4, and WP15B, as well as to the sequence of a BAC clone of laboratory strain K181 (Smith et al., 2008). Notably, the IRFE sequence was found to be highly conserved in all of the strains investigated with no sequence deviation (Fig. 3.3).

Fig. 3.3 Alignment of *m152* promoter sequences from laboratory and wild mouse strains of mCMV. Shown is the alignment (Clone Manager Suite software) of *m152* promoter sequences from WT.Smith (NC_004065), a BAC clone of laboratory strain K181 (AM886412), and wild mouse strains C4A (EU579861), G4 (EU579859), and WP15B (EU579860). Nucleotide positions (n), 5' start site of transcription, and IRFE are indicated.

As a next step, the influence of this regulatory element on *m152* promoter activity was investigated. With the knowledge of the promoter structure (Fig. 3.2), various reporter plasmids had been generated beforehand (S. Emde, C. Janssen), containing different *m152* promoter constructs linked to the luciferase gene. These plasmids were here used for reporter gene assays (see 3.2).

3.2 The Transfected *m152* Promoter is Activated by IFN in an IRFE-Dependent Manner

When the presence of the IRFE in the *m152* promoter of mCMV had been confirmed, and its conservation in different strains of the virus, both laboratory and wild-mouse derived, had been shown, we aimed to identify the function of this regulatory element.

At first, this question was addressed in transfection experiments using luciferase-encoding reporter plasmids which contain different constructs of the *m152* promoter linked to the intronless firefly *luciferase* gene. As vector backbone for all luciferase reporter plasmids, plasmid pGL3 (Promega) was used. These reporter plasmids are characterized as follows (see Fig. 3.4): plasmid – IRFE contains only a small part of the *m152* promoter from the first base after the IRFE-complementary sequence (n211,525) up to the last base before the 5' start site of transcription (n211,378; includes 5'UTR), plasmid IRFE carries the *m152* promoter with its authentic sequence up to the last base before the 5' start site of transcription (n212,001-211,378), plasmid mutIRFE carries the same authentic *m152* promoter sequence except for a mutation of the IRFE (n211,526-211,537; 5'-GCCCGCGCCCGT-3', mutated bases are underlined), and plasmid perf-ISRE carries the

authentic *m152* promoter sequence except for a mutation in the *m152* IRFE sequence to match the ISRE consensus sequence (n211,525-211,537; 5'-CGAAAGCGAAACT-3', mutated base is underlined), but simultaneously sticking to the IRFE consensus sequence (recall Fig. 3.2).

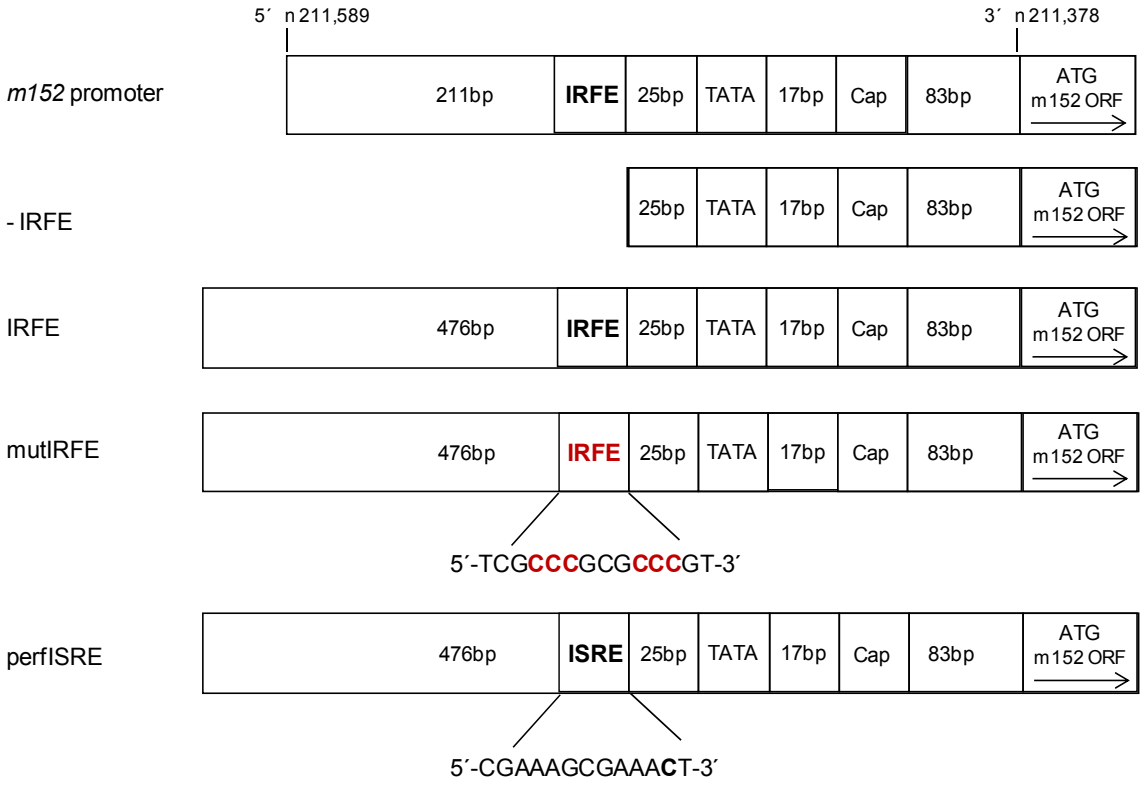

Fig. 3.4 *m152* promoter constructs for luciferase reporter gene plasmids. Schematic overview of the authentic *m152* promoter region (n 211,589-211,378) with base distances and locations of the IRFE (in bold), TATA box, Cap sequence, and 5' start site of transcription (ATG) indicated. *m152* promoter regions of constructs – IRFE, IRFE, mutIRFE, perfISRE are depicted, with mutated bases highlighted. Figure not drawn to scale.

In order to examine the influence of IFN on *m152* promoter activity, NIH 3T3 cells were transiently transfected and subsequently treated for 24h with either IFNα, β, or γ. Promoter activation was then measured by Dual-Luciferase Reporter-Gene (DLR) assays. The experiments were performed as described in 2.2.15.17. Fig. 3.4 shows activation levels of the *m152* promoter constructs with subsequent *luciferase* gene expression as shown by relative luminescence units (RLU).

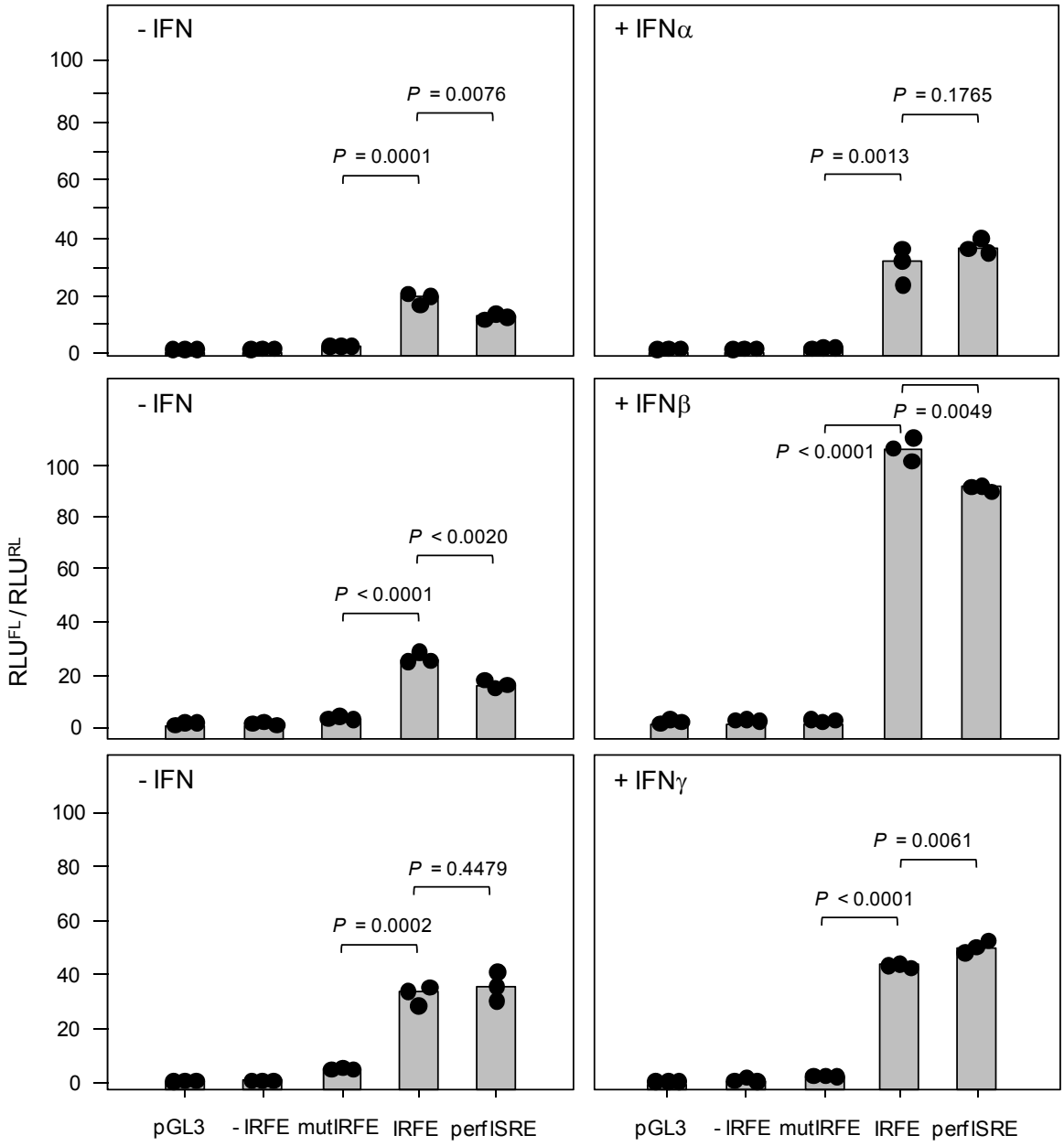

Fig. 3.5 Influence of type I and type II IFN on *m152* promoter activity in NIH 3T3. DLR assays were performed with NIH 3T3 cells, transiently transfected with the *Renilla* luciferase-encoding pRL-TK for standardization of transfection efficiency, and the respective firefly luciferase-encoding reporter plasmid, and were subsequently treated with the respective type of IFN for 24h (Type I 500U/ml, type II 20ng/ml). Vector pGL3, the backbone for all reporter plasmids, was used as negative control. The following reporter plasmids were used: - IRFE containing the first part of the *m152* promoter from transcription start site up to the IRFE sequence (including 5`UTR), mutIRFE with the motif being functionally mutated, IRFE containing the authentic *m152* promoter, and perfISRE containing the *m152* promoter mutated to match the ISRE consensus sequence. Luminescence data are expressed as relative luminescence units (RLU), and are normalized for transfection efficacy dividing firefly luciferase activity (RLU^{FL}) by *Renilla* luciferase activity (RLU^{RL}). Dots. bars, and median values represent data from triplicate transfection cultures and *P* values, determined by unpaired *t* test (http://www.graphpad.com/quickcalcs/ttest1.cfm) are indicated.

In the left panel, data from IFN-untreated samples are depicted. Obviously, plasmids IRFE and perf-ISRE were activated also by intrinsic IFN, which had been produced by the fibroblasts probably due to transfection. However, when compared to the negative control plasmid pGL3, promoter mutIRFE and – IRFE did not display activation. The necessity for a functional motif was obvious by the significant difference between plasmids mutIRFE and IRFE ($P \leq 0.0001$ (for type I IFN) / = 0.0002 (for type II IFN). Note that the left panel presents data from 3 independent experiments, demonstrating that the findings could be reproduced 3x with triplicate cultures each (total of 9). In comparison to that, the right panel gives data from IFN-treated samples. In general, promoter activation of IRFE and perf-ISRE was enhanced by the cytokines whereas the other 3 promoters were still not activated (mutIRFE vs. IRFE: $P = 0.0013$ / < 0.0001). Treatment with IFNβ yielded highest activation levels. Altogether, these data indicate that after transfection in NIH 3T3 fibroblasts, the m152 promoter is activated by type I and type II IFN in an IRFE-dependent manner, with IFNβ having the strongest impact. For that reason, subsequently, an IFNβ dose-response experiment was performed (Fig.3.5) to figure out the range of promoter activation, and interpret the result for future experiments investigating m152 RNA and protein levels after treatment with IFNβ.

In order to measure an IFNβ dose response curve, transfection and IFNβ treatment were performed similar to the experiment described above, with the only difference that here, as the reporter plasmid, only plasmid IRFE was transfected, followed by treatment of the cell cultures with different doses of IFNβ ranging from 500-1,500U/ml. Promoter activation was then measured using the DLR assay. The two panels in Fig. 3.6 depict two independent experiments, showing activation levels of the *m152*-IRFE promoter as indicated by RLU. The dose response experiments confirm the data from Fig. 3.5 insofar as the amount of intrinsic IFN was sufficient to activate the *m152*-IRFE promoter, and that this activation was increased approximately by a factor of 2 after additional treatment with 500U/ml of the cytokine ($P = 0.0013/0.0079$). Furthermore, by doubling the amount of IFNβ (1,000U/ml), promoter activation was slightly enhanced (P = 0.3950/0.1519). Actually, the activation level appeared to be at a maximum, since a further increase in the IFNβ dose (1,500U/ml) did only result in further increased activation levels. Altogether, these data confirm the conclusion that the IRFE promoter is activated by IFNβ after transfection, and that treatment with 500U/ml of the cytokine almost induces maximum activation levels, which can be finally achieved by 1,000U/ml. For this reason, in subsequent experiments investigating m152-RNA and protein levels, cells were treated exemplary with an IFNβ dose of 500-750U/ml.

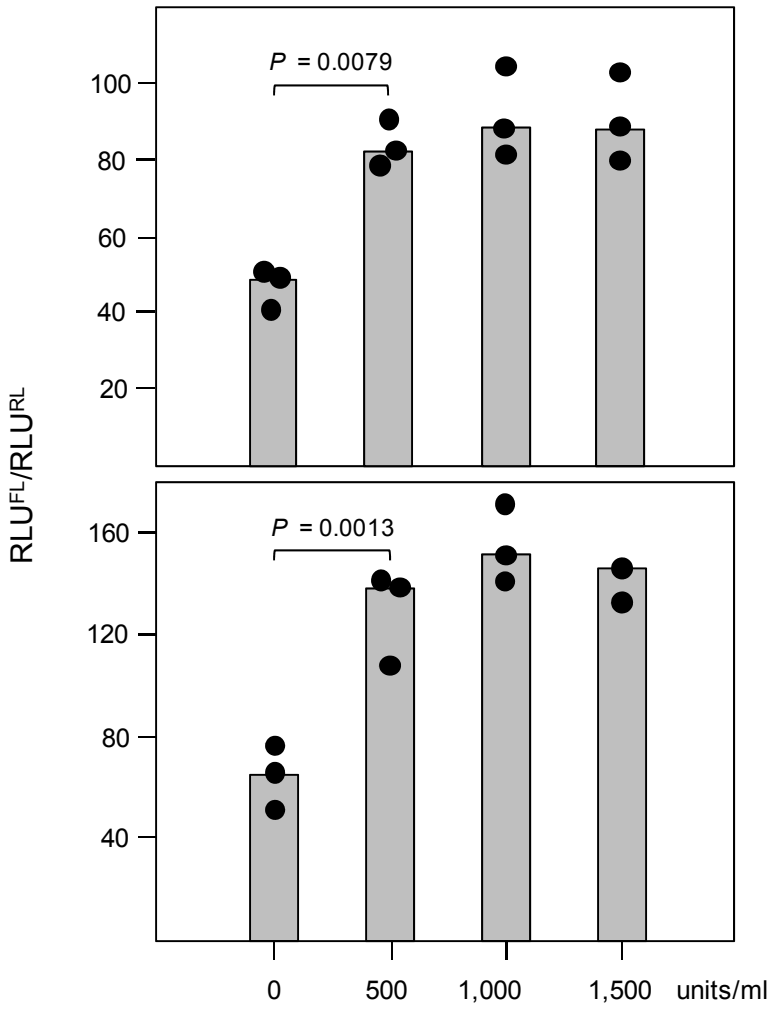

Fig. 3.6 IFNβ dose response. DLR assays were performed with NIH 3T3 cells, transiently transfected with *Renilla* luciferase-encoding pRL-TK for standardization of transfection efficiency, and firefly luciferase-encoding reporter plasmid IRFE, and subsequently treated with the indicated amounts of IFNβ for 24h. Luminescence data are expressed as relative luminescence units (RLU), and are normalized for transfection efficacy dividing firefly luciferase activity (RLU^{FL}) by *Renilla* luciferase activity (RLU^{RL}). The two panels show data from 2 independent experiments. Dots, bars, and median value represent data from triplicate transfection cultures. *P* values determined by unpaired *t* test (http://www.graphpad.com/quickcalcs/ttest1.cfm) are indicated.

Transfection experiments are limited to certain interactions of proteins or factors of interest with the introduced gene promoter, but cannot reveal the whole interplay of viral and cellular factors taking place after infection of cell cultures. As a first approach to the infection system, the BAM25 cells, which stably express viral immediate-early (IE) proteins IE1 and IE3 (Angulo et al., 2000) were used in transfection experiments comparing *m152*-promoter activation in IFN-treated vs. untreated cells, as they were performed above with NIH 3T3 cells (recall Fig. 3.5). This should combine the influence of IFN on *m152* promoter activity with the known transactivator function of the IE proteins (Angulo et al., 2000; Busche et al., 2008; Gribaudo et al., 2000; Lembo et al., 2000;

Messerle et al., 1992; Wilhelmi et al., 2008). Fig. 3.7 presents data from these transfection experiments measured with DLR assays as indicated by RLU.

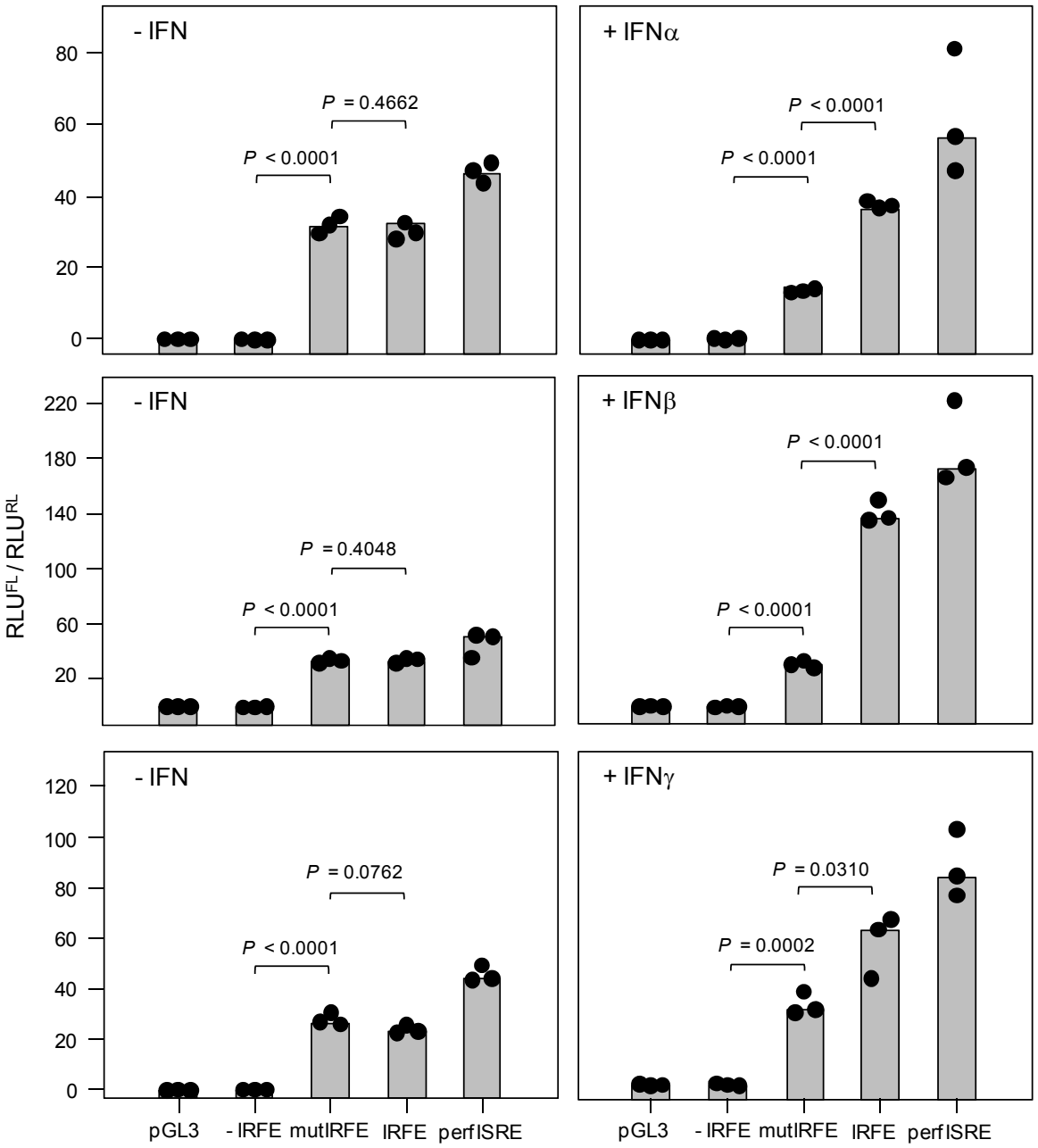

Fig. 3.7 Influence of IFN type I and II on *m152* promoter activity in BAM25 cells. DLR assays were performed with BAM25 cells as described for NIH 3T3 (see Fig. 3.2). Luminescence data are expressed as relative luminescence units (RLU), and are normalized for transfection efficacy dividing firefly luciferase activity (RLU^{FL}) by *Renilla* luciferase activity (RLU^{RL}). Dots, bars, and median values represent data from triplicate transfection cultures. *P* values determined by unpaired *t* test (http://www.graphpad.com/quickcalcs/ttest1.cfm) are indicated.

Also here, in the left panel data from IFN-untreated samples are shown. In comparison to the activation levels seen in NIH 3T3 cells (Fig. 3.5), the promoters in plasmids IRFE and perf-ISRE appeared to be even more activated. Interestingly, and in sharp contrast to the data from NIH 3T3, promoter mutIRFE was activated likewise (*P* = 0.4662/0.4048/0.0762).

These two effects are most probably due to the action of IE1 and/or IE3, and suggest a transactivator function of one or both of the viral proteins, independent of the IRFE motif. However, promoter – IRFE was still not activated, suggesting that the interaction motif for the IEs is missing just like the IRFE motif. Also here, the left panel presents data from 3 independent experiments, demonstrating that the findings could be reproduced 3x with triplicate cultures each (9x). In the right panel, data from IFN-treated samples are given. As a result of the cytokine treatment, only activation of promoters IRFE (P = < 0.0001 / = 0.0310) and perf-ISRE was enhanced, with highest levels after IFNβ treatment, whereas mutIRFE activation levels either were not changed or even reduced (IFNα). The other two reporter plasmids (– IRFE, pGL3) were still not activated. These data support the assumption that IE1 and/or IE3 transactivate the *m152*-promoter independent of the IRFE. To summarize, these data indicate that after transfection in BAM25 fibroblasts, the *m152* promoter is activated by the constitutively expressed viral proteins IE1 and/or IE3 independent of IRFE, and in addition to that, the promoter is activated by type I and type II IFN in an IRFE-dependent manner.

After the influence of viral IE proteins on *m152* promoter activity had been shown, the focus of the studies was laid on the infection system. As an initial experiment, and to switch from transfection to infection, NIH 3T3 cells were at first transiently transfected with luciferase-encoding reporter plasmids *m152*-IRFE or mutIRFE, and one day later they were infected at an MOI of 4 with mCMV-WT.BAC (in the following briefly referred to as WT.BAC), and were incubated for 24h. Then, promoter activation was measured by DLR assays and expressed in RLU, as shown in Fig. 3.8.

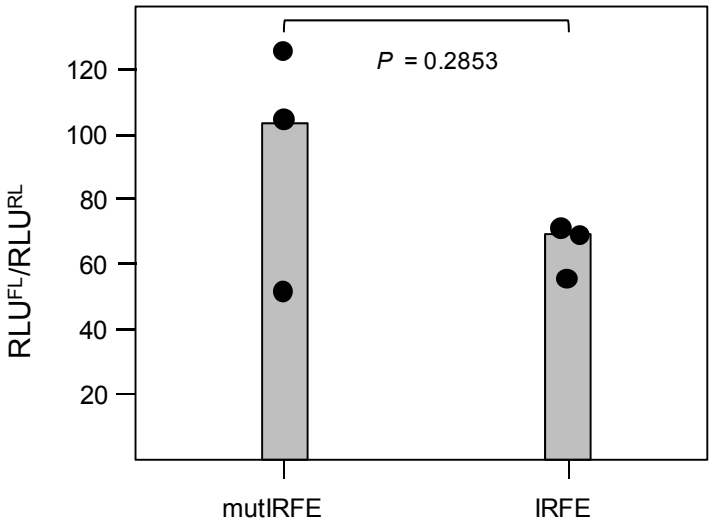

Fig. 3.8 *m152* promoter activity after mCMV-infection. DLR assays were performed with NIH 3T3 cells, transiently transfected with *Renilla* luciferase-encoding pRL-TK for standardization of transfection efficiency, and firefly luciferase-encoding reporter plasmid IRFE or mutIRFE, and one day later they were infected with WT.BAC (MOI 4) for 24h. Luminescence data are expressed as relative luminescence units (RLU), and are normalized for transfection efficacy dividing firefly

luciferase activity (RLU^{FL}) by *Renilla* luciferase activity (RLU^{RL}). Dots, bars, and median values represent data from triplicate transfection cultures. *P* values determined by unpaired *t* test (http://www.graphpad.com/quickcalcs/ttest1.cfm) are indicated.

Apparently, the promoter containing the IRFE was activated, either by intrinsic IFN, which is induced by the process of transfection-infection, and/or by viral factors such as IE proteins, and the level of activation was higher as compared to IFN-untreated samples in the preceeding experiments, where intrinsic IFN was induced only by transfection (Figs. 3.5, 3.6, 3.7). However, contrary to what one would have expected from the preceeding experiments, the promoter with the mutIRFE sequence appeared to be activated after infection at even higher levels as compared to the promoter with the authentic IRFE. Thus, activation of mutIRFE can only be due to the action of viral factors, since the motif required for IFN action is destroyed. This leads to the assumption that maybe the IRFE promoter was inhibited by IFN in this setting. However, one of the replicate values from plasmid mutIRFE deviated from the other two, which makes the difference non significant ($P = 0.2853$), unless this value is omitted ($P = 0.0147$). These deviations were probably due to the transfection/infection procedure, which is stressful for the cells (visible in phenotype), and transfection efficiency is not always alike. Even so, in a preliminary experiment, which also included 3 samples of mutIRFE transfected and WT.BAC infected cells, the relative luminescence in all samples was >100, which provides a legitimate reason for omitting the low value (data not shown). Nonetheless, the data from both experiments cannot be joined in one figure due to the above mentioned variations. Whether the influence of IFN on *m152* promoter activity is indeed different in the infection system was addressed in the following experiments.

Together, these experiments have revealed that the *m152* promoter is activated after transfection by type I and type II IFN in an IRFE-dependent manner, and that the range of activation depends on the type and the amount of cytokine used, with 500-1,000U/ml of IFNβ being the strongest inducer. Furthermore, mCMV IE proteins 1 and/or 3 appear to activate the *m152* promoter via a different mechanism. Both influences lead to an additive effect. However, after infection the influence of IFN but not viral factors appears to be different but has to be investigated further in other settings.

3.3 Generation and Characterization of Recombinant mCMV

In order to investigate the influence of the IRFE motif on *m152* expression and function, a recombinant virus carrying a functional deletion of the motif (mCMV-mutIRFE, in the following shortly denoted mutIRFE had been generated by a former colleague (S. Emde), and was herein reconstituted from the BAC-DNA, propagated in cell culture, and purified as described in 2.2.2 and 2.2.3. As a standard technique used in the lab, the mutIRFE

virus was tested for its replicative fitness in cell culture as well as in the immunocompromised host, in order to exclude any possible influence of the introduced mutation on virus replication in the absence of an immune response.
In addition to that, at a later stage of the project, a revertant virus (mCMV-mutIRFErev, in the following briefly referred to as mutIRFErev) was generated by two-step Tischer recombination (Tischer et al., 2006; 2.2.15.16) to be used as a direct comparison (like WT) to mutant virus. After successful reversion of the mutation by recombination of the PCR product into the mutated BAC-plasmid (mutIRFE), the revertant virus was reconstituted, propagated, and purified (2.2.2, 2.2.3).

3.3.1 Successful Reversion of the Functional IRFE Mutation

A revertant virus mutIRFErev was generated by reversion of the mutation in the *m152* promoter of mutant virus mutIRFE using Tischer recombination (see 2.2.15.16). For this, a 2-step PCR was performed (2.2.15.7) to produce a linearized DNA fragment containing part of the *m152*-promoter sequence with the reverted IRFE, a kanamycin cassette, and an *I-SceI* restriction site. The fragment was generated in 2 PCR steps (touchdown). The first PCR was run with plasmid pEPkan-S as template DNA and with long forward primer pepKan-S_IRFErev-For and short reverse primer rev5. The amplicon was then extracted from a gel band (see 2.2.15.12), and was used as template in the second PCR, together with long reverse primer pepKan-S_IRFErev-Rev and short forward primer IRFE_For5 (see 2.2.16.1). Afterwards, this fragment was transformed into GS1783 bacteria which carry the mutated BAC-plasmid mutIRFE (2.2.15.16.1+2). For this, the Red-genes had to be thermo-induced at first and bacteria had to be made electrocompetent for the first Red-mediated recombination (see 2.2.15.16.1) before transformation. Afterwards, BAC-DNA was purified (2.2.15.14) from Cam+Kan resistant clones, digested with *EcoRI* and *I-SceI* (2.2.15.15.1), and the incorporation of the fragment and the integrity of the BAC-plasmid was verified by gel electrophoresis (see 2.2.15.11). Fig. 3.9 shows the picture of the BAC-gel taken under UV-light. DNA from clones 1-9 was loaded together with DNA purified from WT.BAC bacterial cultures (left panel). Because WT DNA is only weakly displayed, a picture of a different BAC-gel of WT was added (right panel). The white arrows indicate that one band was missing in the clones (>5,090bp), but instead, a smaller band was present (<3,054bp). All clones appeared to display this pattern, although many of the DNA samples of the clones were only weakly visible. Thus, by the 1st recombination the PCR fragment including the Kan cassette and the *I-SceI* restriction site had been successfully integrated, and the clones could be further used for virus generation.

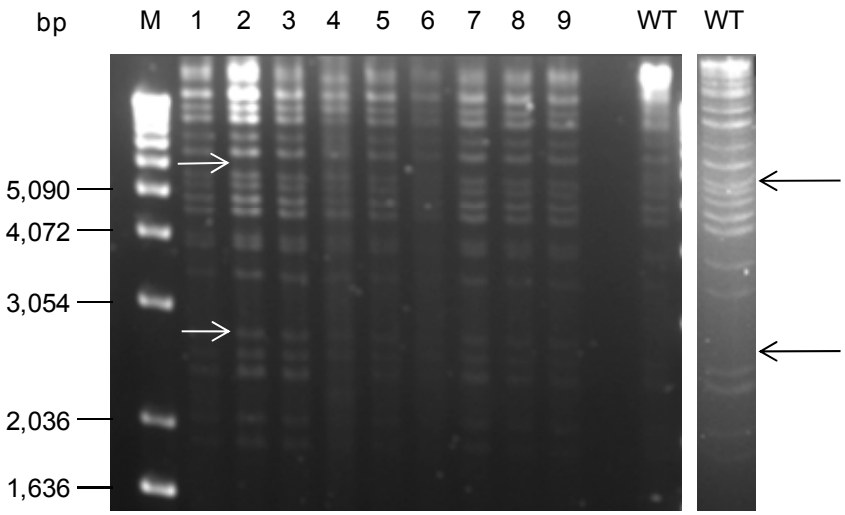

Fig. 3.9 Integrity of the BAC-DNA and incorporation of the I-SceI site. Shown is a BAC-gel of purified DNA from Cam+Kan resistant clones 1-9 (left panel) after the transformation of the PCR product, containing the reversed *m152*-promoter sequence, a Kan cassette and an *I-SceI* restriction site, and after 1st Red-recombination, and restriction digest with *EcoRI* and *I-SceI* (NE(B). For a comparison, purified BAC DNA from WT was loaded (left panel, last lane; separate panel). M: 1-kb DNA ladder (Invitrogen). White arrows indicate missing (upper) and additional (lower) bands in samples 1-9 as compared to WT (black arrows).

As a next step, these cultures were subjected to the 2nd Red-recombination with 1% arabinose in the medium. Thereby, the Kan cassette should be cut out by the induced *I-SceI* enzyme. Colonies were grown on replica plates (Cam; Cam+Kan), and BAC DNA from Kan-sensitive clones (2) was purified and used as template DNA to amplify part of the *m152* promoter containing the IRFE, by PCR with primers *Kpn*I_m152Prom_for and *Hind*III_m152Prom_rev (2.2.15.7). The PCR product of these 2 clones, together with a product from WT DNA was sequenced. Fig. 3.10 shows the chromatograms for WT.BAC, mutIRFE, and mutIRFErev. The mutant virus was sequenced after propagation in MEF cultures and purification, and was included in this figure. Obviously, the IRFE sequence in WT.BAC (5´-CGAAAGCGAAAGT-3`) is successfully mutated in mutIRFE (5`-CGCCCGCGCCCGT-3`), and reversed to the WT sequence in mutIRFErev.

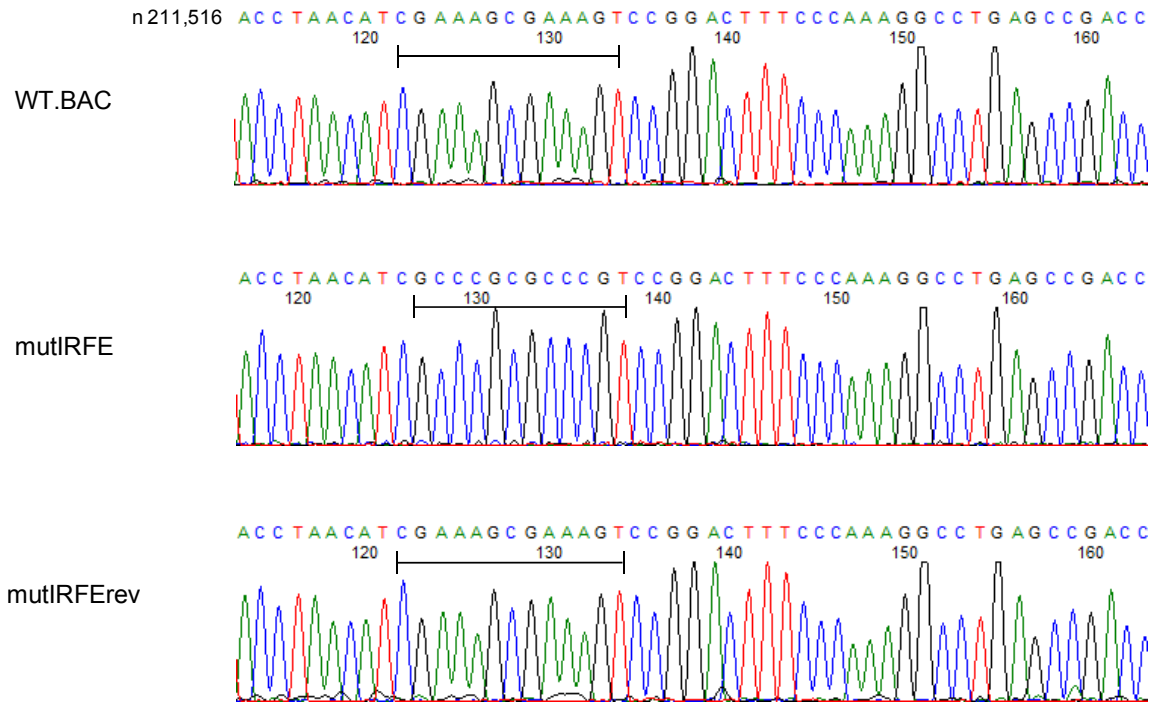

Fig. 3.10 Chromatograms of the sequencing of DNA from WT.BAC, mutIRFE, and mutIRFErev. DNA from the *m152* promoter region of the indicated bacterial clones was amplified by PCR and sequenced. Nucleotide position (n) in the WT.Smith genome (Rawlinson et al., 1996) is given. Black bar markers indicate the IRFE sequence in all samples.

3.3.2 Reconstitution, Propagation, and Purification of recombinant mCMV

The verified BAC DNA which contained the mutIRFErev sequence was then transfected into MEF, and virus supernatants were collected from completely lysed cultures (P0). The supernatants were further propagated by infection of new cultures until passage P6 to eliminate the BAC-vector sequence from the viral genomes (2.2.2). The same was performed on supernatants from mutant virus mutIRFE. The efficiency of this process was quantitated by qPCR specific for viral *M55/gB* and the BAC-sequence (2.2.15.7), with viral DNA purified from the supernatants (2.2.15.5) as template. Log_{10} titrations of plasmid pDrive_gB_PTHrP_BAC (2.2.15.9) were used as standard to determine the copy numbers of BAC and gB. Then, the ratios of BAC sequences/10^6 genomes were calculated. Tab. 3.1 is exemplary of the numbers of BAC sequences per 10^6 viral genomes as determined by qPCR. In both viruses the BAC sequence had been sufficiently eliminated after P5, where the desired value of maximally ~$2x10^2$ BAC/10^6 genomes was achieved (Lemmermann et al., 2010). In the following, the BAC-free virus supernatants of mutIRFE and mutIRFErev were used to infect MEF cultures and purify virus in large-scale (2.2.3). Virus titers (PFU/ml) of the purified viruses were then determined by plaque assay (2.2.4.1).

Virus	Supernatant	BAC sequence	Genomes (*M55/g(B)*	BAC / 10^6 genomes
mutIRFE	P0	$2.62x10^6$	$3.73x10^6$	$7.02x10^5$
	P1	$5.70x10^5$	$2.57x10^6$	$2.22x10^5$
	P2	$3.24x10^5$	$3.33x10^6$	$9.73x10^4$
	P3	$1.02x10^4$	$6.34x10^5$	$1.61x10^4$
	P5	$3.48x10^0$	$1.37x10^4$	$2.55x10^2$
	P6	undetectable	$5.26x10^6$	
mutIRFErev	P0	$2.1x10^5$	$2.9x10^5$	$7.25x10^5$
	P1	$1.3x10^4$	$9.14x10^4$	$1.42x10^5$
	P2	$8.37x10^3$	$4.77x10^5$	$1.76x10^4$
	P3	$3.75x10^3$	$1.19x10^6$	$3.15x10^3$
	P5	undetectable	$1x10^6$	
	P6	$2.78x10^{-0.1}$	$4.72x10^5$	$5.88x10^{-1}$

Tab. 3.1 Quantification of BAC-sequences after virus propagation in cell culture. The number of viral genomes and BAC sequences (mean values of duplicates) was determined by qPCR using plasmid pDrive_gB_PTHrP_BAC as standard. Virus DNA was purified from 200µl of the indicated passages (P0-6) of supernatants and 2µl of the eluate were used as template in qPCR.

As a next step, the genome-to-infectivity ratio was determined. This number mirrors the amount of viral genomes which is necessary to produce 1 plaque in a permissive cell culture (1PFU). The genome-to-infectivity ratio for mCMV-WT.Smith has been reported to be ~500:1 (Kurz et al., 1997). The quantification was made by qPCR with $\log_{10}$ titrations of plasmid pDrive_gB_PTHrP_Tdy (2.2.15.9) as standard, and the corresponding primers (2.2.15.1). As template DNA, 15µl virus stock solution was used for DNA purification. Dilution series were prepared of each sample ($1\log_2$ followed by $4\log_{10}$ steps) and used for quantification in duplicates. Tab. 3.2 gives virus titers and genome-to-infectivity ratios for both recombinant viruses in comparison to WT.BAC. Obviously, they do not significantly differ from the reference value of WT.Smith (Lemmermann et al., 2010).

Virus	Virus titer (PFU/ml)	Genomes / PFU (mean)
mutIRFE	$2.4x10^8$	265 : 1
mutIRFErev	$1.0x10^9$	136 : 1
WT.BAC batch V	$2.8x10^8$	361 : 1

Tab. 3.2 Genome-to-infectivity ratios. The number of viral genomes in serial titrations ($\log_{10}$) of purified DNA was determined by *M55/gB*-specific qPCR (duplicates), using plasmid pDrive_gB_PTHrP_Tdy as standard. Shown are virus titers and mean values of calculated DNA levels.

3.3.3 Mutant Virus mCMV-mutIRFE Replicates Similar to WT Virus

Replicative fitness studies were conducted *in vitro* and subsequently *in vivo*, comparing viral genomes and virus titers of mutant and WT virus in infected cell cultures and different organs in a time-dependent manner (see 2.2.5). Revertant virus mutIRFErev, which was generated almost at the end of the project, for verification of the major conclusions in key

cell-culture experiments (Northern Blot, Western Blot, ELISPOT assay) to exclude an unintended phenotype of mutIRFE was not yet available at the time of these studies.

For the *in vitro* assay, MEF were seeded in starvation medium in 6-well plates at a density of $2x10^5$ cells/well, in order to reflect the *in vivo* situation. Triplicate cultures were done for each sample. The cells were growth arrested for 72h. Subsequently, they were centrifugally infected with 0.02 PFU/cell (MOI 0.4). At different time points after infection (0, 4, 16, 24, 40, 48, 64, 72h p.i.), supernatants and cells (trypsinized and pelleted) were collected. Fig. 3.11 shows data of the multistep growth curve.

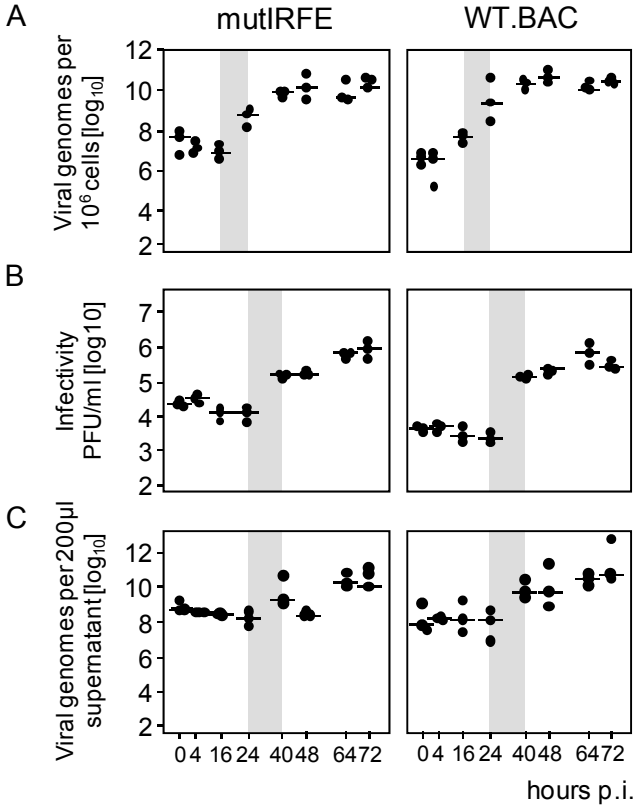

Fig. 3.11 Viral replicative fitness in MEF cultures. MEF were centrifugally infected at an MOI of 0.4 (0.02 PFU/cell x 20; centrifugal enhancement of infectivity) with the virus indicated. (A) Quantitation of viral genomes per 10^6 infected cells, determined by *M55(gB)*-specific real-time PCR with normalization to cellular gene *pthrp*. (B) Quantitation of infectious virus per ml cell culture supernatant, determined by virus plaque assay. (C) Quantitation of viral genomes per 200µl cell culture supernatant, determined as in (A). Multistep growth curves are depicted for a 72h p.i. time course, corresponding to 3 viral replication cycles. Time 0 is set after the 30min centrifugation period, determining the inoculum values for viral genomes and infectivity. Dots represent logarithmized data from 3 different 6-well cultures at each time point. Median values are marked by horizontal lines. The gray shaded area highlights the productivity after the first viral replication cycle, with the onset of DNA-replication at 16h p.i. and virus release after 24 h p.i..

Panel (A) shows the number of viral genomes per 10^6 cells determined by absolute quantification. It appears as though from the onset of viral DNA-replication at 16h p.i. to 64h p.i. the titers are slightly lower in cells infected with mutIRFE, but considering the

range, these deviations are not significant. Panel (B) depicts the infectivity per 10^6 cells as determined by virus plaque assay, and panel (C) gives the number of viral genomes per 200µl cell culture supernatant. Also here, insignificant deviations, rather due to assay procedures, are present, but the onset of virus release is at 24h p.i. as determined by both assays. Taken together, the different methods verify that there is no notable difference in the replicative fitness of mutant and WT virus.

In the next step, the mutant virus was tested for its replicative capacity *in vivo*. For this, 3-5 BALB/c mice (8-9wk-old) per time point were γ-irradiated with a single dose of 6.5Gy, and were infected i.pl. (2.2.7) with 10^5 PFU/25µl PBS of virus Δm152, mutIRFE, or WT.BAC. At days 2, 4, 6, 8, and 10 p.i., organs were dissected. Livers were subjected to IE1-specific IHC (2.2.17), whereas lungs, salivary glands, and spleens were taken to purify DNA and use it in qPCR analyses for an absolute quantification of viral genomes per cell. Using linear regression analyses, the doubling times (DT) of the different viruses were then determined from these data. Virus Δm152 was included in the experiment as indicator for the influence of a complete loss of m152 on virus replication. It is known that deletion of this gene leads to growth attenuation of the virus in lungs and spleens of immunocompromised mice (Krmpotić et al., 1999; Slavuljica et al., 2010). Fig. 3.12 (A) displays the numbers of viral genomes per 10^6 cells in lungs and spleens, Fig. 3.12 (B) the number of infected liver cells for all 3 viruses tested. Viral genomes were detectable from 2d p.i. onwards in all virus samples. Virus replication and dissemination of Δm152 and mutIRFE appeared to be comparable to that of WT.BAC in all organs, and for the indicated time points tested. To support this observation, with the use of regression analyses, the most probable number (MPN), the slope of the regression line x, and the 95% confidence intervals of the slope were determined to calculate the doubling times according to the formula: DT = log 2/x. In the case of an overlap of the DTs (95% confidence intervals) of the viruses tested, replication is defined as being comparable. In this respect, the DTs of the three viruses were alike in all organs under test, verifying that these viruses are comparable in their ability to replicate and disseminate from the portal of entry to distant target organs. Only virus titers of Δm152 in the spleen at 2d p.i. appeared to be lower as compared to the other viruses, which might be due to a residual innate immune response in this organ.

Taken together, for this project, the replication kinetics assay has in cell culture as well as in severely immunocompromised mice proven that any selective immunological phenotype to be shown in mutant virus mutIRFE could be assigned to the deletion of the IRFE motif.

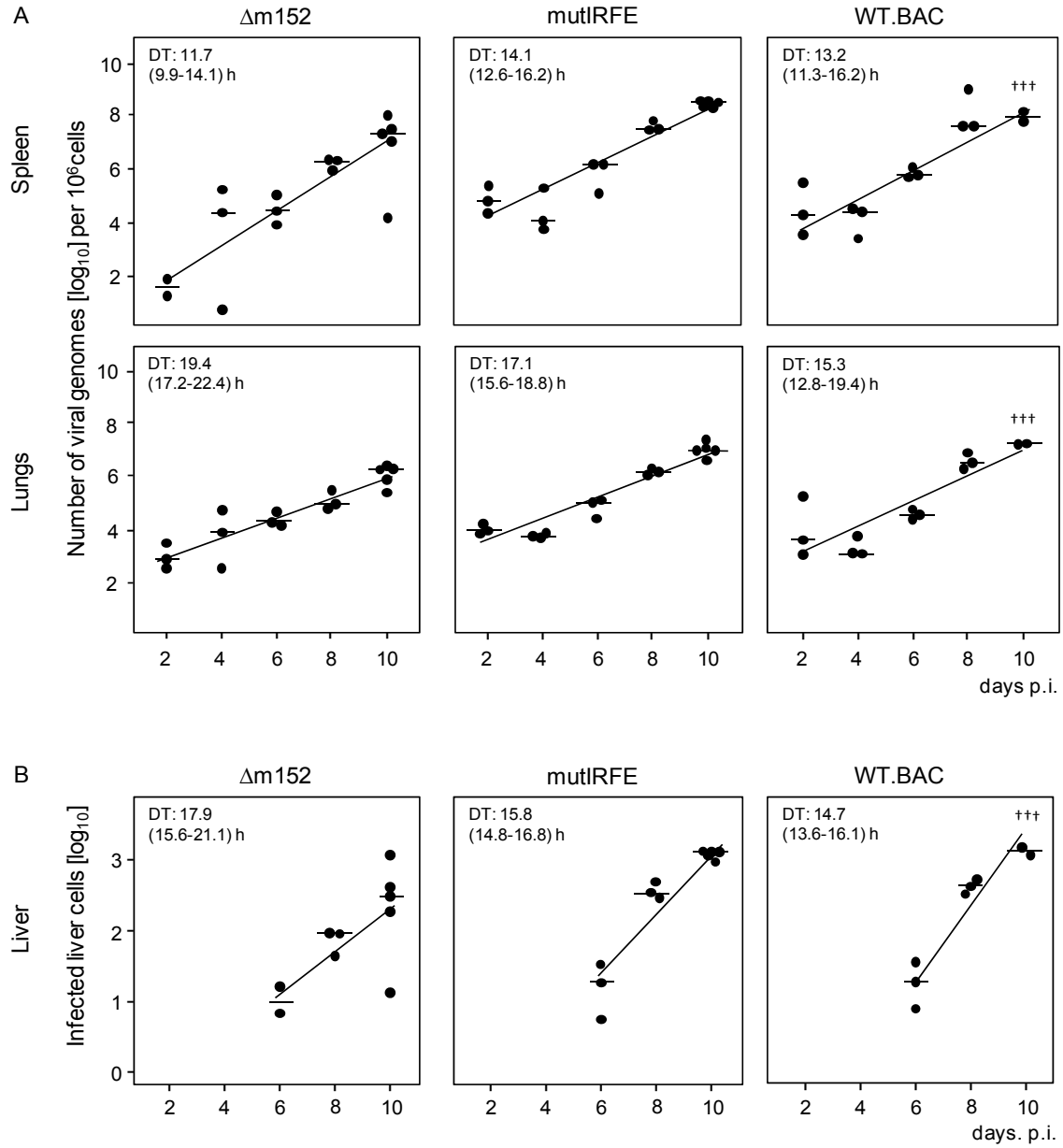

Fig. 3.12 Viral replicative fitness in host tissues. 3-5 BALB/c mice (8-9wk-old) per time point were immunocompromised and subsequently infected with 10^5 PFU (corresponding to ~5x10^7 viral genomes) of mCMV-Δm152, mutIRFE, or WT.BAC. At the indicated days p.i. organs were dissected and subjected to qPCR (spleens and lungs) or IE1-specific IHC (liver). (A) Quantitation of viral genomes per 10^6 infected cells in spleens and lungs as determined by real-time PCR specific for viral gene *M55/gB* normalized to cellular gene *pthrp*. (B) Quantitation of liver infection as determined by the numbers of IE1-positive liver cells counted in representative 10mm^2 liver tissue section areas. Semilogarithmic growth curves for the indicated viruses are plotted. The solid circles represent data from 3 individual mice (5 at day 10), and median values are marked by horizontal lines. The DTs and their 95% confidence intervals (in parentheses) are calculated from the slopes x (95% confidence intervals of x) of the calculated log-linear regression lines according to the formula: DT = log 2/x.

3.4 *m152* Gene Expression is Inhibited by IFN in an IRFE-Dependent Manner

In transfection experiments it was shown that *m152* promoter activity is enhanced by IFN via the IRFE (see 3.2). In order to investigate *m152* promoter activity after infection, as

being the relevant system here, *m152* gene expression was monitored in transcription analyses in infected MEF cultures. RNA was isolated (2.2.16.3) at different time points after infection, and was used in qRT-PCR analyses (2.2.16.5) to determine the relative expression values of m152 RNA. These values were calculated as ddCT values (Livak and Schmittgen, 2001) from the CT of the internal reference β-actin, and the CT of the target m152 and calibrated to time point 0 (after 30min centrifugation) after infection of the corresponding sample. At first, a duplex qRT-PCR was established to guarantee detection of the CT value of both targets in one sample. This makes the calculation much more accurate. The primer sequences for cellular *β-actin* and viral *m152* are shown in 2.2.16.1 with the amplicon sizes indicated as being 87 and 68bp, respectively. In order to verify the accuracy of the RT-PCR, the PCR products were loaded together with a no-template control (NTC) on a 3% agarose gel and separated by gel electrophoresis. Fig. 3.13 confirms the two DNA bands from the β-actin and m152 amplicons in both PCR samples, but not in the NTC. In the following experiments, this method was used to determine the relative expression of *m152* gene expression.

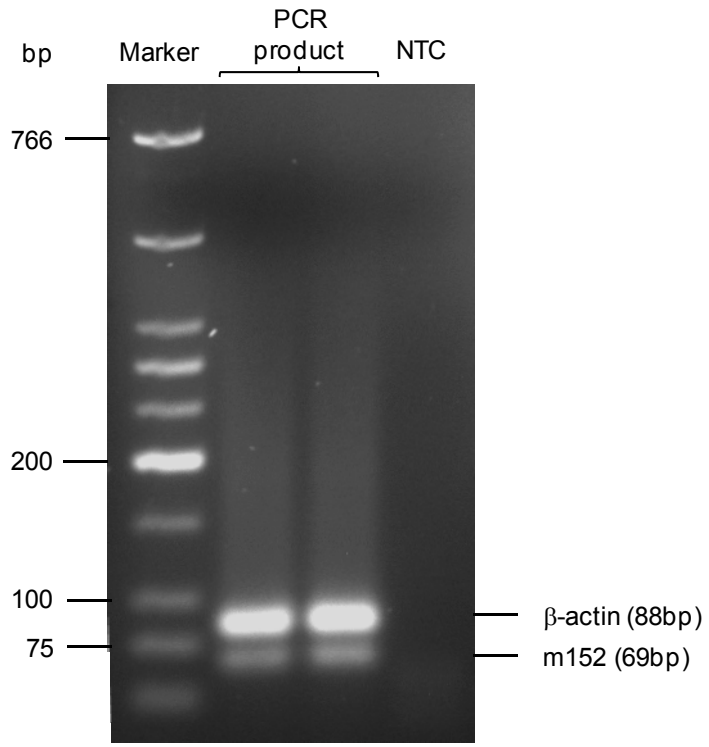

Fig. 3.13 Verification of duplex RT-PCR amplicons by gel electrophoresis. Total RNA was purified from infected MEF cultures at 120min p.i., and 500ng were used in duplex qRT-PCR targeting cellular *β-actin* and viral *m152*. As negative control, H_2O instead of RNA was pipetted (NTC = no template control). The PCR products of two samples were loaded on a 3% agarose gel, and were separated by gel electrophoresis. Low molecular weight DNA ladder (New England BioLabs) was used as standard. Indicated are the DNA bands of β-actin and m152, with their respective sizes of 88 or 69bp.

At first, the influence of IFN on *m152* gene expression was investigated. For this, triplicate MEF cultures were pretreated for 48h with 500U/ml IFNβ, exemplary for type I IFN as determined in Fig. 3.6, and were afterwards infected with WT.BAC (MOI 4) over an early time course after infection. At 0, 30, 60, 75, 90, 120, 180, and 240min p.i. total RNA was isolated and used as template in real time duplex qRT-PCR analysis specific for *m152*. Fig. 3.14 shows relative expression levels of m152 (ddCT values, see above) at the indicated time points. Already at T(0), i.e. after 30min of centrifugal infection, m152 RNA is detectable in both groups, but is set as 1 to be used as calibrator for the calculation of the ddCT values. The left panel shows data from IFN-untreated cultures. Here, the amount of m152 increases rapidly (~$2\log_{10}$/30min) over the first 90min p.i., and then reaches a plateau level. Contrary to that, the right panel displays that IFNβ inhibits and delays m152 transcription over the time course of infection, and that the plateau level is reached only at 240min p.i..

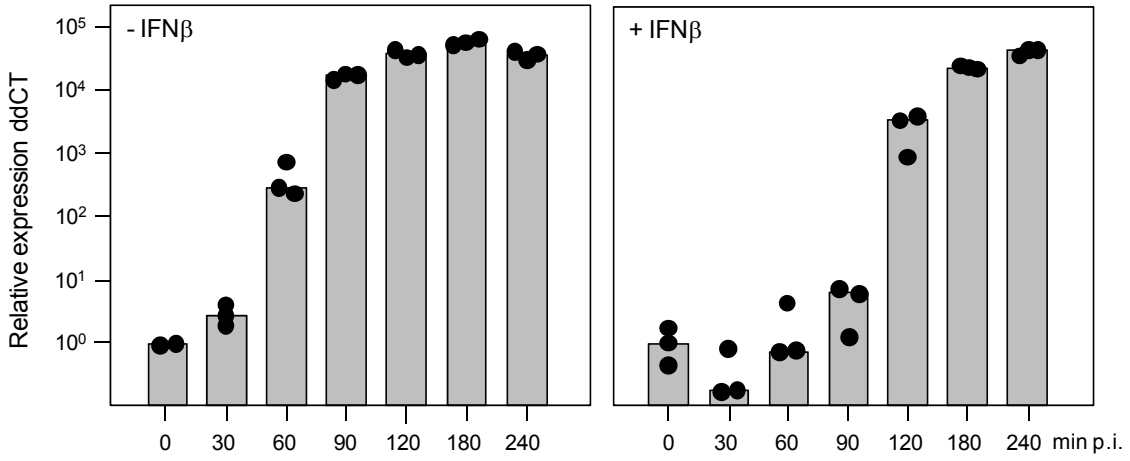

Fig. 3.14 Influence of IFNβ on *m152* gene expression. Relative quantification of m152 transcripts by real time duplex RT-PCR in MEF cultures, pretreated with 500U/ml IFNβ for 48h, and subsequently infected with WT.BAC for the indicated time points. Shown are expression levels (ddCT values, see 2.2.16.5) relative to β-actin transcripts. Total RNA was purified at the indicated time points p.i., where T(0) is defined as being after the 30-min centrifugation period. 500ng RNA per sample was used. Solid circles represent data of triplicate cultures and bars their median values.

Next, in order to confirm the finding that IFN inhibits *m152* gene expression, the mutant virus mutIRFE, which carries a functional deletion of the motif, was used in this assay system and compared to WT.BAC. For this, triplicate MEF cultures were infected with either mutant or WT virus (MOI 4) over a time course (0-240min p.i.), and were processed as described above. Fig. 3.15 shows the relative expression levels of *m152* at the indicated time points p.i.. In the left panel (A), data from mutIRFE-infected cells show in comparison to those from WT.BAC-infected cells (right) that functional deletion of the motif yields higher *m152*-expression levels at 60 and 90min p.i.. At later time points in

infection, the plateau-level of expression is reached in both groups. However, calculating the ddCT cannot display actual differences in m152 levels at T(0), as the values are set to 1 for serving as the calibrator. Therefore, in panel (B), dCT values (= CTm152 - CTβ-actin) are depicted for both groups. Here, it can be seen that samples from mutIRFE-infected cells already start with higher m152 levels at T(0), and the difference to WT.BAC is maintained until 180min p.i.. It has to be considered that depicting the dCT is inverse of the ddCT, which means that low levels in dCT correspond to higher expression of *m152*.

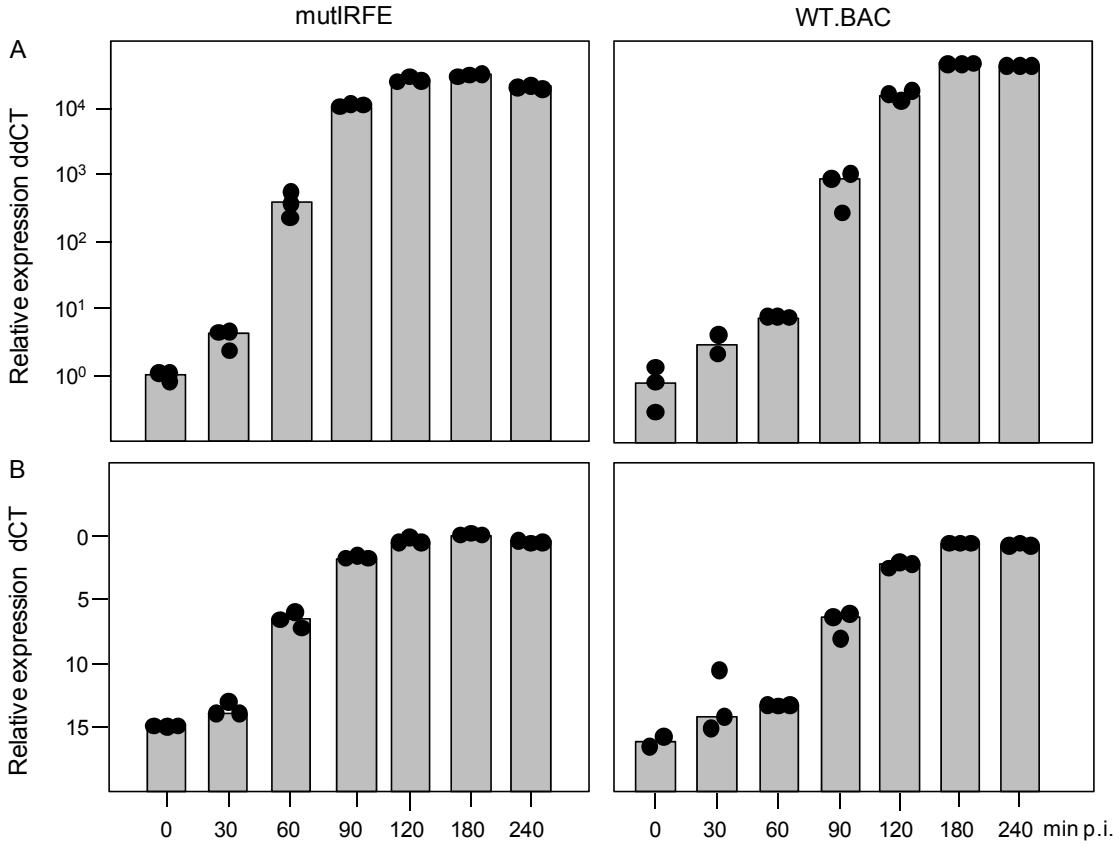

Fig. 3.15 Influence of the IRFE on *m152* gene expression. Relative quantification of m152 transcripts by real time duplex RT-PCR in MEF cultures infected with either, mutIRFE or WT.BAC for the indicated time points. Shown are expression levels as (A) ddCT values or (B) dCT values relative to β-actin transcripts. Total RNA was purified at the indicated time points p.i., where T(0) is defined as being after the 30min centrifugation period. 500ng RNA per sample was used. Solid circles represent data of triplicate cultures and bars their median values.

Up to now, both the influence of IFN on *m152* promoter activity and *m152* gene expression have been investigated using 2 different approaches, namely treatment with recombinant IFN or destruction of the IRFE in mutant virus mutIRFE. At this point, a third approach was introduced in the project, namely the use of IFNAR-/- knock-out mice (C57BL/6 background; see 2.1.9), which lack expression of the type I IFN signaling receptor IFNAR. Primary MEF were prepared from this mouse strain and used in the above described m152-transcription kinetics in comparison to MEF from C57BL/6.

Fig. 3.16 shows the relative expression levels of *m152* (ddCT). In the left panel, data from infected IFNAR-/- MEF cultures are depicted. Obviously, at 45 and 60min p.i., m152 transcription levels are higher as compared to MEF from C57BL/6 (right panel). However, already at 90min, the plateau level, which was also observed in BALB/c MEF, is reached in both MEF cultures. This shows that if type I IFN signaling is missing, *m152* gene expression cannot be inhibited, which thus leads to higher transcription levels.

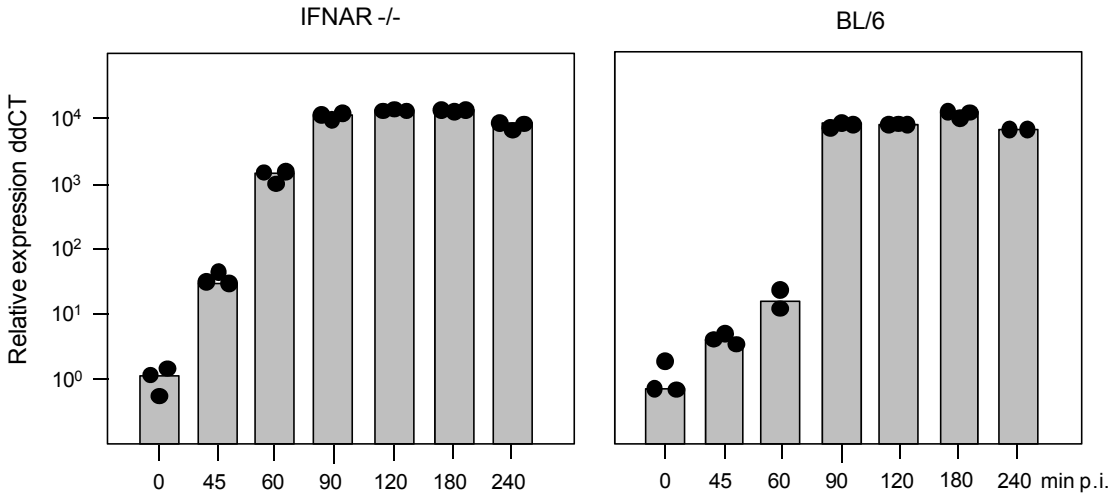

Fig. 3.16 Influence of type I IFN signaling on *m152* gene expression. Relative quantification of m152 transcripts by real time duplex RT-PCR in MEF cultures prepared from IFNAR-/- knock-out mice or C57BL/6 mice, infected with WT.BAC for the indicated time points. Shown are expression levels as ddCT values relative to β-actin transcripts. Total RNA was purified at the indicated time points p.i., where T(0) is defined as being after the 30-min centrifugation period. 500ng RNA per sample was used. Solid circles represent data of triplicate cultures and bars their median values.

In summary, these analyses of m152-transcription kinetics in infected MEF cultures have revealed that the relative expression of the viral gene is inhibited at early time points after infection by treatment with IFNβ (Fig. 3.14) and by type I IFN signaling (Fig. 3.16), and that this inhibition appears to be dependent on the IRFE in the *m152* promoter (Fig. 3.15). In order to further corroborate these findings, a different method detecting and visualizing m152 RNA in these samples (60min p.i.) was used, namely the Northern-Blot technique with a DIG-labeled m152 probe (2.2.16.6). Before that, this method had to be established in the lab. At first, DIG-labeled m152 probes were generated using plasmid pDrive_m152, which had been generated by a colleague (A. Fink) and carries the complete *m152* ORF (see Fig. 3.17).

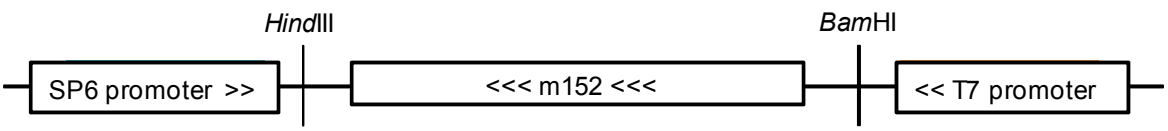

Fig. 3.17 Plasmid pDrive_m152. Indicated are restriction sites for enzymes *Hind*III and *Bam*HI, as well as promoters of RNA polymerase SP6 and T7. Figure not drawn to scale. Modified from A. Fink.

This plasmid was linearized either with restriction enzyme *Bam*HI or *Hind*III (see 2.2.15.15.2) and was *in vitro* transcribed by either SP6 or T7 polymerase (2.2.16.6.1), respectively. Thereby, two complementary ssRNA probes of m152 were generated of which the first one should be complementary and thus bind to m152 mRNA. Dot blots were performed to confirm the functionality of these probes for all concentrations tested (1, 10, 100ng; see 2.2.16.6.2, blots not shown). When this was shown, both probes were tested on RNA samples from infected cells. For this, total RNA purified from infected MEF (IFNAR-/- and C57BL/6) at 90min p.i. (transcription kinetics experiment, Fig. 3.16), and total RNA purified at 24h p.i. from infected BALB/c, was loaded (1-2µg) on a denaturing formaldehyde gel containing ethidium bromide, and was separated by gel electrophoresis (2.2.16.6.3). Thereafter, the RNA was visualized under UV light (Fig. 3.18(A)). In all RNA samples loaded, 2 specific bands of 18S and 28S rRNA were visible, demonstrating that the RNA was intact. In the next step, the RNA was blotted on a nylon membrane by capillary transfer (2.2.16.6.4), and was then cut in half to be incubated with either the SP6 or T7 probe for hybridization (2.2.16.6.5). The signals were subsequently detected by X-ray film in a chemiluminescent reaction (2.2.16.6.6).

Fig. 3.18(B) shows that the expected band for m152 mRNA at a size of ~1,413b (recall Fig. 3.2) was only detectable on the membrane incubated with the DIG-labeled probe generated with the SP6 polymerase (left panel), but not with T7 where only the DIG-labeled RNA marker was visible. This confirms the orientation of the *m152* gene in pDrive_m152 (Fig. 3.17), since the SP6 polymerase, like other polymerases, uses this 3´-5` strand as template for the synthesis of a complementary 5´-3´ RNA strand. For hybridization and detection of a specific mRNA (here: m152), the probe must consist of the complementary sequence. However, the fact that the other probe did not bind and produce a signal proved the specificity of the signal produced by the SP6 probe. As a consequence, only this probe was used in the following Northern blots. Notably, the different amounts of RNA loaded did not produce signals of accordingly different strength, indicating that this technique is not very sensitive. In order to enhance sensitivity, RNA samples were titrated in the following Northern blots to reproduce differences in *m152* expression seen with relative expression analyses using qRT-PCR.

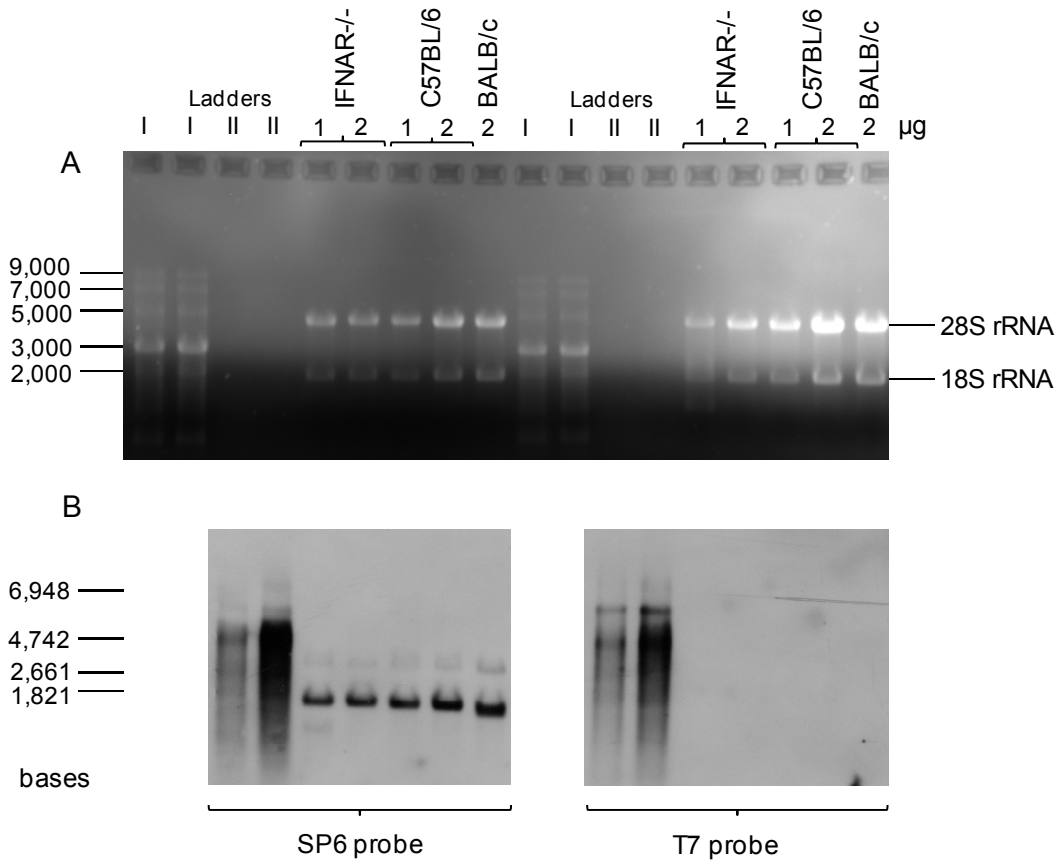

Fig. 3.18 Establishment of the Northern-blot technique with DIG-labeled m152 probes. Total RNA was purified from WT.BAC-infected MEF cultures (MOI 4), either at 90min p.i., in the case of IFNAR-/- and C57BL/6, or at 24h p.i for BALB/c MEF. RNA was titrated, denatured, and each sample was loaded twice on a 1% formaldehyde gel, and separated by gel electrophoresis. The RNA was blotted onto a nylon membrane by capillary transfer. The membrane was cut in half, with each part containing the same samples. One membrane was incubated with a DIG-labeled m152-RNA probe generated with SP6 polymerase, the other membrane was incubated with an m152-RNA probe generated by T7 polymerase. m152 RNA was then detected by a chemiluminescent reaction. (A) Photograph of the gel, stained with ethidium bromide, after electrophoresis, showing intact total RNA with the two specific bands for 28S and 18S rRNA, together with an ssRNA ladder (New England BioLabs). (B) Photograph of the chemiluminescent signal of the DIG-labeled RNA molecular-weight marker I (Roche) and m152 RNA-RNA hybrids as detected by X-ray film.

The aim was to visualize the differences in *m152* gene expression, which were detected by qRT-PCR in samples from mutIRFE- and WT.BAC-infected MEF (Fig. 3.15), on a Northern-blot membrane. Since in the initial experiment this technique appeared to be less sensitive, the samples that were shown to have the highest difference in relative expression of *m152* (60min p.i.) were used first. One of the three RNA samples per virus was titrated from 1µg-250ng and subjected to Northern-blot analysis, as described above. Although the RNA was visible in the gel under UV light, no signal could be detected on the membrane after transfer, apart from the DIG-labeled RNA marker (data not shown). This excludes the possibility that the RNA had been degraded. As to the amount of total RNA applied herein, 1µg had been detectable in the preliminary experiment, which argues

against a low loading amount. However, it has to be considered that at 60min p.i., the relative expression of *m152* (ddCT) was only <5x10^2 in mutIRFE-infected cells and ~1x10^3 in WT.BAC-infected cells, whereas at 90min p.i. it was 10^4 and 10^3, respectively (Fig. 3.15(A). This means that the relative amount of m152 RNA loaded might have been too low. To check this, for the next Northern-Blot analysis, one of the three RNA samples per virus (90min p.i, Fig. 3.15) was titrated in 4 steps (2.5, 1.5, 0.75, 0.25µg), and analyzed as described above, except that more DIG-labeled m152 probe was used (400ng/100cm^2 membrane). Fig. 3.19 depicts the results from this Northern blot.

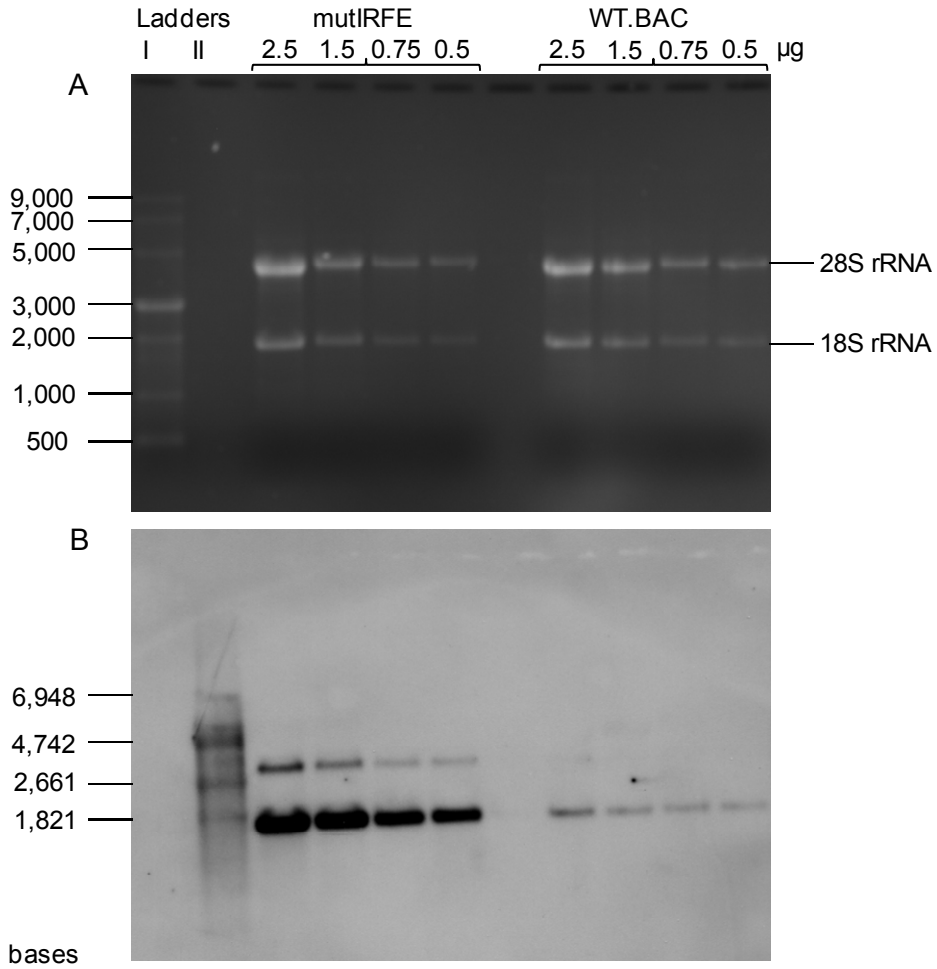

Fig. 3.19 Northern Blot with DIG-labeled m152 probe. Total RNA, purified at 90min p.i. from MEF cultures infected (MOI 4) with either virus mutIRFE or WT.BAC, was titrated, denatured, loaded on a 1% formaldehyde gel, and separated by gel electrophoresis. The RNA was blotted onto a nylon membrane by capillary transfer, and was incubated with the DIG-labeled m152 RNA probe for hybridization. The RNA was then detected by a chemiluminescent reaction. (A) Picture of the ethidium-bromide stained gel after electrophoresis, showing intact total RNA with the two specific bands for 28S and 18S rRNA, together with an ssRNA ladder (New England BioLabs). (B) Picture of DIG-labeled RNA molecular weight marker I (Roche) and m152 RNA hybrids as detected by X-ray film.

Panel (A) shows a picture of the ethidium-bromide stained gel under UV light. The two bands which are visible in all RNA samples loaded on the gel, are characteristic of the 28S and 18S rRNA present in intact total RNA. Panel (B) shows a picture of the X-ray film which was used to detect the chemiluminescent signal produced by the DIG-labeled m152 probe (generated with SP6 polymerase, see 2.2.16.6), bound to its target sequence, an antibody against DIG conjugated with alkaline phosphatase, and the substrate (CSPD). The lower band (~1,821b) visible on the gel fitted the expected size of m152 of ~1,413b. Importantly, throughout the titrated RNA sample from mutIRFE-infected cells, the amount of m152 RNA was always higher than in the corresponding sample from WT.BAC-infected cells. A second band (>2,661b), almost invisible in samples from WT.BAC, was also detected. However, it was unclear whether this was an m152-specific or unspecific signal. To verify the specificity of the upper band and to confirm the results, a second Northern blot was performed with total RNA from MEF infected for 90min with virus Δm152, mutIRFE or mutIRFErev, or were left uninfected.

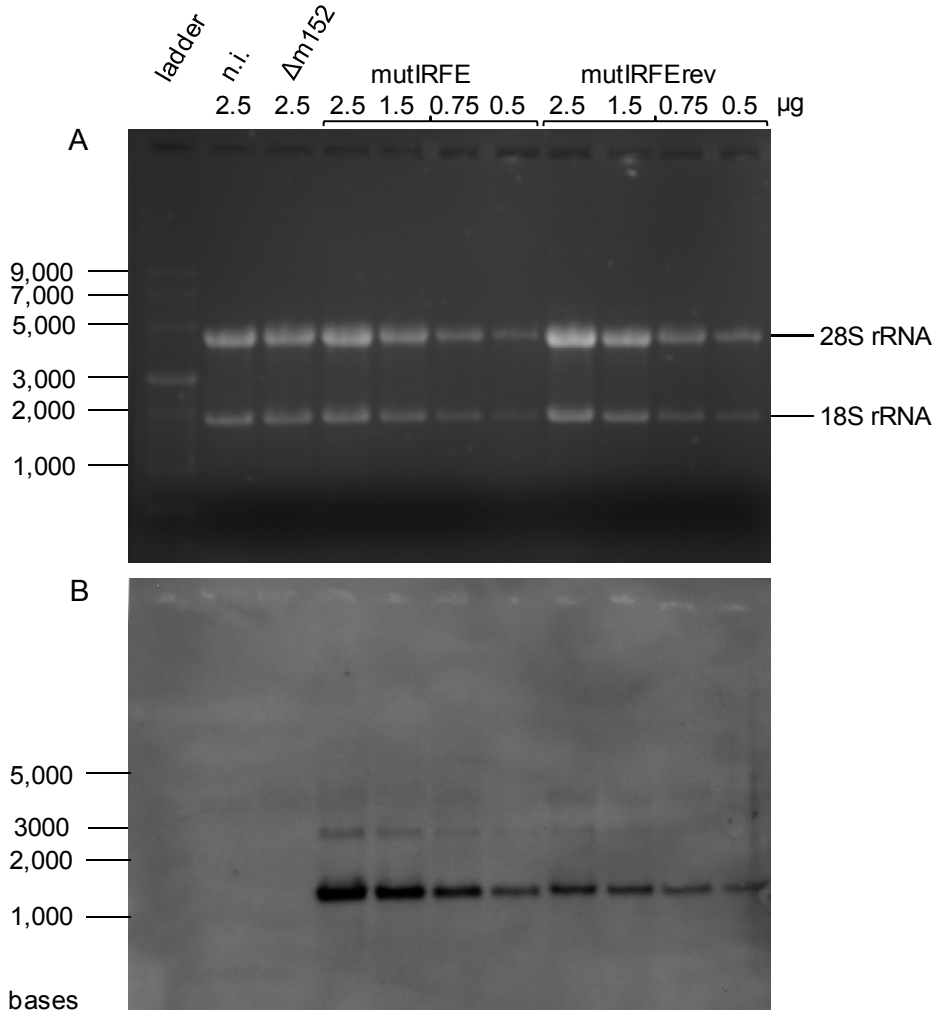

Fig. 3.20 Northern Blot with DIG-labeled m152 probe. Total RNA, purified at 90min p.i. from MEF cultures infected with either virus mutIRFE or mutIRFErev (MOI 4), was titrated, denatured, loaded on a 1% formaldehyde gel, and separated by gel electrophoresis. The RNA was blotted

onto a nylon membrane by capillary transfer, and was incubated with the DIG-labeled m152 RNA probe for hybridization. The RNA was then detected by a chemiluminescent reaction. (A) Picture of the ethidium-bromide stained gel, after electrophoresis, showing intact total RNA with the two specific bands for 28S and 18S rRNA, together with an ssRNA ladder (New England BioLabs). (B) Picture of the hybrids of DIG-labeled m152 probe and m152-specific RNA as detected by X-ray film.

Here again, the amount of RNA was titrated as was done in the preceding experiment. For all of the samples tested the loading-amount and integrity of the RNA was verified by UV light (Fig. 3.20(A)). In Fig. 3.20(B), it is clearly visibly that neither samples from uninfected MEF nor from Δm152-infected MEF contained m152-specific RNA. Essentially, the amount of m152-specific RNA was higher in all of the samples from cells infected with mutant virus as compared to the corresponding RNA samples from cells infected with the revertant. Taken together, with the Northern-blot technique it could clearly be confirmed that *m152*-expression levels are higher in MEF infected with mutant virus mutIRFE than with WT.BAC or revertant virus.

The finding that the IRFE element in the *m152* promoter is indeed operational and leads to a transcriptional inhibition of the *m152* gene in WT.BAC was quite intriguing. We were therefore interested in finding out, whether m152 protein levels that can be detected in samples from WT.BAC-infected cell cultures are actually decreased levels of the protein when compared to mutIRFE-infected samples (see 3.5).

3.5 m152 Protein Expression is Inhibited in an IRFE-Dependent Manner

So far, it could be shown herein that both *m152*-promoter activation (3.2) and gene expression (3.4) are influenced by IFN in an IRFE-dependent manner. In this respect, *m152* gene expression was significantly decreased in IFN-pretreated samples (Fig. 3.14) at early time points after infection. In order to check whether this was also true for translation of the viral protein, the same approaches as for transcription analyses, i. e. IFNβ treatment, comparison of mutIRFE vs. WT.BAC, and IFNAR-/- vs. C57BL/6, were used at this point. At first, MEF cultures were pretreated for 48h with 750U/ml of either IFNα or β, or with 20ng/ml of IFNγ, and were subsequently infected with WT.BAC (MOI 4). Protein was prepared from whole-cell lysates at different time points after infection (see figures), and was used in Western blots detecting m152 and IE1 (2.2.14). Fig. 3.21 compares m152 protein amounts in these samples. For m152, two specific bands were visible, which probably refer to isoforms of 37 and 40kDa (Ziegler et al., 1997). Also for the IE1 protein, two specific bands were visible, derived from the known 76 and 89kDa isoforms (Keil et al., 1987).

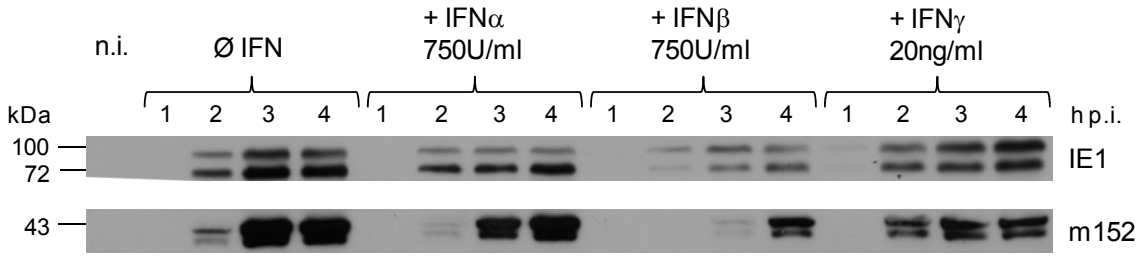

Fig. 3.21 Influence of type I and II IFN on m152 protein expression. Time course of m152- and IE1-protein expression. Shown is a Western blot of whole-cell protein (50µg per sample), isolated from cells pretreated for 48h with the indicated amounts and types of IFN, or left untreated, at the indicated time points after infection with WT.BAC (MOI 4). n.i., not infected, lysates from uninfected cells.

Evidently, treatment with IFNα led to reduced m152 protein levels at 2 and 3h p.i.. In comparison to that, treatment with IFNβ inhibited m152 protein expression even more and at all time points under test. However, also IE1 expression appeared to be decreased by type I IFN, but to a lower extent. Treatment with IFNγ reduced protein levels at 3 and 4h p.i. to a lower extent, whereas at 2h p.i. the amount was rather increased. Yet, expression of the IE1 protein was not affected at all. A Coomassie stain of the blot membrane was routinely performed to verify that equal amounts of protein had been loaded on the gel (Welinder & Ekblad, 2011; stained blot membranes not shown). Taken as a whole, this experiment has demonstrated that type I IFN inhibits m152 protein expression at early time points after infection, with IFNβ having the strongest effect, and that the effect of type II IFN might differ from that. The type I IFN effect was further investigated in a 24h infection-kinetics experiment, using 750U/ml IFNβ to pretreat MEF cultures for 48h, and subsequently infect them with WT.BAC (MOI 4). The purified protein from whole-cell lysates was analyzed in Western blots detecting viral proteins m152 and IE1. In Fig. 3.22, the time course of protein expression in these samples is depicted. At 1h p.i., no viral protein was detected. The expression of m152 was inhibited by IFNβ at 2, 3, and 4h p.i.. At 6 and 8h p.i., in the untreated sample, higher-order proteins, probably isoforms with 2 and 3 glycosylations (Ziegler et al., 1997), appeared, whereas the lowest band was disappearing. Contrary to that, in the IFNβ-treated sample, the lowest band remained and the high order bands were not visible, neither at 24h p.i.. At this time point in the untreated sample, however, all 4 bands were present, probably due to newly synthesized, still un-glycosylated protein. As to the IE1 protein, amounts were mainly comparable in IFN-treated and untreated samples, contrary to what was seen in the preceding experiment (recall Fig. 3.21). Also here, a Coomassie stain of the membrane served as a loading control (stain not shown).

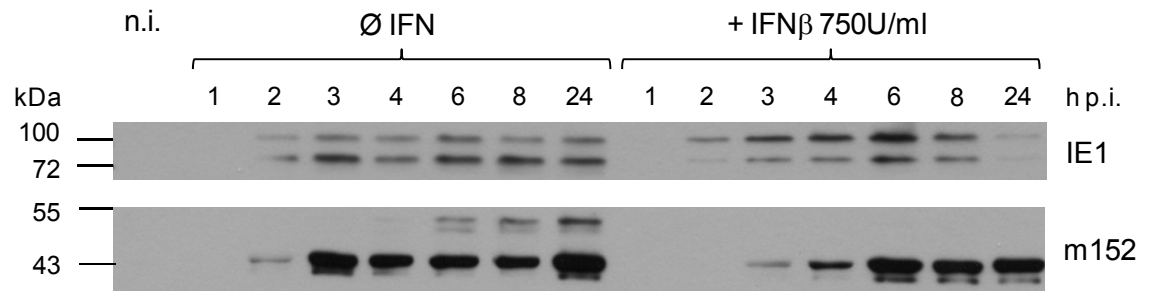

Fig. 3.22 Influence of IFNβ on m152 protein expression. Time course of m152- and IE1-protein expression. Shown is a Western blot of whole-cell protein (50µg per sample), isolated from cells pretreated for 48h with 750U/ml IFNβ, or left untreated, at the indicated time points after infection with WT.BAC (MOI 4). n.i., not infected, lysates from uninfected cells.

This experiment has confirmed the observation made from the first Western blot (Fig. 3.21) insofar as it could be shown that m152 protein expression is inhibited by IFNβ during a 24h-time course after infection. Furthermore, the decrease in certain m152 isoforms after treatment with IFNβ suggests an effect, direct or indirect, on protein modification.

In a second approach, the influence of the IRFE on m152 protein expression was investigated by comparing expression levels in mutIRFE- and WT.BAC-infected cell cultures. For this, protein was purified from whole-cell lysates at 2, 4, 6, 8, 10, 12, and 24h after infection. With these, Western blots were performed detecting viral proteins m152 and IE1. Fig. 3.23 demonstrates that throughout the time course of infection, the amount of m152 protein of all isoforms was higher in samples from mutIRFE-infected cells as compared to those from WT.BAC-infected cells. However, the amount of the IE1 protein was not different between the samples confirming comparable infection efficiencies. A Coomassie stain of the blot membrane verified equal loading amounts (not shown). Thus, the increase in m152 protein levels seen with mutIRFE is due to functional deletion of the motif, the only difference between the two viruses.

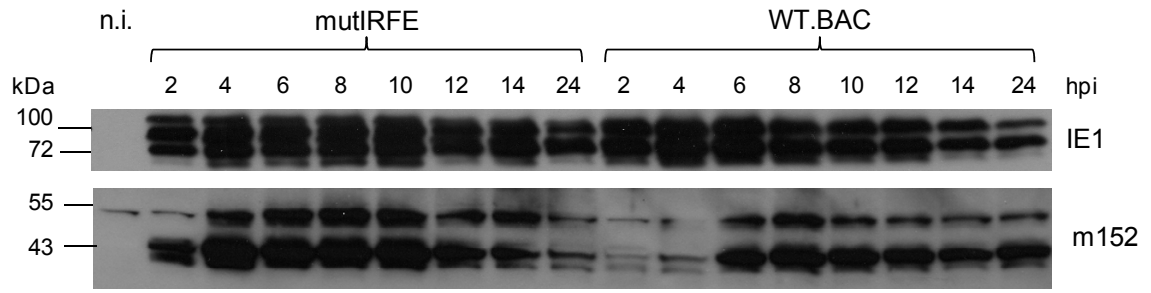

Fig. 3.23 Influence of the IRFE on m152 protein expression. Time course of m152 protein expression. Shown is a Western blot from whole-cell protein (50µg per sample), isolated at the indicated time points after infection with either virus mutIRFE or WT.BAC (MOI 4). n.i., not infected, lysates from uninfected cells. Viral IE1 serves as an infection control.

In this Western blot, an unspecific band was detected by the m152 antibody. This band colocalized with the signal from the higher glycosylated isoform of m152. In order to confirm the difference in m152 protein expression seen between mutant and WT virus, a similar experiment was performed with MEF infected with either mutant virus mutIRFE or its revertant. In addition, MEF were left uninfected or were infected with the Δm152-deletion mutant for 6h to serve as a control for the specificity of the signal. Protein was purified from whole-cell lysates at 2, 4, 6, and 8h after infection and was subjected to Western-blot analysis to detect cellular β-actin and viral m152. Obviously, the amount of m152-specific protein is higher in mutIRFE-infected cells as compared to mutIRFErev-infected cells at all time points tested (Fig. 3.24). Importantly, the amount of β-actin is comparable between the samples, which guarantees equal loading amounts. Moreover, in the control samples, no m152-specific signal is detectable.

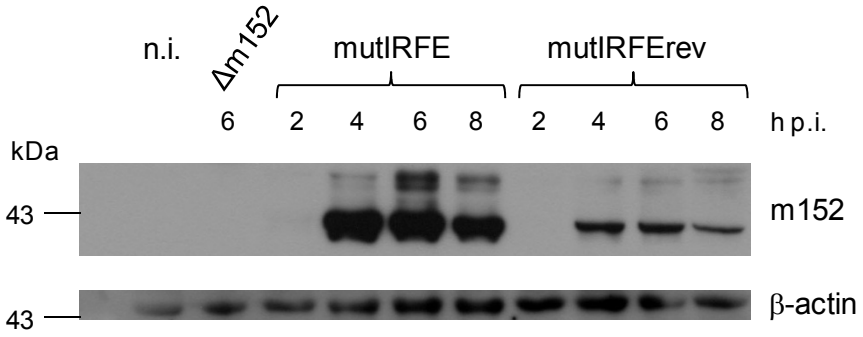

Fig. 3.24 Influence of the IRFE on m152 protein expression. Time course of m152 protein expression. Shown is a Western blot from whole-cell protein (50µg per sample), isolated at the indicated time points after infection with virus Δm152, mutIRFE or mutIRFErev (MOI 4). n.i., not infected, lysates from uninfected cells. β-actin serves as a loading control.

So far, these findings are in perfect accordance with the observations made on the gene-transcription level, where *m152* gene expression was higher in mutIRFE infected cells (Fig. 3.14). As a next step, also the third approach applied in transcription analyses, namely the use of IFNAR knock-out mice, was tested on the translation level. This should disclose whether the inhibitory effect on m152 protein expression could not only be reversed by functional deletion of the motif (Fig. 3.23+24), but also by knocking-out type I IFN signaling. For this, MEF from IFNAR-/- knock-out mice together with the control group of MEF from C57BL/6 were pretreated with 750U/ml IFNβ to enhance any potential effect, and were subsequently infected with WT.BAC (MOI 4). Protein was prepared from whole-cell lysates and analyzed for the expression of m152 and IE1. Fig. 3.25 compares the amounts of protein from both cell cultures, including an uninfected control (n.i.) for each of the mouse type.

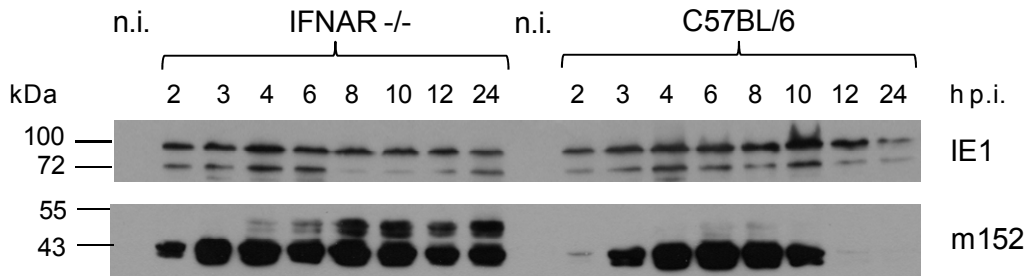

Fig. 3.25 Influence of type I IFN signaling on m152 protein expression. Time course of m152 expression. Shown is a Western blot of whole-cell protein (50µg per sample), isolated from MEF pretreated for 48h with 750U/ml IFNß, at the indicated time points after infection with WT.BAC (MOI 4). n.i., not infected, lysates from uninfected cells derived from IFNAR-/- and C57BL/6. Viral IE1 serves as an infection control.

The IE1 protein in all samples appeared to be of comparable amount, demonstrating that infection efficiency was identical between the different samples. A Coomassie stain of the blot membrane confirmed comparable loading amounts (not shown). Thus, it is even more impressive that in infected IFNAR-/- MEF the amount of m152 protein was higher at all time points under test. Remarkably, from 4h p.i. onwards, all four isoforms were present and were maintained; this was in sharp contrast to infected C57BL/6 MEF, where only the two lower order isoforms were strongly visible. Obviously, the inhibitory effect of IFNβ on m152 protein expression and post-translational modification was abrogated in IFNAR-/- mice.

Overall, these different Western-blot analyses have revealed that m152 protein expression is significantly inhibited by type I IFN (Figs. 3.21+22), and that this inhibitory effect can be reversed, either by functionally deleting the IRFE in the m152 promoter (Fig. 3.23+24), or by preventing type I IFN signaling (Fig. 3.25). In this context, the data totally agree with the findings of the transcriptional analyses conducted herein (3.4). Having shown that the IRFE apparently influences m152-RNA and protein levels, it was of interest to find out whether this would also have a functional effect with respect to the immune-modulatory function of m152. This question was addressed in the following experiments.

3.6 IRFE-Dependent Inhibition of m152 Restores Direct Antigen Presentation for CD8 T-Cell Activation by Infected APC

Thus far, the influence of the IRFE on m152 promoter activity, gene and protein expression has been investigated, and revealed that the overall effect was inhibitory. However, whether this would also lead to effects on the immune-modulatory function of m152 had to be determined in the next step. One of the main targets of m152 is the activation of CD8 T cells by peptide-loaded MHC class I complexes on the cell surface which is subverted by the retention of these complexes in the ERGIC (Ziegler et al., 1997 & 2000). This function was initially addressed in the single-cell ELISPOT assay (2.2.18.1)

to reveal the frequencies of IFNγ-secreting effector cells upon stimulation with epitope-presenting cells. For this, as APC, MEF were infected (MOI 4) for 20h with virus Δm152, mutIRFE, or Δm152rev/WT.BAC and were seeded in triplicates together with graded numbers of *ex-vivo* isolated CD8 T cells (2.2.8) or m164-peptide specific CTLL (2.2.10) as effector cells. Fig. 3.26 displays the recognition of infected cells by CD8 T cells, isolated from spleens of BALB/c mice in the acute phase of infection (1wk p.i.) with WT.BAC. Shown are most probable numbers (MPN) of spots per $5x10^4$ effector cells, with their 95% confidence intervals, as determined by linear regression analysis (Mathematica 8.0). The potential of the effector cells to recognize mCMV-infected MEF and become activated was demonstrated by infection with Δm152. In this mutant virus, deletion of gene *m152* prevents the retention of peptide-loaded MHC class I molecules, so that peptide presentation to effector cells can take place. This resulted in a high number of spots. Contrary to that, effector cells were not activated by uninfected MEF. Obviously, MEF infected with WT.BAC could also activate the T cells by mCMV-peptide presentation, but to a much lower extent than Δm152 infected cells. This was due to the immune-modulatory function of m152. Interestingly, cells infected with mutIRFE appeared to activate even less effector cells, namely half of the amount of WT.BAC. This finding was the first hint at a functional effect of the IRFE, which could be well explained by the decreased amount of m152 protein found in WT virus as compared to mutant virus mutIRFE (Fig. 3.23+24).

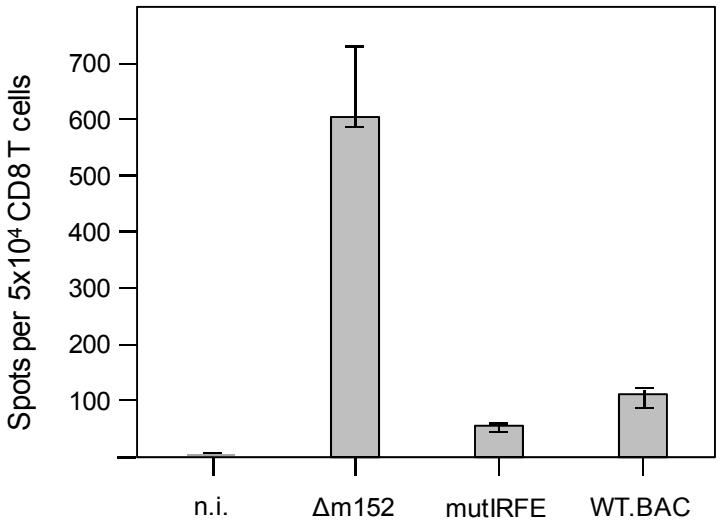

Fig. 3.26 Recognition of infected cells by acute CD8 T cells. Presentation of antigenic peptides on cells infected with m152 mutants and WT.BAC. MEF (BALB/c) were infected (MOI 4) for 20h with the indicated viruses. n.i., uninfected MEF. Shown are data from an IFNγ-based ELISPOT assay, using *ex vivo* isolated CD8 T cells (from spleens, 1wk p.i.) as effector cells by seeding graded numbers (1,000, 5,000, 10,000, 50,000) in triplicates together with the infected MEF as target cells. Grey bars indicate the frequencies of responding cells (most probable number of spots

per 5x10^4 effector cells), with error bars depicting their 95% confidence intervals. Values were determined by intercept-free linear regression analysis of spot numbers (Mathematica 8.0).

In order to test, whether an increased activation by WT-infected cells as compared to mutIRFE-infected cells was also found in *ex vivo* isolated memory CD8 T cells, another ELISPOT assay was performed. Therein, pretreatment of the APC with IFNβ was applied, as was done before in other experiments (3.2-4). On the one hand, this should point out the direct effect of this cytokine on m152's immune-modulatory function. On the other hand, this should enhance peptide presentation, which was already low in WT.BAC-infected cells (Fig. 3.26), and thereby increase the difference to mutIRFE. For this, APC were pretreated for 48h with 500U/ml IFNβ, or were left untreated, and were subsequently infected as described above. The effector cells were isolated from spleens of BALB/c mice >3mo p.i. (repeated with effectors from different time points p.i.) with WT.BAC (2.2.8).

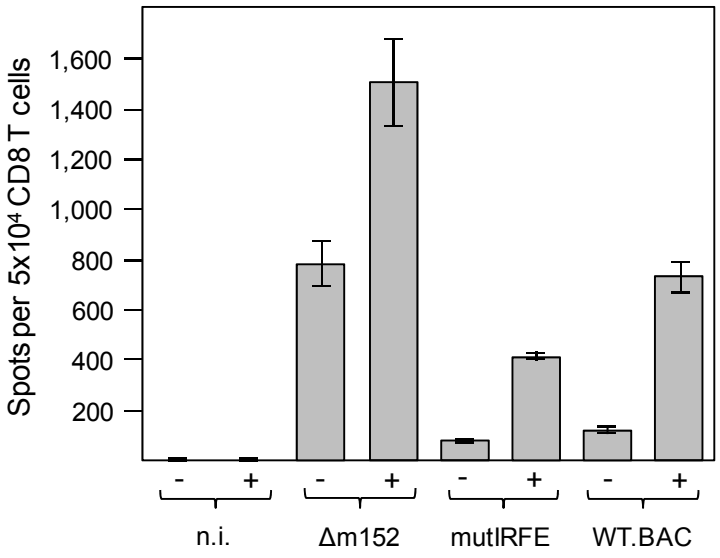

Fig. 3.27 Recognition of infected cells by memory CD8 T cells. Presentation of antigenic peptides on cells infected with m152 mutants and WT.BAC. MEF (BALB/c) were pretreated for 48h with 500U/ml IFNβ (+), or were left untreated (-), and were subsequently infected (MOI 4) for 20h with the indicated viruses. n.i., uninfected MEF. Shown are data from an IFNγ-based ELISPOT assay, using *ex-vivo* isolated CD8 T cells (>3mo p.i. with WT.BAC) as effector cells by seeding graded numbers (400, 2,000, 10,000, 50,000) in triplicates together with the infected MEF as target cells. Grey bars indicate the frequencies of responding cells (most probable number of spots per 5x10^4 effector cells), with error bars depicting their 95% confidence intervals. Values were determined by intercept-free linear regression analysis of spot numbers (Mathematica 8.0).

Fig. 3.27 presents the MPN of activated effector cells (spots) per 5x10^4 cells, for each of the viruses under test, from one experiment. Also here, the potential to recognize mCMV-infected MEF is shown in Δm152-infected samples. As intended, pretreatment with IFNβ resulted in increased numbers of activated effector cells, almost by a factor of 2. Untreated, WT.BAC-infected cells activated only ¼ of the effector cells as compared to

Δm152 (untreated). However, after IFNβ treatment, about half of the effector cells as compared to Δm152 (pretreated) were activated. In mutIRFE-infected cells, the numbers of activated effectors were lower as compared to WT virus, which was more pronounced after IFNβ pretreatment, although also here, this resulted in a higher number of activated effector cells. However, this is not surprising, because although IFNβ cannot act on m152 via IRFE in the mutant, it can certainly enhance peptide presentation by cellular mechanisms. Taken together, this experiment has revealed that WT.BAC-infected MEF appear to present more viral antigen, whereby effector cells from the memory phase are activated as compared to activation by mutIRFE-infected MEF. This confirms the findings from effector cells of the acute phase.

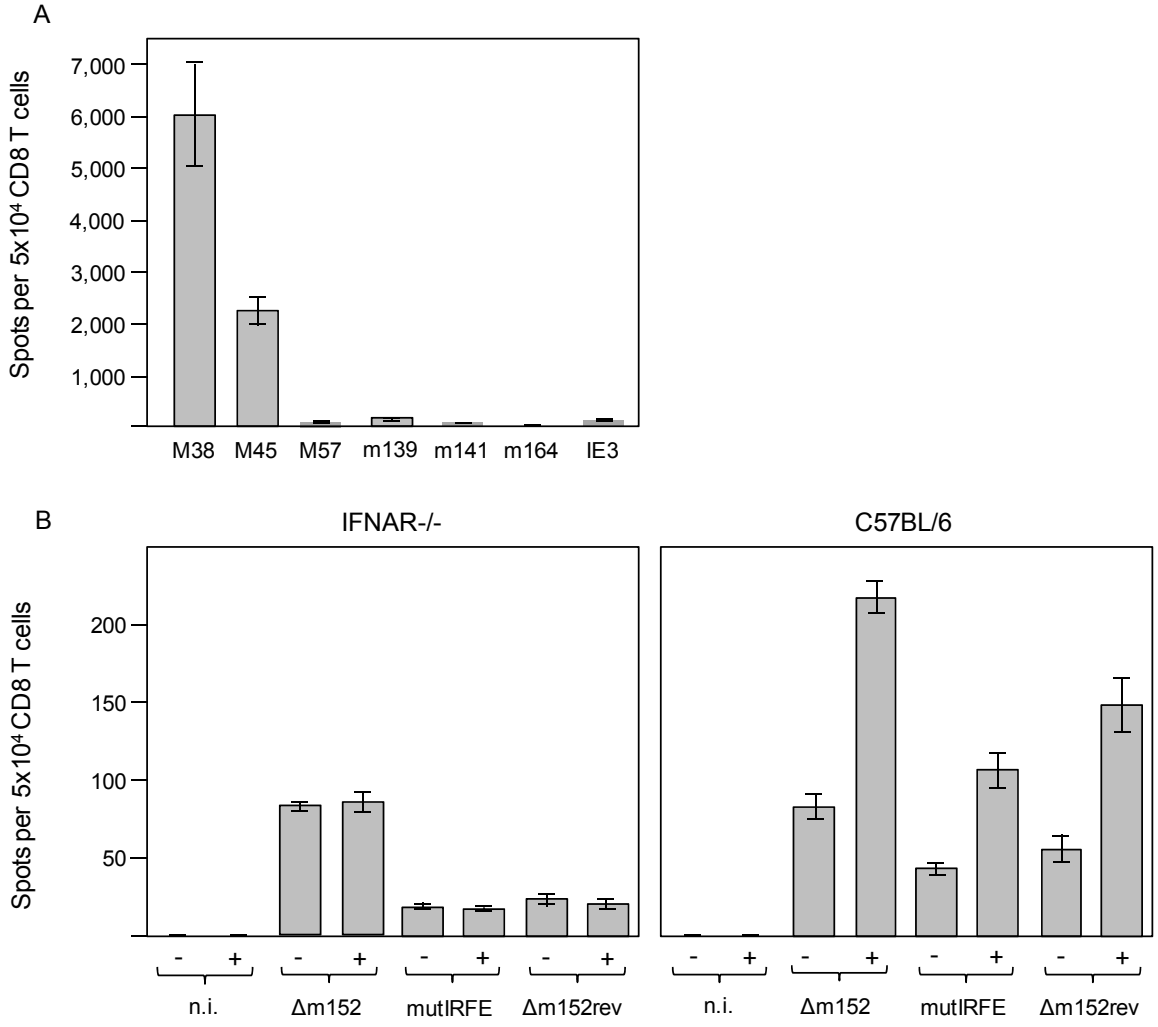

Fig. 3.28 Recognition of infected cells by *ex vivo* isolated memory (WT.Smith) CD8 T cells. (A) Activation of effector cells by synthetic, antigenic peptides (H-2^b haplotype) presented by EL-4 target cells, exogenously loaded with 10^{-6}M of the corresponding peptide. (B) Presentation of antigenic peptides on cells infected with m152-mutants and Δm152rev (WT). MEF, derived from IFNAR-/- or C57BL/6, were pretreated for 48h with 500U/ml/100mm dish IFNβ (+), or were left untreated (-), and were subsequently infected (MOI 4) for 20h with the indicated viruses. n.i., uninfected MEF. Shown are data from IFNγ-based ELISPOT assays, using *ex vivo* isolated CD8 T

cells (from spleens of mice >3mo p.i.) as effector cells, by seeding graded numbers (1,000, 5,000, 10,000, 50,000) in triplicates together with the different targets. Grey bars indicate the frequencies of responding cells (most probable number of spots per $5x10^4$ effector cells), with their 95% confidence intervals given by error bars. Values were determined by intercept-free linear regression analysis of spot numbers (Mathematica 8.0).

So far, the functional effect of IRFE-dependent m152 inhibition had been investigated in ELISPOT assays by comparing mutant and WT virus, and by using IFNβ to enhance the effect. As a third approach, in preceding experiments, type I IFN-signaling knock-out mice (IFNAR-/-) had been used in comparison to C57BL/6 (same genetic background). This system should also be tested at this point. As effector cells, memory CD8 T cells were *ex vivo* isolated from spleens of C57BL/6 mice >3mo p.i. with WT.Smith, and were used in the ELISPOT assay at titrated dilutions. At first, the activity of these effector cells was tested using EL-4 as target cells, loaded with synthetic, antigenic peptides.

Fig. 3.28(A) shows that target cells presenting the mCMV-peptide M38 activated the highest number of effector cells (shown as MPN). Presentation of the other antigenic peptides, namely M45, m139, IE3, M57, m141, and m164 also activated the effector cells, but with decreasing numbers, in this order. This demonstrated that the effector cells were functional and in addition revealed the distribution of epitope specificities in the polyclonal and polyspecific memory CD8 T-cell population. Then, in a second assay, MEF, derived from either IFNAR-/- or C57BL/6 mice, were pretreated with IFNβ or were left untreated and were then infected with Δm152, mutIRFE, or Δm152rev (WT) as described above, before their use as APC in the ELISPOT assay. Fig. 3.28(B) depicts the numbers of activated effector cells (MPN) for each of the targets. As assumed, pretreatment with IFNβ had no effect on peptide presentation in IFNAR-/- cells, which lack type I IFN signaling, but in C57BL/6. The number of activated effector cells by mutIRFE and Δm152rev, but not Δm152 infected (untreated) targets was lower in IFNAR-/- MEF than in C57BL/6. Thereby, the influence of IFNβ on antigen presentation in general was shown. Furthermore, in both types of MEF, Δm152-infected cells activated effectors the most, and mutIRFE the least, as was shown before with BALB/c MEF (Fig. 3.27). This demonstrates that also in the H-2^b haplotype, the IRFE-dependent negative influence on m152 restores direct antigen presentation for CD8 T-Cell activation.

At this point, the functional inhibition of m152 by IRFE had been shown in connection with effector functions of *ex vivo* isolated polyclonal and polyspecific acute or memory CD8 T cell populations. In order to investigate the activation of epitope-monospecific effector cells, a cytolytic T lymphocyte line (CTLL) with the specificity for a known antigenic peptide of the H-2^d haplotype, namely m164 (Holtappels et al., 2002a+b), was generated next. A synthetic m164 peptide was used to *in vitro* repetitively stimulate memory CD8 T cells isolated from the spleen of donor mice (BALB/c). For this, it had to be considered

that the molar concentration of the peptide during restimulations is important, although m164-CTLL are known to tolerate a wide range of peptide concentrations (Podlech et al., 2002). Nonetheless, two concentrations to generate two different CTLL were used herein, namely 10^{-8}M and 10^{-10}M. At first, these CTLL were tested for their functional avidity in two assays of effector-cell functions, namely the cytolytic assay (^{51}Cr-release assay, 2.2.18.2) to measure lysis of epitope-presenting target cells, and the ELISPOT assay to quantitate frequencies of responding effector cells.

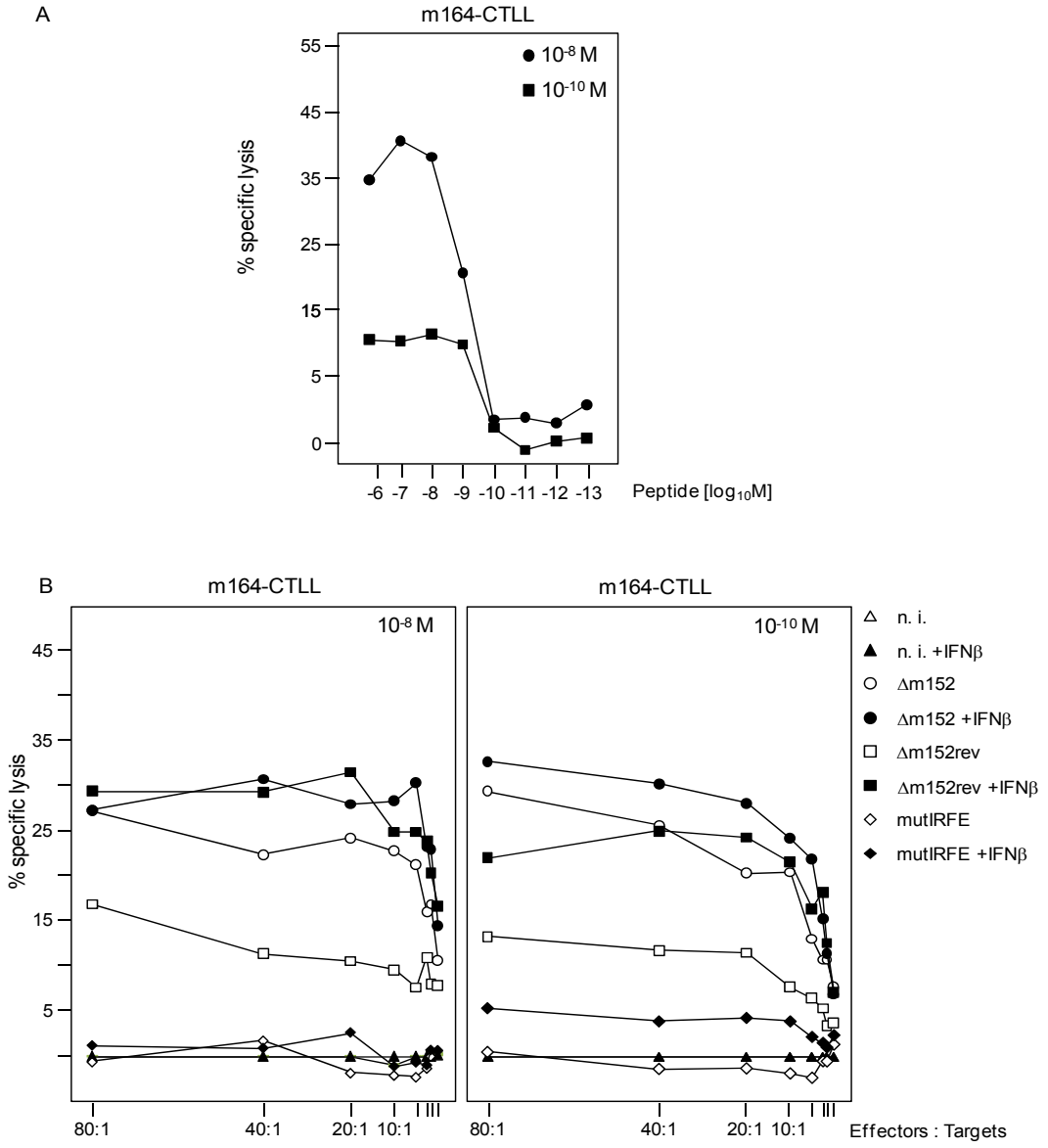

Fig. 3.29 Comparison of functional avidities of two different m164 CTLL. Cytolytic 4h ^{51}Cr-release assay. Effector cells were m164-peptide specific CTLL, stimulated with different molarities of the antigenic, synthetic peptide, 10^{-8}M or 10^{-10}M. Target and stimulator cells were MEF, derived from BALB/c. (A) MEF target cells were exogenously loaded with the indicated concentrations of synthetic m164 peptide. Cytolytic activity was determined at an effector:target cell ratio of 15:1. (B) MEF target cells were pretreated for 48h with 500U/ml/100mm dish IFNβ, or were left untreated, and were subsequently infected (MOI 4) with the indicated panel of viruses. n.i., uninfected MEF.

Cytolytic activity was determined at the indicated effector:target cell ratios. Dots represent the mean of triplicate measurements.

In both assays, to stimulate the effector cells, two different types of targets were used, namely MEF, either exogenously loaded with the antigenic, synthetic peptide at defined concentrations, or pretreated with IFNβ and infected with the m152 mutants or Δm152rev, as described above. As shown in Fig. 3.29(A), the threshold peptide concentration for triggering cytolytic activity was between 10^{-9} and 10^{-10}M for both CTLL. However, the percentage of specific lysis at all peptide concentrations was higher for the 10^{-8}M CTLL. Though, the percentage of specific lysis was generally low, particularly by the 10^{-10}M CTLL. Fig. 3.29(B) reveals the cytolytic activities of both CTLL (left panel, 10^{-8}M; right panel, 10^{-10}M) after stimulation by antigen-presenting infected MEF. Interestingly, neither of the mutIRFE samples (+/- IFNβ) could induce cytolytic activity of the 10^{-8}M CTLL, as was the case for the uninfected controls in both CTLL. Only the IFNβ pretreated, mutIRFE infected sample could induce a low percentage of lysis in the 10^{-10}M CTLL. This demonstrated a somewhat higher avidity of this line at low peptide concentrations. In accordance with that, also the other samples infected with Δm152 or Δm152rev induced a stronger cytolytic activity in the 10^{-10}M CTLL as compared to the 10^{-8}M CTLL, with IFNβ pretreated samples always inducing the highest percentages. Only at high effector:target ratios (80:1) did the 10^{-8}M CTLL display higher lysis of Δm152rev-infected target cells than the other line. In summary, this demonstrated that the inhibition of the cytolytic activity of these CTLL by m152, present in Δm152rev-infected cells, is decreased in an IRFE-dependent manner. Fig. 3.30(A) gives the frequencies of the CTLL (left panel, 10^{-8}M; right panel, 10^{-10}M) responding to the different concentrations of synthetic m164 peptide in the ELISPOT assay. Here, the threshold for IFNγ secretion was 10^{-10}M for both CTLL, but the number of effector cells activated by this concentration of synthetic peptide was higher in the 10^{-10}M CTLL. Stimulation with 10^{-9}M peptide yielded equal numbers of responding cells. However, higher peptide concentrations in the assay induced higher numbers in the 10^{-8}M CTLL. These findings were partly in accordance with the cytolytic assay (Fig. 3.29(A)), but the activity of the 10^{-10}M CTLL appeared to be stronger as shown by the cytolysis assay. For the situation *in vivo*, lower peptide concentrations are more realistic, which suggests that the 10^{-10}M CTLL is more suitable in these settings.

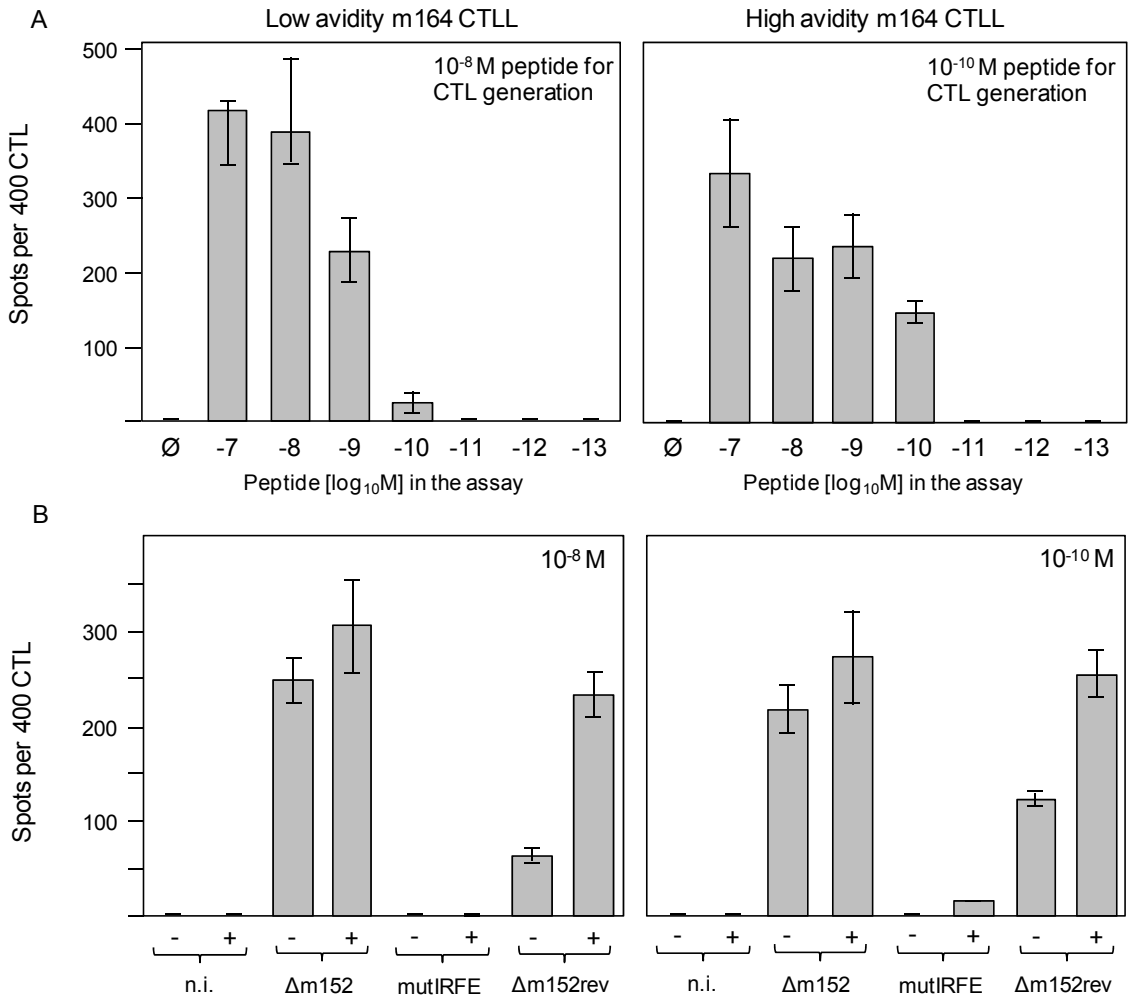

Fig. 3.30 Recognition of mCMV-antigen presentation by m164 peptide-specific CTLL. Comparison of two m164 peptide-specific CTLL stimulated with different molarities of the synthetic peptide. Stimulator cells were P815-B7 cells irradiated and exogenously loaded with the synthetic m164 peptide at a concentration of either 10^{-8}M or 10^{-10}M. (A) Functional avidities of the two different CTLL. MEF were exogenously loaded with the indicated concentrations of the synthetic m164 peptide and used as stimulator cells in the IFNγ-based ELISPOT assay. Ø: MEF with no peptide added. (B) Presentation of the m164 peptide by MEF, after a 48h IFNβ pretreatment with 500U/ml/100mm dish (+), and subsequent infection (MOI 4) for 20h with m152 mutants and Δm152rev (WT). (-), IFNβ untreated cells. n.i., uninfected MEF. Frequencies of responsive cells in the IFNγ-based ELISPOT assays were determined by seeding graded numbers of effector cells (50, 100, 200, 400) in triplicates together with the different stimulator cells, followed by intercept-free linear regression analysis of spot numbers. Grey bars indicate the frequencies of responding cells (most probable number of spots per 400 effector cells), with error bars depicting their 95% confidence intervals. Values were determined by intercept-free linear regression analysis of spot numbers (Mathematica 8.0).

Fig. 3.30(B) shows the frequencies of responding CTL after stimulation by antigen-presenting infected MEF. Interestingly, and completely matching the results from the cytolytic assay, neither of the mutIRFE samples (+/- IFNβ) could induce IFNγ secretion by the 10^{-8}M CTL, as was the case for the uninfected controls in both CTLL. Importantly, also here, only the IFNβ-pretreated, mutIRFE-infected cells could activate a low number of the

10^{-10}M CTL. However, CTL of both specificities were activated by cells infected with WT virus (Δm152rev), with IFN-β treatment leading to an enhanced activation. Thus, also this assay demonstrated that the capacity of m152 to prevent antigen presentation is inhibited in an IRFE-dependent manner.

Additionally, CTL of two other specificities, namely m145 peptide-specific CTLL (10^{-9}M) and m105 peptide-specific CTLL (10^{-10}M) were used as effector cells to detect their activation by MEF infected with Δm152, mutIRFE or mutIRFErev in the same setting.

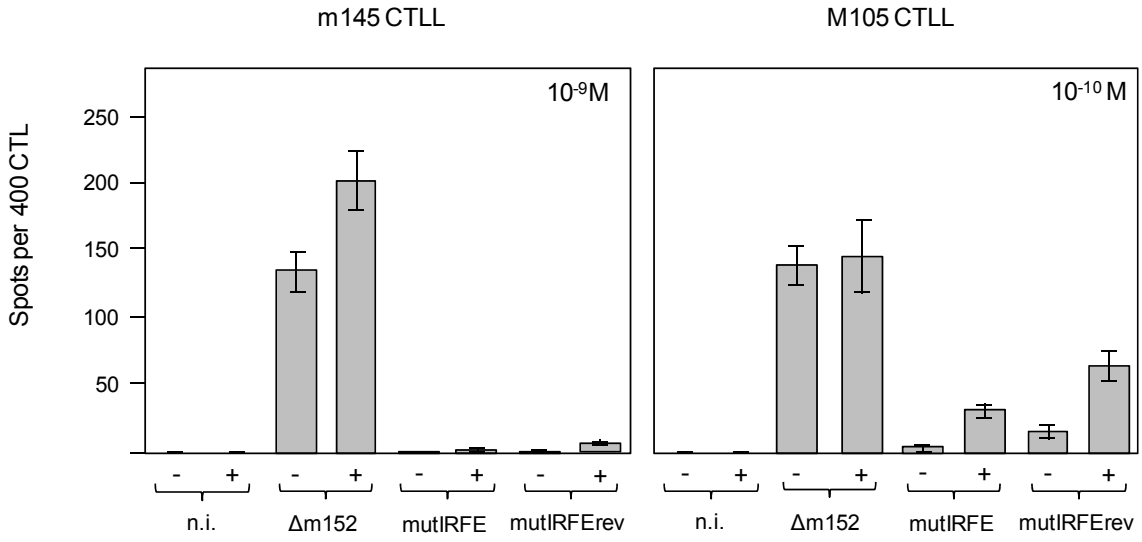

Fig. 3.31 Recognition of mCMV-antigen presentation by m145 and M105 peptide-specific CTLL. Presentation of the m145 peptide (left panel) or M105 peptide (right panel) by MEF, after a 48h IFNβ pretreatment with 500U/ml/100mm dish (+), and subsequent infection (MOI 4) for 20h with m152 mutants and Δm152rev (WT). (-), IFNβ untreated cells. n.i., uninfected MEF. Frequencies of responsive cells in the IFNγ-based ELISPOT assays were determined by seeding graded numbers of effector cells (50, 100, 200, 400) in triplicates together with the different targets, followed by intercept-free linear regression analysis of spot numbers. Grey bars indicate the frequencies of responding cells (most probable number of spots per 400 effector cells), with error bars depicting their 95% confidence intervals. Values were determined by intercept-free linear regression analysis of spot numbers (Mathematica 8.0).

Fig. 3.31 shows the frequencies of responding cells per 400 CTL. The potential of the m145-peptide specific CTL was revealed by APC infected with the m152-deletion mutant. Yet, neither cells infected with mutant nor revertant virus were able to activate high numbers of effector cells except for IFN-β-pretreated, revertant-infected cells which induced slightly elevated activation levels. However, M105 antigen-specific CTL were able to recognize cells infected with either virus, with the highest numbers by the m152-deletion mutant and decreased numbers by mutant and revertant virus. In essence, with both CTLL the lowest activation was observed when the stimulator cells were infected with mutIRFE, regardless of whether or not the cells were pretreated with IFN.

Taken together, the ELISPOT assays with polyclonal acute or memory effector cells as well as with epitope-specific CTL have revealed that the inhibition of m152 RNA and protein expression in the presence of the IRFE motif after infection with WT-equivalent virus actually has an effect on the immune-modulatory function of m152 in terms of enhanced presentation of peptide-loaded MHC class I molecules. Whether this functional effect of the IRFE on m152 was also of importance for viral replication and pathogenicity in the natural host was determined in the next step.

3.7 IRFE-Dependent Inhibition of m152 Restores the Protective Antiviral Activity of CTLL

Up to this point, the functional effect of the IRFE-dependent inhibition of *m152* gene and protein expression has been shown in cell-culture assays (ELISPOT assay, cytolysis assay, see 3.6) using *ex vivo* isolated CD8 T cells and epitope-specific CTLL. It was shown that the activation of effector cells by WT-infected MEF was dependent on the inhibition of m152. As a next step, the *in vivo* relevance of this IRFE-dependent inhibition of m152 for the protective function of CTLL was investigated. The state-of-the-art approach to determine the protective antiviral activity is the adoptive transfer (AT) of these cells into immunocompromised and mCMV-infected (i.pl.) recipients. Normally, mice die of multiple-organ CMV disease, unless intravenously transferred CD8 T cells protect against infection (Reddehase et al., 1985). For this reason, the AT is an approach of experimental cytoimmunotherapy. It was applied herein in two different settings.

In the first AT experiment, two m164-CTLL of different avidities (see 3.6), tested for their functionality in ELISPOT assays and cytolysis assays (Figs. 3.29+30), were used as effector cells. As indicator recipients, 8-9wk-old BALB/c mice were immune suppressed by γ-irradiation (single dose 6.5Gy). The m164 peptide-specific CTLL were titrated (10^2-10^6/0.5ml PBS/mouse) and injected intravenously. As negative control, 7 mice were left without T-cell transfer (no transfer control). Subsequently, mice were infected (i.pl.) with 10^5PFU/25µl PBS of virus Δm152, mutIRFE, or Δm152rev. Normally, organ infection is monitored 11-13d after cell transfer and infection, at the time when recipient mice of the no-transfer group succumb to multi-organ CMV disease. However here, already by 10d p.i. 12% of the mice had died (indicated by a black daggers), whereof 8.5% were from mutIRFE-infected groups. For this reason, the experiment was ended, and organs were dissected. Virus replication in spleen and lungs was evaluated by quantitating infectivity (plaque assay, see 2.2.4) and the number of viral genomes (qPCR, see 2.2.15.10). In the liver, infected cells were detected by IE1-specific immunohistology together with CD3ε-specific staining of CD8 T cells in this organ (IHC, see 2.2.17). Fig. 3.32 gives the results from both analyses and for all groups tested. The data obtained from animals having

received the same amount (10^4, 10^5, 10^6) of either the 10^{-8}M (n=5) or the 10^{-10}M (n=5) m164-CTL were combined to increase the number of individuals tested per group (n=10). However, to discriminate between data obtained from either of the CTLL, two different colors were used in Fig. 3.32, namely black (10^{-8}M) and grey (10^{-10}M). In the left panel, data from ∆m152-infected mice are shown. This group was included in the experiment mainly as a control for the protective potential of the two different m164-CTLL. In general, CTLL of this specificity are known to efficiently control mCMV-infection in indicator recipients after AT (Holtappels et al., 2002a). In the no transfer control group virus titers were about $1\log_{10}$ decreased as compared to ∆m152rev and mutant virus. This was not so surprising, because as mentioned above (3.3), it is a known fact that deletion of the *m152* gene leads to growth attenuation of the virus in lungs, and spleens of immunocompromised mice (Krmpotić et al., 1999). Obviously, transfer of 10^5 m164-CTL already protected the recipients from infection with ∆m152, which was shown by a significant decrease (P = 0.0001) in virus titers in spleen (A) and lungs (B). However, in the liver (C) the numbers of infected cells were already significantly reduced (P = 0.0358) after transfer of 10^4 CD8 T cells. These results demonstrated the high efficiency of the m164-CTL in controlling mCMV-infection in indicator recipients, and confirmed their functionality, which was shown before in ELISPOT assays and cytolysis assays. In comparison, the titers of revertant virus (right panel) after transfer of 10^5 m164-CTL were also significantly reduced (P = 0.0145) in the spleen (A), as were the numbers of infected liver cells (C) (P = 0.0081). On the contrary, in lungs virus titers appeared to be slightly increased after transfer of 10^4 CD8 T cells, whereas they were found to be significantly decreased (P = 0.0393) only by 10^6 adoptively transferred m164-CTL. Strikingly, and in sharp contrast to the other two viruses used herein, the virus titers of mutIRFE (mid panel) in spleen (A) and lungs (B) of indicator recipients, as well as the number of infected liver cells (C), were rather unaltered or increased as compared to the control group, independent of the amount or avidity of the m164-CTL transferred. The fact that most of the mice that had died before 10 d p.i. were infected with the mutant virus (8.5%) supports this result, which probably results from a higher virus load in these animals. Based on the findings from preceding experiments in cell culture, where mutation of the IRFE led to increased *m152*-expression levels and prevented an activation of the m164-CTL (Fig. 3.29), the absence of a protective antiviral activity in the mutIRFE-infected recipient was now confirmed in accordance with the prediction.

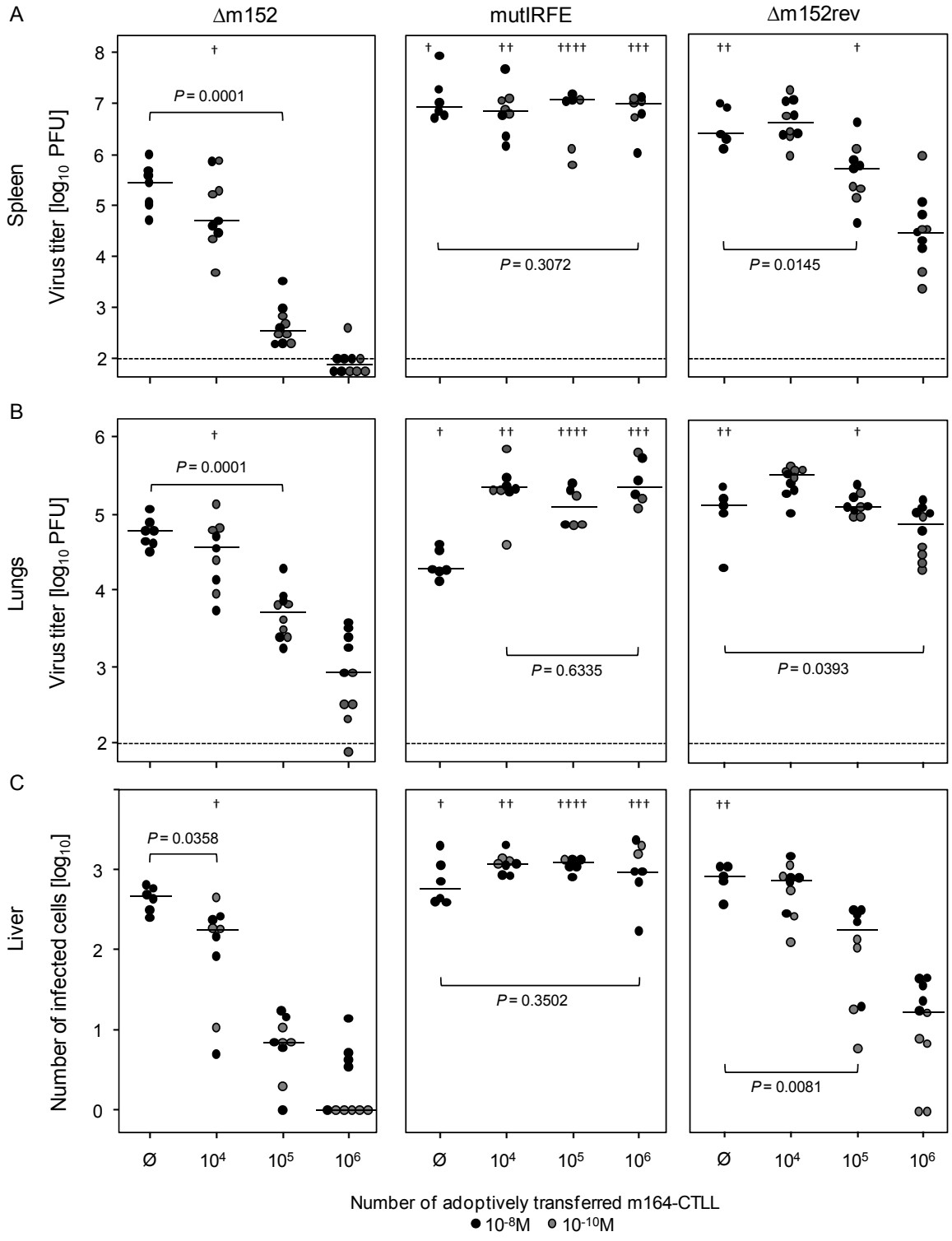

Fig. 3.32 Protective antiviral activity of m164-CTLL depending upon the expression of viral m152. Graded numbers of cells (m164-CTL) specific for the m164 peptide of mCMV were transferred into immunocompromised 8-9wk-old BALB/c recipients infected with virus Δm152, mutIRFE, or Δm152rev. Virus replication was monitored at 10d after infection and cell transfer by plaque assay in homogenates of spleen (A) and lungs (B), and by immunohistological quantitation of infected liver cells in representative 10mm^2 areas of tissue sections (C) (IE1-specific IHC). Ø control group of infected mice, left without cell transfer. Black dots represent logarithmized data for individual recipients of the 10^{-8}M m164-CTL, and grey dots for individual recipients of the 10^{-10}M m164-CTL. Median values are marked by horizontal bars. The dotted line indicates the detection limit of the plaque assay. Black daggers show the number of mice which had died before day 10. *P*

values, determined by unpaired *t* test are indicated (http://www.graphpad.com/quickcalcs/ttest1.cfm).

Fig. 3.33 shows immunohistological images, illustrating extensive pathology of the liver tissues with plaque-like virus foci in the absence of therapy (no transfer groups, upper panels), whereas lower panels illustrate almost complete prevention of liver infection with ∆m152 and ∆m152rev by 10^5 adoptively transferred m164-CTL (10^{-10}M). In contrast to that, infection was not controlled by the same number of CTL in mutIRFE infected recipients (center panel), and CD8 T cells appeared to be randomly distributed rather than assembled around virus foci, unlike the situation observed after infection with the other two viruses.

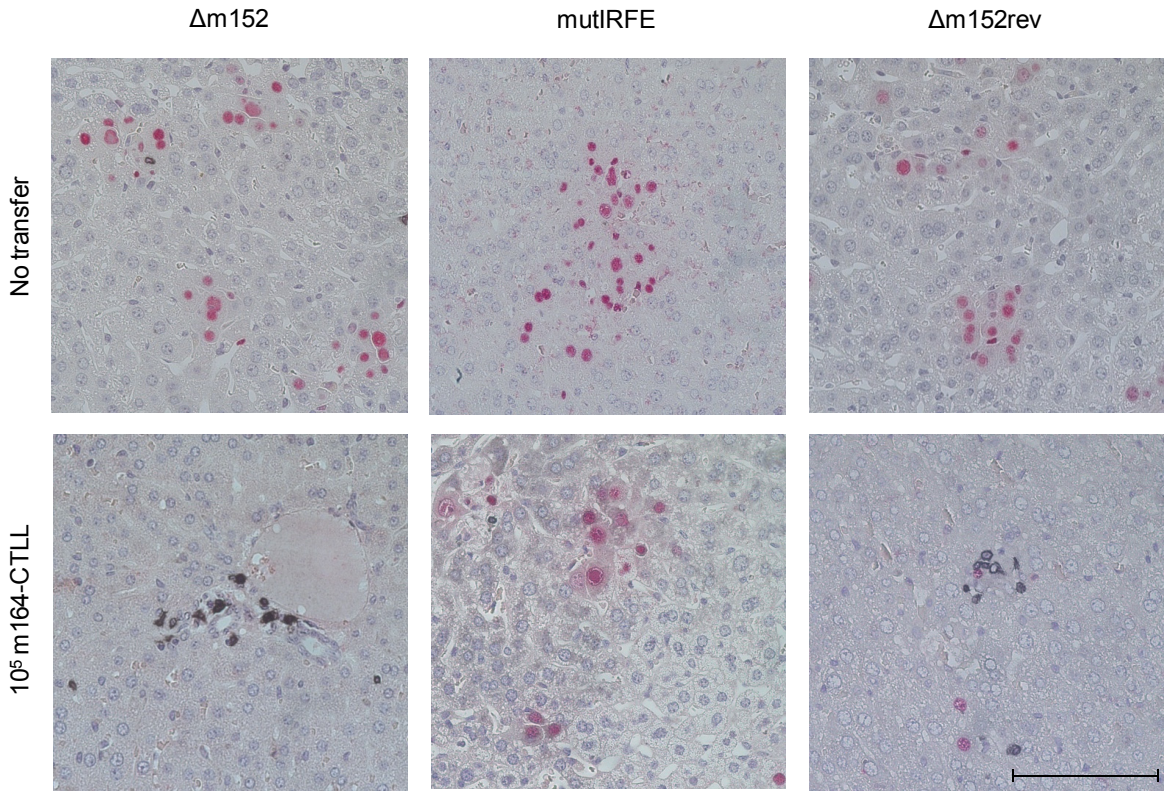

Fig. 3.33 Protective antiviral activity of m164-CTLL depending upon the expression of viral m152. Shown are two-color IHC images of intranuclear IE1 antigen (red) and CD8 T cell surface antigen CD3ε (black) in liver tissue sections derived from 8-9wk-old BALB/c mice 10d after infection with ∆m152, mutIRFE, or ∆m152rev, and either no transfer (upper row) or transfer (lower row) of 10^5 cells (m164-CTL stimulated with 10^{-10}M peptide) specific for the m164 peptide of mCMV. The bar marker represents 100µm.

Taken together, the protective effect of the m164-CTL in recipients infected with revertant virus, which could be shown in this AT for all organs tested, appears to be dependent on the inhibition of the major immune modulator m152 via the IRFE, which guarantees the presentation of the m164 antigen by mCMV-infected cells to cognate T cell receptors.

The hypothesis that the protective effect of the m164-CTL depends on the inhibition of m152 via the IRFE, implies that at least for an enhancement of this effect, type I IFN signaling is required. Some of the IRF, which bind to these elements, are constitutively expressed and can be further induced by IFN signaling, for others this signaling is obligatory for their expression (Mamane et al., 1999). In order to reproduce the findings from the first AT, a second experiment was conducted using type I IFN signaling knock-out mice, IFNAR-/-, and C57BL/6 as indicator recipients. In preliminary cell culture studies it could already be shown that activation of *ex vivo* isolated polyclonal effector cells by mCMV-infected IFNAR-/- MEF was generally impaired. However, it has to be considered that lack of IFN signaling also prevents cellular mechanisms to enhance MHC class I antigen presentation. In this second AT experiment, the above mentioned recipients (8-9wk-old) were immunocompromised by γ-irradiation (single dose 7.5Gy), 24h before the infection and cell transfer. SIINFEKL-specific CD8 T cells were isolated from the spleen of an OT1 mouse, which express a transgenic T-cell receptor with specificity for a peptide from ovalbumin on the H-2K^b background (Hogquist et al., 1994). A number of 10^3 cells/mouse were transferred intravenously into one group of mice (n=6), for each of the two mouse strains. In addition to that, one control group (n=7) for each strain was left without transfer. The recipients were then infected i.pl. with recombinant virus Δm157Luc-m164SIINFEKL (10^5PFU/25µl). This virus expresses the K^b-presented antigenic peptide SIINFEKL in place of the D^d-presented viral peptide m164 of the carrier protein (Lemmermann et al., 2010). This setting of infection with virus Δm157Luc-m164SIINFEKL and transfer of SIINFEKL-specific CD8 T cells from OT1 mice was chosen for two reasons. Firstly, because it is known that an amount of as low as 10^3 transferred CD8 T cells efficiently protects C57BL/6 mice from mCMV-SIINFEKL infection, which minimizes any possible unspecific, cross-reactive effect on virus replication. Secondly, because generation of a functional mCMV peptide-specific CTLL takes a long time. Since it is known that, the susceptibility of IFNAR-/- mice to viral infection is generally quite high (Hwang et al., 1995; Müller et al., 1994), mice were monitored every day from the 2nd day onwards. For this experiment, a virus lacking the expression of *m157* was chosen, because the m157 protein is known to be a ligand for the activating NK-cell receptor Ly49H (Arase et al., 2002; Scalzo et al., 2007 & 2008) and the inhibitory receptor Ly49i (Arase et al., 2002), thereby modulating virus titers by activation or inhibition of NK cell-mediated innate immunity. As expected, 8d after infection and transfer, the experiment had to be stopped, because IFNAR-/- mice were severely affected (extremely swollen hind footpad) and about to die.

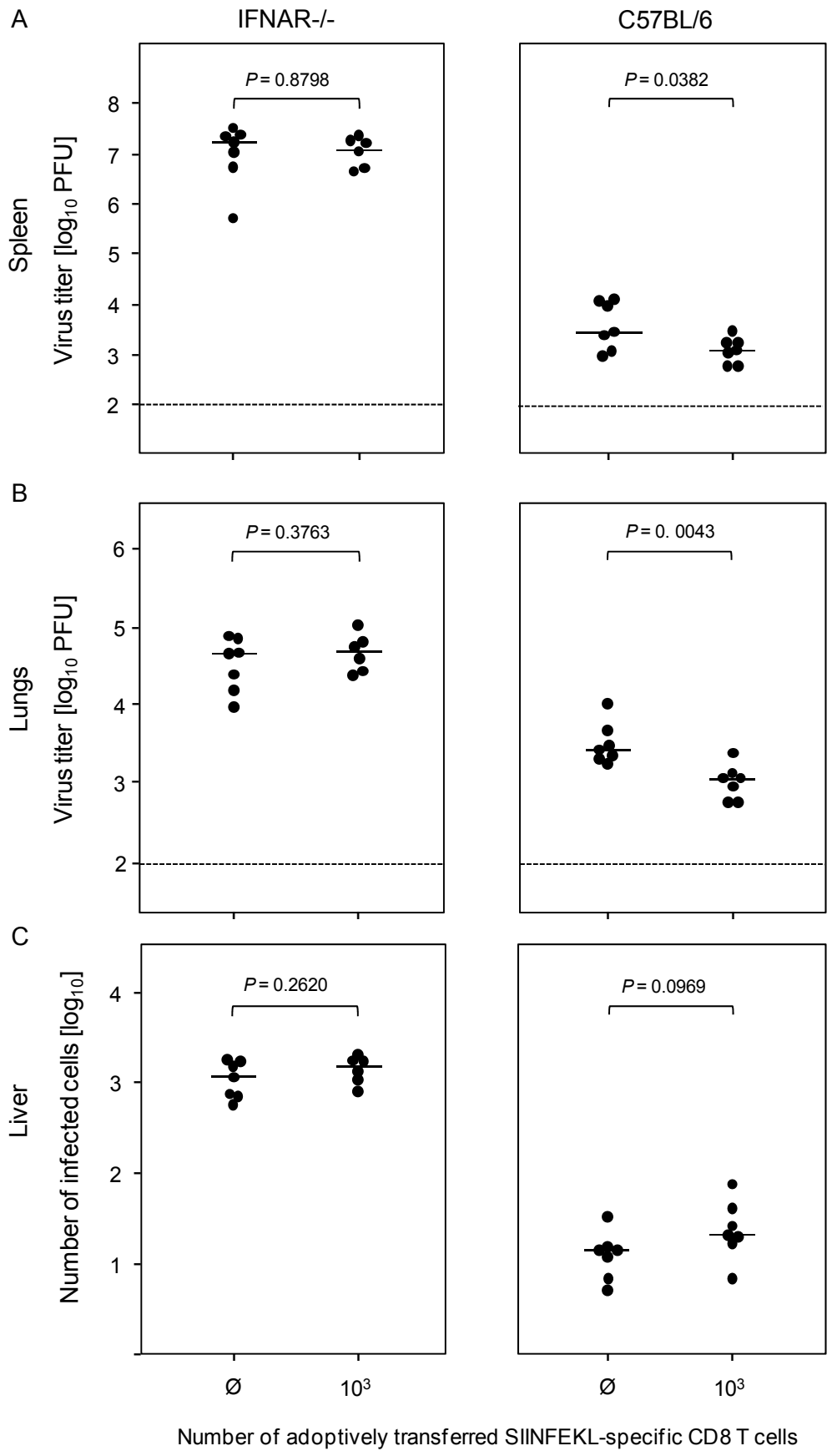

Fig. 3.34 Protective antiviral activity of SIINFEKL-specific CD8 T cells dependent on type I IFN signaling. A number of 10^3 *ex vivo* isolated CD8 T cells from OT-1 mice (8mo-old), specific for the antigenic SIINFEKL peptide, were transferred into immunocompromised 8-9wk-old IFNAR-/- or

C57BL/6 recipients infected with mCMV-Δm157Luc-m164SIINFEKL. Virus replication was monitored 8d after infection and cell transfer, by plaque assay in homogenates of spleen (A) and lungs (B), and by immunohistological quantitation of infected liver cells in representative 10mm^2 areas of tissue sections (C) (IE1-specific IH(C). Ø, control group of infected mice, left without transfer. Black dots represent logarithmized data for individual recipients. Median values are marked by horizontal bars. The dotted line indicates the detection limit of the plaque assay. *P* values, determined by unpaired *t* test are indicated (http://www.graphpad.com/quickcalcs/ttest1.cfm).

For this, virus titers in spleen and lungs were quantified by plaque assay (2.2.4.2), and the number of infected cells in the liver was determined by IE1-specific IHC (2.2.17.3) as shown in Fig. 3.34, together with CD3ε-specific staining of CD8 T cells in this organ (data not shown). As expected, virus titers in IFNAR-/- mice were higher in spleen (~4log$_{10}$) and lungs (~1log$_{10}$), as was the number of infected liver cells (~2log$_{10}$), compared to C57BL/6 mice. Interestingly, transfer of 10^3 SIINFEKL-specific CD8 T cells did not reduce the amount of virus in any of the tissues tested. In contrast to that, and although virus titers were already low in the control group of C57BL/6 mice, adoptively transferred CD8 T cells significantly reduced the viral burden in the spleens (P = 0.0382) and lungs (P = 0.0043), but, somewhat surprisingly, not in the liver. This demonstrated the functional activity of these cells. In conclusion, the results obtained from this AT experiment support the assumption that type I IFN signaling is required for efficient protection of the host from mCMV infection. However, since this knock-out leads to a broad range of effects, the exact contribution of m152 to the failure in protective activity could not be determined in this setting. In order to investigate this aspect, another AT experiment was performed likewise. As described above, 8-9-wk-old IFNAR-/- and C57BL/6 mice were immunocompromised, adoptively transferred with 10^3 SIINFEKL-specific CD8 T cells or were left without cell transfer, and were infected with the deletion mutant Δm152m06-m164SIINFEKL (Lemmermann et al., 2010). Organs were dissected 8d p.i. and were subjected to the above mentioned analyses for virus titers in spleens and lungs, and for the number of IE1-specific liver cells. Unfortunately, only a recombinant virus on the m164-SIINFEKL background which lacks both immune modulators m152 and m06 was available in the lab and therefore used for this experiment. Fig. 3.35 compares the data from IFNAR-/- infected with either virus Δm157-m164SIINFEKL (left panel, reproduced from Fig. 3.34) or Δm152m06-m164SIINFEKL (right panel). Data from C57BL/6 mice are not shown due to overall low titers. In accordance with our hypothesis, the protective antiviral activity of the SIINFEKL-specific effector CD8 T cells was restored by deletion of the two immune modulators, which resulted in a significantly decreased viral burden in all organs under test (panels (A), (B), and (C)).

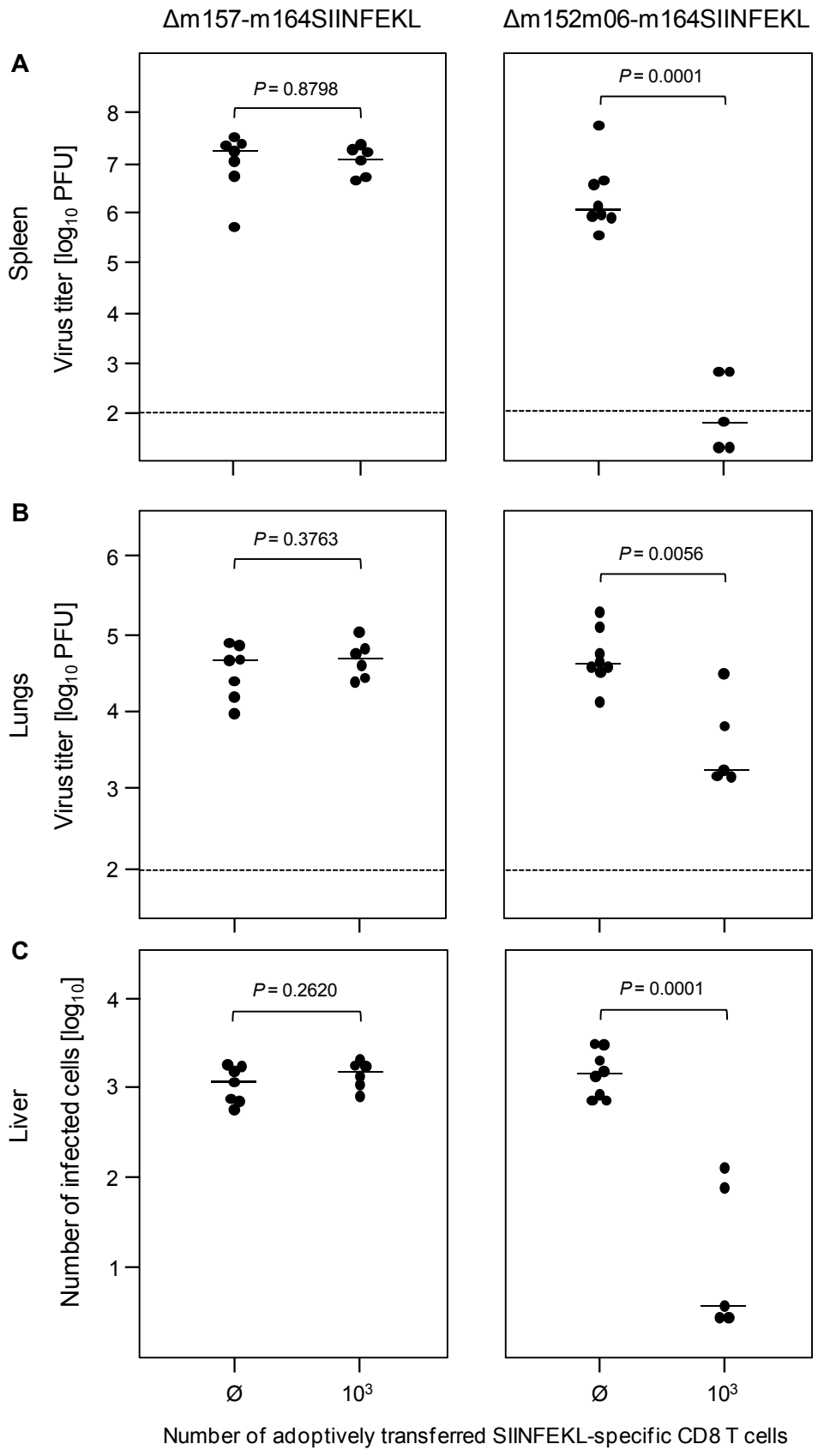

Fig. 3.35 Immune modulators inhibit the protective antiviral activity of SIINFEKL-specific CD8 T cells. Right panel: a number of 10^3 *ex vivo* isolated CD8 T cells from OT-1 mice (3mo-old), specific for the antigenic SIINFEKL peptide, were transferred into immunocompromised 8-9wk-old IFNAR-/- recipient mice infected with mCMV-Δm152m06-m164SIINFEKL. Left panel: for reasons of

comparability, the IFNAR-/- group from Fig. 3.34 (left panel) was reproduced in this figure. Virus replication was monitored 8d after infection and cell transfer, by plaque assay in homogenates of spleen (A) and lungs (B), and by immunohistological quantitation of infected liver cells in representative 10mm^2 areas of tissue sections (C) (IE1-specific IHC). Ø, control group of infected mice, left without transfer. Black dots represent logarithmized data for individual recipients. Median values are marked by horizontal bars. The dotted line indicates the detection limit of the plaque assay. *P* values, determined by unpaired *t* test are indicated (http://www.graphpad.com/quickcalcs/ttest1.cfm).

Since it was shown here that of all so-far-described immune modulators of mCMV only *m152* is controlled via an IRFE in its promoter, this experiment supports the assumption that inhibition of m152 guarantees the protective effector function of CD8 T cells in terms of antigen-recognition on infected target cells.

3.8 IRFE-Dependent Inhibition of m152 Counteracts an Enhanced Activation of NK Cells after Acute mCMV Infection

So far, the downmodulation of MHC class I molecules on infected target cells by m152 in evading from CD8 T-cell activation was investigated in the context of an IRFE-dependent inhibition of m152 expression by mCMV-WT. However, downmodulation of MHC class I molecules also leads to a decrease in interactions of these molecules with inhibitory receptors on NK cells. Because of the fact that NK-cell activity is regulated by the balance of activating and inhibitory signals (Lanier 2008; Ortaldo and Young, 2005; Yokoyama et al., 1998), in this case, NK cells ought to be activated via the 'missing-self' mechanism (Kärre et al., 1986). In this context, m152 has adopted another important function, namely the downmodulation of RAE-1 (Krmpotić et al., 2002; Lodoen et al., 2003), which is a ligand for the activating NK-cell receptor NKG2D, thereby decreasing the threshold for NK-cell activation via 'missing self'. In order to investigate the impact of IRFE-dependent inhibition of m152 in mCMV-WT on the activation of NK cells, virus replication in the NK-cell depleted but otherwise immunocompetent host was assessed in comparison to the undepleted immunocompetent host. For this, current protocols for NK-cell depletion were applied herein (Arapović et al., 2009; Babić et al., 2010; Bantug et al., 2008; Krmpotić et al., 2002; Slavuljica et al., 2010; see 2.2.12). Five 8-9wk-old BALB/c mice were NK-cell depleted by i.v. injection of anti-asialo GM1 antibodies (20µl/500µl PBS). The same number of mice was left without NK-cell depletion as a control. The next day, all mice, depleted or not depleted, were infected i.v. either with virus mutIRFE or WT.BAC, 5 mice per group. As infection doses, the commonly used dose of 2x10^5 PFU/500µl PBS i.v. and a lower dose of 4x10^4 PFU was used in order to possibly enhance an effect of NK-cell depletion under conditions of lower virus burden. At day 3 p.i. the organs were dissected. From the spleen of each mouse, a piece representing ca. 20% of the organ was collected for isolating spleen leukocytes from pools of five mice per group to verify efficient NK-cell

depletion by flow cytofluorometry (2.2.13), although this has not been a standard procedure in the above mentioned protocols. Organ homogenates were prepared from pools of the remaining portions of the spleens and from additional organs for quantitating viral burden. For cytofluorometry, $1x10^6$ cells were used for staining of NK cells with fluorescence-labeled antibodies to cell surface markers CD3ε and CD335, the latter of which is uniquely found on NK cells and serves to discriminate between NKT cells and NK cells (Walzer et al., 2007; personal communication S. Jonjić). Fig. 3.36 is exemplary for all NK-depletion experiments, and gives the numbers (%) of double positive cells, whereby the original amount of NK cells in naive mice was defined as being 100%.

A

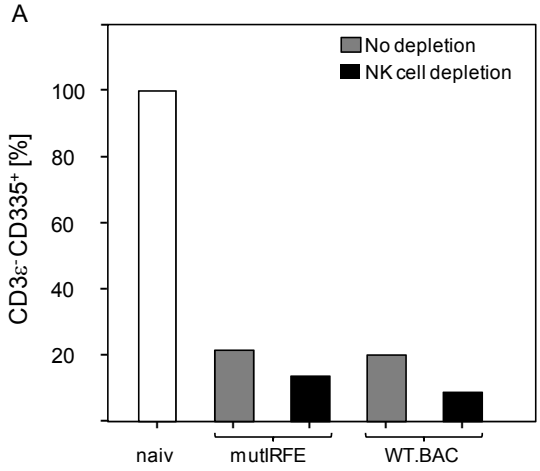

B

	Number of CD3ε⁻ CD335⁺ cells	
	No depletion	NK-cell depletion
Naiive	1902	–
mutIRFE	410	266
WT.BAC	375	170

Fig. 3.36 Verification of NK-cell depletion in spleens of mCMV-infected mice. The number of cells positive for NK-cell surface marker CD335 but negative for T-cell marker CD3ε was determined by flow cytofluorometry of organ homogenates (B). Per group, 5 BALB/c mice (8-9wk-old) were NK-cell depleted by i.v. injection of 20µl/500µl PBS anti-asialo GM1 antibody 24h before i.v. infection with $2x10^5$ PFU of virus mutIRFE or WT.BAC. Organs were dissected 3d p.i., $1/5^{th}$ of the spleen was pooled for each group of 5 mice. An age-matched naïve mouse (white bar) was tested for the amount of NK cells, which was defined as 100%. Grey bars indicate the relative numbers of NK cells after mCMV-infection with the indicated viruses (no depletion), black bars the numbers after NK-cell depletion and mCMV-infection (A).

Obviously, the number of NK cells was dramatically decreased (to ~20%) by the process of i.v. infection with either virus mutIRFE or WT.BAC. NK-cell depletion could further decrease this number by a factor of two. However, this means that altogether only ~10% of the original number remained in the spleen. Probably, for an NK-cell effect the absolute number of residual NK cells is relevant rather than the relative difference between depleted or non-depleted groups (~50%).

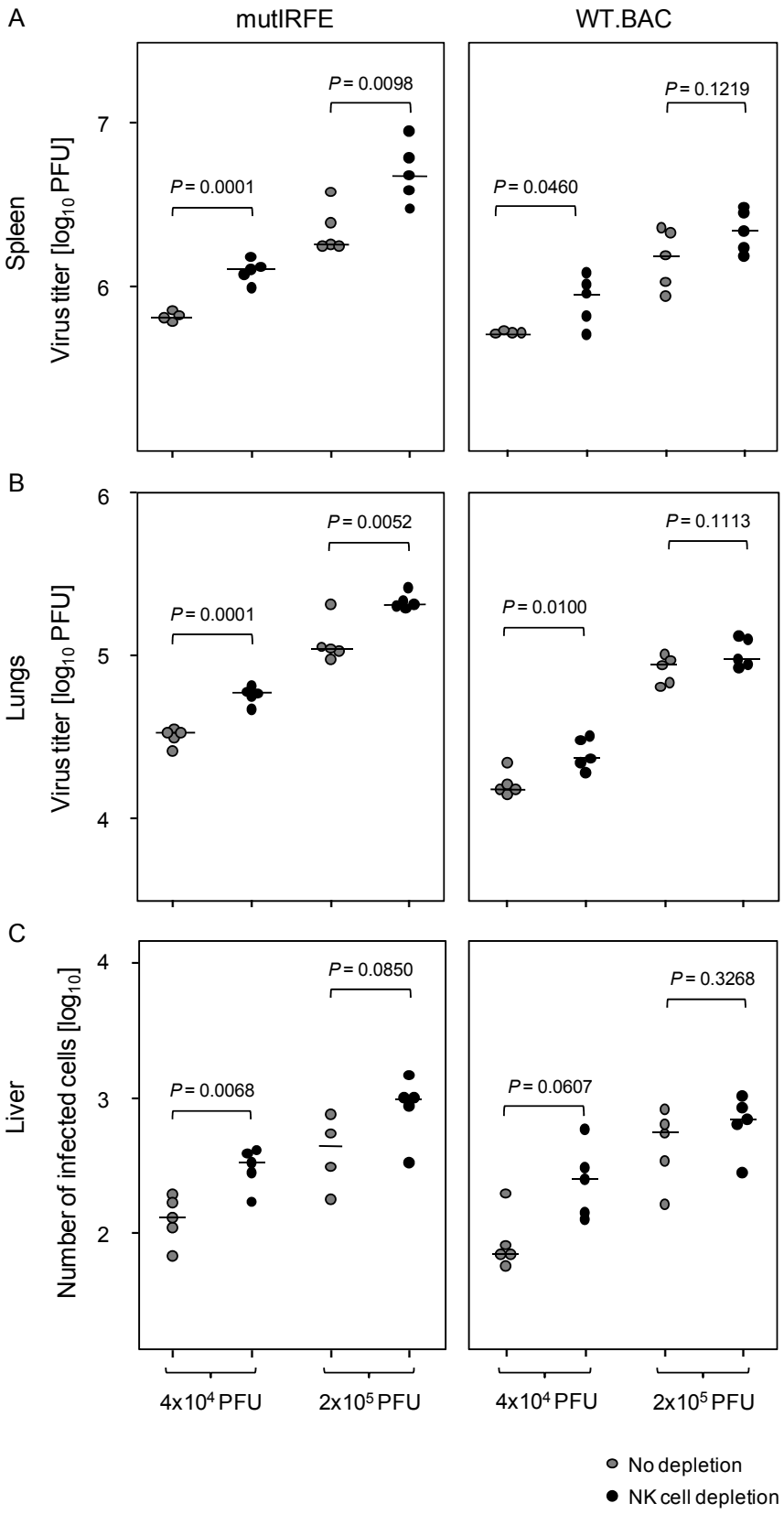

Fig. 3.37 Control of acute mutIRFE infection is mediated by NK cells. 8-9wk-old BALB/c mice (5 per group) were depleted of NK cells by i.v. injection of 20µl/mouse anti-asialo GM1/500µl PBS, or were left without depletion. 24h later they were infected i.v. with the indicated doses of either mCMV-mutIRFE or WT.BAC in 500µl PBS. 3d p.i., organs were dissected to monitor virus titers in spleen (A) and lungs (B) by plaque assay, and by quantitating the number of infected liver cells by

IE1-specific IHC (C). Dots represent logarithmized data for individual recipients with median values marked by horizontal bars. *P* values, determined by unpaired *t* test are indicated (http://www.graphpad.com/quickcalcs/ttest1.cfm).

Fig. 3.37 depicts virus titers in spleen (A) and lungs (B) as determined by plaque assay, and the number of infected liver cells (C) quantified by IE1-specific IHC. In case of the spleen (A), depletion of NK cells led to a significant increase in virus titers (*P* = 0.0001 and *P* = 0.0098) in hosts infected with either dose of mutIRFE virus (left panel), whereby the effect was enhanced by low-dose infection, as intended. This also demonstrated that the above described NK-cell depletion was indeed functional. In spleens from WT.BAC infected mice ($2x10^5$ PFU), NK cell depletion did not cause a significant rise in virus titers, which confirms previous results from other groups (Babić et al., 2010), but after infection with the low dose the increase was significant (*P* = 0.046). Essentially the same results for both viruses and infection doses were found for the lungs. In the liver, the number of infected cells was significantly increased after NK-cell depletion in low-dose mutIRFE infected mice (*P* = 0.0068), but not in WT-infected mice. In a second experiment, which was conducted alike, the results were similar, but with slight deviations. The results are given in Fig. 3.38. The only difference in the spleen (A) was that NK-cell depletion in WT-infected mice did not cause a significant increase in virus titers, whereas in mutIRFE-infected mice it always did (*P* = 0.0002 / 0.0134), independent of the infection dose. In the case of the lungs (B), the results were inconsistent, since here NK-cell depletion did never contribute to virus replication, regardless which virus or infection dose was used. The only difference concerning the number of infected liver cells after NK-cell depletion was a significant increase after infection with $2x10^5$ PFU of WT virus (*P* = 0.0154). Taken together, this outlines the variance in this experimental setting, which might at least in part be due to the above mentioned (Fig. 3.33) incomplete efficiency to deplete NK cells from the host. Nevertheless, it could without doubt be reproduced that a depletion of NK cells led to enhanced replication of mutIRFE in spleens and livers of infected hosts. As to WT virus, considering published data from other groups (see above), the tendency for an enhanced replication might be present, however much weaker as compared to mutant virus. With regard to that, NK cells in the acute infected host seem to inhibit replication of mutant virus, which only becomes obvious by depletion of the cells in question, because the initial titers are not lower as compared to WT virus.

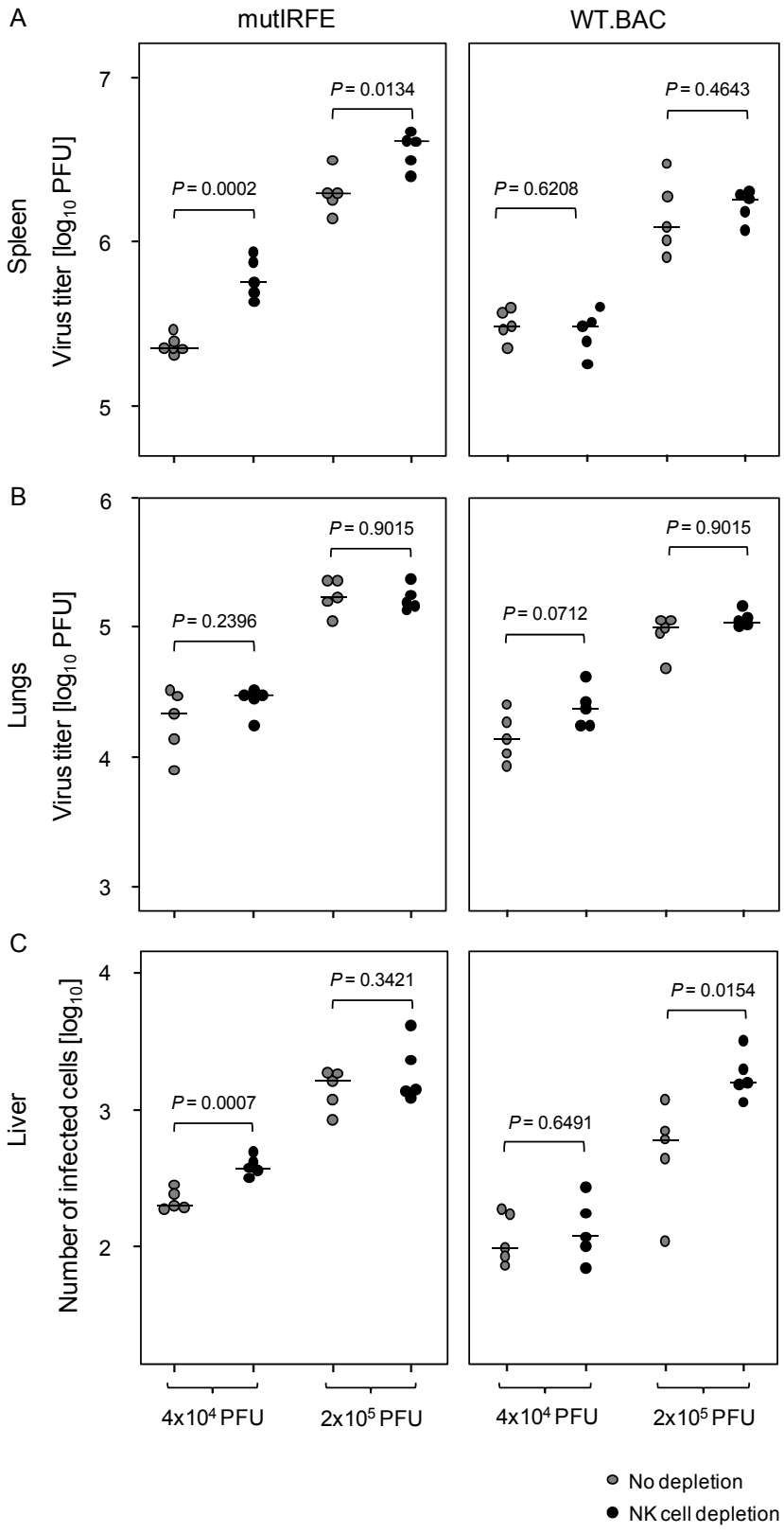

Fig. 3.38 Control of acute mutIRFE infection in the immunocompetent host is mediated by NK cells. 8-9wk-old BALB/c mice (5 per group) were depleted of NK cells by i.v. injection of 20µl/500µl PBS/mouse anti-asialo GM1 (black dots), or were left without depletion (dark grey dots). 24h later they were infected i.v. with the indicated doses of either mCMV-mutIRFE or WT.BAC in 500µl PBS. 3d p.i., organs were dissected to monitor virus titers in spleen (A) and lungs (B) by plaque assay, and by quantitating the number of infected liver cells by IE1-specific IHC (C). Dots

represent logarithmized data for individual recipients with median values marked by horizontal bars. *P* values, determined by unpaired *t* test are indicated (http://www.graphpad.com/quickcalcs/ttest1.cfm).

Before an inhibitory effect could be attributed to NK cells, a possible role of CD8 T cells in this experimental setting had to be excluded. However, a contribution of these lymphocytes at such an early stage of primary infection is not very likely. Nonetheless, a third experiment was conducted, in which CD8 T cells were depleted, according to current protocols (Bantug et al., 2008; Krmpotić et al., 2002) by i.v. injection of monoclonal anti-CD8α antibody (1mg/500µl PBS; kindly provided by Prof. Jonjić) 24h before infection. In total, 3 groups of 5 BALB/c mice each (8-9wk-old) were included in the experiment, with either no depletion as control, NK-cell depletion (as described above), or CD8 T-cell depletion, and subsequent infection with $2x10^5$ PFU of mutIRFE virus. 3d p.i. organs were dissected. The efficiency of CD8 T-cell depletion was assessed by flow cytofluorometry in organ homogenates from pools of spleen pieces, by staining for surface markers CD3ε and TCRβ. In addition, the efficiency of NK-cell depletion was verified as described above (data not shown). Fig. 3.39 gives the numbers (%) of double positive cells, whereby the number of CD8 T cells in spleens from mutIRFE infected mice was defined as being 100%. After depletion with the monoclonal antibody, CD3ε^+ TCRβ^+ cells were found to be almost completely erased from the organ.

A

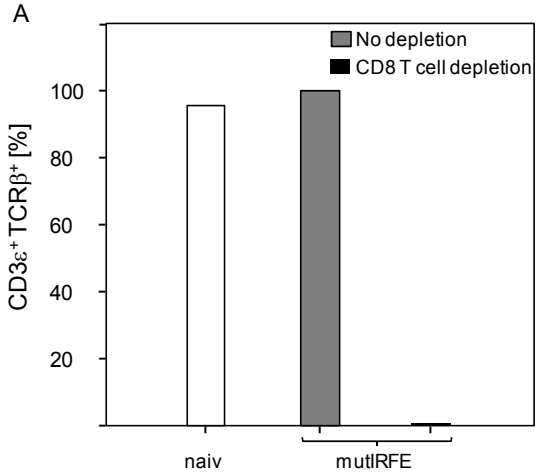

B

	Number of CD3ε+ TCRβ+ cells	
	No depletion	T-cell depletion
Naiive	8998	–
mutIRFE	9409	36

Fig. 3.39 Verification of CD8 T-cell depletion in spleens of mCMV-infected mice. The number of double positive cells for CD8 T-cell surface markers CD3ε and TCRβ was determined by flow cytofluorometry of organ homogenates (B). Per group, 5 BALB/c mice (8-9wk-old) were CD8 T-cell depleted by i.v. injection of 1mg/500µl PBS monoclonal anti-CD8α antibody 24h before i.v. infection with $2x10^5$ PFU of virus mutIRFE or WT.BAC. Organs were dissected 3d p.i., $1/5^{th}$ of the spleen was pooled for each group of 5 mice. An age-matched naïve mouse (white bar) was tested for the amount of CD3ε^+ TCRβ^+ cells. The grey bar indicates the relative number of CD3ε^+ TCRβ^+ cells after mCMV-infection with the indicated viruses (no depletion), which was defined as 100%. The black bar indicates the numbers after CD8 T-cell depletion and mCMV-infection (A).

In the pooled remaining portion of the spleen, and in the lungs, virus titers were determined by plaque assay, whereas the number of infected cells in the liver was quantitated by IE1-specific IHC.

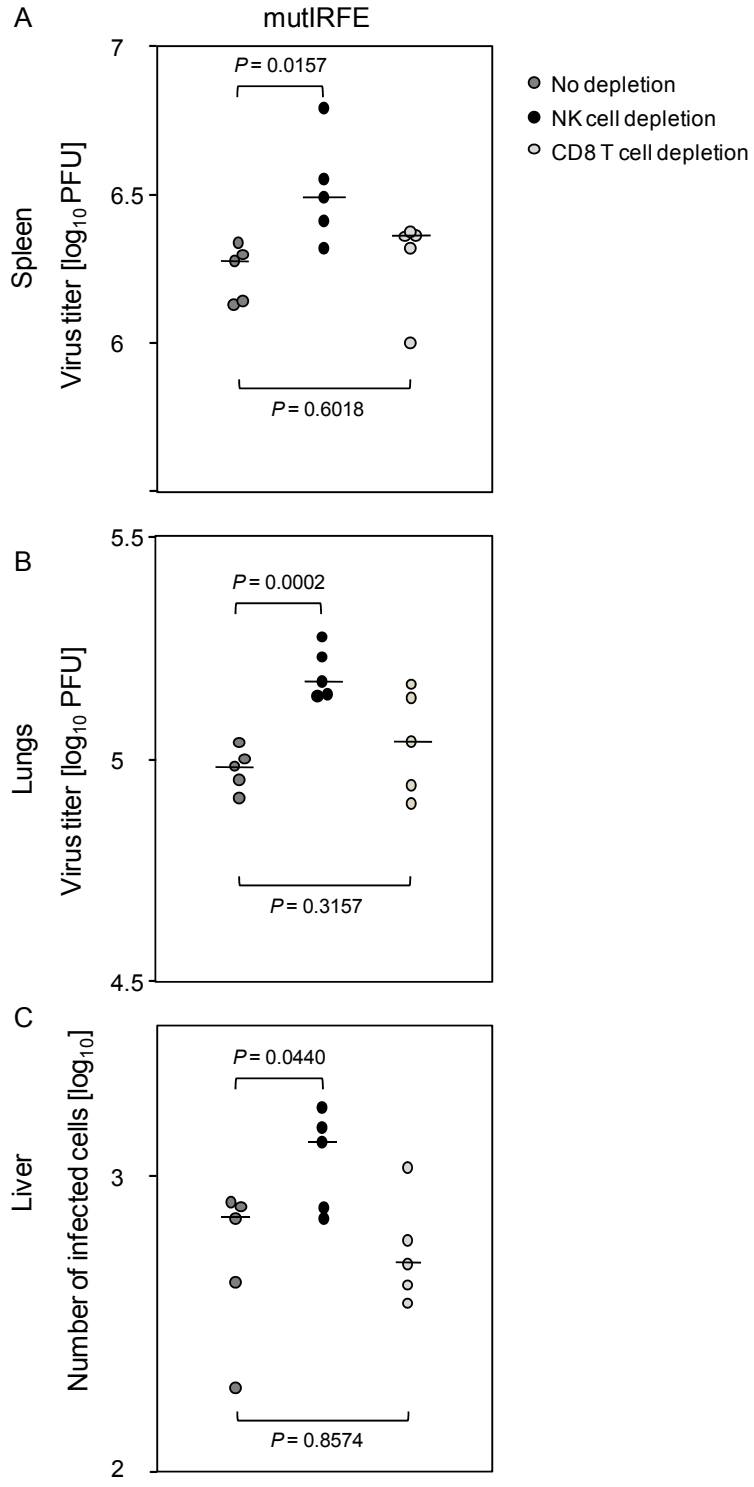

Fig. 3.40 CD8 T cells do not contribute to the control of acute mutIRFE infection in the immunocompetent host. 5 BALB/c mice per group (8-9wk-old) were depleted of CD8 T cells by i.v. injection of 1mg/500µl PBS/mouse of monoclonal anti-CD8α antibody (light grey dots), or were depleted of NK cells by i.v. injection of 20µl/500µl PBS/mouse anti-asialo GM1 (black dots), or

were left without depletion (dark grey dots). 24h later they were infected i.v. with $2x10^5$ PFU/500µl PBS of virus mutIRFE. 3d p.i., organs were dissected to monitor virus titers in spleen (A) and lungs (B) by plaque assay, and by quantitating the number of infected liver cells by IE1-specific IHC (C). Dots represent logarithmized data for individual recipients with median values marked by horizontal bars. *P* values, determined by unpaired *t* test are indicated (http://www.graphpad.com/quickcalcs/ttest1.cfm).

Fig. 3.40 shows that the virus titers after NK-cell depletion were significantly higher in the spleen (P = 0.0157), the lungs (P = 0.0002), and in the liver (P = 0.0440). Hence, this experiment has reproduced the findings from the other two depletion experiments, with regard to NK cells. Importantly here, a contribution of CD8 T cells could be ruled out, since depletion of these lymphocytes did not increase virus titers or numbers of infected liver cells in any of the organs tested. Thus, the inhibitory function on replication of virus mutIRFE in the acute phase of infection (3d p.i.) could be assigned to NK cells.

Altogether, it could be shown that the replication of mutant virus mutIRFE was inhibited in the acutely infected host in an NK-cell-dependent manner, which was not the case for WT virus. This difference between both viruses is likely to be caused by the increased levels of m152 in the mutant virus. Curiously enough, considering the inhibitory function of m152 on the activatory ligand RAE-1, an increase in m152 has rather suggested a decrease in the activation of NK cells via NKG2D. Thus, the effect of m152 on RAE-1 expression cannot explain the enhanced activation of NK cells during acute infection and consequent inhibition of virus replication. To test the assumption that in the case of mutIRFE infection, NK-cell activation was independent of NKG2D, we used another current protocol (Babić et al., 2010) to block NKG2D. For this, 300µg of anti-NKG2D monoclonal antibody (kindly provided by Prof. Jonjić) were injected i.v. into BALB/c mice (8-9wk-old). As control group, mice were left untreated. In addition, one group was NK-cell depleted with anti-asialo GM1, as described above. 24h later, all mice were infected with $2x10^5$ PFU/500µl PBS/mouse of either virus Δm152 or mutIRFE, and organs were dissected 3d p.i.. In this experiment, the deletion mutant Δm152 was used as a positive control for the blockade of NKG2D. In the case of the spleen, it is known that the attenuation of virus Δm152 in the infected host can be reversed blockade of NKG2D signaling (Slavuljica et al., 2010).

At first, the efficiency of the blockade was assessed in splenic cells, as described above for the other experiments, but staining for surface markers TCRβ, CD49b, and NKG2D (Fig. 3.41). Obviously, and in consistence with NK-cell depletion using anti-asialo GM1 antibody, the number of $NKG2D^+$ cells was dramatically decreased by the process of i.v. infection, namely to 14% by Δm152 and to 3% by mutIRFE as compared to the total number of $NKG2D^+$ cells in naïve mice. However in both groups, NKG2D blockade further reduced the numbers of stainable NK cells almost completely.

A

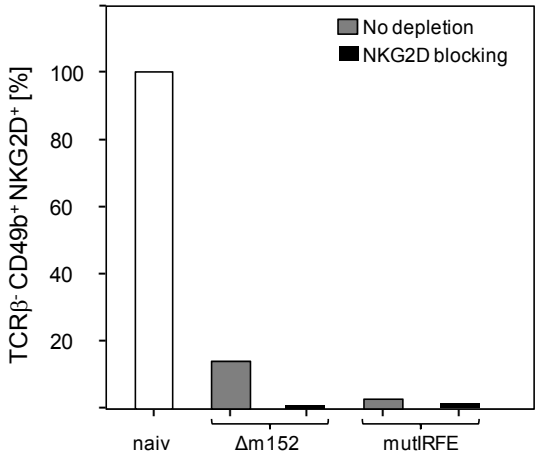

B

	Number of TCRβ- CD49b+ NKG2D+ cells	
	No blockade	NKG2D blockade
Naiive	1233	–
Δm152	174	9
mutIRFE	38	19

Fig. 3.41 Verification of NKG2D blockade in spleens of mCMV-infected mice. The number of cells positive for NK-cell surface markers CD49b and NKG2D but negative for T cell marker TCRβ was determined by flow cytofluorometry of organ homogenates (B). Per group, 5 BALB/c mice (8-9wk-old) were NKG2D blocked by i.v. injection of α-mouse NKG2D antibody (300µg/500µl PBS/mouse) 24h before i.v. infection with $2x10^5$ PFU Δm152 or mCMV-mutIRFE. Organs were dissected 3d p.i., $1/5^{th}$ of the spleen was pooled for each group of 5 mice. A naïve mouse (white bar) of the same age was tested for the original amount of NKG2D-positive cells, which was defined as 100%. Grey bars indicate the relative numbers of NKG2D+ cells after mCMV-infection with the indicated viruses (no depletion). Black bars indicate the numbers after NKG2D blockade and mCMV-infection (A).

The same assays as for the depletion experiments were applied here to determine virus titers in the pooled remaining portions of the spleens and in the lungs, and the number of infected liver cells. Fig. 3.42 shows the results for Δm152-infected mice (left panels) and mutIRFE-infected mice (right panels) for all organs under test. As was expected for the deletion mutant, in mice infected with Δm152 the virus titers in spleens (A) and lungs (B) and numbers of infected liver cells (C) were appreciably lower as compared to mutIRFE-infected mice. Furthermore, this attenuation could be reversed in the spleen by depletion of NK cells in an NKG2D-dependent manner (Slavuljica et al., 2010), as displayed by increased titers after NK-cell depletion (black dots, $P < 0.0001$) and NKG2D blockade (grey dots, $P < 0.0001$). However, in the lungs, only NK-cell depletion ($P = 0.0008$) but not NKG2D blockade ($P = 0.2882$) led to increased titers. Astonishingly in the liver, virus titers were not significantly increased by NK-cell depletion ($P = 0.2103$), but were significantly decreased ($P = 0.0222$) after NKG2D blockade. The same was true for the livers of mutIRFE-infected mice ($P = 0.4738$ and $P = 0.0001$, respectively). Also in the lungs, mutIRFE titers after NKG2D blockade were significantly decreased ($P = 0.0002$), and not affected by NK-cell depletion. As for the spleen, the mutIRFE titers were significantly increased ($P = 0.0029$) after NK-cell depletion but not after NKG2D blockade where they were rather decreased ($P = 0.0052$).

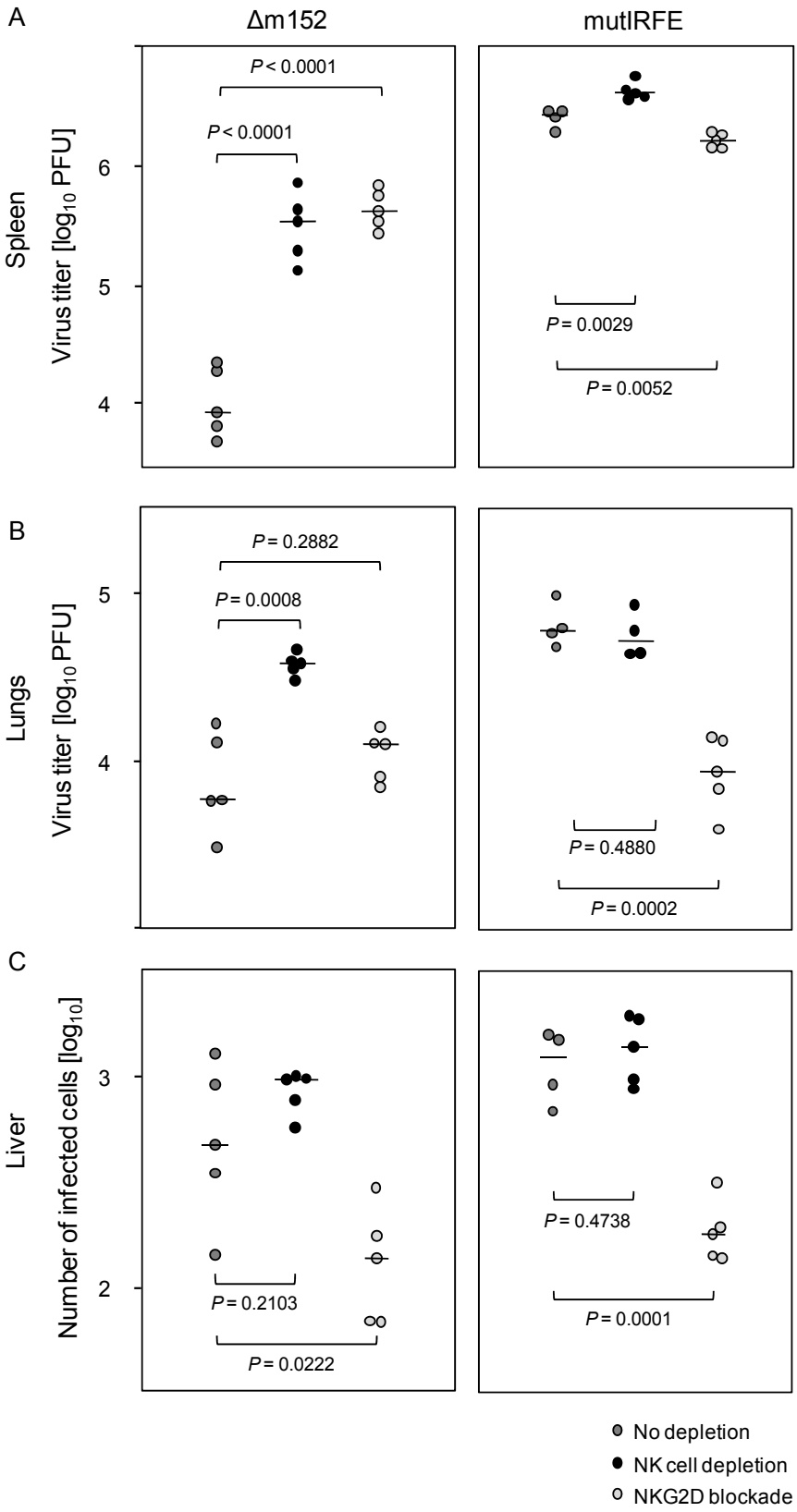

Fig. 3.42 Control of acute mutIRFE infection in the immunocompetent host is mediated by NK cells. 5 BALB/c mice per group (8-9wk-old) were depleted of NK cells (black dots) by i.v. injection of 20µl/500µl PBS/mouse anti-asialo GM1, or were NKG2D blocked (light grey dots) by i.v. injection of 300µg anti-NKG2D monoclonal antibody, or were left without depletion (dark grey dots). 24h later they were infected i.v. with $2x10^5$ PFU/ 500µl PBS of either virus Δm152 or mutIRFE. 3d p.i., organs were dissected to monitor virus titers in spleen (A) and lungs (B) by

plaque assay, and by quantitating the number of infected liver cells by IE1-specific IHC (C). Dots represent logarithmized data for individual recipients with median values marked by horizontal bars. *P* values, determined by unpaired *t* test are indicated (http://www.graphpad.com/quickcalcs/ttest1.cfm).

Thus, what was assumed for the activation of splenic NK cells by virus mutIRFE could be shown, namely that it is not mediated by NKG2D signaling. Moreover, in case of lungs and liver, NKG2D rather appeared to contribute positively to virus replication, since blockade of the receptor decreased virus titers of both, ∆m152 and mutIRFE. The previously published data for WT virus were only derived from the spleen (Babić et al., 2010; Bantug et al., 2008; Slavuljica et al., 2010), so it remains unknown whether NKG2D positively influences WT virus titers in lungs and liver.

Taken together, this set of depletion and blockade experiments in immunocompetent BALB/c mice has confirmed that early replication of WT virus in the spleen is not inhibited by NK cells. However, they have also revealed that an increase in m152 expression (in mutIRFE) leads to an activation of NK cells independent of NKG2D, whereby virus replication in the spleen, lungs, and liver, with decreasing effects in this order, is inhibited. A contribution of CD8 T cells to this inhibition was excluded here. The initial aim of these experiments was to investigate, whether the IRFE-dependent decrease in the levels of m152 in WT virus had a functional influence on the activation of NK cells via RAE-1. Instead, it rather appears as if the inhibition of *m152* expression in WT virus guarantees the prevention of an NKG2D-independent NK-cell activation or the maintenance of a certain level of NK-cell inhibition, which is probably mediated via the ‘missing-self’ axis.

4 Discussion

Upon viral infection, the innate and adaptive immune system mount an immunological response with IFN being a major player of both systems thereby linking one to the other. Initially, the action of IFN is characterized by the expression and antiviral activity of IFN-stimulated genes (ISG) (reviewed in Katze et al., 2002). Simultaneously, herpesviruses, like CMV, have evolved several strategies to counteract the host's immune reponse to infection, and thereby enable themselves to establish persistent infection in specific cell types, such as macrophages, lymphocytes, epithelial and endothelial cells (reviewed in Paludan et al., 2011). In this respect, some of the currently well-studied interactions between CMV and the host's immune system are given here as examples:

Transcription and translation of mCMV *immediate-early (ie)* genes is impaired in infected cell cultures pretreated with IFNα or IFNγ (Martinotti et al., 1993; Gribaudo et al., 1993; IFNβ was not included in the studies). Only recently, it has been reported that at very early times p.i. the *ie* promoter activity is blocked in macrophages by IFNγ treatment (Kropp et al., 2011).

Toll-like receptors (TLR) 3, 7, and 9 were described to be activated by mCMV (Krug et al., 2004; Tabeta et al, 2004; Zucchini et al., 2008), TLR 2 and 9 by hCMV (Boehme et al., 2006; Varani et al., 2007), and to induce downstream pro-inflammatory and antiviral activities (reviewed in Kawai and Akira, 2010; Paludan et al., 2011).

The IE1 protein of hCMV forms a complex with the cellular transcription factors (TF) 'signal transducer and activator of transcription' (STAT) 1 and STAT 2. Thereby, it prevents their association with IRF-9 to form the IFN-stimulated gene factor (ISGF) 3, which binds to IFN-stimulated response elements (ISRE) present in many ISG (Paulus et al., 2006).

The influence of the mCMV IE1 protein on the expression of ISG in terms of transactivation of a luciferase reporter plasmid under control of a promoter containing 5 consecutive ISRE in stably and transiently transfected cells was investigated and found to be activatory (Busche et al., 2008).

In cooperation with the group of Prof. P. Ghazal, we have identified the IE1 protein of mCMV as being an inhibitor of *IFNβ* gene expression in macrophages, as well as in the immunocompromised model of mCMV infection (Rodriguez-Martín et al., manuscript in preparation).

The M27 protein of mCMV was reported to bind, downregulate, and induce the proteasomal degradation of STAT 2 (Zimmermann et al., 2005). Moreover, the same

group also described a simultaneous downregulation of *IFNβ* and *IFNα4* gene expression in mCMV-infected fibroblasts (Le et al., 2008).

With regard to NK cells, it is known that hCMV encodes ligands for inhibitory NK-cell receptors (reviewed in Tortorella et al., 2000), whereas mCMV encodes proteins that downmodulate ligands for the activating NK-cell receptor NKG2D (Arapović et al., 2009; Krmpotić et al., 2002; reviewed in Lisnić et al., 2010).

Investigation of the complex network of virus-host interactions is crucial to understand the mechanisms of virus persistence in face of a competent immune response, and may disclose new targets for antiviral therapy (Katze et al., 2002; Levy & García-Sastre, 2001).

In this work, a new connection between two major interaction partners of either site, namely of cellular IFN and viral m152 could be identified. The relevance of this interaction for the antiviral activity of CD8 T lymphocytes and NK cells, key players of adaptive and innate immunity, respectively, and for virus replication in the host was a key point of interest in the studies conducted herein.

4.1 The *m152* Promoter Contains Regulatory Motifs of IFN Signaling

IFN are known to be cytokines that interfere with viral replication directly from the beginning of infection onwards (Levy & García-Sastre, 2001; reviewed in Samuel, 2001), and can also function as immune modulators during later stages (Biron, 2001). In this respect, it was intriguing to find that the expression of viral m152, being a major immune modulator itself, in infected cell cultures was influenced by pretreatment with IFNγ (preliminary experiments S. Emde). In order to check, whether this was due to a direct effect on a molecular basis, and not only downstream of the inhibition of *ie* gene expression and transactivation (Gribaudo et al., 1993; Martinotti et al., 1993), a search of the *m152* promoter region for transcription factor binding sites was conducted. Indeed, a potential binding site for murine IFN-regulatory factor (IRF)-1 and IRF-2 was found in the promoter region on the non-coding strand of *m152* (5´-TCGAAAGCGAAAGT-3´) (Fig. 3.1). In accordance with the literature on these IRF (Harada et al., 1989; Tanaka et al., 1993), this binding site was identified herein as being an IRF-element (IRFE), completely matching the consensus sequence 5´-G(A)AAA G/C T/C GAAA G/C T/C-3´, as indicated by underlined bases. Moreover, it also matches the recognition sequence 5´-AANNGAAA-3´ assigned to IRF-2 (Fujii et al., 1999). The fact that the IRFE is located in the *m152* promoter region on the non-coding strand is not an unusual feature of this motif. It was shown for the *H-2D^d* gene that the contact site for both IRF-1 and IRF-2 lies on the non-coding strand (Harada et al., 1989). These two IRF, which are potential interaction partners of the *m152* IRFE, are described as `*trans*-acting factors´ with IRF-2 being a repressor of IRF-1 mediated activation through direct competition for binding to the

common motif in the *IFNβ* gene (Fujita et al., 1988 & 1989; Harada et al., 1989; Tanaka et al., 1993). In general, IRF-1 and IRF-2 belong to the mammalian IRF family of 9 currently known members in humans and mouse that bind defined consensus DNA sequences, such as IRFE and ISRE present in enhancers and promoters of type I IFN genes and ISG (Honda & Taniguchi, 2006; preceding review by Nguyen et al., 1997; Sato et al., 2001; Taniguchi et al., 2001). The expression of IRF is virus and IFN inducible (Fujita et al., 1988; Harada et al., 1989, Myamoto et al., 1988). Moreover, IRF-2 appears to be cross-regulated by IRF-1 (Harada et al., 1994). IRF are known to bind to both single and tandem repeats of the GAAA sequence (Fujii et al., 1999), whereby the latter is true for the sequence found in *m152*. Exactly the same sequence of the dimeric repeats with 2 base pairs spacer (5´-GAAAGCGAAAG-3´) can be found in the myeloid differentiation primary-response protein 88 (MyD88) (Fujii et al., 1999), which is an adaptor molecule in TLR signaling pathways, and can be bound by IRF-1, IRF-5, and IRF-7, which leads to the induction of ISG and type I IFN (reviewed in Honda and Taniguchi, 2006; Savitsky et al., 2010). This suggests the functionality of the sequence found in the *m152* promoter and might give a hint at a potential binding partner. In this respect it has been reported that upon virus infection of the cell, IRF-3 and IRF-7 form a complex, termed virus-activated factor (VAF), together with the histone acetyltransferases p300 and 'cAMP response element binding protein (CREB) binding protein' (CBP). This VAF then assembles together with a heterodimer of 'activating TF' (ATF)-2 and c-jun, NF-κB, and other factors on the positive regulatory domains (PRD) within the IFNβ promoter and thereby activate transcription (Falvo et al., 2000; Wathelet et al., 1998). In this connection it is interesting to note that a potential NFκB and CREB binding site is located next to the IRFE in the *m152* promoter (recall Fig. 3.1). Notably, IRF-3, which is constitutively expressed in most cell types (Marié et al., 1998), was shown to be induced by infection with hCMV (Preston et al., 2001) and mCMV (Navarro et al., 1998). IRF-7 was described as being the `master regulator of type I IFN dependent immune responses´ (Honda et al., 2008), however in the case of mCMV infection, previous studies have claimed that IRF-7 is not essential for IFNβ signaling and early resistance to infection carried out by NK cells (Steinberg et al., 2009); although in general, IRF-7 has been reported to be the key factor in positive feedback regulation of type I IFN production (Marié et al., 1998; Sato et al., 1998). For the case of hCMV it has been reported that a complex consisting of IRF-3, CBP, and p300, probably reflecting the VAF, is formed upon infection and induces the induction of ISG54 via ISRE. Moreover, it has been shown that IRF-3 and IRF-7 bind to the same consensus binding sequence as IRF-1 and IRF-2, 5'-GAAANNGAAANN-3' (Lin et al., 2000), which is also present in the *m152* promoter region. Altogether, these facts point out that both IRF-3 and IRF-7 might play a role in the regulation of *m152* expression.

The functional diversity of the IRF family of transcription factors ranging from regulation of the immune response and immune-cell differentiation, to regulation of cell growth/death, which depends on the cell type or stimulus, or on its posttranslational modification, or interaction with other factors, became known only later (Savitsky et al., 2010; preceding review by Taniguchi et al., 2001). For instance, the activatory and inhibitory role of IRF-1 and IRF-2, respectively, on *IFNβ* gene expression does not apply to all genes regulated by these IRF (Vaughan et al., 1995, Vaughan et al., 1998; Yamamoto et al., 1994). With regard to these two IRF it is also interesting to note that the murine transcriptional repressor Blimp-1 has been shown to selectively compete with IRF-1 and IRF-2 for binding sites containing the GAAAG sequence, and that its consensus sequence (5´ A/C AG T/C GAAAG T/C G/T 3´) is very similar to both the IRFE (matching bases are underlined) and ISRE (Kuo & Calame, 2004).

Taken together, it is hard to predict which IRF or other TF could actually bind the IRFE, and which effect it could have on *m152* expression and functionality.

A fact that makes the situation even more complex is that the ISRE sequence, which resides in genes that are induced by IFN signaling, has a consensus sequence similar to the IRFE sequence, namely 5´-G/ANGAAANNGAAACT-3´ (Darnell et al., 1994) (reviewed in Taniguchi et al., 2001). IRF contact sites are known to sometimes coexist within an ISRE, a fact which permits enhanced gene expression in response to IFN (Israel et al., 1986; Korber et al., 1988; Sugita et al., 1987). This explains why IRF also bind to the ISRE of some ISG (Harada et al., 1989; Tanaka et al., 1993). A comparison of the IRFE in the *m152* promoter with the ISRE consensus sequence revealed that they were almost identical except for 2 bases (matching bases are underlined in the consensus sequence). Thus, potentially both motifs can be functional in the *m152* promoter, which enlarges the number of possible interaction partners (other IRF) and thereby the variety of effects.

Notably, herein an ISRE was also found in the *ie* transcription unit of mCMV, in intron 2 (5´-AGGAAATGGAAACA-3´), however not localized to the promoter region. Nevertheless, this element might be the reason for the inhibition of *ie* gene expression and transactivation by IFN (Gribaudo et al., 1993; Martinotti et al., 1993).

Moreover, the presence of an IRFE in the whole mCMV genome of WT.Smith (Rawlinson et al., 1996) is restricted to only three locations, namely the promoter region of *m152*, the ORF *m29/29.1*, and the ORF *M78*. This shows that the IRFE is not a common viral motif, and suggests that it should be of relevance for the virus. For m29 currently no function is known. M78 was reported to be a G-protein-coupled receptor (GPCR) homolog (Gompels et al., 1995; Rawlinson et al., 1996), receptors which generally are known to transfer signals from bacterial peptides, mediators of inflammatory response, and chemokines (in Janeway, 6th ed., 2005). This fact suggests an immune-modulatory function for the M78

protein as well. However, the functionality of an IRFE located in an ORF has not been determined, and so far it is also unclear whether the corresponding opposite strands of *m29/m29.1*, *M78*, and *m152* also contain coding regions. With regard to the corresponding homologous proteins of hCMV (strain AD169), an IRFE could only be identified in ORF *UL28*. This ORF has been reported to encode a spliced mRNA together with ORF *UL29*, and was shown to stimulate the accumulation of IE RNA (Mitchell et al., 2009). In this respect, it is interesting to note that also here, a motif of IFN signaling is located at a site of alternative splicing, as it is the case for the *ie* transcription unit of mCMV. However, whether this is just coincidence or a common feature of IRFE has to be determined elsewhere.

In addition to that, the IRFE originally identified in the genome sequence of mCMV-WT.Smith (Rawlinson et al., 1996) was found to be evolutionary conserved among various established laboratory strains of mCMV and more recent low-passage wild-derived virus isolates (Smith et al., 2008) (Fig. 3.3). Notably, in strain K181, an additional adenine base at the 5´end of the IRFE improves the sequence to better match the consensus ISRE, here except for one base only.

Taken together, comparisons with the current literature on IFN signaling and IRF support the assumption that *m152* may be transcriptionally influenced by IFN signaling and IRF via the promoter-resident IRFE. However, the diversity of functions and interactions, mentioned above, makes it hard to predict an interaction partner and a possible influence on m152. For that reason, these aspects were addressed in this work initially by RNA and protein expression analyses followed by functional analyses of m152.

4.2 The IRFE-Containing *m152* Promoter Construct is Activated by Type I IFN

Early studies on the functions of IRF-1 and IRF-2 on *IFNβ* gene activity were conducted with reporter gene assays. For instance, a truncated *IFNβ* promoter with AAGTGA hexamer repeats linked to the bacterial Chloramphenicol acetlytransferase (CAT) gene (Fujita et al., 1988) was cotransfected with IRF-1 or IRF-2 encoding plasmids, and the subsequent CAT activity was detected (Harada et al., 1989). In this setting, it could be shown that IRF-2 suppresses the activating function of IRF-1 through competitive binding to the hexamer repeats, but also demonstrated that IRF-2 had only a weak effect on the natural *IFNβ* gene in cotransfection experiments (Harada et al., 1989). This mirrors the limitations of transfection experiments with reporter-plasmid constructs.

Nevertheless, in initial studies, a similar approach was adopted herein to investigate the influence of the IRFE motif on *m152* promoter activity. For this, reporter-gene assays were performed with 5 reporter plasmids containing different *m152* promoter constructs linked to the firefly luciferase gene (Fig. 3.4).

At first, the influence of the IRFE on *m152* promoter activity was investigated by pretreatment of the transiently transfected cells with IFN. Treatment with type I IFN was shown before to induce the expression of IRF-1 and IRF-2 (Harada et al., 1989), as well as IRF-5 (Taniguchi et al., 2001) and IRF-7 (Marié et al., 1998; Sato et al., 1998). Inducibility by these cytokines was also ascribed to complex formation of ISGF3 (IRF-9+STAT1+STAT2) and its nuclear translocation, followed by binding to ISRE (Kessler et al., 1990; Levy et al., 1989). Also, IFNγ treatment was shown to activate ISGF3 in MEF (Matsumoto et al., 1999). Furthermore, this cytokine was reported to induce IRF-1 via an IFNγ-activated sequence (GAS) residing in the promoter (Harada et al., 1994), as well as IRF-9 (reviewed in Savitsky et al., 2010). Although it is known that IFNα and IFNβ are constitutively produced in cells, which modifies cellular responsiveness to these cytokines (Gresser, 1990; Taniguchi & Takaoka, 2001), and although the process of introducing foreign DNA into the cells induces IFN production itself (Park et al., 2003; Zhang et al., 2011), additional treatment of the cells with the cytokines should augment any possible effect of the IRFE on *m152* promoter activity.

The effect of intrinsic IFN signaling was displayed by a significant activation of only reporter plasmids containing the *m152* promoter with the authentic IRFE sequence (IRFE), or a perfect-match ISRE sequence (perfISRE 5´-GCGAAAGCGAAACT-3´, mutated bases are underlined), in contrast to lack or functional deletion of the IRFE (Fig. 3.5, left panels). As intended, treatment with either cytokine augmented the activating effect, with IFNβ having the strongest influence. Thus, this assay has revealed the functionality of both elements via type I and II IFN signaling.

As a next step, the full potential of this effect was tested by treatment of cells with increasing doses of the strongest activator, IFNβ. However, the effect was only marginally enhanced by treatment with higher doses as compared to the initial dose of 500U/ml (Fig. 3.6). Obviously, at some point the system is saturated or blocked. This result was taken as an indicator for succeeding experiments, which also included an IFNβ pretreatment.

In these two settings, of course only the interactions of cellular TF with the *m152* promoter are investigated. For mCMV, IE proteins are well-known for their transactivator function on both cellular and viral genes (Angulo et al., 2000; Busche et al., 2008; Gribaudo et al., 2000; Lembo et al., 2000; Messerle et al., 1992; Wilhelmi et al., 2008). In order to include this aspect in the experiments, a different cell line, stably transfected with viral IE1 and IE3, was transiently transfected with the *m152* reporter plasmid constructs and pretreated with IFNβ. Also in this cell line, the effect of intrinsic IFN signaling was displayed by a significant activation of the reporter plasmids IRFE and perfISRE (Fig. 3.7, left panel). Remarkably, also plasmid mutIRFE was activated likewise, which hints at a direct effect of either IE1 or IE3 on *m152* promoter activity. This assumption was corroborated by the

finding that IFN treatment, in contrast, only augmented the activation of plasmids IRFE and perfISRE, as was seen in NIH 3T3 cells, but not of mutIRFE, which was rather inhibited by IFNα treatment or not affected by the other cytokines. These results suggest that the *m152* promoter is induced by either IE1 or IE3 in an IRFE-independent manner, and that the contact site must lie upstream beyond the IRFE in 5´direction (n>211,525), since the minimal *m152* promoter construct, termed – IRFE, was not activated. This finding is certainly of importance for infection studies where viral and cellular factors interact with each other, and has to be considered when interpreting results. Furthermore, it underlined the necessity for this type of studies.

In this regard, we performed a preliminary experiment combining transfection and infection, where cells were transfected with either plasmid mutIRFE or IRFE, and were subsequently infected with WT.BAC. Disregarding some variance, luciferase activity was found to be higher due to activation of the mutIRFE promoter, probably by IE proteins, as compared to the IRFE construct (Fig. 3.8). Here, it rather seemed as though *m152* promoter activity was inhibited in an IRFE-dependent manner. However, this experiment was certainly only the beginning of the infection studies, but should later be proven to have pointed in the right direction.

4.3 m152 Gene Expression is Inhibited in an IRFE-Dependent Manner

IRF are known to be TF that recognize a consensus sequence (IRFE or ISRE) in promoters of various genes and regulate their expression (reviewed in Taniguchi et al., 2001). The presence of a perfect-match IRFE in the *m152* promoter region led us to investigate the expression of *m152* transcripts dependent upon of this motif.

The expression kinetics of m152 mRNA was first described by Ziegler et al. (1997). Therein, total RNA was isolated at different time points p.i. (MOI 10, Ø CEI) and was subjected to Northern Blot analysis. Transcription was shown to be present from 2h p.i. onward, with a maximum at 4h p.i., and continued troughout the 24h replication cycle of mCMV.

Herein, at first we applied the more sensitive method of a duplex qRT-PCR (Fig. 3.13) to determine the expression of m152 transcripts. For this, cells were infected according to our standard procedure (MOI 4, CEI), and also here, total RNA was isolated at different time points p.i., but already starting at T=0 (30min after virus encounter) on account of the low detection limit of qRT-PCR, and ending at 4h p.i. for which maximum levels had been reported (Ziegler et al., 1997). This procedure was performed in different experimental settings to investigate *m152* transcription with regard to presence or absence of a functional IRFE.

In the first setting, the cells were pretreated with IFNβ, or were left untreated before infection to augment any possible effect, which the IRFE or even ISRE site might exert on *m152* gene expression. The experiment revealed that the relative expression of *m152* was inhibited by IFNβ treatment throughout the time course of infection, although maximum levels could be achieved, but only with delayed kinetics (Fig. 3.14). This was the first hint at an inhibitory effect of type I IFN on *m152* gene expression. However, it has to be considered that IFN at least additionally inhibits the expression of IE1 (see above), which is why any effect seen here cannot be attributed as a direct effect on *m152* but rather an effect downstream of IE1 inhibition. Supposedly, both contribute to the effect. For that reason, in a second setting, it was tested whether this effect was due to the IRFE sequence, by infecting cells with either virus mutIRFE or WT.BAC. Indeed, the relative expression of *m152* in cells infected with the mutant virus was found to be not inhibited and thus higher and with earlier kinetics as compared to WT virus (Fig. 3.15). However, differences in m152 mRNA steady-state levels were only detectable at early times, because later a plateau level was reached in both groups. For that reason, generally, the time points at which cells are harvested for total RNA must be exactly identical for both viruses, and different experiments are not reliably comparable. The effect seen with mutant and WT virus relies on the constitutive expression of IRF and IFN, because no enhancing pretreatment with IFNβ was applied. As a third approach, to further support the relevance of the IRFE for the inhibitory effect on *m152* gene expression, MEF from type I IFN receptor knock-out mice (IFNAR-/-) and C57BL/6 (genetic background) were infected with WT.BAC. It was published previously, that mice lacking the type I IFN receptor subunit, or MEF cultures of these mice, do not respond to IFNα or IFNβ, and are highly susceptible to various viral infections (Hwang et al., 1995; Müller et al., 1994). A high susceptibility of IFNAR-/- mice to mCMV infection was shown by others (Gil et al., 2001; Presti et al., 1998). Moreover, it was reported that signaling by IFNγ also depends on type I IFN receptor components, but not vice versa (Takaoka et al., 2000). Notably, the relative expression of *m152* in IFNAR-/- MEF was found to be higher at early times p.i. as compared to the expression in C57BL/6 MEF (Fig. 3.16).

Taken together, all of the 3 settings have independently shown that *m152* expression is inhibited by treatment with IFN, and that the inhibitory effect depends on a functional IRFE as well as on functional IFN signaling.

To come back to the initial studies on *m152* gene expression conducted by Ziegler et al. (1997), we also performed Northern blot analyses with RNA samples from cells infected with either virus mutIRFE or WT.BAC. Total RNA was diluted to various concentrations in order to visualize differences in the amount of m152 mRNA. Hybridization with a DIG-labeled strand-specific RNA probe (complementary to the *m152* coding sequence)

revealed 2 transcripts of <1,821b and >2,661b (Fig. 3.19(B)) originating from the coding strand, since the probe complementary to the non-coding strand did not detect any transcripts. Obviously, the amount of m152 mRNA was higher in mutIRFE-infected cells than in WT-infected cells, as became obvious for all dilutions of total RNA. Equal loading amounts were confirmed by 18S and 28S rRNA in the ethidium-bromide stained gel under UV light (Fig. 3.19(A)). In WT-infected cells, the upper band is not even visible, but would be after a longer exposure time to X-ray film (data not shown). The same two bands were also detected in the work of Ziegler et al. (1997), where the smaller one was assumed to be the m152 mRNA, according to the predicted size. This suggestion was also made here, with the expected size of m152 of ~1,413b (recall Fig. 3.2). As for the heavier band, no suggestion was made by Ziegler et al., but one could assume that it might be a splicing variant of the m153/m152/m151 mRNA, or otherwise modified mRNA species of lower abundance. Regarding splicing variants of mRNA, it is tempting to draw a comparison to hCMV UL28 and UL29 (4.1), which were identified to carry an IRFE in the UL28 ORF, and were reported earlier to encode a spliced mRNA from both ORF (Mitchell et al., 2009), as well as to the presence of an ISRE in the *ie* transcription unit. This would suggest transcription to occur over the borders of the *m152* locus. However, this assumption would have to be further investigated. In this respect, a RNA sample from cells infected with virus Δm152 was included in a repetition of the experiment but comparing m152 mRNA levels in cells infected with mutant and revertant virus (Fig. 3.20(B)). On the one hand, it confirmed the decreased levels in WT/revertant-infected cells and on the other hand, it proved the specificity for m152 of both bands, since both were absent in RNA samples from Δm152-infected cells.

It is important to note that in the first Northern blot analysis (Fig. 3.18), performed with total RNA samples from IFNAR-/- and C57BL/6 MEF infected with WT.BAC (90min), no difference between the two groups was detectable. However, also in the corresponding qRT-PCR analysis at this time point the steady-state expression levels were alike. Another Northern Blot, performed with 1µg of total RNA from 60min p.i. did not detect any m152 mRNA (data not shown), because the relative amount of m152 was apparently below the detection limit.

Thus, it is not trivial to detect viral mRNA with standard protocols, especially not at such early time points after infection, when the amount of transcripts is only starting to increase. However, the Northern Blot confirmed the findings from qRT-PCR analyses and although it is a less sensitive technique it could even visually reveal the difference in m152 mRNA, which is due to a direct, IRFE-dependent inhibition in WT virus.

4.4 m152 Protein Expression is Inhibited in an IRFE-Dependent Manner

The finding that *m152* gene expression was inhibited by type I IFN (signaling) via the promoter-resident IRFE was quite intriguing. It was tempting to hypothesize that this would also have an influence on m152 protein expression. Therefore, this aspect was addressed in the next step.

The first studies on m152 protein expression were again conducted by Ziegler et al. (1997). The amino acid sequence was there predicted to code for a type I transmembrane glycoprotein of 42kDa with three potential N-glycosylation sites. In cells infected with WT.Smith over the time course of the mCMV replication cycle (24h p.i.), they detected three protein species after immunoprecipitation of m152 and detection by Western blot, and claimed gp40 synthesis to start at 3-4h p.i, with a maximum of expression at 5-6h p.i., and a decline from 14h p.i. onward. In a second experiment, these authors detected two protein species at 12h p.i., which they claimed to be two differently glycosylated forms, namely gp37 and gp40. The unglycosylated protein (~34kDa) was detected after tunicamycin treatment, which inhibits *de novo* N-glycosylation. The viral proteins were reported to have a half-life of ~2.5h, and become endoglycosidase-H resistant 3h after translation, meaning that they leave the ERGIC at this time. This study was among the first, together with Del Val et al., 1992, to report the retention of mouse MHC class I molecules by m152, which thereby blocks antigen presentation in this pathway.

Here, we performed Western blot analyses of m152 protein expression with whole cell protein lysates from infected MEF cultures, in the three different settings tested earlier for gene expression. In the first setting, cell cultures were pretreated with IFN, or were left untreated, and were subsequently infected with WT.BAC. In the IFN-untreated samples, two m152 protein species, possibly representing gp37 and gp40 as reported by Ziegler et al. (1997), were detectable already at 2h p.i. with increasing amounts over the next 2h (Fig. 3.21). Pretreatment with either IFNα or IFNβ inhibited the expression of both protein species, thereby delaying the start of detectable protein expression. Pretreatment with IFNγ appeared to slightly enhance protein expression at early times p.i. but inhibited it later. The IE1 protein was detected on the same Western blot, originally with the intention to use it as a loading control. However, in this case the IE protein itself appeared to be inhibited by the cytokines; a fact, which had been reported earlier at least for IFNα (Gribaudo et al., 1993; Martinotti et al., 1993), and has to be considered for interpretation of the results. However, as standard procedure, BCA assays were performed to determine the amount of protein in cell lysates for loading equal amounts onto the gel, and moreover blot membranes were stained by Coomassie Blue (Welinder & Ekblad, 2011) to verify comparable amounts of protein actually present in the samples. Anyway, the result was confirmed by another expression kinetics experiment performed after pretreatment with

IFNβ, and infection with WT.BAC (Fig. 3.22). In addition to the inhibitory effect of the cytokine and delay of detectable m152 protein expression, this experiment revealed that two higher order protein species, probably representing 2-fold and 3-fold glycosylated m152 isoforms, which were detectable in IFN-untreated samples, were not visible after IFNβ treatment. Whether the inhibition of glycosylation was due to a direct effect of the cytokine, or due to overall low levels of m152 remains unknown.

In the second setting, the expression kinetics of m152 in mutIRFE- or WT.BAC-infected cells (without IFN pretreatment) was compared. For all time points tested, the amount of m152 protein was higher in mutIRFE infected cells (Fig. 3.23). Only late in infection, the amounts appeared to be comparable. In this Western blot, the IE1 protein verified equal infection efficiencies of all samples, because there was no obvious difference. In conclusion, this demonstrated that m152 protein expression in WT.BAC is actually inhibited in an IRFE-dependent manner, which was suggested in the preceding Western blot analyses to be mediated by IFN. Since the control sample displayed a nonspecific band which colocalized with the signal from the higher-glycosylated m152 isoform, this experiment was repeated in a similar manner. essentially here, m152 protein expression was inhibited in cells infected with revertant virus mutIRFErev as compared to the expression in cells infected with mutant virus (Fig. 3.24). In this assay, β-actin served as a control for equal loading amounts.

In the third setting, MEF from IFNAR-/- mice and C57BL/6 were both pretreated with IFNβ and subsequently infected with WT.BAC. Overall m152 protein expression in MEF from C57BL/6 started with delayed kinetics, and was reduced at all time points (Fig. 3.25). Notably, the expression of the two highest order protein species was almost undetectable, whereas simultaneously in the MEF from the knock-out mice all glycosylated species were present already at early times p.i. This is in accordance with the observation from a previous Western blot (Fig. 3.22), where treatment with IFNβ appeared to inhibit the accumulation of these protein species. Yet, in IFNAR-/- the cytokine cannot exert its function. Also in this blot, the IE1 protein verified equal infection eficiencies of all samples. Thus, this approach has shown that the inhibition of m152 protein expression in WT is dependent on IFN signaling.

In summary, all of the three settings have independently shown that IFN inhibits m152 protein expression, as it does with gene expression, and that the inhibitory effect depends on a functional IRFE, as well as on functional IFN signaling.

4.5 CD8 T Cell Activation is Restored by IRFE-Dependent Inhibition of m152

So far, the IRFE residing in the *m152* promoter was shown to be a functional element in reporter-gene assays, and to have an inhibitory effect on *m152* gene and protein

expression in infected cells. Thus, possibly, the decline in m152 levels, although not complete, could have an effect on the functions of m152. For that reason, we set out to investigate the two major functions of this viral protein regarding its immune-modulatory role.

The first function of m152 to be addressed herein was the retention of peptide-loaded MHC class I complexes in the ERGIC/cis-Golgi compartment (Del Val et al., 1992; Ziegler et al., 1997; Ziegler et al., 2000). In early studies on this effect using the 4h ^{51}Cr release assay, it could be shown that m152 blocks antigen presentation by MHC class I, (Ziegler et al., 1997), and that presentation could be restored in cells infected with the m152 deletion mutant (Krmpotić et al., 1999). In later studies, m152 was identified as being the major immune modulator in terms of negatively regulating mCMV-peptide presentation in the MHC class I pathway, but not for regulating MHC class I cell surface expression, as shown by flow cytofluorometry, ELISPOT and cytolysis assays, comparing various immune modulator deletion mutants (Holtappels et al., 2006).

In order to test whether the inhibition of m152 via IRFE had an influence on peptide presentation, single-cell ELISPOT assays were performed to reveal the frequencies of effector cells secreting IFN-γ upon stimulation with infected APC. Also here, the three different approaches as used for *m152* expression analyses were applied, in addition to using different kinds of effector cells. As an initial experiment, the activation of CD8 T cells isolated from acute-infected mice by MEF infected with viruses Δm152, mutIRFE or WT.BAC was compared. The m152 deletion mutant was used throughout as a control for the activation of CD8 T cells, in the complete absence of immune modulator m152 but still presence of other immune modulators, of m06/gp48 in particular (Holtappels et al., 2006; Krmpotić et al., 1999). The activation by Δm152-infected APC was revealed by a high number of spots (Fig. 3.26). In contrast to that, and also in accordance with previous findings (Böhm et al., 2008b; Holtappels et al., 2006; Lemmermann et al., 2011), in WT.BAC-infected APC the phenomenon of negative immune modulation became apparent from decreased numbers of activated effector cells. In comparison to that, infection with mutant virus mutIRFE obviously prevented activation of the effector cells to an even higher degree, implying that the inhibition of peptide presentation by the mutant virus is more pronounced. Hence, this finding fits quite nicely to the previous results showing that with WT virus the expression of m152 was lower than with the mutant.

In order to reproduce this initial finding, a further ELISPOT assay was performed likewise which included IFNβ treatment of the APC to enhance MHC class I peptide presentation (Bukowski et al., 1985; Israel et al., 1986; Korber et al., 1988; Sugita et al, 1987). As effector cells, *ex vivo* isolated memory CD8 T cells were used. The results demonstrate that IFNβ has worked in favor of peptide presentation in all of the APC, and has thereby

increased the numbers of activated CD8 T cells (Fig. 3.27). Yet, the magnitude of the difference in activation by IFN-treated and untreated MEF was lower in mutIRFE-infected cells as compared to WT.BAC-infected cells, and the same was true for the overall activation of effector cells by these APC. In conclusion, this assay confirmed the findings from the first experiment, insofar as peptide presentation by WT.BAC-infected APC appeared to be partly restored, in an IRFE-dependent manner.

In the third approach, the dependence of this effect on IFN signaling was investigated. To this end, the activation of memory CD8 T cells by IFNβ-pretreated and mCMV-infected IFNAR-/- MEF was compared to the activation by C57BL/6 MEF treated likewise. The activation of effector cells by synthetic antigenic peptides of haplotype H-2^b showed that most of the effector cells are specific for peptides M38 and M45 (Fig. 3.28(A)). Regarding the requirement of IFN signaling for MHC class I peptide presentation and activation of effector cells, as expected, pretreatment with IFNβ did not have any influence in MEF from IFNAR-/- mice, whereas MEF from C57BL/6 mice induced an increased number of activated effector cells (Fig. 3.28(B)). However, the effect of IFN signaling on the function of m152 became apparent from the numbers of effector cells activated by IFN-untreated APC infected with WT virus, which were lower in the case of IFNAR-/- MEF, which is supposedly due to loss of the inhibitory function of IFN signaling on m152 expression. Hence, the difference between mutIRFE and WT was only marginal in these MEF. Moreover, this experiment showed that the findings from BALB/c MEF (haplotype H-2^d) were also true for C57BL/6 MEF (haplotype H-2^b), insofar as the number of activated effector cells by mutIRFE-infected APC was lower than by WT.BAC-infected APC.

As a final approach in this respect, the activation of clonal effector cells from two cytolytic T lymphocyte line (CTLL), with the same specificity for the known antigenic immunodominant m164 peptide of the H-2^d haplotype (Holtappels et al., 2002a+b) but differing in their avidity (10^{-8}M and 10^{-10}M peptide stimulated), was investigated. Specific lysis was generally low by both lines particularly by the 10^{-10}M CTLL, and their threshold peptide concentration for triggering cytolytic activity was shown to be between 10^{-9} and 10^{-10}M (Fig. 3.29(A)). Yet remarkably, mutIRFE-infected APC could only induce a minor percentage of lysis after pretreatment with IFNβ, and only by the 10^{-10}M CTLL of higher avidity, in sharp contrast to the other APC. Reproduced by the ELISPOT assay, only the 10^{-10}M CTL were activated very weakly by mutIRFE-infected APC, and only if these had been pretreated with IFNβ (Fig. 3.30(A)). In the case of WT-infected APC, both types of CTL were activated, with lower numbers by IFN-untreated APC, and generally lower as compared to Δm152-infected APC. By performing the same ELISPOT experiment with two other CTLL specific for either the mCMV peptide m145 (10^{-9}M) or M105 (10^{-10}M), at least with the latter CTLL it could be shown that reduced amounts of m152 in MEF infected with

revertant virus mutIRFErev led to an enhanced activation of effector cells by these APC as compared to APC infected with the mutant (Fig. 3.31).

The results obtained from the studies with CTLL have thus clearly demonstrated that antigen presentation is restored by an IRFE-dependent inhibition of m152 after infection with WT virus. In this respect, the functional data are in perfect accordance with the findings from gene and protein expression studies having shown that m152 mRNA and protein synthesis is inhibited in WT virus via the IRFE.

4.6 The Protective Antiviral Activity of CD8 T Cells is Restored by IRFE-Dependent Inhibition of m152

During CMV disease, various cell types in different organs are infected in the host. Studies in fibroblasts can only give a limited insight into mechanisms regarding m152's modulation of the CD8 T-cell-mediated immune control. For that reason, studies in the infected host are critical to corroborate findings from `*in vitro´*.

As a next step, adoptive transfer (AT) experiments were conducted to investigate the effect of the m152 protein, expressed at different concentrations in three different viruses, on the protective antiviral activity of effector CD8 T cells in immunocompromised and mCMV-infected recipients. Early studies in mCMV-infected mice (weanlings) have shown that a virus-specific, H-2-restricted CTL response is operational at 6-20d p.i. (Quinnan et al; 1978). Due to the fact that m164-CTLL have been shown before to have a protective antiviral capacity in the acute-infected host (Holtappels et al., 2002a), and that herein these cells clearly revealed a link between levels of m152 and effector-cell activity, the m164-peptide specific CTLL were adoptively transferred at graded numbers into indicator recipients infected with viruses ∆m152, mutIRFE, or ∆m152rev (WT). The protective effect of the CTL was monitored at 10d p.i. by assessing virus replication in spleen, lungs, and liver. In the case of ∆m152, it is known that this virus has an attenuated phenotype in spleen and lungs of immunocompromised (neonatal) mice, and that this phenotype is on the one hand mediated by T-cells and on the other hand by residual NK-cell activity, in that depletion of CD8 and CD4 T cells restores virus replication (Krmpotić et al., 1999) and adoptive transfer of NK cells protects neonatal mice (Bukowski et al., 1985c). This group was included as an indicator for the protective capacity of the CTL in the absence of m152. Indeed, virus titers of ∆m152 were shown to be lower in the spleen and in the lungs as compared to WT titers, and AT of as low as 10^4 m164-CTL significantly reduced these titers in spleen and lungs, as well as the numbers of infected cells in the liver (Fig. 3.32). Replication of WT virus was less affected by AT. Strikingly, and in sharp contrast to the other two viruses, replication of mutIRFE was not affected at all in any of the organs under test by AT of any number of m164-CTL. The IE1- and CD3ε-specific IHC of liver tissue

sections showed that CD8 T cells were apparently not attracted by mutIRFE-infected liver cells, as distinguished from Δm152- and Δm152rev-infected cells (Fig. 3.33). This was certainly a very impressive finding of an unequivocally clear effect of the increased amount of m152 preventing m164-peptide presentation by MHC class I molecules on infected cells almost completely.

This result tempted us to hypothesize that if inhibition of m152 via the IRFE was indeed required for the antiviral activity of effector cells, then lack of type I IFN signaling in IFNAR-/- mice should likewise prevent a protective effect against WT infection. As mentioned above, these knock-out mice do not respond to IFNα or β, and are highly susceptible to various viral infections already at early times p.i. (Hwang et al., 1995; Müller et al., 1994), including mCMV infection (Gil et al., 2001; Presti et al., 1998). Specifically, Slavuljica et al. (2010) have demonstrated an increased mortality in mice infected with the WT virus. This tendency was maintained throughout the experiment. They and others (Presti et al., 1998) claimed these knock-out mice to be much more susceptible to mCMV infection than the parental strain. With regard to type II IFN it was reported that signaling by IFNγ at least in part depends on type I IFN receptor components, but not the other way round (Takaoka et al., 2000). Müller et al. (1994) pointed out that depending on the virus both IFN systems were essential for the immune response and were functionally nonredundant. Thus, it has to be considered that usage of IFNAR-/- is not complete in preventing IFN signaling, but affects signaling pathways of both type I and II IFN. These knock-out mice together with C57BL/6 mice were used as indicator recipients in another AT experiment. Due to the fact that IFNAR-/- are very susceptible to mCMV infection (see above) it was most likely that the experiment would have to be ended before 10d p.i.. In order to yield higher virus titers in general, mice were infected with an mCMV-Δm157 virus. This mutant virus is known to be more virulent in mCMV-resistant C57BL/6 (Ly49H+) mice as compared to WT virus (Bubić et al., 2004). This increased virulence results from a failure in NK-cell activation because the mutant lacks the ligand (m157) which binds the activating NK-cell receptor Ly49H (Arase et al., 2002). With the use of this virus, titers should be detectable also prior to d10 also in the WT-infected control group. Moreover, we chose to use a recombinant virus expressing the K^b-presented dominant ovalbumin peptide SIINFEKL in place of the immunodominant m164 peptide of the carrier protein (Lemmermann et al., 2010). OT1 cells express a transgenic TCR specific for the K^b-SIINFEKL complex (Hogquist et al., 1994) and hence recognize infected cells expressing SIINFEKL (Kedl et al., 2000). In immunocompromised C57BL/6 mice infected with Δm157Luc-m164SIINFEKL it was shown previously that already low numbers (10^3) of adoptively transferred OT1 effector cells exert a significant protective effect (Gergely et al., 2011). This reduces the probability that unspecific effects are induced by transfer of

high numbers of effector cells, which is another reason for choosing this approach. However, it could also be shown that higher numbers of adoptively transferred OT1 cells do not reduce viral titers to below 10^3 PFU in spleens (Gergely et al., 2011). Thus, complete protection from mCMV infection cannot be achieved by OT-1 cells, which is probably due to a narrow functional avidity distribution of CD8 T cells that carry a defined, transgenic TCR. Accordingly, polyclonal SIINFEKL-specific CD8 T cells were more efficient in clearing low-titer residual infection.

As expected, on account of clinical signs in IFNAR-/- mice, which were manifested by extremely swollen hind foot pads at the portal of entry of mCMV, hunched postures, and ruffled fur, the AT experiment had to be ended 8d p.i and transfer. The severity of infection became also apparent from a pronounced viral replication of Δm157Luc-m164SIINFEKL in spleen, lungs and liver (Fig. 3.34), as compared to virus titers in the parental strain C57BL/6, which were generally quite low due to the early time point p.i.. Nevertheless, AT of 10^3 SIINFEKL-specific OT1 CD8 T cells significantly reduced virus titers in spleen and lungs of C57BL/6 mice. In contrast, replication of mCMV in organs of IFNAR-/- mice was not affected at all by these effector cells. Actually, this finding is in accordance with our hypothesis that lack of type I IFN signaling in IFNAR-/- mice prevents a protective effect on account of the increased levels of m152. Of course, one could argue that this phenomenon seen herein could also be due to the fact that lack of IFN signaling negatively affects the activity of the effector cells (Biron et al., 1998; Young and Hardy, 1995). Yet, early studies with IFNAR-/- mice have only reported abnormalities of hematopoietic cells and elevated levels of cells from the myeloid lineage (Hwang et al., 1995), but did not mention an impaired activity of lymphoid cells. In order to assign the here observed effect to an increase in m152 and thereby an enhanced inhibition of antigen presentation, an experiment with IFNAR-/- recipients infected with an m152 deletion mutant (Δm157Luc-Δm152m06-m164SIINFEKL) and 10^3 adoptively transferred OT1 cells was performed (Fig. 3.35). Essentially, the here observed restoration of the protective antiviral activity of OT1 effector cells in IFNAR-/- mice substantiated our hypothesis.

4.7 NK-Cell Activation in Acute mCMV Infection

Another noted function of m152 is the downmodulation of RAE-1 (Krmpotić et al., 2002; Lodoen et al., 2003), which is a ligand for the activating NK-cell receptor NKG2D, thereby preventing activatory interactions and shifting the balance towards inhibitory signals (Lanier 2008; Ortaldo and Young, 2005; Yokoyama et al., 1998). This is presumably essential to compensate for the activation of NK cells via the ‘missing-self’ axis (Babić et

al., 2010; Kärre et al., 1986), which is caused by the decline in MHC class I cell surface expression by m152.

Here, we addressed this function with regard to the IRFE-dependent inhibition of m152 by conducting NK-cell depletion experiments in mCMV-infected mice. Earlier studies have shown that antibody to asialo GM1 selectively depletes NK-cell activity *in vivo*, without having an effect on CD8 T cells provided that depletion is performed prior to infection and CD8 T-cell activation (Habu et al., 1981; Kasai et al., 1980; Slifka et al., 2000). As to mCMV infection, mice treated with this antibody were reported to have significantly higher virus titers in their lungs, liver, and most pronounced in the spleen at days 3, 5, 7, and 9 p.i. (Bukowski et al., 1983 & 1984), and severe viral pathogenesis in spleen and liver, but less in the lungs. In recent studies, this antibody was used as well to investigate the interaction of mCMV immune modulators with activating and inhibitory NK-cell receptors (Arapović et al., 2009; Babić et al., 2010; Krmpotić et al., 2002). These authors could show that WT virus titers in the lungs were significantly increased after NK-cell depletion in C57BL/6 mice, but only weakly in BALB/c mice, whereas ∆m152 titers in lungs of either BALB/c or C57BL/6 mice were significantly increased after depletion (Krmpotić et al., 2002). Furthermore, they could demonstrate that this m152-mediated control was independent of CD4 and CD8 T cells. In cooperation with the group of Prof. Jonjić (Department of Histology and Embryology, Faculty of Medicine, University of Rijeka, Croatia) we have received antibodies and applied their protocols to conduct similiar studies.

On the basis of these previous findings, we sought to investigate the effect of the IRFE-dependent inhibition of m152 on NK-cell activity. Considering the increased levels of m152 in cells infected with mutant virus mutIRFE, one would suggest that this leads to an augmented downmodulation of RAE-1, and thereby to an even more complete inhibition of NK-cell activation. This would imply that virus titers would not be affected by NK-cell depletion. To test this hypothesis, immunocompetent BALB/c mice were depleted of NK cells and were infected either virus mutIRFE or WT.BAC. Different infection doses were applied to account for a possible influence of virus burden on the effect of NK cells. Viral replication in spleen, lungs, and liver was monitored 3d p.i., according to the finding that NK-cell activity to mCMV peaks at 3-5d p.i. (Babić et al., 2010; Bancroft et al., 1981; Krmpotić et al., 2002; Quinnan et al., 1982).

At first, the efficacy of NK-cell depletion was verified in the spleen by flow cytofluorometry. Yet, apparently this has not been a standard control in other groups. Interestingly, we found that the process of i.v. infection reduced the number of NK cells to ~20% as compared to naïve mice (Fig. 3.36). Treatment with the depleting antibody reduced these levels a residual of 10% of the initial number. Probably, for an NK-cell effect the absolute

number of residual NK cells is relevant, rather than the relative difference between depleted or undepleted groups (~50%). At least, the applied depletion protocol has been shown to be sufficient for inducing an effect in the above-mentioned studies as well as herein. Interestingly, it has been reported in early studies (Bukowski et al., 1984) that in contrast to i.v. and i.p. infection, NK-cell depletion has no effect on mCMV replication after intranasal infection, and thus depends on the infection route. Herein, flow cytofluorometry has shown that the process of i.v. infection itself largely reduces the number of NK cells in the spleen (Fig. 3.36), whereas other experiments from our group (unpublished data) have revealed that after footpad infection the reduction is much weaker. In terms of the innate defense, it has been shown before that the route of infection can make a difference in the induction of the IFN response (Lewy et al., 2002). Together, these findings suggest that depletion of NK cells by anti-asialo GM1 might not be sufficient and requires the augmenting effect of i.v. or i.p. infection to effectively reduce the absolute number of NK cells in the spleen.

Contrary to what one would have expected, depletion of NK cells in mutIRFE-infected mice led to significantly increased virus titers in spleen and lungs, and increased numbers of infected liver cells, with augmented effects by the low infection dose as was intended by the experimental design (Fig. 3.37). In comparison to that, statistically significant but quantitatively lower increases in titers of WT virus could only be detected in all tested organs after low-dose infection. In a repetition of the experiment, these results could be confirmed, more or less, insofar as mutIRFE-infected mice displayed higher numbers of infected liver cells, and higher virus titers in the spleen, but not in the lungs, after NK-cell depletion (Fig. 3.38). This might be due to a lower efficiency of depletion in the lungs. Moreover, this corresponds to the findings from earlier studies, namely that the effect of NK cells in the lungs is not quite as pronounced as it is in spleen and liver (Bukowski et al., 1994). For WT virus, the increase was not consistently significant in any organ under test. However, these slight variances in the case of WT infection have been shown before by other groups (Babić et al., 2010; Krmpotić et al., 2002).

Taken together, these results suggest that replication of mutIRFE is inhibited by NK cells at early times p.i., but not to below levels of WT replication. This implies that the increase in m152, which is the only known difference between mutant and WT virus, is causative for this phenomenon. An explanation for that might be an enhanced inhibition of cell surface trafficking of MHC-peptide complexes and thus of peptide presentation by MHC class I molecules, and a consequent reduction in overall cell-surface levels of MHC class I molecules (Lemmermann et al. 2010) (3.6), which would favor activation of NK cells via ‘missing-self’ recognition, i.e. by missing ligation of inhibitory NK-cell receptors.

It has been reported that anti-asialo GM1 antibody-treated mice have higher plasma IFN levels than control mice (Bukowski et al., 1983). This observation is in accordance with previous studies (Robbins et al., 2007) reporting that by the early control of CMV infection NK cells limit type I IFN production to levels being immune stimulatory by preventing an expansion of plasmacytoid dendritic cells (pDC), which are the major producers of IFN (reviewed in Gilliet et al., 2008), and influence the accrual of virus-specific NK and CD8 T cells (Swiecki et al., 2010). As we have shown herein, an increase in IFN signaling leads to decreased levels of m152 in WT virus, and thereby restores peptide presentation via MHC class I, which, at least in part, activates antigen-specific T cells. In addition, it was reported that type I IFN can promote CD8 T-cell survival and differentiation, mechanisms that further strengthen an antiviral CD8 T cell response (Wiesel et al., 2010).

For excluding a possible involvement of early-primed CD8 T cells (Böhm et al., 2008b) in the control of mutIRFE virus replication in the spleen, an experiment was performed including three groups of BALB/c mice, which were either NK-cell depleted, CD8 T-cell depleted, or left undepleted, and were infected with virus mutIRFE. The efficacy of cell depletions was verified in the spleen by flow cytofluorometry. In contrast to NK-cell depletion, the levels of CD8 T cells were slightly increased by infection as compared to a naïve mouse (Fig. 3.39), and treatment with the depleting antibody almost completely removed this lymphocyte population. Regarding virus titers, it could be confirmed (for the third time) that depletion of NK cells results in significantly increased titers of mutIRFE in spleen and lungs, with a more variable and less significant effect on the liver (Fig. 3.40). Importantly, control of mutIRFE virus replication in the spleen proved to be independent of CD8 T cells, which is in accordance with the literally complete inhibition of antigenic peptide presentation by the enhanced level of m152.

As mentioned above, the activation of NK cells by mutant virus mutIRFE could possibly be due to a lack of interactions of inhibitory receptors with MHC class I molecules, leading to activation, or more precisely derepression by the ‘missing-self’ signal. In this respect, it was reported that the early activation of NK cells by mCMV infection, as displayed by IFNγ production 36h p.i., is independent of Ly49H expression, whereas later in infection the percentage of splenic and liver Ly49+ NK cells is found to be preferentially increased from day 2 p.i. onward (Dokun et al., 2001). However, in the case of the deletion mutant Δm152, it could be shown that the attenuated phenotype of this virus displayed in spleens and lungs of infected BALB/c mice 3d p.i. could be reversed by blockade of NKG2D positive cells (Slavuljica et al., 2010), which demonstrates that the missing downregulation of RAE-1 by m152 restores NK-cell activation via NKG2D receptors. Moreover, replication of WT virus was shown in this study to be not significantly affected by NKG2D blockade.

In order to exclude that interactions with the activating NK-cell receptor NKG2D are responsible for the NK-cell effect on replication of mutIRFE, NKG2D+ cells were blocked in BALB/c mice , which were afterwards infected with virus ∆m152 or mutIRFE. The m152 deletion mutant was included in this experiment to verify the efficiency of the blockade. Notably, replication of mutIRFE in the spleen was inhibited by NK cells as demonstrated by the preceding experiments, but apparently independent of NKG2D (Fig. 3.42). This observation is in accordance with the hypothesis that NK-cell activation by mutIRFE is mediated via the 'missing-self' axis. Yet, the functionality of the NKG2D blockade was primarily seen from the reversion of the attenuated phenotype of the m152 deletion mutant in the spleen. Surprisingly, blockade of NKG2D+ cells resulted in a significantly reduced replication of mutIRFE in liver and lungs, and of ∆m152 virus in the liver. These results suggest that the action of NKG2D+ cells in the spleen somehow differs from that in the other organs. At this point, it would be interesting to compare the effect of NKG2D blockade on WT virus. Slavuljica et al. (2010), have shown that in the case of the lungs, replication was insignificantly decreased, and in the spleen not affected at all, whereas Babić et al. (2010) have also demonstrated an insignificant decrease in the case of the spleen. This would suggest that the weak (insignificant) effect of NKG2D+ cells present in WT-virus-infected mice is augmented by the mutant virus. However, it remains unclear how and why viral replication could be supported by these cells, and, specifically, why this depends on the amount of m152.

With regard to this finding, it has to be considered that activated CD8 T cells also express NKG2D, but it has been reported that it serves only as a co-stimulatory molecule for TCR triggering, and that RAE-1/NKG2D interaction alone fails to signal in T cells (Lanier, 2004; Vivier et al., 2002). Nevertheless, NKG2D blockade was shown to affect the killing of mCMV-infected cells for some epitopes, but NKG2D signaling was suggested to contribute only weakly to CTL lysis (Pinto et al., 2007). Moreover, a role of CD8 T cells on early replication of mutIRFE had been excluded in the preceding experiment.

Taken together, the depletion studies have aimed to identify whether the IRFE-dependent inhibition of m152 has a functional effect concerning the activation of NK cells, which is a target of this viral immune modulator. Apparently, inhibition of *m152* expression in WT virus prevented the activation of NK cells by ligation of inhibitory NK-cell receptors, which in the case of mutIRFE virus infection is prevented by an enhanced retention of MHC class I molecules. Moreover, the expression levels of *m152* in WT virus are sufficient to downmodulate RAE-1 and thereby prevent the activation of NK cells via NKG2D signaling, which obviously cannot be further reduced by increased levels of m152 in cells infected with the mutIRFE virus. In conclusion, inhibition of m152 by IFN signaling in the acute phase of infection might be crucial to balance viral immune modulation to achieve a

certain degree of inhibition of the adaptive immune response to infection while simultaneously preventing stimulation of the innate immune system.

4.8 Conclusions and Perspectives

The interaction of host and viral factors determines the development of CMV infection (Scalzo et al., 2007). In the case of the host, two lines of defense are operational, the innate and the adaptive immune system. CMV is known to express immune-modulatory proteins, which target key players of both systems IFN and NK cells, and CD8 T cells (Arapović et al., 2009; Krmpotić et al., 2002; reviewed in Lisnić et al., 2010; Paulus et al., 2006; Rodriguez-Martín et al., submitted for publication; Ziegler et al., 1997). Conducting research on these interactions not only identifies viral strategies to withstand the immune response, but also discloses general principles of immunology in the context of infection. Both aspects are critical to develop new targets for antiviral therapy.

In this work, a striking connection between the major viral immune modulator m152 and a key cytokine of the immune system IFN (reviewed in Katze et al., 2002), has been revealed. The promoter region of *m152* was identified to contain regulatory elements of the IFN signaling pathway, namely a perfect-match sequence of an IRFE, and an imperfect sequence of an ISRE, which are both evolutionary conserved among different strains of the virus. The focus of this study lies on the identification of the functional role of this element on *m152* promoter activity, gene expression, and the immune-modulatory function. Herein, the functionality of this element could be confirmed *in vitro* and *in vivo* by revealing a connection between IFN signaling, inhibition of *m152* expression, and a decline in the functional impact of m152. However, in cell-transfection-based reporter gene assays also an activating effect of IFN signaling on *m152* promoter activity was shown. Initially, a search for transcription factor binding sites had identified the sequence to be potentially bound by IRF-1 or IRF-2, because it completely matches their binding motif IRFE (Tanaka et al., 1993). In the case of type I IFN gene expression, and IFN-inducible MHC class I gene expression, these factors were initially shown to be `trans-acting factors´, both acting on the same regulatory element, but IRF-1 as a positive factor and IRF-2 as suppressor (Fujita et al., 1989; Harada et al., 1989). Furthermore, IRFE were reported to have a `dual function as positive and negative regulators´, because they can be bound by active or inactive IRF molecules, depending on the differentiation status of the cell (Harada et al., 1990). The complexity of the function of IRF was further revealed in succeeding studies demonstrating that these factors also act antagonistically in the regulation of cell growth, with IRF-2 leading to cell transformation and IRF-1 to reversion of this effect. These studies also demonstrated the ‘presence of a latent activation domain’ in IRF-2, which possibly contributes to gene activation under certain conditions

(Yamamoto et al., 1994; Vaughan et al., 1995). These studies have disclosed that the two IRF, which can potentially act on the IRFE in *m152*, can both exert activating and inhibitory effects, depending on the type of gene, cell, cell-cycle phase, and differentiation status. Moreover, as the literature review in this work has revealed (see 4.1), also other TF (Blimp-1) including members from the IRF family (IRF-3 and IRF-7) share the same recognition sequence and are thus also potential binding partners of the *m152* promoter-resident IRFE. In addition, as mentioned above, the IRFE in the *m152* promoter could also be functional as an ISRE, although the sequence does not completely match the consensus sequence. This further increases the number of possible binding partners and the effects on *m152* expression.

For the interpretation of the results, it might be important to consider that in embryonic fibroblasts, virus-induced type I IFN gene expression is reduced, and the expression pattern of IFNα subtypes altered (Sato et al., 2000), which is why herein treatment with exogenous IFN has often enhanced the effect decisively.

The previous finding that in infected macrophages, which predominantly express TLR to identify pathogens and produce downstream IFN among other cytokines (Flint et al., 2009), the antigenic IE1 peptide is constitutively presented by MHC class I, because m152 immune modulation is prevented (Hengel et al., 2000), might as well be a function of the IRFE-dependent inhibition of m152. In this respect, it is of interest to note that macrophages are also suggested to be a site of CMV latency (reviewed in Paludan et al., 2011).

With regard to the complexity of the functions of IRF, it is conceivable that under certain conditions, *m152* expression might be activated via the IRFE. In this context, it is tempting to consider this to play a role in the establishment of latency. In this respect, it is interesting that for another member of the herpesvirus family, EBV, transcriptional activation of the viral *EBNA-1* gene was described to be mediated by different IRF. The promoter Qp, which is used for *EBNA-1* transcription in cells in the infection state of type I latency, but not in type III latency, was reported to be constitutively activated by both IRF-1 and IRF-2, but not ISGF3 (Nonkwelo et al., 1997; Schaefer et al., 1997). Moreover, an ISRE sequence was identified in Qp, and the binding of IRF-7, which is abundantly expressed in type III latency cells, to this sequence with a repressive effect was demonstrated (Zhang & Pagano, 1997). This aspect might also be important in the context of the here identified ISRE sequence present in the *ie1/3* transcription unit of mCMV.

In the context of viral infection of the cell and induction of pathogen recognition pathways including IFN signaling, the results obtained from this work regarding the IRFE-dependent inhibition of *m152* gene expression and its impact on the immune modulatory function are summarized in Fig. 4.1.

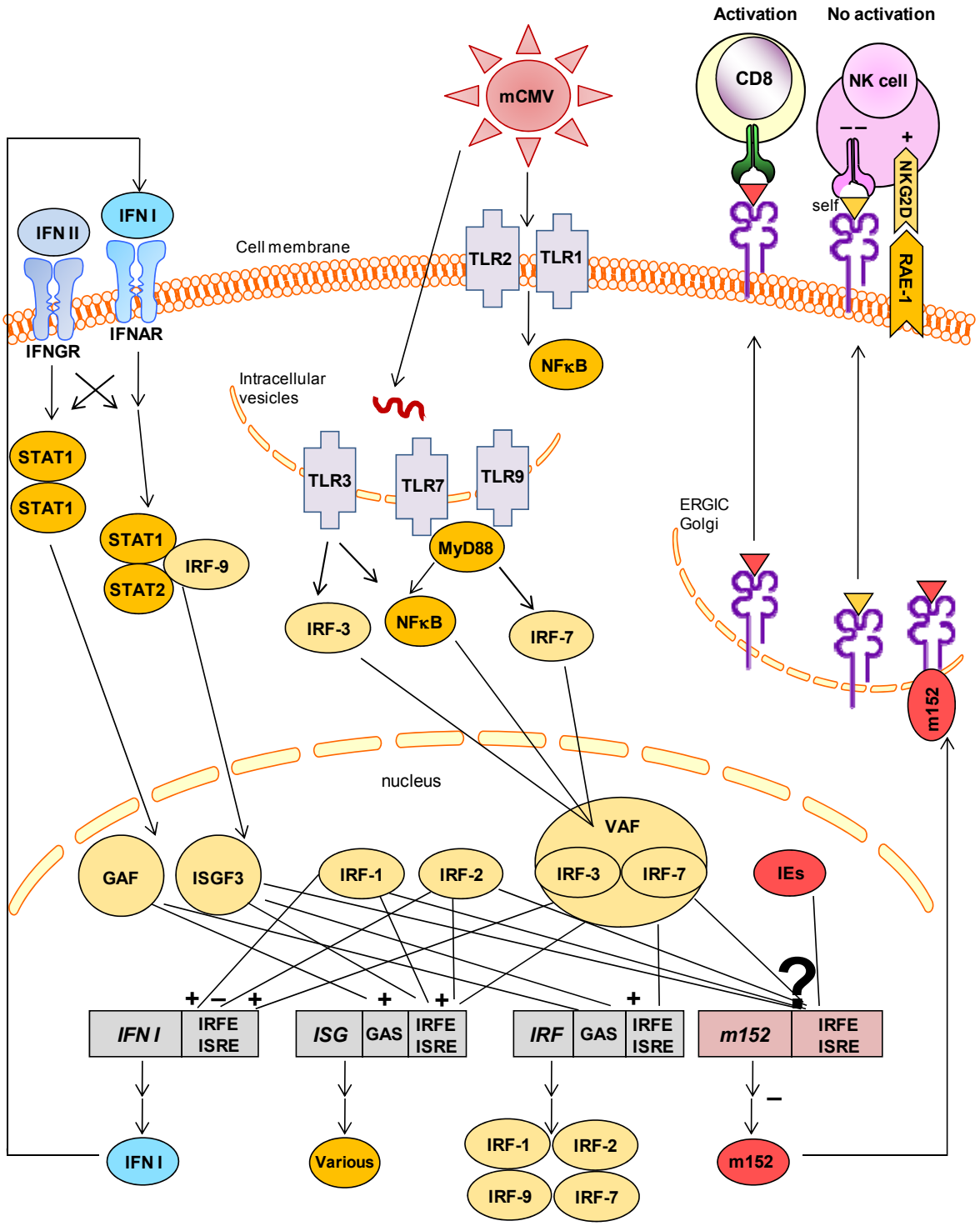

Fig. 4.1 Sketch of the IRFE-dependent regulation of *m152* gene expression and immune modulatory function in the case of mCMV infection of the cell. Virus entry is sensed via cell-membrane-resident TLR (TLR1, TLR2), which leads to activation of NFκB. Virus nucleic acids in intracellular vesicles are sensed via TLR3, which leads to activation of IRF-3, and via TLR7 and TLR9, which leads to the recruitment of MyD88 and the formation of the VAF complex (IRF-3, IRF-7, p300, CBP) that translocates to the nucleus and induces the expression of various *ISG*, *IFN I*, and *IRF* via the IRFE. IRF-1 and IRF-2 also regulate the expression of some *ISG* as well as of *IFN I via the* IRFE. Production and secretion of IFN I leads to binding to the IFNAR receptor, whereas exogenous IFN II binds to the IFNGR receptor. Receptor activation induces downstream complex formation of ISGF3γ and GAF, respectively, which translocate to the nucleus and activate genes via their corresponding recognition sequences ISRE and GAS, respectively. The viral *m152* gene

containing an IRFE/ISRE sequence in its promoter region can potentially be bound and regulated by ISGF3γ, IRF-1, IRF-2, and the VAF. Moreover, it can be bound by viral IE transactivator proteins. Inhibition of *m152* gene expression restores MHC class I antigen presentation at the cell surface, whereby effector CD8 T cells can be activated. Simultaneously, MHC class I molecules loaded with self peptides are presented at the cell surface and can engage with inhibitory receptors of NK cells, whereby the activatory signal via RAE-1/NKG2D ligand/receptor interaction is repressed. Some of the forms are taken from motifolio.com©. Figure not drawn to scale.

Entry of mCMV into the cell is sensed by cell-membrane resident TLR1 and TLR2, which leads to the activation of NFκB (Barbalat et al., 2009; Szomolanyi-Tsuda et al., 2006). Moreover, viral nucleic acids in intracellular vesicles are recognized on the one hand by TLR3, which leads to the activation of IRF-3, and on the other hand by TLR7 (Tabeta et al., 2004) and TLR9 (Krug et al., 2009; Zucchini et al., 2008), which leads to recruitment of the adaptor protein MyD88, and the induction of IRF-7 and NFκB. Both IRF-3 and IRF-7 form a complex, termed virus-activated factor (VAF), also including p300 and CBP, which translocates to the nucleus, and binds the promoters of *IFNβ* and various ISG that have been described to be virus inducible (Wathelet et al., 1998). Production and secretion of IFNβ leads to activation of the IFNAR downstream signaling pathway, which leads to the formation of ISGF3 (STAT1, STAT2, IRF-9) that activates various ISG via the ISRE, including *IRF-2*, *IRF-7*, and *IRF-9*. In contrast, exogenous IFNγ binds to the IFNGR receptor, which leads to the formation of GAF (homodimer STAT1-STAT1) that activates various ISG via the GAS, including *IRF-1*. Constitutively expressed IRF-1 and IRF-2 regulate the expression of *IFNβ*, as well as of various ISG via the IRFE (reviewed in Honda & Taniguchi, 2006). This figure illustrates the potential binding partners of the *m152* promoter-resident IRFE/ISRE present in the nucleus of an infected cell. Moreover, in the current work viral IE proteins were also suggested to contribute to *m152* gene expression. However, the IRFE-dependent effect on *m152* was shown herein to be inhibitory in the acute phase of infection, which restores direct antigen presentation via MHC class I molecules on infected cells for the activation of CD8 T cells, and probably also restores presentation of 'self' peptides to NK cells, which leads to ligation with inhibitory receptors.

In any case, to shed light on the interactions taking place at the *m152* promoter site, as a next step, electrophoretic mobility shift assays (EMSA) should be performed to identify the binding partner/s of the IRFE. In the present thesis, the focus was laid on the functionality and relevance of the IRFE on *m152* expression and its immune modulatory function, which is why the search for the IRFE interaction partners is the subject of ongoing research.

Furthermore, with the findings from this study, the action of another viral protein, M27, was identified to be involved in the regulation of m152. This protein is known to bind and

downregulate STAT 2, which leads to disruption of IFN signaling (Zimmermann et al., 2005), and thereby at least in part prevents inhibition of *m152* expression in acute infection with WT virus. Gene and protein expression experiments should be performed with a deletion mutant ΔM27 and the revertant virus ΔM27rev to reproduce the findings from herein. A protein-expression kinetics in fact revealed that in the deletion mutant the expression of m152 was weaker as compared to expression levels in revertant virus (data not shown).

In the case of the interaction of m152 with NK cells, the hypothesis that an increase in the viral protein leads to activation of NK cells via the 'missing-self' axis, will be further investigated with an assay established by the group of Prof. Jonjić (Babić et al., 2010). Therein, reporter cells expressing an inhibitory Ly49 receptor are co-cultured with MEF infected with WT virus or a mutant. In the case of WT infection, the inhibitory receptor is engaged, which in part is due to the action of m04 that binds to MHC class I molecules and escorts them to the cell surface (Kleijnen et al., 1997). In the case of an infection with virus mutIRFE, the increase in m152 and hence of MHC class I retention might prevent trafficking of m04-MHC complexes to the cell surface and thereby prevent the ligation of inhibtory Ly49 receptors on NK cells. Showing this would confirm our hypothesis.

In summary, this study has demonstrated a so far unknown mechanism of IFN signaling to control acute mCMV infection in the immunocompromised and immunocompetent host, and might also present an important aspect for persistent infection. In this respect, previous studies have demonstrated that i.p. or i.m. IFNγ-treatment prior to infection with mCMV reduced the mortality in a dose- and time-dependent manner (Fennie et al., 1988). In another study, a low-dose daily oral administration of type I IFN was shown to significantly reduce early replication of mCMV in spleen and liver of infected BALB/c mice (Beilharz et al., 1997). Moreover, intramuscular gene therapy with plasmids encoding IFN transgenes was reported to lead to significantly lower mCMV titers in mice expressing the transgene (Yeow et al., 1998). On the basis of these findings, recent studies have used type I IFN for co-immunization with gB CMV DNA constructs, and have revealed an enhanced protective immunity in mice, as displayed by reduced viral titers and severity of pathogenesis in infected organs, as well as increased early antiviral IgG titers (Cull et al., 2002). With the knowledge of the results from this thesis, these descriptive findings, which may be due to common effects of IFN signaling, might also be explained by an IRFE-dependent regulation of *m152* gene expression.

5. References

Akira, S., K. Takeda, and T. Kaisho. 2001. Toll-like receptors: critical proteins linking innate and acquired immunity. Nat. Immunol. **2**:675-680.

Akira, S., S. Uematsu, and O. Takeuchi. 2006. Pathogen recognition and innate immunity. Cell **124**:783-801.

Angulo, A., P. Ghazal, and M. Messerle. 2000. The major immediate-early gene ie3 of mouse cytomegalovirus is essential for viral growth. J. Virol. **74**:11129-11136.

Arapović, J., T. Lenac, R. Antulov, B. Polić, Z. Ruzsics, L. N. Carayannopoulos, U. H. Koszinowski, A. Krmpotić, and S. Jonjić. 2009. Differential susceptibility of RAE-1 isoforms to mouse cytomegalovirus. J. Virol. **83**:8198-8207.

Arase, H., E. S. Mocarski, A. E. Campbell, A. B. Hill, L. L. Lanier. 2002. Direct recognition of cytomegalovirus by activating and inhibitory NK cell receptors. Science **296**:1323-1326.

Autenrieth, I. B., M. Beer, E. Bohn, S. H. Kaufmann, and J. Heesemann. 1994. Immune responses to Yersinia enterocolitica in susceptible BALB/c and resistant C57BL/6 mice: an essential role for gamma interferon. Infect. Immun. **62**:2590-2599.

Babić, M., M. Pyzik, B. Zafirova, M. Mitrović, V. Butorac, L. L. Lanier, A. Krmpotić, S. M. Vidal, and S. Jonjić. 2010. Cytomegalovirus immunoevasin reveals the physiological role of "missing self" recognition in natural killer cell dependent virus control in vivo. J. Exp. Med. **207**:2663-2673.

Bach, E. A., M. Aguet, and R. D. Schreiber. 1997. The IFN gamma receptor: a paradigm for cytokine receptor signaling. Annu. Rev. Immunol. **15**:563-591.

Bancroft, G. J., G. R. Shellam, and J. E. Chalmer. 1981. Genetic influences on the augmentation of natural killer (NK) cells during murine cytomegalovirus infection: correlation with patterns of resistance. J. Immunol. **126**:988-994.

Bantug, G. R., D. Cekinović, R. Bradford, T. Koontz, S. Jonjić, and W. J. Britt. 2008. CD8+ T lymphocytes control murine cytomegalovirus replication in the central nervous system of newborn animals. J. Immunol. **181**:2111-2123.

Barbalat, R., L. Lau, R. M. Locksley, and G. M. Barton. 2009. Toll-like receptor 2 on inflammatory monocytes induces type I interferon in response to viral but not bacterial ligands. Nat. Immunol. **10**:1200-1207.

Beilharz, M. W., W. McDonald, M. W. Watson, J. Heng, J. McGeachie, and C. M. Lawson. 1997. Low-dose oral type I interferons reduce early virus replication of murine cytomegalovirus in vivo. J. Interferon Cytokine Res. **17**:625-630.

Biron, C. A. 1998. Role of early cytokines, including alpha and beta interferons (IFN-alpha/beta), in innate and adaptive immune responses to viral infections. Semin. Immunol. **10**:383-390.

Biron, C. A. 2001. Interferons alpha and beta as immune regulators--a new look. Immunity **14**:661-664.

Biron, C. A., K. S. Byron, and J. L. Sullivan. 1989. Severe herpesvirus infections in an adolescent without natural killer cells. N. Engl. J. Med. **320**:1731-1735.

Biron, C. A., K. B. Nguyen, G. C. Pien, L. P. Cousens, and T. P. Salazar-Mather. 1999. Natural killer cells in antiviral defense: function and regulation by innate cytokines. Annu. Rev. Immunol. **17**:189-220.

Biron, C. A., L. R. Turgiss, and R. M. Welsh. 1983. Increase in NK cell number and turnover rate during acute viral infection. J. Immunol. **131**:1539-1545.

Boehm, U., T. Klamp, M. Groot, and J. C. Howard. 1997. Cellular responses to interferon-gamma. Annu. Rev. Immunol. **15**:749-795.

Boehme, K. W., M. Guerrero, and T. Compton. 2006. Human cytomegalovirus envelope glycoproteins B and H are necessary for TLR2 activation in permissive cells. J. Immunol. **177**:7094-7102.

Böhm, V., J. Podlech, D. Thomas, P. Deegen, M. F. Pahl-Seibert, N. A. Lemmermann, N. K. Grzimek, S. A. Oehrlein-Karpi, M. J. Reddehase, and R. Holtappels. 2008a. Epitope-specific in vivo protection against cytomegalovirus disease by CD8 T cells in the murine model of preemptive immunotherapy. Med. Microbiol. Immunol. **197**:135-144.

Böhm V., C. O. Simon, J. Podlech, C. K. Seckert, D. Gendig, P. Deegen, D. Gillert-Marien, N. A. Lemmermann, R. Holtappels, and M. J. Reddehase. 2008b. The immune evasion paradox: immunoevasins of murine cytomegalovirus enhance priming of CD8 T cells by preventing negative feedback regulation.J. Virol. **82**:11637-11650.

Boppana, S. B., L. B. Rivera, K. B. Fowler, M. Mach, and W. J. Britt. 2001. Intrauterine transmission of cytomegalovirus to infant of women with preconceptional immunity. N. Engl. J. Med. **344**:1366-1371.

Boyle, K. A., and T. Compton. 1998. Receptor-binding properties of a soluble form of human cytomegalovirus glycoprotein B. J. Virol. **72**:1826-1833.

Brown, M. G., A. O. Dokun, J. W. Heusel, H. R. Smith, D. L. Beckman, E. A. Blattenberger, C. E. Dubbelde, L. R. Stone, A. A. Scalzo, and W. M. Yokoyama. 2001. Vital involvement of a natural killer cell activation receptor in resistance to viral infection. Science **292**:934-937.

Bubić, I., M. Wagner, A. Krmpotić, T. Saulig, S. Kim, W. M. Yokoyama, S. Jonjić, and U. H. Koszinowski. 2004. Gain of virulence caused by loss of a gene in murine cytomegalovirus. J. Virol. **78**:7536-7554.

Bühler, B., G. M. Keil, F. Weiland, and U. H. Koszinowski. 1990. Characterization of the murine cytomegalovirus early transcription unit e1 that is induced by immediate-early proteins. J. Virol. **64**:1907-1919.

Bukowski, J. F., and R. M. Welsh. 1985a. Interferon enhances the susceptibility of virus-infected fibroblasts to cytotoxic T cells. J. Exp. Med. **161**:257-262.

Bukowski, J. F., and R.M. Welsh. 1985b. Inability of interferon to protect virus-infected cells against lysis by natural killer (NK) cells correlates with NK cell-mediated antiviral effects in vivo. J. Immunol. **135**:3537-3541.

Bukowski J. F., J. F. Warner, G. Dennert, and R. M. Welsh. 1985c. Adoptive transfer studies demonstrating the antiviral effect of natural killer cells in vivo. J. Exp. Med. **161**:40-52.

Bukowski, J. F., B. A. Woda, S. Habu, K. Okumura, and R. M. Welsh. 1983. Natural killer cell depletion enhances virus synthesis and virus-induced hepatitis in vivo. J. Immunol. **131**:1531-1538.

Bukowski, J. F., B. A. Woda, and R. M. Welsh. 1984b. Pathogenesis of murine cytomegalovirus infection in natural killer cell-depleted mice. J. Virol. **52**:119-118.

Busche, A., A. Angulo, P. Kay-Jackson, P. Ghazal, and M. Messerle. 2008. Phenotypes of major immediate-early gene mutants of mouse cytomegalovirus. Med. Microbiol. Immunol. **197**:233-240.

Calame, K. 2010. Blimp-1's maiden flight. J. Immunol. **185**:3-4.

Carnaud, C., D. Lee, O. Donnars, S. H. Park, A. Beavis, Y. Koezuka, and A. Bendelac. 1999. Cutting edge: Cross-talk between cells of the innate immune system: NKT cells rapidly activate NK cells. J. Immunol. **163**:4647-4650.

Chan, S., Akira, A. Vicari, C. A. Biron, G. Trinchieri, and F. Brière. MyD88-dependent and -independent murine cytomegalovirus sensing for IFN-alpha release and initiation of immune responses in vivo. 2005. J. Immunol. **175**:6723-6732.

Chang, Y., E. Cesarman, M. S. Pessin, F. Lee, J. Culpepper, D. M. Knowles, and P. S. Moore. 1994. Identification of herpesvirus-like DNA sequences in AIDS-associated Kaposi's sarcoma. Science **266**:1865-1869.

Cobbold, M., N. Khan, B. Pourgheysari, S. Tauro, D. McDonald, H. Osman, M. Assenmacher, L. Billingham, C. Steward, C. Crawley, E. Olavarria, J. Goldman, R. Chakraverty, P. Mahendra, C. Craddock, and P. A. Moss. 2005. Adoptive transfer of cytomegalovirus-specific CTL to stem cell transplant patients after selection by HLA-peptide tetramers. J. Exp. Med. **202**:379-386.

Compton, T., R. R. Nepomuceno, and D. M. Nowlin. 1992. Human cytomegalovirus penetrates host cells by pH-independent fusion at the cell surface. Virology **191**:387-395.

Compton, T., D. M. Nowlin, and N. R. Cooper. 1993. Initiation of human cytomegalovirus infection requires initial interaction with cell surface heparan sulfate. Virology **193**:834-841.

Cull, V. .S, S. Broomfield, E. J. Bartlett, N. L. Brekalo, and C. M. James. 2002. Coimmunisation with type I IFN genes enhances protective immunity against cytomegalovirus and myocarditis in gB DNA-vaccinated mice. Gene Ther. **9**:1369-1378.

Darnell, J. E. Jr., I. M. Kerr, and G. R. Stark. 1994. Jak-STAT pathways and transcriptional activation in response to IFNs and other extracellular signaling proteins. Science **264**:1415-1421.

Davison, A. J., and D. Bhella. 2006. Comparative genome and virion structure, p.175-201. *In* Arvin, A. M., E. S. Mocarski, P. Moore et al., (eds). Human Herpesviruses: Biology, Therapy, Immunoprophylaxis. Cambridge: Cambridge Press.

DeFilippis, V. R., D. Alvarado, T. Sali, S. Rothenburg, and K. Früh. 2010. Human cytomegalovirus induces the interferon response via the DNA sensor ZBP1. J. Virol. **84**:585-598.

Delale, T., A. Paquin, C. Asselin-Paturel, M. Dalod, G. Brizard, E. E. Bates, P. Kastner, S. Chan, S. Akira , A. Vicari, C. A. Biron, G. Trinchieri, and F. Brière. 2005. MyD88-dependent

and -independent murine cytomegalovirus sensing for IFN-alpha release and initiation of immune responses in vivo. J. Immunol. **175**:6723-6732.

Del Val, M., H. Hengel, H. Häcker, U. Hartlaub, T. Ruppert, P. Lucin, and U. H. Koszinowski. 1992. Cytomegalovirus prevents antigen presentation by blocking the transport of peptide-loaded major histocompatibility complex class I molecules into the medial-Golgi compartment. J. Exp. Med. **176**:729-738.

Doherty, P. C. 1993. Cell-mediated cytotoxicity. Cell **75**:607-612.

Dokun, A. O., D. T. Chu, L. Yang, A. S. Bendelac, and W. M. Yokoyama. 2001a. Analysis of in situ NK cell responses during viral infection. J. Immunol. **167**:5286-5293.

Dokun, A. O., S. Kim, H. R. Smith, H. S. Kang, D. T. Chu, and W. M. Yokoyama. 2001b. Specific and nonspecific NK cell activation during virus infection. Nat. Immunol. **2**:951-956.

Dolan, A., C. Cunningham, R. D. Hector, A. F. Hassan-Walker, L. Lee, C. Addison, D. J. Dargan, D. J. McGeoch, D. Gatherer, V. C. Emery, P. D. Griffiths, C. Sinzger, B. P. McSharry, G. W. Wilkinson, and A. J. Davison. 2004. Genetic content of wild-type human cytomegalovirus. J. Gen. Virol. **85**:1301-1312.

Doody, G. M., S. Stephenson, C. McManamy, and R. M. Tooze. 2007. PRDM1/BLIMP-1 modulates IFN-g-dependent control of the MHC class I antigen-processing and peptide-loading pathway. J. Immunol. **179**:7614-7623.

Dumas, A. M, J. L. Geelen, W. Maris, and J. Van der Noorda. 1980. Infectivity and molecular weight of varicella-zoster virus. J. Gen. Virol. **47**:233-235.

Emery, V. C., and P. D. Griffiths. 1990. Molecular biology of cytomegalovirus. Int. J. Exp. Pathol. **71**:905-918.

Epstein, M., W. Henle, B. Achoing, and Y. Barr. 1965. Morphological and biological studies on a virus in cultured lymhpoblasts from Burkitt`s lymphoma. J. Exp. Med. **121**:761-770.

Erlandsson, L, R. Blumenthal, M. L. Eloranta, H. Engel, G. Alm, S. Weiss, and T. Leanderson. 1998. Interferon-beta is required for interferon-alpha production in mouse fibroblasts. Biol. **8**:223-226.

Falvo J. V., B. S. Parekh, C. H. Lin, E. Fraenkel, and T. Maniatis. 2000. Assembly of a functional beta interferon enhanceosome is dependent on ATF-2-c-jun heterodimer orientation. Mol. Cell Biol. **20**:4814-4825.

Fauci, A. S., D. Mavilio, and S. Kottilil. 2005. NK cells in HIV infection: paradigm for protection or targets for ambush. Nat. Rev. Immunol. **5**:835-843.

Fennie, E. H., Y. S. Lie, M. A. Low, P. Gribling, and K. P. Anderson. 1988. Reduced mortality in murine cytomegalovirus infected mice following prophylactic murine interferon-gamma treatment. Antiviral Res. **10**:27-39.

Frenkel, N., E. C. Schirmer, L. S. Wyatt, G. Katsafanas, E. Roffmann, R. M. Danovich, and C. H. June. 1990. Isolation of a herpesvirus from human CD4+ T cells. Proc. Natl. Acad. Sci. USA **87**:748-752.

Fujita, T., J. Sakakibara, Y. Sudo, M. Miyamoto, Y. Kimura, and T. Taniguchi. 1988. Evidence for a nuclear factor(s), IRF-1, mediating induction and silencing properties to human IFN-beta gene regulatory elements. EMBO J. **7**:3397-3405.

Fujita, T., Y. Kimura, M. Miyamoto, E. L. Barsoumian, and T. Taniguchi. 1989. Induction of endogenous IFN-alpha and IFN-beta genes by a regulatory transcription factor, IRF-1. Nature **337**:270-272.

Gergely, K., B. Plachter, M. J. Reddehase, R. Holtappels, and N. A. W. Lemmermann. 2011. Immunization with recombinant dense bodies protects mice from cytomegalovirus infection. 13th International CMV/BetaHerpesvirus Workshop. Abstract No. 4.05.

Gil, M. P., E. Bohn, A. K. O'Guin, C. V. Ramana, B. Levine, G. R. Stark, H. W. Virgin, and R. D. Schreiber. 2001. Biologic consequences of Stat1-independent IFN signaling. Proc. Natl. Acad. Sci. U S A **98**:6680-6685.

Gilliet, M., W. Cao, and Y. J. Liu. 2008. Plasmacytoid dendritic cells: sensing nucleic acids in viral infection and autoimmune diseases. Nat. Rev. Immunol. **8**:594-606.

Gompels, U. A., J. Nicholas, G. Lawrence, M. Jones, B. J. Thomson, M. E. Martin, S. Efstathiou, M. Craxton, and H. A. Macaulay. 1995. The DNA sequence of human herpesvirus-6: structure, coding content, and genome evolution. Virology **209**:29-51.

Gough, D. J., N. L. Messina, L. Hii, J. A. Gould, K. Sabapathy, A. P. Robertson, J. A. Trapani, D. E. Levy, P. J. Hertzog, C. J. Clarke, and R. W. Johnstone. 2010. Functional crosstalk between type I and II interferon through the regulated expression of STAT1. PLoS Biol. **8**:e1000361.

Grandér, D, O. Sangfelt, and S. Erickson. 1997. How does interferon exert its cell growth inhibitory effect? Eur. J. Haematol. **59**:129-35.

Gresser I. 1990. Biologic effects of interferons. J. Invest. Dermatol. **95**:66S-71S.

Gribaudo, G., S. Ravaglia, A. Caliendo, R. Cavallo, M. Gariglio, M. G. Martinotti, and S. Landolfo. 1993. Interferons inhibit onset of murine cytomegalovirus immediate-early gene transcription. Virology **197**:303-311.

Gribaudo, G., L. Riera, D. Lembo, M. De Andrea, M. Gariglio, T. L. Rudge, L. F. Johnson, and S. Landolfo. 2000. Murine cytomegalovirus stimulates cellular thymidylate synthase gene expression in quiescent cells and requires the enzyme for replication. J. Virol. **74**:4979-4987.

Gruter, W. 1924. Das Herpesvirus, seine aetiologische und klinische Bedeutung. Muench. Med. Wochenschr. **71**:1058-1060.

Gubbay, J., J. Collignon, P. Koopman, B. Capel, A. Economou, A. Münsterberg, N. Vivian, P. Goodfellow, and R. Lovell-Badge. 1990. A gene mapping to the sex-determining region of the mouse Y chromosome is a member of a novel family of embryonically expressed genes. Nature **346**:245-250.

Habu, S., H. Fukui, K. Shimamura, M. Kasai, Y. Nagai, K. Okumura, and N. Tamaoki. 1981. In vivo effects of anti-asialo GM1. I. Reduction of NK activity and enhancement of transplanted tumor growth in nude mice. J. Immunol. **127**:34-38.

Hansen T. H., and M. Bouvier. 2009. MHC class I antigen presentation: learning from viral evasion strategies. Nat. Rev. Immunol. **9**:503-513.

Harada, H., T. Fujita, M. Miyamoto, Y. Kimura, M. Maruyama, A. Furia, T. Miyata, and T. Taniguchi. 1989. Structurally similar but functionally distinct factors, IRF-1 and IRF-2, bind to the same regulatory elements of IFN and IFN-inducible genes. Cell **58**:729-739.

Harada, H., K. Willison, J. Sakakibara, M. Miyamoto, T. Fujita, and T. Taniguchi. 1990. Absence of the type I IFN system in EC cells: transcriptional activator (IRF-1) and repressor (IRF-2) genes are developmentally regulated. Cell **63**:303-312.

Harty J. T., A. R. Tvinnereim, and D. W. White. 2000. CD8+ T cell effector mechanisms in resistance to infection. Annu. Rev. Immunol. **18**:275-308.

Hengel, H., U. Reusch, G. Geginat, R. Holtappels, T. Ruppert, E. Hellebrand, and U. H. Koszinowski. 2000. Macrophages escape inhibition of major histocompatibility complex class I-dependent antigen presentation by cytomegalovirus. J. Virol. **74**:7861-7868.

Ho, E. L., L. N. Carayannopoulos, J. Poursine-Laurent, J. Kinder, B. Plougastel, H. R. Smith, and W. M. Yokoyama. 2002. Costimulation of multiple NK cell activation receptors by NKG2D. J. Immunol. **169**:3667-3675.

Hogquist, K. A., S. C. Jameson, W. R. Heath, J. L. Howard, M. J. Bevan, and F. R. Carbone. 1994. T cell receptor antagonist peptides induce positive selection. Cell **76**:17-27.

Holtappels, R., V. Böhm, J. Podlech, and M. J. Reddehase. 2008a. CD8 T-cell-based immunotherapy of cytomegalovirus infection: "proof of concept" provided by the murine model. Med. Microbiol. Immunol. **197**:125-134.

Holtappels, R., N. K. Grzimek, C. O. Simon, D. Thomas, D. Dreis, and M. J. Reddehase. 2002a. Processing and presentation of murine cytomegalovirus pORFm164-derived peptide in fibroblasts in the face of all viral immunosubversive early gene functions. J. Virol. **76**:6044-6053.

Holtappels, R., M. W. Munks, J. Podlech, and M. J. Reddehase. 2006. CD8 T-cell-based immunotherapy of cytomegalovirus disease in the mouse model the immunocompromised bone marrow transplantation recipient, p. 383-418. *In* M. J. Reddehase (ed.), Cytomegaloviruses: Molecular biology and Immunology. Caister Academic Press, Wymondham, Norfolk, United Kingdom.

Holtappels, R., D. C. O. Simon, M. W. Munks, D. Thomas, P. Deegen, B. Kühnapfel, T. Däubner, S. Emde, J. Podlech, N. K. Grzimek, S. A. Oehrlein-Karpi A. B. Hill, and M. J. Reddehase. 2008b. Subdominant CD8 T-cell epitopes account for protection against cytomegalovirus independent of immunodomination. J. Virol. **82:**5781-5796.

Holtappels, R., D. Thomas, J. Podlech, and M. J. Reddehase. 2002b. Two antigenic peptides from genes m123 and m164 of murine cytomegalovirus quantitatively dominate CD8 T-cell memory in the H-2d haplotype. J. Virol. **76**:151-164.

Honda, K., and T. Taniguchi. 2006. IRFs: master regulators of signalling by Toll-like receptors and cytosolic pattern-recognition receptors. Nat. Rev. Immunol. **6**:644-658.

Honda, K., H. Yanai, H. Negishi, M. Asagiri, M. Sato, T. Mizutani, N. Shimada, Y. Ohba, A. Takaoka, N. Yoshida, and T. Taniguchi. 2005. IRF-7 is the master regulator of type-I interferon-dependent immune responses. Nature **434**:772-777.

Honess, R. W., and B. Roizman. 1974. Regulation of herpesvirus macromolecular synthesis. I. Cascade regulation of the synthesis of three groups of viral proteins. J. Virol. **14**:8-19.

Huang, S. 1994. Blimp-1 is the murine homolog of the human transcriptional repressor PRDI-BF1 [letter]. Cell **78**:9.

Hudson, J. B., V. Misra, and T. R. Mosmann. 1976. Cytomegalovirus infectivity: analysis of the phenomenon of centrifugal enhancement of infectivity. Virology **72**:235-243.

Hwang, S. Y., P. J. Hertzog, K. A. Holland, S. H. Sumarsono, M. J. Tymms, J. A. Hamilton, G. Whitty, I. Bertoncello, and I. Kola. 1995. A null mutation in the gene encoding a type I interferon receptor component eliminates antiproliferative and antiviral responses to interferons alpha and beta and alters macrophage responses. Proc. Natl. Acad. Sci. U S A **92**:11284-11288.

Isaacs, A., and Lindenmann J. 1957. Virus interference. I. The interferon. J. Interferon Res. **147**:258-267.

Ishii, K. J., C. Coban, H. Kato, K. Takahashi, Y. Torii, F. Takeshita, H. Ludwig, G. Sutter, K. Suzuki, H. Hemmi, S. Sato, M. Yamamoto, S. Uematsu, T. Kawai, O. Takeuchi, and S. Akira. 2006. A Toll-like receptor-independent antiviral response induced by double-stranded B-form DNA. Nat. Immunol. **7**:40-48.

Israel, A., A. Kimura, A. Fournier, M. Fellous, and P. Kourilsky. 1986. Interferon response sequence potentiates activity of an enhancer in the promoter region of a mouse H-2 gene. Nature **322**:743-746.

Janeway, C. A. Jr., and R. Medzhitov. 2002. Innate immune recognition. Annu. Rev. Immunol. **20**:197-216.

Jaworska, J., A. Gravel, K. Fink, N. Grandvaux, and L. Flamand. 2007. Inhibition of transcription of the beta interferon gene by the human herpesvirus 6 immediate-early 1 protein. J. Virol. **81**:5737-5748.

Jonjić, S., W. Mutter, F. Weiland, M. J. Reddehase, and U. H. Koszinowski. 1989. Site-restricted persistent cytomegalovirus infection after selective long-term depletion of CD4+ T lymphocytes. J. Exp. Med. **169**:1199-1212.

Jonjić, S., I. Pavić, B. Polić, I. Crnković, P. Lucin, and U. H. Koszinowski. 1994. Antibodies are not essential for the resolution of primary cytomegalovirus infection but limit dissemination of recurrent virus. J. Exp. Med. **179**:1713-1717.

Kärre, K., H. G. Ljunggren, G. Piontek, and R. Kiessling. 1986. Selective rejection of H-2-deficient lymphoma variants suggests alternative immune defence strategy. J. Immunol. **174**:6566-6569.

Kasai, M., M. Iwamori, Y. Nagai, K. Okumura, and T. Tada. 1980. A glycolipid on the surface of mouse natural killer cells. Eur. J. Immunol. **10**:175-180.

Kavanagh, D. G., U. H. Koszinowski, and A. B. Hill. 2001. The murine cytomegalovirus immune evasion protein m4/gp34 forms biochemically distinct complexes with class I MHC at the cell surface and in a pre-Golgi compartment. J. Immunol. **167:**3894-3902.

Kawai, T., and S. Akira. 2010. The role of pattern-recognition receptors in innate immunity: update on Toll-like receptors. Nat. Immunol. **11**:373-384.

Kedl, R. M., W. A. Rees, D. A. Hildeman, B. Schaefer, T. Mitchell, J. Kappler, and P. Marrack. 2000. T cells compete for access to antigen-bearing antigen-presenting cells. J. Exp. Med. **192**:1105-1113.

Keil, G. M., A. Ebeling-Keil, and U. H. Koszinowski. 1984. Temporal regulation of murine cytomegalovirus transcription and mapping of viral RNA synthesized at immediate early times after infection. J. Virol. **50**:784-795.

Keil, G. M., A. Ebeling-Keil, and U. H. Koszinowski. 1987. Immediate-early genes of murine cytomegalovirus: location, transcripts, and translation products. J. Virol. **61**:526-533.

Keller, A. D., and T. Maniatis. 1991. Identification and characterization of a novel repressor of β-interferon gene expression. Genes Dev. **5**:868-879.

Kenneson A., and M. J. Cannon. 2007. Review and meta-analysis of the epidemiology of congenital cytomegalovirus (CMV) infection. Rev. Med. Virol. **17**:253-276.

Kessler, D. S., S. A. Veals, X. Y. Fu, and D. E. Levy. 1990. Interferon-alpha regulates nuclear translocation and DNA-binding affinity of ISGF3, a multimeric transcriptional activator. Genes Dev. **4**:1753-1765.

Kielczewska, A., M. Pyzik, T. Sun, A. Krmpotic, M. B. Lodoen, M. W. Munks, M. Babić, A. B. Hill, U. H. Koszinowski, S. Jonjić, L. L. Lanier, and S. M. Vidal. 2009. Ly49P recognition of cytomegalovirus-infected cells expressing H2-Dk and CMV-encoded m04 correlates with the NK cell antiviral response. J. Exp. Med. **206**:515-523.

Kimura, T., K. Nakayama, J. Penninger, M. Kitagawa, H. Harada, T. Matsuyama, N. Tanaka, R. Kamijo, J. Vilcek, and T. W. Mak. 1994. Involvement of the IRF-1 transcription factor in antiviral responses to interferons. Science **264**:1921-1924.

Kleijnen, M. F., J. B. Huppa, P. Lucin, S. Mukherjee, H. Farrell, A. E. Campbell, U. H. Koszinowski, A. B. Hill, and H. L. Ploegh. 1997. A mouse cytomegalovirus glycoprotein, gp34, forms a complex with folded class I MHC molecules in the ER which is not retained but is transported to the cell surface. EMBO J. **16**:685-694.

Korber, B., N. Mermod, L. Hood, and I. Stroynowski. 1988. Regulation of gene expression by interferons: control of H-2 promoter responses. Science **239**:1302-1306.

Krauss, S., J. Kaps, N. Czech, C. Paulus, and M. Nevels. 2009. Physical requirements and functional consequences of complex formation between the cytomegalovirus IE1 protein and human STAT2. J. Virol. **83**:12854-12870.

Krmpotić, A., I. Bubić, B. Polić, P. Lucin, S. Jonjić. 2003. Pathogenesis of murine cytomegalovirus infection. Microbes Infect. **5**:1263-1277.

Krmpotić, A., D. H. Busch, I. Bubić, F. Gebhardt, H. Hengel, M. Hasan, A. A. Scalzo, U. H. Koszinowski, S. Jonjić. 2002. MCMV glycoprotein gp40 confers virus resistance to CD8+ T cells and NK cells in vivo. Nat. Immunol. **3**:529-535.

Krmpotić, A., M. Messerle, I. Crnković-Mertens, B- Polić, S. Jonjić, and U. H. Koszinowski. 1999. The immunoevasive function encoded by the mouse cytomegalovirus gene m152 protects the virus against T cell control in vivo. J. Exp. Med. **190**:1285-1296.

Kropp, K. A., K. A. Robertson, G. Sing, S. Rodriguez-Martin, M. Blanc, P. Lacaze, M. F. Noor Hassim, M. R. Khondoker, A. Busche, P. Dickinson, T. Forster, B. Strobl, M. Mueller, S. Jonjić, A. Angulo, and P. Ghazal. 2011. Reversible inhibition of MCMV replication by IFN{gamma} in primary macrophages involves a primed type I IFN signaling sub-network for full establishment of an immediate-early antiviral-state. J. Virol. **85**:10286-10299.

Krug, A., A. R. French, W. Barchet, J. A. Fischer, A. Dzionek, J. T. Pingel, M. M. Orihuela, S. Akira, W. M. Yokoyama, and M. Colonna. 2004. TLR9-dependent recognition of MCMV by IPC and DC generates coordinated cytokine responses that activate antiviral NK cell function. Immunity **21**:107-119.

Kuo, T. C., and K. L. Calame. 2004. B lymphocyte-induced maturation protein (Blimp)-1, IFN regulatory factor (IRF)-1, and IRF-2 can bind to the same regulatory sites. J. Immunol. **173**:5556-5563.

Kurz S., H. P. Steffens, A. Mayer, J. R. Harris, and M. J. Reddehase. 1997. Latency versus persistence or intermittent recurrences: evidence for a latent state of murine cytomegalovirus in the lungs. J. Virol. **71**:2980-2987.

Lanier, L. L. 2005. NKG2D in innate and adaptive immunity. Adv. Exp. Med. Biol. **560**:51-56.

Lanier, L. L. 2008. Up on the tightrope: natural killer cell activation and inhibition. Nat. Immunol. **9**:495-502.

Lee, S. H., S. Girard, D. Macina, M. Busà, A. Zafer, A. Belouchi, P. Gros, and S. M. Vidal. 2001. Susceptibility to mouse cytomegalovirus is associated with deletion of an activating natural killer cell receptor of the C-type lectin superfamily. Nat. Genet. **28**:42-45.

Lembo, D., G. Gribaudo, A. Hofer, L. Riera, M. Cornaglia, A. Mondo, A. Angeretti, M. Gariglio, L. Thelander, and S. Landolfo. 2000. Expression of an altered ribonucleotide reductase activity associated with the replication of murine cytomegalovirus in quiescent fibroblasts. J. Virol. **74**:11557-11565.

Lemmermann N. A., V. Böhm, R. Holtappels, and M. J. Reddehase. 2011. In vivo impact of cytomegalovirus evasion of CD8 T-cell immunity: facts and thoughts based on murine models. Virus Res. **157**:161-174.

Lemmermann, N. A., K. Gergely, V. Böhm, P. Deegen, T. Däubner, and M. J. Reddehase. 2010. Immune evasion proteins of murine cytomegalovirus preferentially affect cell surface display of recently generated peptide presentation complexes. J. Virol. **84**:1221-1236.

Levy, D. E. 2002. Whence interferon? Variety in the production of interferon in response to viral infection. J. Exp. Med. **195**:F15-18.

Levy, D. E., and A. García-Sastre. 2001. The virus battles: IFN induction of the antiviral state and mechanisms of viral evasion. Cytokine Growth Factor Rev. **12**:143-156.

Levy, D. E., D. S. Kessler, R. Pine, and J. E. Jr. Darnell. 1989. Cytoplasmic activation of ISGF3, the positive regulator of interferon-alpha-stimulated transcription, reconstituted in vitro. Genes Dev. **3**:1362-1371.

Livak K. J., and T. D. Schmittgen. 2001. Analysis of relative gene expression data using real-time quantitative PCR and the 2(-Delta Delta C(T)) Method. Methods **25**:402-8.

Li, M., H. Lee, J. Guo, F. Neipel, B. Fleckenstein, K. Ozato, and J. U. Jung. 1998. Kaposi's sarcoma-associated herpesvirus viral interferon regulatory factor. J. Virol. **72**:5433-5440.

Lin R., P. Génin, Y. Mamane, and J. Hiscott. 2000. Selective DNA binding and association with the CREB binding protein coactivator contribute to differential activation of alpha/beta interferon genes by interferon regulatory factors 3 and 7. Mol. Cell Biol. **20**:6342-6353.

Lindquester, G. J., and P. E. Pellett. 1991. Properties of the human herpesvirus 6 strain Z29 genome: G+C content, length, and the presence of variable-length directly repeated terminal sequence elements. Virology **182**:102-110.

Lisnić, V. J., A. Krmpotić, and S. Jonjić. 2010. Modulation of natural killer cell activity by viruses. Curr Opin Microbiol. **13**:530-539.

Lodoen, M., K. Ogasawara, J. A. Hamerman, H. Arase, J. P. Houchins, E. S. Mocarski, and L. L. Lanier. 2003. NKG2D-mediated natural killer cell protection against cytomegalovirus is impaired by viral gp40 modulation of retinoic acid early inducible 1 gene molecules. J. Exp. Med. **197**:1245-1253.

Loewendorf, A., and C. A. Benedict. 2010. Modulation of host innate and adaptive immune defenses by cytomegalovirus: timing is everything. J. Intern. Med. **267**:483-501.

Mamane, Y., C. Heylbroeck, P. Génin, M. Algarté, M. J. Servant, C. LePage, C. DeLuca, H. Kwon, R. Lin, and J. Hiscott. 1999. Interferon regulatory factors: the next generation. Gene **237**:1-14.

Mangin, M., K. Ikeda, and A. E. Broadus. 1990. Structure of the mouse gene encoding parathyroid hormone-related peptide. Gene **95**:195-202.

Marié, I., J. E. Durbin, and D. E. Levy. 1998. Differential viral induction of distinct interferon-alpha genes by positive feedback through interferon regulatory factor-7. EMBO J. **17**:6660-6669.

Marks, J. R., and D. H. Spector. 1988. Replication of the murine cytomegalovirus genome: structure and role of the termini in the generation and cleavage of concatenates. Virology **162**:98-107.

Martinotti, M. G., G. Gribaudo, M. Gariglio, A. Caliendo, D. Lembo, A. Angeretti, R. Cavallo, and S. Landolfo. 1993. Effect of interferon-alpha on immediate early gene expression of murine cytomegalovirus. J. Interferon Res. **13**:105-109.

Masopust, D., V. Vezys, A. L. Marzo, and L. Lefrançois. 2001. Preferential localization of effector memory cells in nonlymphoid tissue. Science **291**:2413-2417.

Matsumoto, M., N. Tanaka, H. Harada, T. Kimura, T. Yokochi, M. Kitagawa, C. Schindler, and T. Taniguchi. 1999. Activation of the transcription factor ISGF3 by interferon-gamma. Biol. Chem. **380**:699-703.

Meier, J. L., and M. F. Stinski. 2006. Major Immediate-early enhancer and its gene products, p. 151-166. *In* M. J. Reddehase (ed.), Cytomegaloviruses: Molecular biology and Immunology. Caister Academic Press, Wymondham, Norfolk, United Kingdom.

Melroe, G. T., N. A. DeLuca, and D. M. Knipe. 2004. Herpes simplex virus 1 has multiple mechanisms for blocking virus-induced interferon production. J. Virol. **78**:8411-8420.

Messerle, M., B. Bühler, G. M. Keil, and U. H. Koszinowski. 1992. Structural organization, expression, and functional characterization of the murine cytomegalovirus immediate-early gene 3. J. Virol. **66**:27-36.

Messerle, M., and I. Crnkovic. 1997. Cloning and mutagenesis of a herpesvirus genome as an infectious bacterial artificial chromosome. Proc. Natl. Acad. Sci. USA **94**:14759-14763.

Meurs, E, K. Chong, J. Galabru, N. S. Thomas, I. M. Kerr, B. R. Williams, and A. G. Hovanessian. 1990. Molecular cloning and characterization of the human double-stranded RNA-activated protein kinase induced by interferon. Cell **62**:379-90.

Mitchell, D. P., J. P. Savaryn, N. J. Moorman, T. Shenk, and S. S. Terhune. 2009. Human cytomegalovirus UL28 and UL29 open reading frames encode a spliced mRNA and stimulate accumulation of immediate-early RNAs. J. Virol. **83**:10187-10197.

Miyahira, Y., K. Murata, D. Rodriguez, J. R. Rodriguez, M. Esteban, M. M. Rodrigues, and F. Zavala. 1995. Quantification of antigen specific CD8+ T cells using an ELISPOT assay. J. Immunol. Methods **181**:45-54.

Mocarski, E. S., T. Shenk, and R. F. Pass. Cytomegaloviruses, p. 2701-22772. *In* Knipe D. M., and P. M. Howley (eds.), Field`s Virology 5th edition. Lippincott Williams & Wilkins, Philapeldphia, PA, USA.

Mogensen, T. H. 2009. Pathogen recognition and inflammatory signaling in innate immune defenses. Clin. Microbiol. Rev. **22**:240-273.

Moore, P. S., and Y. Chang. 1995. Kaposi's sarcoma findings. Science **270**:15b

Müller, U., U. Steinhoff, L. F. Reis, S. Hemmi, J. Pavlovic, R. M. Zinkernagel, and M. Aguet. 1994. Functional role of type I and type II interferons in antiviral defense. Science **264**:1918-1921.

Mullis, K. B., and F. A. Faloona. 1987. Specific synthesis of DNA in vitro via a polymerase-catalyzed chain reaction. Methods Enzymol. **155**:335-50.

Munks, M. W., K. S. Cho, A. K. Pinto, S. Sierro, P. Klenerman, and A. B. Hill. 2006a. Four distinct patterns of memory CD8 T cell responses to chronic murine cytomegalovirus infection. J. Immunol. **177**:450-458.

Munks, M. W., M. C. Gold, A. L. Zajac, C. M. Doom, C. S. Morello, D. H. Spector, and A. B. Hill. 2006b. Genome-wide analysis reveals a highly diverse CD8 T cell response to murine cytomegalovirus. J. Immunol. **176**:3760-3766.

Mutter, W., M. J. Reddehase, F. W. Busch, H. J. Bühring, and U. H. Koszinowski. 1988. Failure in generating hemopoietic stem cells is the primary cause of death from cytomegalovirus disease in the immunocompromised host. J. Exp. Med. **167**:1645-1658.

Navarro, L., K. Mowen, S. Rodems, B. Weaver, N. Reich, D. Spector, and M. David. 1998. Cytomegalovirus activates interferon immediate-early response gene expression and an interferon regulatory factor 3-containing interferon-stimulated response element-binding complex. Mol. Cell Biol. **18**:3796-3802.

Nguyen, H., J. Hiscott, and P. M. Pitha. 1997. The growing family of interferon regulatory factors. Cytokine Growth Factor Rev. **8**:293-312.

Nonkwelo, C., I. K. Ruf, and J. Sample. 1997. Interferon-independent and -induced regulation of Epstein-Barr virus EBNA-1 gene transcription in Burkitt lymphoma. J. Virol. **71**:6887-6897.

Novotny, J., I. Rigoutsos, D. Coleman, and T. Shenk. 2001. In silico structural and functional analysis of the human cytomegalovirus (HHV5) genome. J. Mol. Biol. **310**:1151-1166.

Orange, J. S., and C. A. Biron. 1996. Characterization of early IL-12, IFN-alphabeta, and TNF effects on antiviral state and NK cell responses during murine cytomegalovirus infection. J. Immunol. **156**:4746-4756.

Orr M.T., W. J. Murphy, and L. L. Lanier. 2010. 'Unlicensed' natural killer cells dominate the response to cytomegalovirus infection. Nat. Immunol. **11**:321-327.

Ortaldo, J. R., and H. A. Young. 2005. Mouse Ly49 NK receptors: balancing activation and inhibition. Mol. Immunol. **42**:445-450.

Pahl-Seibert M. F., M. Juelch, J. Podlech, D. Thomas, P. Deegen, M. J. Reddehase, and R. Holtappels. 2005. Highly protective in vivo function of cytomegalovirus IE1 epitope-specific memory CD8 T cells purified by T-cell receptor-based cell sorting. J. Virol. **79**:5400-5413.

Park, M. S., M. L. Shaw, J. Muñoz-Jordan, J. F. Cros, T. Nakaya, N. Bouvier, P. Palese, A. García-Sastre, and C. F. Basler. 2003. Newcastle disease virus (NDV)-based assay demonstrates interferon-antagonist activity for the NDV V protein and the Nipah virus V, W, and C proteins. J. Virol. **77**:1501-1511.

Paulus, C., S. Krauss, and M. Nevels. 2006. A human cytomegalovirus antagonist of type I IFN-dependent signal transducer and activator of transcription signaling. Proc. Natl. Acad. Sci. U S A **103**:3840-3845.

Pellett, P. E., and B. Roizman. 2007. The family *herpesviridae*: a brief introduction, p. 2479-2499. *In* Knipe D. M., and P. M. Howley (eds.), Field`s Virology 5th edition. Lippincott Williams & Wilkins, Philapeldphia, PA, USA.

Pestka, S., J. A. Langer, K. C. Zoon, and C. E. Samuel. 1987. Interferons and their actions. Annu. Rev. Biochem. **56**:727-777.

Pinto, A. K., A. M. Jamieson, D. H. Raulet, and A. B. Hill. 2007. The role of NKG2D signaling in inhibition of cytotoxic T-lymphocyte lysis by the Murine cytomegalovirus immunoevasin m152/gp40. J. Virol. **81**:12564-12571.

Plummer, G. 1967. Comparative virology of the herpes group. Prog. Med. Virol. **9**:302-340.

Podlech, J., R. Holtappels, M. F. Pahl-Seibert, H. P. Steffens, and M. J. Reddehase. 2000. Murine model of interstitial cytomegalovirus pneumonia in syngeneic bone marrow transplantation: persistence of protective pulmonary CD8-T-cell infiltrates after clearance of acute infection. J. Virol. **74**:7496-7507.

Podlech, J., R. Holtappels, N. Wirtz, H. P. Steffens, and M. J. Reddehase. 1998. Reconstitution of CD8 T cells is essential for the prevention of multiple-organ cytomegalovirus histopathology after bone marrow transplantation. J. Gen. Virol. **79**:2099-2104.

Presti, R. M., J. L. Pollock, A. J. Dal Canto, A. K. O'Guin, and H. W. Virgin. 1998. Interferon gamma regulates acute and latent murine cytomegalovirus infection and chronic disease of the great vessels. J. Exp. Med. **188**:577-588.

Preston, C. M., A. N. Harman, and M. J. Nicholl. 2001. Activation of interferon response factor-3 in human cells infected with herpes simplex virus type 1 or human cytomegalovirus. J. Virol. **75**:8909-8916.

Quinnan, G. V., J. E. Manischewitz, and F. A. Ennis. 1978. Cytotoxic T lymphocyte response to murine cytomegalovirus infection. Nature **273**:541-543.

Quinnan, G. V. Jr, J. F. Manischewitz, N. Kirmani. 1982. Involvement of natural killer cells in the pathogenesis of murine cytomegalovirus interstitial pneumonitis and the immune response to infection. J. Gen. Virol. **1**:173-180.

Rathinam V. A., Z. Jiang, S. N. Waggoner, S. Sharma, L. E. Cole, L. Waggoner, S. K. Vanaja, B. G. Monks, S. Ganesan, E. Latz, V. Hornung, S. N. Vogel, E. Szomolanyi-Tsuda, and K. A. Fitzgerald. 2010. The AIM2 inflammasome is essential for host defense against cytosolic bacteria and DNA viruses. Nat. Immunol. **11**:395-402.

Rawlinson, W. D., H. E. Farrell, and B. G. Barrell. 1996. Analysis of the complete DNA sequence of murine cytomegalovirus. J. Virol. **70**:8833-8849.

Reddehase, M. J. 2002. Antigens and immunoevasins: opponents in cytomegalovirus immune surveillance. Nat. Rev. Immunol. **2**:831-844.

Reddehase M. J., M. Balthesen, M. Rapp, S. Jonjić, I. Pavić, and U. H. Koszinowski. 1994. The conditions of primary infection define the load of latent viral genome in organs and the risk of recurrent cytomegalovirus disease. J. Exp. Med. **179**:185-193.

Reddehase, M. J, F. Weiland, K. Münch, S. Jonjić, A. Lüske, and U. H. Koszinowski. 1985. Interstitial murine cytomegalovirus pneumonia after irradiation: characterization of cells that limit viral replication during established infection of the lungs. J. Virol. **55**:264-273.

Reusch, U., W. Muranyi, P. Lucin, H. G. Burgert, H. Hengel, and U. H. Koszinowski. 1999. A cytomegalovirus glycoprotein re-routes MHC class I complexes to lysosomes for degradation. EMBO J. **1**8:1081-1091.

Riddell, S. R., K. S. Watanabe, J. M. Goodrich, C. R. Li, M. E. Agha, and P. D. Greenberg. 1992. Restoration of viral immunity in immunodeficient humans by the adoptive transfer of T cell clones. Science **257**:238-241.

Robbins, S. H., G. Bessou, A. Cornillon, N. Zucchini, B. Rupp, Z. Ruzsics, T. Sacher, E. Tomasello, E. Vivier, U. H. Koszinowski, and M. Dalod. 2007. Natural killer cells promote early CD8 T cell responses against cytomegalovirus. PLoS Pathog. **3**:e123.

Rötzschke, O., K. Falk, S. Stevanović, G. Jung, P. Walden, H. G. Rammensee. 1991. Exact prediction of a natural T cell epitope. Eur. J. Immunol. **21**:2891-2894.

Rudolph, M. G., R. L. Stanfield, and I. A. Wilson. 2006. How TCRs bind MHCs, peptides, and coreceptors. Annu. Rev. Immunol. **24**:419-466.

Saiki, R. K., D. H. Gelfand, S. Stoffel, S. J. Scharf, R. Higuchi, G. T. Horn, K. B. Mullis, H. A. Erlich. 1988. Primer-directed enzymatic amplification of DNA with a thermostable DNA polymerase. Science **239**:487-491.

Salazar-Mather T. P., C. A. Lewis, and C. A. Biron. 2002. Type I interferons regulate inflammatory cell trafficking and macrophage inflammatory protein 1alpha delivery to the liver. J. Clin. Invest. **110**:321-330.

Samuel, C. E. 2001. Antiviral actions of interferons. Clin. Microbiol. Rev. **14**:778-809.

Sato, M., N. Hata, M. Asagiri, T. Nakaya, T. Taniguchi, and N. Tanaka. 1998a. Positive feedback regulation of type I IFN genes by the IFN-inducible transcription factor IRF-7. FEBS Lett. **441**:106-110.

Sato, M., H. Suemori, N. Hata, M. Asagiri, K. Ogasawara, K. Nakao, T. Nakaya, M. Katsuki, S. Noguchi, N. Tanaka, and T. Taniguchi. 2000. Distinct and essential roles of transcription factors IRF-3 and IRF-7 in response to viruses for IFN-alpha/beta gene induction. Immunity **13**:539-548.

Sato, M, N. Tanaka, N. Hata, E. Oda, and T. Taniguchi. 1998b. Involvement of the IRF family transcription factor IRF-3 in virus-induced activation of the IFN-beta gene. FEBS Lett. **425**:112-116.

Sato, M., T. Taniguchi, and N. Tanaka. 2001. The interferon system and interferon regulatory factor transcription factors -- studies from gene knockout mice. Cytokine Growth Factor Rev. **12**:133-42.

Savitsky, D., T. Tamura, H. Yanai, and T. Taniguchi. 2010. Regulation of immunity and oncogenesis by the IRF transcription factor family. Cancer Immunol. Immunother. **59**:489-510.

Schaefer, B. C., E. Paulson, J. L. Strominger, and S. H. Speck. 1997. Constitutive activation of Epstein-Barr virus (EBV) nuclear antigen 1 gene transcription by IRF1 and IRF2 during restricted EBV latency. Mol. Cell Biol. **17**:873-886.

Scalzo, A. A., A. J. Corbett, W. D. Rawlinson, G. M. Scott, and M. A. Degli-Esposti. 2007. The interplay between host and viral factors in shaping the outcome of cytomegalovirus infection. Immunol. Cell Biol. **85**:46-54.

Scalzo, A. A., and W. M. Yokoyama. 2008. Cmv1 and natural killer cell responses to murine cytomegalovirus infection. Curr. Top. Microbiol. Immunol. **321**:101-122.

Schneider, K, A. Loewendorf, C. De Trez, J. Fulton, A. Rhode, H. Shumway, S. Ha, G. Patterson, K. Pfeffer, S. A. Nedospasov, C. F. Ware, and C. A. Benedict. 2008. Lymphotoxin-mediated crosstalk between B cells and splenic stroma promotes the initial type I interferon response to cytomegalovirus. Cell Host Microbe **3**:67-76.

Schneweis, K. E. 1962. Serologische Untersuchungen zur Typendifferenzierung des Herpesvirus Hominis. Z. immunitätsforsch. Exp. Ther. **124**:24-48.

Schulz O., S. S. Diebold, M. Chen, T. I. Näslund, M. A. Nolte, L. Alexopoulou, Y. T. Azuma, R. A. Flavell, P. Liljeström, and C. Reis e Sousa. 2005. Toll-like receptor 3 promotes cross-priming to virus-infected cells. Nature **433**:887-892.

Sen, N., M. Sommer, X. Che, K. White, W. T. Ruyechan, and A. M. Arvin. 2010. Varicella-zoster virus immediate-early protein 62 blocks interferon regulatory factor 3 (IRF3) phosphorylation at key serine residues: a novel mechanism of IRF3 inhibition among herpesviruses. J. Virol. **84**:9240-9253.

Simon, C. O., R. Holtappels, H. M Tervo, V. Böhm, T. Däubner, S. A. Oehrlein-Karpi, B. Kühnapfel, A. Renzaho, D. Strand, J. Podlech, M. J. Reddehase, and N. K. Grzimek. 2006. CD8 T cells control cytomegalovirus latency by epitope-specific sensing of transcriptional reactivation. J. Virol. **80**:10436-10456.

Simon, C. O., C. K. Seckert, D. Dreis, M. J. Reddehase, and N. K. Grzimek. 2005. Role for tumor necrosis factor alpha in murine cytomegalovirus transcriptional reactivation in latently infected lungs. J. Virol. **79**:326-340.

Slavuljica, I., A. Busche, M. Babić, M. Mitrović, I. Gašparović, D. Cekinović, E. Markova Car, E. Pernjak Pugel, A. Ciković, V. J. Lisnić, W. J. Britt, U. H. Koszinowski, M. Messerle, A. Krmpotić, and S. Jonjić. 2010. Recombinant mouse cytomegalovirus expressing a ligand for the NKG2D receptor is attenuated and has improved vaccine properties. J. Clin. Invest. **120**:4532-4545.

Slifka M. K., R. R. Pagarigan, and J. L. Whitton. 2000. NK Markers Are Expressed on a High Percentage of Virus-Specific CD8+ and CD4+ T Cells. J. Immunol. **164**:2009-2015

Smith, M. G. 1965. Propagation in tissue cultures of a cytopathogenic virus from human salivary gland virus (SGV) disease. Proc. Soc. Exp. Biol. Med. **92**:224-230.

Smith, P. K., R. I. Krohn, G. T. Hermanson, A. K. Mallia, F. H. Gartner, M. D. Provenzano, E. K. Fujimoto, N. M. Goeke, B. J. Olson, and D. C. Klenk. 1985. Measurement of protein using bicinchoninic acid. Anal. Biochem. **150**:76-85.

Smith, L. M., A. R. McWhorter, L. L. Masters, G. R. Shellam, and A. J. Redwood. 2008. Laboratory strains of murine cytomegalovirus are genetically similar to but phenotypically distinct from wild strains of virus. J. Virol. **82**:6689-6696.

Stark, G. R., I. M. Kerr, B. R. Williams, R. H. Silverman, and R. D. Schreiber. 1998. How cells respond to interferons. Annu. Rev. Biochem. **67**:227-264.

Steinberg, C., K. Eisenächer, O. Gross, W. Reindl, F. Schmitz, J. Ruland, and A. Krug. 2009. The IFN regulatory factor 7-dependent type I IFN response is not essential for early resistance against murine cytomegalovirus infection. Eur. J. Immunol. **39**:1007-1018.

Stenberg, R. M., D. R. Thomsen, and M. F. Stinski. 1984. Structural analysis of the major immediate early gene of human cytomegalovirus. J. Virol. **49**:190-199.

Stetson, D. B., and R. Medzhitov. 2006. Recognition of cytosolic DNA activates an IRF3-dependent innate immune response. Immunity **24**:93-103.

Sugita, K., J. Miyazaki, E. Appella, and K. Ozato. 1987. Interferons increase transcription of a major histocompatibility class I gene via a 5' interferon consensus sequence. Mol. Cell Biol. **7**:2625-3260.

Swiecki, M., S. Gilfillan, W. Vermi, Y. Wang, and M. Colonna. 2010. Plasmacytoid dendritic cell ablation impacts early interferon responses and antiviral NK and CD8(+) T cell accrual. Immunity **33**:955-966.

Szomolanyi-Tsuda, E., X. Liang, R.M. Welsh, E. A. Kurt-Jones, and R. W. Finberg. 2006. Role for TLR2 in NK cell-mediated control of murine cytomegalovirus in vivo. J. Virol. **80**:4286-4291.

Tabeta, K., P. Georgel, E. Janssen, X. Du, K. Hoebe, K. Crozat, S. Mudd, L. Shamel, S. Sovath, J. Goode, L. Alexopoulou, R. A. Flavell, and B. Beutler. 2004. Toll-like receptors 9 and 3 as essential components of innate immune defense against mouse cytomegalovirus infection. Proc. Natl. Acad. Sci. U S A **101**:3516-3521.

Taguchi, T., J. R. McGhee, R. L. Coffman, K. W. Beagley, J. H. Eldridge, K. Takatsu, and H. Kiyono. 1990. Detection of individual mouse splenic T cells producing IFN-gamma and IL-5 using the enzyme-linked immunospot (ELISPOT) assay. J. Immunol. Methods. **128**:65-73.

Takaoka, A., Y. Mitani, H. Suemori, M. Sato, T. Yokochi, S. Noguchi, N. Tanaka, and T. Taniguchi. 2000. Cross talk between interferon-gamma and -alpha/beta signaling components in caveolar membrane domains. Science **288**:2357-2360.

Tanaka, N., T. Kawakami, and T. Taniguchi. 1993. Recognition DNA sequences of interferon regulatory factor 1 (IRF-1) and IRF-2, regulators of cell growth and the interferon system. Mol. Cell Biol. **13**:4531-4538.

Taniguchi, T., K. Ogasawara, A. Takaoka, and N. Tanaka. 2001. IRF family of transcription factors as regulators of host defense. Annu. Rev. Immunol. **19**:623-655.

Taniguchi, T., and A. Takaoka. 2001. A weak signal for strong responses: interferon-alpha/beta revisited. Nat. Rev. Mol. Cell Biol. **2**:378-386.

Taniguchi, T., and A. Takaoka. 2002. The interferon-alpha/beta system in antiviral responses: a multimodal machinery of gene regulation by the IRF family of transcription factors. Curr. Opin. Immunol. **14**:111-116.

Taylor, R. T., and W. A. Bresnahan. 2006. Human cytomegalovirus immediate-early 2 protein IE86 blocks virus-induced chemokine expression. J. Virol. **80**:920-928.

Thäle R., U. Szepan, H. Hengel, G. Geginat, P. Lucin, and U. H. Koszinowski. 1995. Identification of the mouse cytomegalovirus genomic region affecting major histocompatibility complex class I molecule transport. J. Virol. **69**:6098-6105.

Thanos, D., and T. Maniatis. 1992. The high mobility group protein HMG I(Y) is required for NF-kappa B-dependent virus induction of the human IFN-beta gene. Cell **71**:777-789.

Tischer, B. K., J. von Einem, B. Kaufer, and N. Osterrieder. 2006. Two-step red-mediated recombination for versatile high-efficiency markerless DNA manipulation in Escherichia coli. Biotechniques **40**:191-197.

Tjian, R., and T. Maniatis. 1994. Transcriptional activation: a complex puzzle with few easy pieces. Cell **77**:5-8.

Tortorella, D., B. E. Gewurz, M. H. Furman, D. J. Schust, and H. L. Ploegh. 2000. Viral subversion of the immune system. Annu. Rev. Immunol. **18**:861-926.

Turner, C. A. Jr., D. H. Mack, and M. M. Davis. 1994. Blimp-1, a novel zinc finger-containing protein that can drive the maturation of B lymphocytes into immunoglobulin-secreting cells. Cell **77**:297-306.

Varani, S., M. Cederarv, S. Feld, C. Tammik, G. Frascaroli, M. P. Landini, and C. Söderberg-Nauclér. 2007. Human cytomegalovirus differentially controls B cell and T cell responses through effects on plasmacytoid dendritic cells. J Immunol. **179**:7767-7776.

Vaughan, P. S., F. Aziz, A. J. van Wijnen, S. Wu, H. Harada, T. Taniguchi, K. J. Soprano, J. L. Stein, and G. S. Stein. 1995. Activation of a cell-cycle-regulated histone gene by the oncogenic transcription factor IRF-2. Nature **377**:362-365.

Vaughan, P. S., C. M. van der Meijden, F. Aziz, H. Harada, T. Taniguchi, A. J. van Wijnen, J. L. Stein, and G. S. Stein. 1998. Cell cycle regulation of histone H4 gene transcription requires the oncogenic factor IRF-2. J. Biol. Chem. **273**:194-199.

Vivier, E., E. Tomasello, and P. Paul. 2002. Lymphocyte activation via NKG2D: towards a new paradigm in immune recognition? Curr. Opin. Immunol. **14**:306-311.

Wagner, M., A. Gutermann, J. Podlech, M. J. Reddehase, and U. H. Koszinowski. 2002. Major histocompatibility complex class I allele-specific cooperative and competitive interactions between immune evasion proteins of cytomegalovirus. J. Exp. Med. **196**:805-816.

Walzer T., M. Bléry, J. Chaix, N. Fuseri, L. Chasson, S. H. Robbins, S. Jaeger, P. André, L. Gauthier, L. Daniel, K. Chemin, Y. Morel, M. Dalod, J. Imbert, M. Pierres, A. Moretta, F. Romagné, and E. Vivier. 2007. Identification, activation, and selective in vivo ablation of mouse NK cells via NKp46. Proc Natl Acad Sci U S A. **104**:3384-3389.

Wang, J. P., E. A. Kurt-Jones, O. S. Shin, M. D. Manchak, M. J. Levin, and R. W. Finberg. 2005. Varicella-zoster virus activates inflammatory cytokines in human monocytes and macrophages via Toll-like receptor 2. J. Virol. **79**:12658-12666.

Wathelet M. G., C. H. Lin, B. S. Parekh, L. V. Ronco, P. M. Howley, and T. Maniatis. 1998. Virus infection induces the assembly of coordinately activated transcription factors on the IFN-beta enhancer in vivo. Mol. Cell. **1**:507-518.

Welinder, C., and L. Ekblad. 2011. Coomassie staining as loading control in Western blot analysis. J. Proteome Res. **10**:1416-1419.

Welsh, R. M. 2001. Assessing CD8 T cell number and dysfunction in the presence of antigen. J. Exp. Med. **193**:F19-22.

Wiesel, M., W. Kratky, and A. Oxenius. 2011. Type I IFN substitutes for T cell help during viral infections. J. Immunol. **186**:754-763.

Wilhelmi, V., C. O. Simon, J. Podlech, V. Böhm, T. Däubner, S. Emde, D. Strand, A. Renzaho, N. A. Lemmermann, C. K. Seckert, M. J. Reddehase, and N. K. Grzimek. 2008. Transactivation of cellular genes involved in nucleotide metabolism by the regulatory IE1 protein of murine cytomegalovirus is not critical for viral replicative fitness in quiescent cells and host tissues. J. Virol. **82**:9900-9916.

Wu, L., E. Fossum, C. H. Joo, K. S. Inn, Y. C. Shin, E. Johannsen, L. M. Hutt-Fletcher, J. Hass, and J. U. Jung. 2009. Epstein-Barr virus LF2: an antagonist to type I interferon. J. Virol. **83**:1140-1146.

Yamamoto, H., M. S. Lamphier, T. Fujita, T. Taniguchi, and H. Harada. 1994. The oncogenic transcription factor IRF-2 possesses a transcriptional repression and a latent activation domain. Oncogene **9**:1423-1428.

Yasukawa, H., A. Sasaki, and A. Yoshimura. 2000. Negative regulation of cytokine signaling pathways. Annu. Rev. Immunol. **18**:143-64.

Yeow, W. S., C. M. Lawson, and M. W. Beilharz. 1998. Antiviral activities of individual murine IFN-alpha subtypes in vivo: intramuscular injection of IFN expression constructs reduces cytomegalovirus replication. J. Immunol. **160**:2932-2939.

Yokoyama, W. M. 1998. Natural killer cell receptors. Curr. Opin. Immunol. **10**:298-305.

Yokoyama W. M., and S. Kim. 2006. Licensing of natural killer cells by self-major histocompatibility complex class I. Immunol. Rev. **214**:143-154.

Yoneyama, M., and T. Fujita. 2010. Recognition of viral nucleic acids in innate immunity. Rev. Med. Virol. **20**:4-22.

Yewdell J. W., and A. B. Hill. 2002. Viral interference with antigen presentation. Nat. Immunol. **3**:1019-1025.

Yoneyama, M., W. Suhara, Y. Fukuhara, M. Fukuda, E. Nishida, and T. Fujita. 1998. Direct triggering of the type I interferon system by virus infection: activation of a transcription factor complex containing IRF-3 and CBP/p300. EMBO J. **17**:1087-1095.

Young, H. A. 1996. Regulation of interferon-gamma gene expression. J. Interferon Cytokine Res. **16**:563-568.

Young, H. A., and K. J. Hardy. 1995. Role of interferon-gamma in immune cell regulation. J. Leukoc. Biol. **58**:373-381.

Zhang, X., T. W. Brann, M. Zhou, J. Yang, R. M. Oguariri, K. B. Lidie, H. Imamichi, D. W. Huang, R. A. Lempicki, M. W. Baseler, T. D. Veenstra, H. A. Young, H. C. Lane, and T. Imamichi. 2011. Cutting edge: Ku70 is a novel cytosolic DNA sensor that induces type III rather than type I IFN. J. Immunol. **186**:4541-4545.

Zhang, L., and J. S. Pagano. 1997. IRF-7, a new interferon regulatory factor associated with Epstein-Barr virus latency. Mol. Cell Biol. **17**:5748-5757.

Zhi, L., J. Mans, M. J. Paskow, P. H. Brown, P. Schuck, S. Jonjić, K. Natarajan, and D. H. Margulies. 2010. Direct interaction of the mouse cytomegalovirus m152/gp40 immunoevasin with RAE-1 isoforms. Biochemistry **49**:2443-2453.

Ziegler, H., W. Muranyi, H. G. Burgert, E. Kremmer, and U. H. Koszinowski. 2000. The luminal part of the murine cytomegalovirus glycoprotein gp40 catalyzes the retention of MHC class I molecules. EMBO J. **19**:870-881.

Ziegler, H., R. Thale, P. Lucin, W. Muranyi, T. Flohr, H. Hengel, H. Farrell, W. Rawlinson, and U. H. Koszinowski. 1997. A mouse cytomegalovirus glycoprotein retains MHC class I complexes in the ERGIC/cis-Golgi compartments. Immunity **6**(1):57-66.

Zimmermann, A., and H. Hengel. 2006. Cytomegalovirus interference with interferon, p. 321-340. *In* M. J. Reddehase (ed.), Cytomegaloviruses: Molecular biology and Immunology. Caister Academic Press, Wymondham, Norfolk, United Kingdom.

Zimmermann, A., M. Trilling, M. Wagner, M. Wilborn, I. Bubić, S. Jonjić, U. H. Koszinowski, and H. Hengel. 2005. A cytomegaloviral protein reveals a dual role for STAT2 in IFN-{gamma} signaling and antiviral responses. J. Exp. Med. **201**:1543-1553.

Zimring, J. C., S. Goodbourn, and M. K. Offermann. 1998. Human herpesvirus 8 encodes an interferon regulatory factor (IRF) homolog that represses IRF-1-mediated transcription. J. Virol. **72**:701-707.

Zucchini, N., G. Bessou, S. Traub, S. H. Robbins, S. Uematsu, S. Akira, L. Alexopoulou, and M. Dalod. 2008. Cutting edge: Overlapping functions of TLR7 and TLR9 for innate defense against a herpesvirus infection. J. Immunol. **180**:5799-5803.

Honorable Declaration

I hereby declare, that this thesis being submitted for examination is a result of my own work and research. The data and results presented are the genuine data and results actually obtained by my research. Where I have used work, ideas and results of others it has been appropriately indicated in the thesis. The thesis has not been presented to any other examination committee or been published before.

Mainz, 24.01.2012: _____